

REMOVAL OF SULFUR DIOXIDE FROM POWER PLANT  
STACKS BY A MODIFIED CLAUS PROCESS

R. T. Struck, M. D. Kulik, and Everett Gorin

CONSOLIDATION COAL COMPANY  
Research Division  
Library, Pennsylvania 15129

A large amount of research and development is being conducted both by government and industry to develop processes for removal of  $\text{SO}_2$  from power plant stack gases. These efforts have been stimulated by the activity of the Federal Government in suggesting to local, state and interstate air pollution control agencies that stringent standards be set up on the maximum permissible ground level concentration of  $\text{SO}_2$ . The suggested criterion<sup>1</sup> calls, for example, for a maximum ground level concentration over a 24-hour period of 0.1 ppm of  $\text{SO}_2$ . It is difficult to relate this criterion to a maximum permissible level of  $\text{SO}_2$  in a typical power plant stack since this depends on many factors such as stack height, presence of other pollution sources, meteorological conditions, etc. However, in many instances this would require reduction of the  $\text{SO}_2$  content in the stack to a level corresponding to the combustion of a fuel containing much less than 1% sulfur.

There is no doubt that wherever such stringent air quality standards may become legally required, power plant operators will be forced either to install  $\text{SO}_2$ -removal equipment or to switch to low-sulfur fuels (if such should be available).

The situation is of particular concern to the coal industry, since over 50% of its production is used for power generation and only a small fraction of the coal produced in the Eastern United States is low enough in sulfur to meet the stringent standards mentioned above.

The most feasible solution to the problem for a coal burning utility at the present time is the installation of  $\text{SO}_2$ -scrubbing facilities since removal of sulfur from the coal to the level required is a much more difficult task.

The first system for flue gas cleanup to undergo trial operation on a full commercial-scale is the combined limestone injection and wet scrubbing process offered by Combustion Engineering.<sup>2</sup> The above system does not produce any valuable by-products and incurs a cost debit for limestone purchase and spent calcium sulfate slurry disposal.

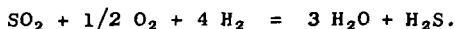
A number of developments is in progress aimed at reducing the net cost of  $\text{SO}_2$  scrubbing by sale of by-products, usually either sulfuric acid or sulfur. Some processes are also aimed at the production of either  $(\text{NH}_4)_2\text{SO}_4$  or liquid  $\text{SO}_2$  as by-products, but these are not of general interest because of restricted markets.

The production of sulfuric acid has a somewhat broader market potential. Two processes are being offered for commercial use, i.e., Monsanto's<sup>3</sup> Cat-Ox process and Lurgi's Sulfacid process.<sup>4</sup> The high cost of shipping sulfuric acid to consuming points, however, also restricts the number of plants to which this approach is applicable.

The production of elemental sulfur on the other hand, considerably broadens the market potential due to its low cost of shipping relative to sulfuric acid. Considerable research and development is underway, therefore, directed at  $\text{SO}_2$  scrubbing processes which yield elemental sulfur as a by-product. None of these, however, is as yet available for commercial use.

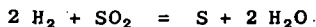
Most of these processes are based on the use of an "alkaline type" absorbent either in form of an aqueous<sup>5</sup> or molten carbonate<sup>6</sup> or an alkalized solid support such as alkalized alumina.<sup>7</sup> The absorption process is associated with unavoidable oxidation, if it is conducted at high temperatures, such that large amounts of alkali sulfate are generally formed. The regeneration system, in general, involves reduction of the alkali sulfate with CO and H<sub>2</sub> mixtures, and recovery of the sulfur as H<sub>2</sub>S which is subsequently converted to sulfur in a conventional Claus plant.

This type of process requires more than 3 and as many as 4 mols of CO plus H<sub>2</sub> reductant per mol of sulfur recovered, as typified by the equation below describing the overall process,



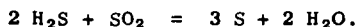
The most convenient way of generating the CO plus H<sub>2</sub> reductant is by way of steam-methane reforming. The thermal efficiency of such plants may be taken as equal to about 70%, based on natural gas feed. It is readily computed on the above basis that the natural gas requirement, where 4 mols of CO + H<sub>2</sub> reductant are required per mol of elemental sulfur recovered, amounts to 48 MM Btu/long ton of sulfur. Present prices for natural gas at most locations in north eastern United States, i.e., in the range of 35-45¢/MM Btu, are such that the reductant cost (\$17-21/long ton of sulfur for a 4/1 mol ratio) places a very high economic burden on such a process even without considering the capital and other significant operating costs of the gas generation and reagent regeneration processes.

It is clear, therefore, that a very large incentive exists to reduce the reductant cost to the theoretical minimum of 2 mols/mol of sulfur recovered as typified by the overall reaction,



or roughly half, as compared with the schemes discussed above.

One method that has been proposed which accomplishes this objective is to inject H<sub>2</sub>S into the flue gas and reduce the SO<sub>2</sub> in situ, to produce sulfur by a Claus type process, i.e.,



Two thirds of the recovered sulfur are reduced to H<sub>2</sub>S and reinjected into the flue gas. This process, in principle, then produces sulfur with a consumption of only 2 mols of reductant/mol of sulfur produced.

The conventional Claus process is usually operated with concentrated gases using an alumina catalyst at sufficiently high temperatures, usually 400-450°F, such that the sulfur vapor produced does not condense on the catalyst.

Thermodynamic limitations in the case of flue gas, however, preclude such a type of operation. This is illustrated by the equilibrium calculations for a typical flue gas to which 2 mols H<sub>2</sub>S/mol SO<sub>2</sub> have been added as illustrated in Figure 1. These calculations were made utilizing the most modern available thermodynamic data.<sup>8</sup> Data are also shown, for an artificial case, where water is removed from the flue gas to illustrate the adverse effect of water vapor on the equilibrium.

It is seen from Figure 1 that efficient removal of SO<sub>2</sub> from flue gas by the modified Claus technique requires operation at temperatures well below those utilized in the standard Claus process. This is necessitated to a large degree, as shown in Figure 1, by the adverse effect of water vapor on the equilibrium. It should be remembered also, that because of the more noticeable odor of H<sub>2</sub>S, the permissible level

of sulfur compounds in the stack should probably be held to a level well under that for  $\text{SO}_2$  alone. Thus, operation at very low temperature, i.e., below about  $240^\circ\text{F}$  is indicated. Under these conditions, more than 98.5% of the sulfur produced will condense on the catalyst. It is clear, therefore, that either a cyclic or moving-burden process is required to periodically remove the deposited sulfur from the catalyst.

The first attempt to apply such a process to gas purification was made to coke oven gas by Audas.<sup>9</sup> In this case, the process was applied in reverse, i.e.,  $\text{SO}_2$  was added to the  $\text{H}_2\text{S}$ -containing gas, and the modified low temperature Claus process was conducted with condensation of the sulfur on the alumina catalyst and its subsequent regeneration.

Application of the concept to flue gas treating was proposed by Kerr<sup>10</sup> in a patent assigned to Peter Spence, Ltd. In both the Audas and Kerr processes, the sulfur-fouled catalyst is cycled through a thermal regeneration step where the sulfur is removed by distillation at about  $900\text{--}950^\circ\text{F}$ .

More recently, Princeton Research has undertaken work to develop this type of process<sup>11</sup> under the auspices of the National Air Pollution Control Administration. Little information is available, however, about the results of their work at this time.

The Consolidation Coal Company undertook evaluation of the "modified Claus Process" in its laboratories since it appears to be potentially one of the most attractive processes for treating flue gas. The work soon showed that the alumina catalyst was rapidly poisoned on cycling through the process, largely due to formation of aluminum sulfate.

A two-step regeneration process now under development is described herein which removes this poison and recovers 93% of the sulfur as elementary sulfur and 7% as ammonium sulfate. The tail gas from the process contains less than 50 ppm of  $\text{H}_2\text{S}$  and  $\text{SO}_2$ .

#### EXPERIMENTAL

The apparatus used is shown in Figure 2. A fixed bed of catalyst is supported on quartz chips in a heated tube through which the simulated stack gas flows. The gases are preheated by passage through Pyrex wool and quartz chips. A central thermo-couple well with adjustable couple position is used to measure the bed temperature. The controlled temperature is taken as the hottest spot in the bed. Water is added to the incoming gases by bubbling one of the gas streams through a water bath held at the proper temperature. Under the conditions used here, elemental sulfur remains on the catalyst and the tail gases pass out through a soda lime trap before being metered. At regular intervals, part of the tail gas is diverted through an iodine scrubber to analyze for  $\text{H}_2\text{S}$  and  $\text{SO}_2$ . Catalyst bed depths of one and three inches were used, and a reactor pressure of 810 mm Hg absolute.

Thermal regeneration of the catalyst is carried out by passing nitrogen at 1 to 4 SCFH over the catalyst as it is heated above the boiling point of sulfur to distill off sulfur. The exit gases pass through a sulfur trap (dotted line on Figure 1) and then through the iodine scrubber to analyze for  $\text{H}_2\text{S}$  and  $\text{SO}_2$  liberated during stripping. The analysis for  $\text{H}_2\text{S}$  and  $\text{SO}_2$  is based on their reactions with iodine as was previously described by Doumani.<sup>12</sup>

Three different aluminas were used as catalysts in these tests. Catalyst A is a commercial dessiccant alumina which contains 1.6% alkali and 2.0% silica. The others are purer, more expensive aluminas with properties given in Table I.

### DISCUSSION OF RESULTS

Table II shows the results of short term tests at 300°F (149°C) feeding the stoichiometric ratio:  $H_2S/SO_2 = 2$ . With neither oxygen or water vapor present, the reaction goes nearly to completion and reaches the thermodynamic equilibrium predicted by Figure 1. With added oxygen, results are nearly equivalent. The presence of both steam and oxygen gives much poorer results (last line, Table II). The thermodynamic equilibrium values of Figure 1 were not approached indicating that the presence of steam has an adverse effect on both the kinetics and equilibrium in the Claus reaction. Results of similar experiments to test the effect of oxygen and steam at higher temperatures, i.e., 360°F, can be seen in Figure 3. The right hand figure gives the results in the absence of oxygen, showing that at this temperature, the reaction, after an initial induction period, gives a tail gas having an even lower content of  $H_2S + SO_2$  (900 ppm) than the predicted thermodynamic equilibrium value of 1100 ppm in Figure 1. The low initial  $SO_2$  content of the tail gas is probably due to absorption of  $SO_2$  on the catalyst. When free oxygen is present (as it always is in power plant stacks), the results shown in the left hand half of Figure 3 are obtained. Although the  $SO_2$  concentration was erratic, the rapidly increasing level of  $H_2S$  shows how the catalyst became quickly poisoned. Following this test, an appreciable amount of sulfate was found on the catalyst. It is thus clear that undesirable oxidation of  $SO_2$  is taking place.

The next tests were made at the lower temperatures of 212°F (100°C) in an attempt to minimize sulfate formation and to improve the completeness of the reaction. The first cycle of this test (Figure 4) showed surprisingly that the reaction was very fast at this low temperature and that nearly sulfur-free tail gas could be obtained at this temperature, as predicted by the equilibrium curve of Figure 1. Some  $H_2S$  breakthrough occurred in the early part of the run and both gases broke through due to filling of pores with product sulfur after about 60 grams of sulfur had been fed per 100 grams of catalyst. During the early period when considerable  $H_2S$  breakthrough was observed, it is noted again that no  $SO_2$  broke through. This again is likely due to adsorption of  $SO_2$  by the alumina catalyst.<sup>13</sup> The adsorptive capacity of alumina for  $SO_2$  is taken advantage of in the Audas<sup>9</sup> process previously cited. After this "break-out," the run was stopped and the catalyst heated to 950°F in a stream of nitrogen to remove sulfur. The simulated stack gas was then fed over the catalyst again and the process repeated through four cycles. Results from the last cycle (right half of Figure 4) show that the capacity to completely remove  $SO_2$  had been reduced from 60 to less than 10 grams of sulfur fed per 100 grams of catalyst. This loss of capacity was found again to be due to formation of sulfate poisons even at the low temperature of 212°F. The origin of the sulfate is not wholly clear at the present time as it was found that some sulfate is formed at 212°F even when oxygen is excluded from the flue gas. This problem is being investigated further at this time.

Several attempts were made to remove sulfur from the catalyst by means of organic solvents, such as toluene and carbon disulfide, in order to avoid the thermal stripping. Other aqueous solvents, such as ammonium hydrosulfide solutions, with the potential of removing both sulfates and sulfur, also were tested. With all of these solvents the catalyst particles were disintegrated or weakened so that mechanical handling would be impossible.

The final regeneration process which was successful in maintaining activity consists of two stages: 1) heat the sulfur-laden catalyst to strip off sulfur, and 2) treat the stripped catalyst with aqueous ammonium hydroxide to remove sulfates and regenerate an active alumina surface.

The second stage was accomplished by dropping the cooled catalyst (after stripping) into about 50 times its weight of 2%  $NH_4OH$  at 75°F. After soaking 15 minutes, the catalyst was removed and rinsed four times with distilled water. After air drying, the catalyst was recharged to the reactor and heated to 400°F in nitrogen to remove ammonia.

Figure 5 shows the results of the first and fifth cycles using the new two-stage catalyst regeneration. Although results of the first cycle are erratic (the SO<sub>2</sub> breakthrough suggests that the feed ratio probably was not exactly at the stoichiometric ratio) it is clear that after five cycles there had been no deterioration. In addition, the initial break-in period with high H<sub>2</sub>S values had been eliminated, so that right from the start there was no detectable H<sub>2</sub>S or SO<sub>2</sub> until breakthrough at 24 grams of sulfur fed per 100 grams of catalyst. The uneven results thereafter represent attempts to explore the effects of changing the H<sub>2</sub>S/SO<sub>2</sub> feed ratio slightly on both sides of 2.0.

No change in catalyst size or weight was detectable after five cycles. After stripping off sulfur, the cooled catalyst was tested for hardness in the Hardgrove Grindability Machine (A.S.T.M. Method D-409). The used catalyst was slightly stronger than fresh catalyst.

Figure 6 shows how the two-stage regeneration has eliminated the poisoning problem. The upper graph shows how the catalyst capacity dropped rapidly when only thermal removal of sulfur was used. The lower graph shows that capacity gradually increased through five cycles with the two-stage regeneration. This may be attributable to precipitation of fresh alumina in the ammonia wash. The overall lower capacity shown by the lower graph is a function of the catalyst used. The catalyst, H, has a pore volume of 0.77 versus 0.55 cc/g for catalyst A. It is also noteworthy that the percentage of sulfur in the products which was recovered as elemental sulfur also gradually increased from cycle to cycle: from 92.2 in Cycle 1 to 95.0 in Cycle 5.

Based on results of Cycle 5, the steady-state sulfur balance for the process would be as follows:

<u>In (As Gases)</u>	<u>Percent of Sulfur Fed to Reactors</u>	
SO <sub>2</sub> in Stack Gas	31.8	
SO <sub>2</sub> Recycled from Stripping	1.5	
H <sub>2</sub> S Recycled from Stripping	1.5	
H <sub>2</sub> S Made from S Produced	<u>65.2</u>	
	100.0	
<u>Out (On Catalyst)</u>		
Elemental Sulfur	95.0	
Sulfate	2.0	
H <sub>2</sub> S	1.5	
SO <sub>2</sub>	<u>1.5</u>	
	100.0	
<u>Net Products</u>		<u>Percent of Sulfur Fed in Stack Gas</u>
Elemental Sulfur	29.8	93.7
Sulfate	<u>2.0</u>	<u>6.3</u>
	31.8	100.0

It should be noted that the process also would handle the small amount of SO<sub>3</sub> present in stack gases, giving a slightly higher yield of sulfate.

The authors would like to express their appreciation to Consolidation Coal Company for permission to publish this work.

REFERENCES

- (1) Chem. & Eng. News, 45, No. 15, p 20 (April 3, 1967).  
Chem. Eng., 70, No. 4, p 38 (February 24, 1969).
- (2) Miller, P. M. and Jonakin, J. - Electrical World, 169, No. 35 (March, 1968).
- (3) Ramirez, Raul - Chem. Eng., 76, No. 9, p 86 (April 21, 1969).
- (4) Scheidel, C. F. - Preprint 6E of Paper Presented at 61st Annual Meeting  
AIChE, Los Angeles (December 1 - 5, 1968).
- (5) Pollock, W. A., Tomany, J. P. and Frieling, Garry - Preprint of Paper Presented  
Before ASME Meeting, New York, N. Y. (November 27 - December 1, 1966).  
Galeono, S. F. and Harding, C. I. - Jour. Air Pollution Control Assoc'n.,  
17, No. 8, p 536 (1937).
- (6) Oldenkamp, R. A. - Paper Presented Before 65th Annual Meeting AIChE (May 5, 1969).  
Heredy, L. A., McKenzie, D. E. and Yosim, S. J. - U.S. Patent 3,483,722  
(May 15, 1967).
- (7) Bienstock, D., Field, J. H., Katell, S. and Plants, K. D. - Jour. Air Pollution  
Control Assoc'n., 15, 459 (October, 1965).
- (8) "Janaf Thermochemical Tables" - Dow Chemical Company, PB 168370 (August, 1968).
- (9) Audas, F. G. - Coke and Gas, 13, p 229 (July, 1951).
- (10) Kerr, John - Brit. Patent 1,097,306 (January 3, 1968).
- (11) Chem. & Eng. News, 46, No. 39, p 22 (September 9, 1968).
- (12) Doumani, T. F., Deery, R. F. and Bradley, W. E. - Ind. Eng. Chem., 36, 329 (1944).
- (13) Munro, L. A. and Johnson, F. M. G. - Ind. Eng. Chem., 17, 99 (1925).

TABLE ICatalyst Analyses

Catalyst Composition, ppm	A	C	H
Na	11,900 <sup>(1)</sup>	5	180
Si	9,300 <sup>(1)</sup>	< 100	560
Fe	840	40	280
Ca	--	37	9,100
Al	Balance	Balance	Balance
Surface Area m <sup>2</sup> /g	390	200	218
Pore Volume, cc/g	0.55	0.42	0.77
Bulk Density, Lb/CF	54	--	32

(1) This corresponds to 2% SiO<sub>2</sub> and 1.6% Na<sub>2</sub>O.

TABLE IIThe Effect of Water and Oxygen on Reaction Efficiency

Conditions: Catalyst C

Temperature 300°F

VHSV = 4200

Bed Height = 1 Inch

<u>Feed Gas Composition, Vol %</u>				<u>Tail Gas Composition, ppm</u>	
SO <sub>2</sub>	H <sub>2</sub> S	O <sub>2</sub>	H <sub>2</sub> O	SO <sub>2</sub>	H <sub>2</sub> S
0.163	0.325	0	0	< 50	< 50
0.159	0.317	1.23	0	< 50	50
0.307	0.614	2.40	6.0	700	1400

Figure 1

## EQUILIBRIUM CONCENTRATION IN TAIL GAS AND PERCENT OF SULFUR FORMED WHICH CONDENSES vs OPERATING TEMPERATURE

<u>VOL. %</u>	<u>NORMAL-○-</u> <u>WET FEED</u>	<u>DRY FEED -△-</u>
H <sub>2</sub> S	0.6	0.6
SO <sub>2</sub>	0.3	0.3
H <sub>2</sub> O	6.0	0.0
OTHER	93.1	99.1

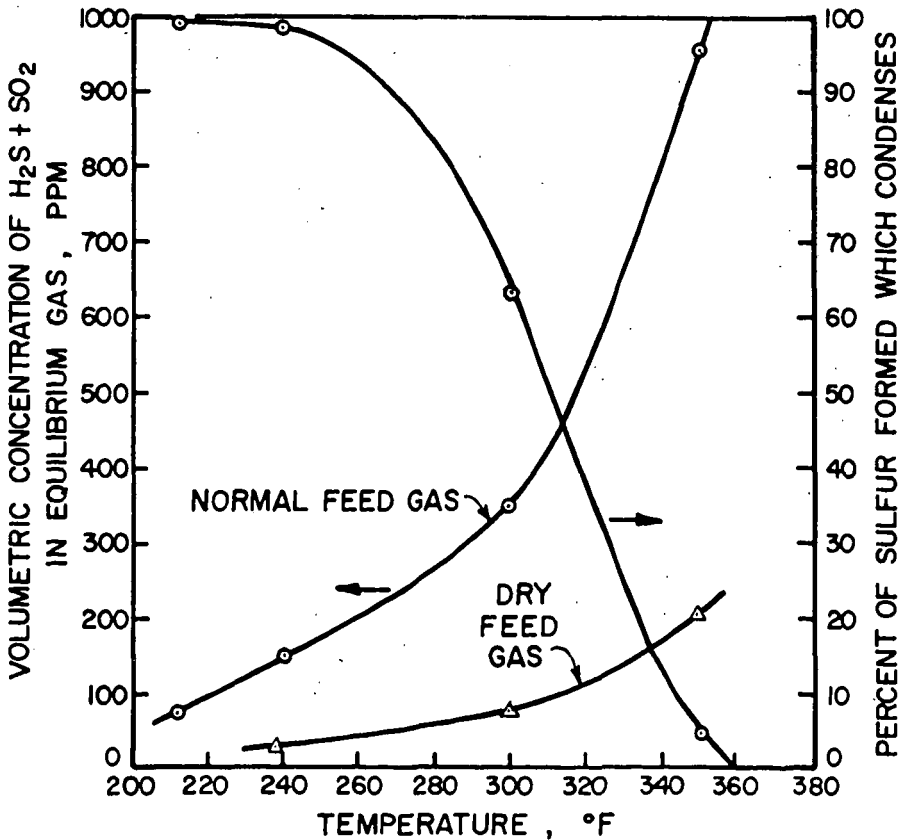


Figure 2

# EXPERIMENTAL APPARATUS

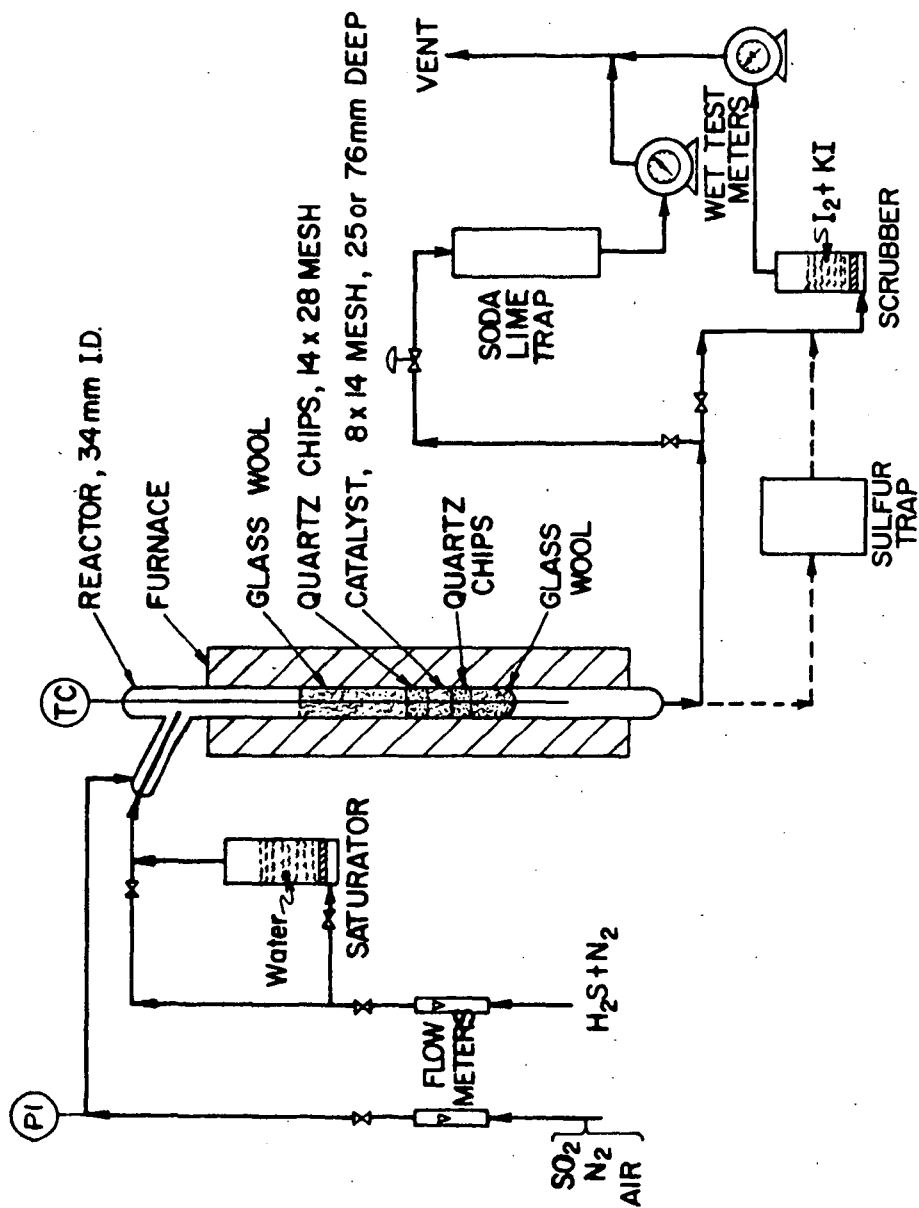


Figure 3

# THE EFFECTS OF OXYGEN AT 360°F

CONDITIONS: CATALYST H  
 TEMP. 360°F  
 VHSV 1500

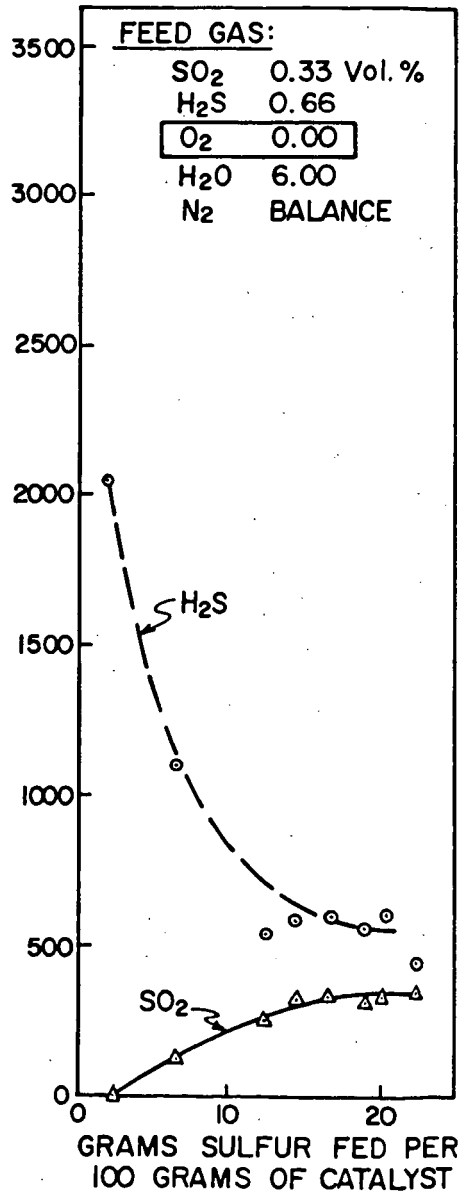
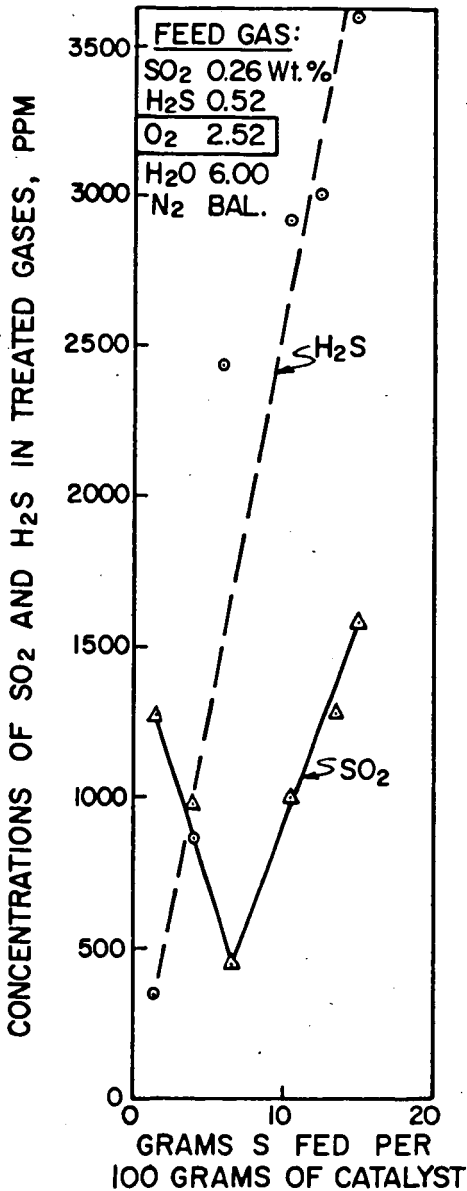


Figure 4

## DECREASE IN CATALYST ACTIVITY USING SINGLE-STAGE THERMAL REGENERATION

CONDITIONS:

CATALYST	H
REACTION TEMP.	212°F
VHSV	1425
REGENERATION IN N <sub>2</sub>	950°F

FEED GASES:

SO <sub>2</sub>	0.24 Vol. %
H <sub>2</sub> S	0.46
O <sub>2</sub>	2.01
H <sub>2</sub> O	6.00
N <sub>2</sub>	BALANCE

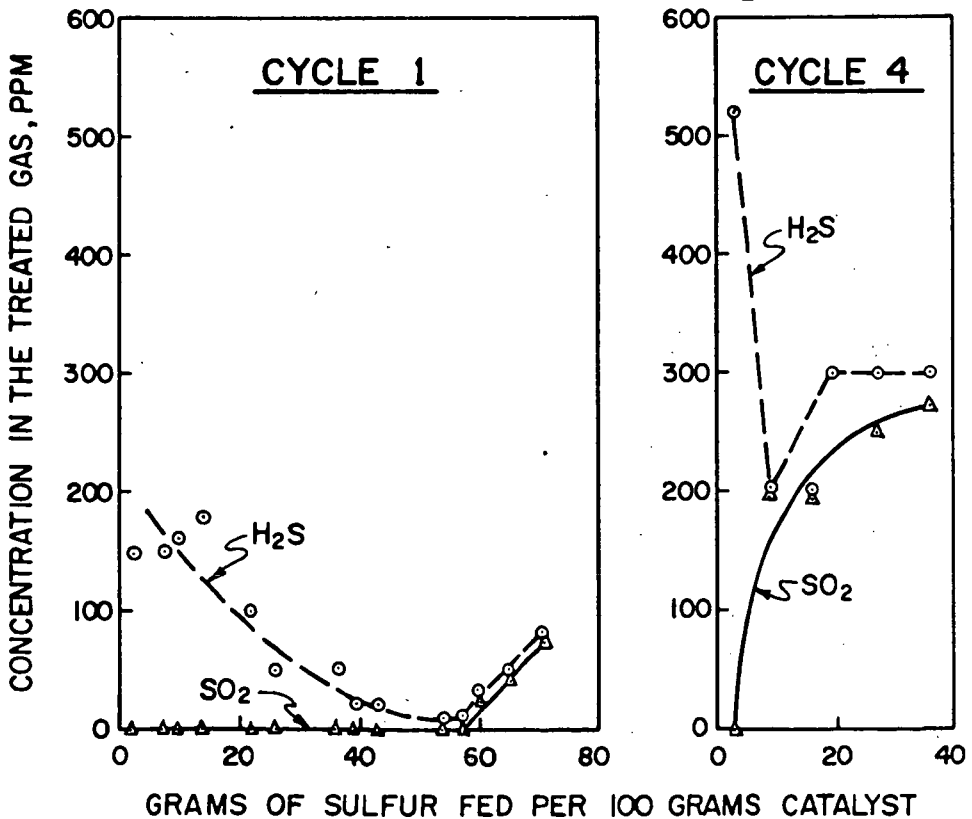


Figure 5

# CATALYST ACTIVITY USING THE CONSOL TWO-STAGE REGENERATION

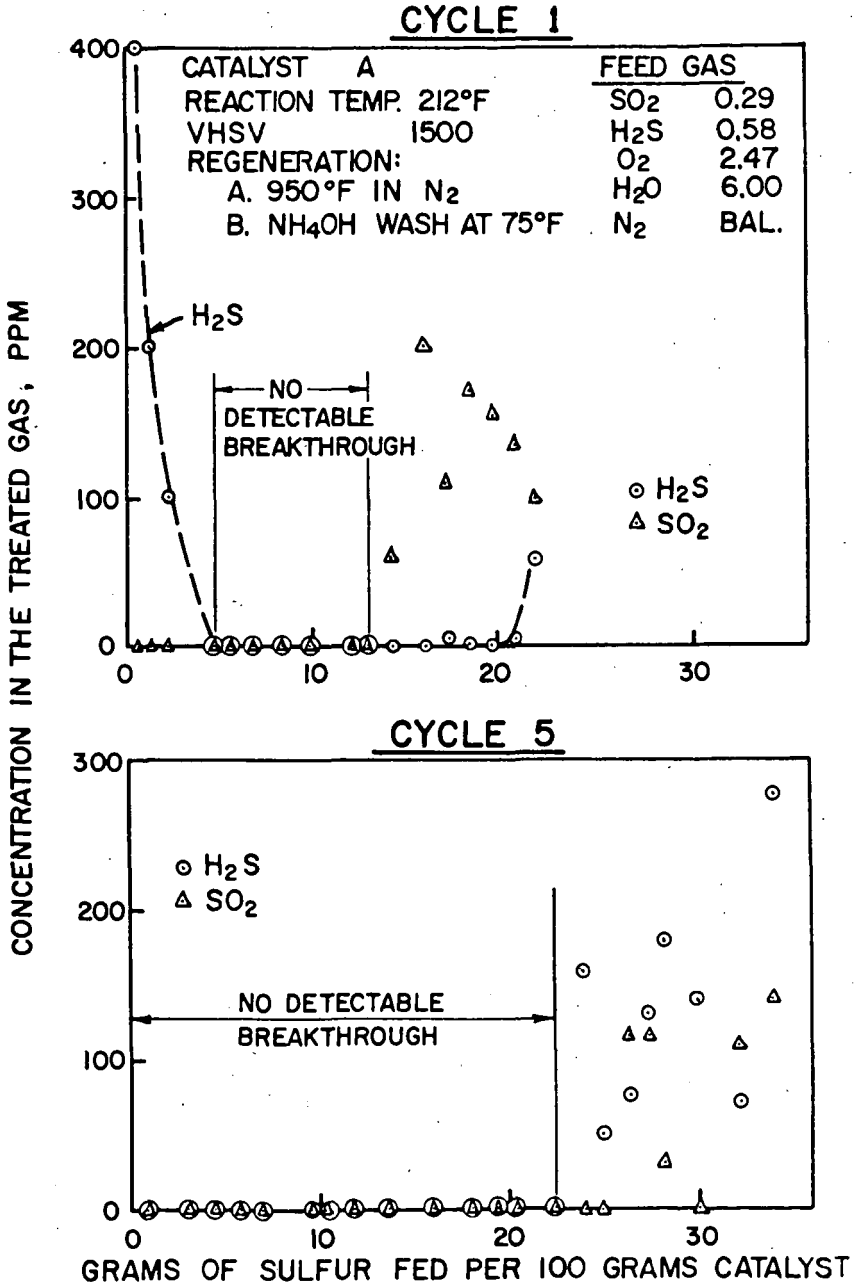
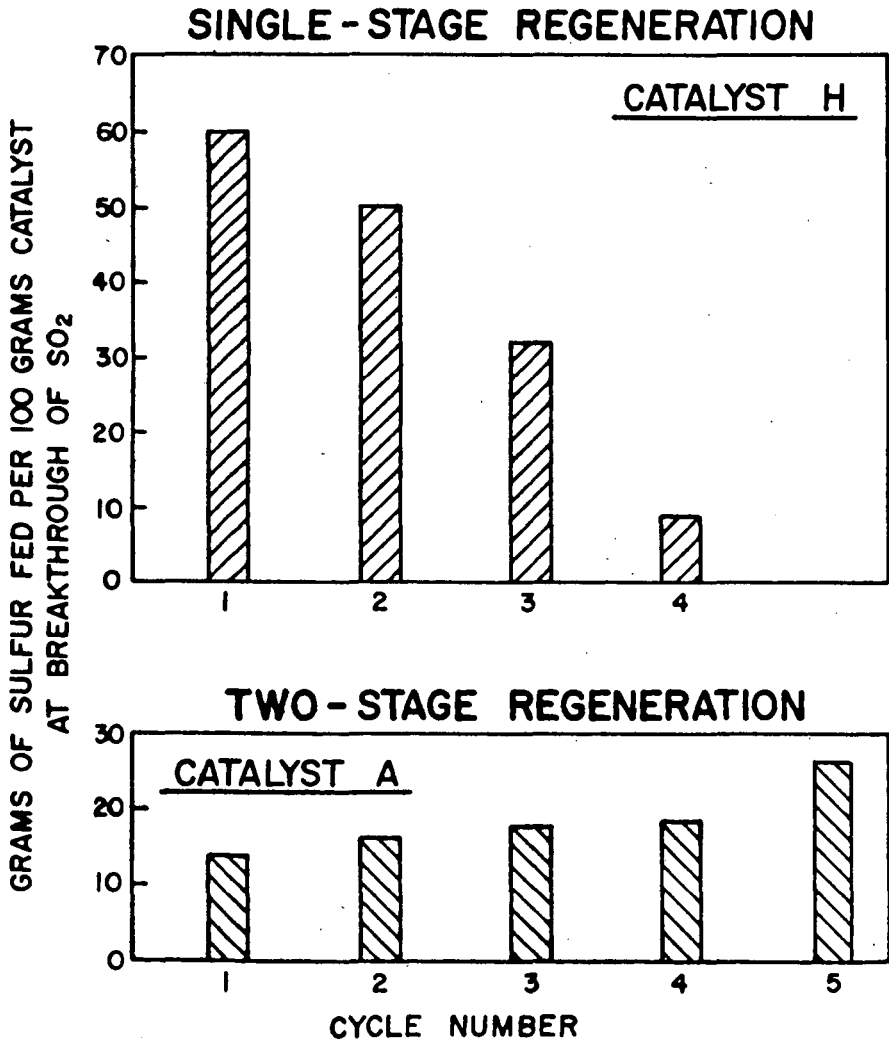


Figure 6AMOUNT OF STACK GAS FED PRIOR  
TO SULFUR DIOXIDE BREAKTHROUGH

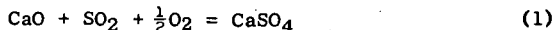
SULFUR REMOVAL DURING COMBUSTION OF  
SOLID FUELS IN A FLUIDIZED BED OF DOLOMITE

C. W. Zielke, H. E. Lebowitz, R. T. Struck, and E. Gorin

Research Division  
Consolidation Coal Company  
Library, Pennsylvania 15129

INTRODUCTION

The national concern over atmospheric pollution has led to extensive research and development on removal of sulfur oxide pollutants from flue gases. There has been considerable effort in this regard using limestone or dolomite to react with the sulfur oxides in dry, high-temperature processes. In these processes, SO<sub>2</sub> in the gases produced during combustion is fixed as CaSO<sub>4</sub> by reaction with CaO:



Usually the raw stone (dolomite or limestone) is fed to the process and calcination immediately takes place by the following reaction:



One method of operation has involved removal of sulfur oxides by direct injection of limestone dust above the burners of power plant boilers. A system such as this requires a minimum of new facilities and is readily adaptable to existing plants. However, the removal of sulfur in this case is carried out in a relatively inefficient and uncontrolled manner. Hence, utilization of limestone is poor and sulfur removal does not exceed 50 to 60%. An excellent article by the Tennessee Valley Authority reviews work done along this line. (1)

More efficient contact between gases and solid, as well as excellent temperature control, can be obtained by passing the combustion gases through a fluidized bed of lime or dolomite. The research reported here was aimed at the ultimate combination along this line: combustion of the fuel within a fluidized bed of lime or dolomite, which, in addition to pollution control, has great potential for reducing boiler size and cost by locating boiler tubes within the fluidized bed. (2,3,4,9)

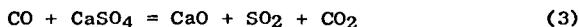
EXPERIMENTAL

The experimental unit consists of a continuous fluidized combustor, four inches in diameter, with a fluidized bed depth of 36 inches. The bed is supported on a perforated plate above a plenum chamber through which fluidizing gas is fed. Figure 1 shows the arrangement of equipment for feeding and recovering products. The combustor fits within an electric furnace for startup, and thereafter, cooling is provided by an air flow between reactor and furnace. The cyclone to recover coal ash and dolomite fines is operated at 350°F, and the filter at 150 to 200°F. The dolomite overflowing the bed via the weir is substantially free of ash. Argon is used for purges to facilitate accurate analysis of off-gases. Operating pressure was 8 psig, the pressure required to force the gases through the recovery train and give adequate control. All runs were preceded by a line-out period at conditions involving at least 3 changes of bed inventory.

In addition to combustion studies under various conditions with once-through use of dolomite, the re-use of dolomite was explored using 6½ cycles of alternate regeneration and SO<sub>2</sub>-absorption.

The SO<sub>2</sub> absorption runs were conducted in a manner similar to the normal combustion runs except that SO<sub>2</sub> gas was added with the fluidizing air as a major source of sulfur; coal was burned to supply heat and supply a minor amount of sulfur. The purpose of adding SO<sub>2</sub> was to produce large amounts of highly sulfated dolomite in a relatively short time. The activity of the regenerated product was measured in these runs by determining the CaO-to-S mol feed ratio required to produce a 20% sulfur breakthrough in the exit gas. The required ratio was reached by adjusting the amount of feed SO<sub>2</sub>; the dolomite residence time was held essentially constant in all cycles. When the desired Ca-to-S ratio was reached, conditions were maintained constant and the usual line-out and balance were made.

The regeneration portion of each cycle was conducted at 1950°F with CO as the reducing gas according to the overall reaction



No solid fuel was used in the regeneration runs. However, excess CO, over that required to carry out the reduction reaction, was burned with air to supply the heat. The gas flows were first established with nitrogen being substituted for the CO carrier gas. A bed of dolomite was established with the bed held at about 1400°F. Sufficient CO was then substituted in place of an equal amount of N<sub>2</sub> such that the bed was heated to 1925°F under a slightly oxidizing atmosphere. The remaining CO was then introduced, the used dolomite feed restarted and the unit lined out at 1950°F. Frequent analyses of the off-gas were made by gas chromatography to determine the CO/CO<sub>2</sub> ratio. Frequent analyses of the SO<sub>2</sub> content of the gas were made by determining the sulfate obtained in hydrogen peroxide scrubbers.

#### Feedstocks

The solid fuels tested in the combustor were Ireland Mine Coal, Disco Char, and Cresap Char. Analyses of these feeds are given in Table I. Ireland mine coal is a highly caking, high volatile, bituminous coal from the Pittsburgh seam. It is typical of the product sold to power stations. Both chars are from low temperature carbonization processes. The Disco char was produced in a rotary kiln from a Pittsburgh seam coal. The Cresap char was derived from Ireland mine coal. It was produced by fluidized low temperature carbonization of the residue remaining after solvent extraction of the coal in the "Project Gasoline" pilot plant operated by Consol for the U. S. Office of Coal Research at Cresap, West Virginia.

The dolomite used is from the Tymochtee formation in western Ohio. This stone was chosen because it had shown good physical strength and good resistance to chemical deactivation in CO<sub>2</sub> acceptor gasification studies.<sup>(6)</sup> Its analyses are given in Table II. The dolomite typically contained 0.05 to 0.10 weight percent moisture as it was fed to the unit.

### RESULTS AND DISCUSSION

#### A. Runs Using Dolomite On a Once-Through Basis

Table III gives results using Disco char and Cresap char. Disco char was used in the initial runs because it is non-caking, thus precluding the possibility of operability problems due to coking. Cresap char was of interest because of its unusually high sulfur and ash content. Table IV gives results with Ireland coal. Superficial velocity is defined as the velocity of the air feed at process conditions based on the empty reactor. Superficial residence time is based on the superficial velocity and fluidized bed depth. Stoichiometric air is defined as that required to completely burn carbon to CO<sub>2</sub>, hydrogen to water, and sulfur to SO<sub>2</sub>.

## 1. Sulfur Removal

Runs 1 through 4 of Table III using Disco char explored the effect of temperature in the range of 1700-1900°F and the effect of residence times of one and two seconds. A large excess of acceptor was used in these runs (Ca/S mol feed ratio of 7.3 to 8.3) while holding the air input substantially constant at 120±5% of stoichiometric. Neither the temperature nor time variation had a significant effect on sulfur absorption which was nearly complete in all runs.

Runs 5 and 6 of Table III with Cresap char and Runs 7 through 10 of Table IV with Ireland coal explored the effect of Ca/S mol feed ratio at a constant temperature of 1800°F, one second gas residence time, and about 120% of stoichiometric air. Figure 2 shows the sulfur removal data for these runs plotted as a function of Ca/S mol feed ratio. Sulfur removal efficiency appears to be independent of the feed sulfur concentration which indicates the absorption reaction is first order with respect to SO<sub>2</sub> at a given Ca/S ratio. There is further evidence of this in the life study data which will be discussed later. Therefore, the data with Disco char were also plotted on Figure 2, although its sulfur content was lower than either the Cresap char or Ireland coal. It is apparent from Figure 2 that a desulfurization efficiency exceeding 90% can be achieved at Ca-to-S ratios of 2 or higher; at a Ca-to-S ratio of 1.0, sulfur removal efficiency was about 78%.

In general, these results with low Ca-to-S ratios (1.0 to 1.5) are superior to those reported in the literature by others for such a coarse dolomite (16 x 28 mesh). In scrubbing SO<sub>2</sub> from flue gases in a fluidized bed of dolomite at 1600°F, Skopp<sup>(4)</sup> found that a high CaO utilization of 75% or more required that the dolomite size be finer than 100 mesh; his results indicate CaO utilization of only 50% or less with 16 x 28 mesh material. Williams, of the National Coal Board of England, ground his limestone to -120 mesh before he got close to 100% sulfur removal at 1.5 Ca-to-S mol ratio. These results are some of the best reported.

Possible reasons for the superior results of this work would be the type of stone, the rapid, but controlled high temperature calcination, sufficient residence time, and good contacting of gas with the absorbent. The importance of good contact and good dispersion can be seen by comparing Run 7 of Table IV with Run 11. The baffle mounted above the feed port, shown in Figure 1, was employed in Run 11 but not in Run 7. With the baffle in place, 93.6% sulfur removal was achieved, but without it, only 66.5% sulfur removal was achieved.

Most workers blame the poor CaO utilization using coarse acceptor on an impervious shell of CaSO<sub>4</sub> which acts as a diffusion barrier preventing utilization of most of the CaO. Our results indicate that, under some conditions, the shell can be permeated reasonably well. For example, with 77% CaO utilization, penetration is at least 39% of the radius assuming spherical particles.

In all of this work, only the CaO fraction of the dolomite has been assumed to be active as a sulfur acceptor; the MgO has been assumed to have no ability for SO<sub>2</sub> removal because of equilibrium limitations.

## 2. Carbon Burnout

Carbon burnout efficiency at 1800°F with one second residence time using coal feed was 97%, as the data of Table IV show. The chars were somewhat less reactive, as would be expected. At conditions similar to the coal runs, Cresap char burnout was 93-94% (Runs 5 and 6 of Table III) and Disco char burnout was 94% (Run 3 of Table III). Increasing the temperature from 1800 to 1900°F, or increasing the residence time from one to two seconds at 1800°F, raised the burnout of Disco char from 94 to 98 or 97%, respectively.

### 3. Dolomite Fines Formation

A substantial amount of the feed dolomite is degraded to fines under some conditions. These fines are elutriated from the bed along with the large majority of the ash and unburned carbon. Figure 3 shows the rate of fines formation as a function of the Ca-to-S ratio in the bed. The ordinate of Figure 3 is defined as follows:

$$\text{Attrition Rate \% / hr} = \frac{\text{lbs(Ca + Mg) in Overhead Fines from Dolomite} \times 100}{\text{lbs(Ca + Mg) in Dolomite Feed} \times \text{Dolomite Res. Time in hrs.}}$$

It is apparent that the highly sulfated dolomite is much more resistant to size degradation than the lightly sulfated dolomite. At low Ca-to-S ratios, the rate of degradation is very low, that is, about 0.5% per hour. The rate of fines formation is also much higher using coal feed than with char feed for some unknown reason. Perhaps the higher reactivity of the coal causes greater thermal stresses in the particles.

### 4. Nitrogen Oxides in the Gases

The nitrogen oxides content of the gases vary considerably from run to run, i.e., 60 to 340 ppm. There is no apparent pattern to the variation. Perhaps this is due to variation in the rate of quenching of the off-gases which was not carefully controlled.

## B. Dolomite Life Study

Potentially, the amount of new acceptor required per ton of coal can be reduced substantially by regenerating the acceptor and recycling the used acceptor back to the combustion process. One advantage of combustion in a bed of coarse acceptor is that the ash and fines are separated naturally by elutriation during combustion leaving substantially pure acceptor for regeneration treatment. To help assess the possibilities of regeneration, a series of cyclical combustion-regeneration runs was made. Results of the combustion runs with sulfur absorption are given in Table V; results of the regeneration runs are given in Table VI.

### 1. Regeneration

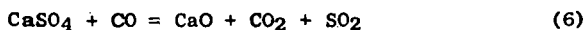
Regeneration comprises converting the  $\text{CaSO}_4$  in the acceptor to  $\text{CaO}$ . In the present work, this was done using  $\text{CO}$  as the reducing gas at  $1950^\circ\text{F}$ . It is first of all necessary to reduce a portion of the  $\text{CaSO}_4$  to  $\text{CaS}$  by the reaction



The ratio of  $\text{CO}_2$  to  $\text{CO}$  in the exit gas needs to be near that which corresponds to equilibrium for the above reaction so as to provide for the co-existence of  $\text{CaSO}_4$  and  $\text{CaS}$ . The concentration of  $\text{SO}_2$  in the off-gas from regeneration in cycle 1 was about 23 times greater than that in a flue gas from burning a 4% sulfur fuel, making its recovery much easier. Sulfur rejection then occurs by the reaction



The overall reaction can be represented by the equation



$$\Delta H = +59.2 \text{ Kcal/mol}$$

Since the overall reaction is endothermic, excess  $\text{CO}$  over that required to carry out the reduction of  $\text{CaSO}_4$  was burned to provide the heat to conduct the regeneration at

1950°F. At 1950°F and 1.5 atmospheric pressure, the equilibrium concentration of SO<sub>2</sub> in the gas is 12 mol %. This provided adequate driving force since the maximum concentration of SO<sub>2</sub> in the gases produced was 7.10%.

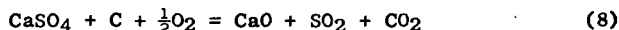
It was found that best results were obtained with the effluent gas slightly richer in CO than the equilibrium CO<sub>2</sub>-to-CO ratio of 46, i.e., 23 to 30. Higher or lower ratios gave lower sulfur rejection. When the appropriate CO<sub>2</sub>/CO ratio was established, rejection of 93% or more of the sulfur was achieved. In Runs 3 and 4, an erroneously low CO concentration was used and sulfur rejection was poorer.

A small amount of COS is produced as shown in the gas analyses. The concentration corresponds roughly to that at equilibrium for the reaction



$$K_p = \frac{(\text{COS})}{(\text{CO}_2)} = .00037 \text{ at } 1950^\circ\text{F}^{(6)}$$

In principle, the regeneration could be carried out in a similar fashion in a single stage by burning coal or char with a deficiency of air according to the overall equation



Fusion of ash, of course, may be a problem if the reaction is to be carried out at 1900°F or more since the ash fusion temperature is lowered under the reducing conditions necessary to carry out the sulfur rejection.

## 2. Sulfation

The results of the sulfation (SO<sub>2</sub> absorption) runs are given in Table V. These runs were conducted in much the same way as the once-through combustion runs except that SO<sub>2</sub> gas was added in order to rapidly produce large amounts of treated dolomite for the cyclical life study. The SO<sub>2</sub> content of the gas was adjusted to give 20% breakthrough of sulfur in the gas, i.e., 80% absorption. The Ca/S ratio obtained then was the measure of dolomite activity. It is apparent from the results that ~80% absorption was obtained in all cycles. In cycle 1, with fresh dolomite, a 0.95 Ca/S mol feed ratio gave 79% sulfur absorption. This point falls approximately on the curve of Figure 2, again showing that the absorption reaction is first order.

The acceptor activity as listed is based only on the CaO in the feed and not the CaSO<sub>4</sub> since, in cycles 3 and 4, regeneration wasn't as complete as desired.

## 3. Dolomite Life

The activity, *a*, of the dolomite sulfur-acceptor from cycle to cycle was measured as the fraction of available calcium which would absorb sulfur while maintaining 20% breakthrough of SO<sub>2</sub>. This is calculated from the spent acceptor analysis on a mol basis: CaSO<sub>4</sub>/(CaO + CaSO<sub>4</sub>). Figure 4 shows how the capacity (activity) of the dolomite decreased with the number of cycles, *n*, of absorption and regeneration.

Using the composite activity for a perfectly-mixed bed as described by Curran,<sup>(6)</sup> the effect of recycling dolomite has been calculated as a function of the rate of recirculation. Figure 5 shows this relationship. The ordinate of Figure 5 is the ratio of the pounds of fresh dolomite feed in the once-through process to that in the regenerative process, with the amount and efficiency of sulfur dioxide pick-up held constant. By going to high recirculation rates of regenerated acceptor, the makeup rate of fresh acceptor can be kept quite low.

Fresh dolomite makeup rate is usually controlled by activity loss since decrepitation loss is generally small. Total loss as fines overhead in 6 $\frac{1}{2}$  cycles was 9.43% or about 1.5% per cycle. The average rate of decrepitation was 0.39%/hr during regeneration and 0.67%/hr during combustion. Discarding the attrition results from cycles 3 and 4, which look erroneously high, the rate during combustion was 0.42%/hr. Thus, it is apparent that makeup requirements due to attrition are probably not more than 1%/cycle.

#### COMMERCIAL IMPLICATIONS

The results of this work suggest two basic processes: 1) a process where dolomite is used on a once-through basis and discarded, or 2) a process in which the dolomite is regenerated and reused. The first process would require at least 0.25 ton of dolomite/ton of coal feed of 4% S. The second process could require 0.05 ton or less of dolomite per ton of coal feed. The cost of regeneration could be partially offset by recovering elementary sulfur from the sulfur-rich regeneration off-gas. If a relatively pure limestone could be found that has the same activity as the dolomite, the stone requirements could be cut substantially because of the greater CaO content in a limestone as compared with a dolomite.

#### REFERENCES

- (1) "Sulfur Oxide Removal from Power Plant Stack Gas", PB-178972, Tennessee Valley Authority, 1968.
- (2) Bishop, J.W., Robinson, E.B., Ehrlich, Shelton, Jain, A.K., Chen, P.M., "Status of the Direct Contact Heat Transferring Fluidized Bed Boiler", ASME Publication 68-WA/FU-4, 1968.
- (3) Moss, G., Paper presented at the "First International Conference on Fluidized Bed Combustion" at Hueston Woods State Park, Oxford, Ohio, Nov. 18-22, 1968.
- (4) Skopp, A.P., Work published in the "Proceedings of the First International Conference on Fluidized Bed Combustion" at Hueston Woods State Park, Oxford, Ohio, Nov. 18-22, 1968.
- (5) Kruel, M., and Juntgen, H., *Chemie-Ingenieur-Technik* 39, No. 9/10, 607, 1967.
- (6) Curran, G.P., Fink, C.E., and Gorin, E., Fuel Gasification, Advances in Chemistry Series, 69, 141, 1967.
- (7) Barney, J.C. and Bertolacini, Anal. Chem., 29, 283, 1957.
- (8) Standard Methods for the Examination of Water and Waste Water; American Public Health Association, Inc., 11th ed. 175, 1960.
- (9) Williams, D.F., Work published in the "Proceedings of the First International Conference on Fluidized Combustion" at Hueston Woods State Park, Oxford, Ohio, Nov. 18-22, 1968.
- (10) Zawadski, J., *Ztschr. Anorg. Chem.*, 205, 180, 1932.
- (11) Marchal, G., *Compt. rend.*, 175, 270, 1922.

TABLE I

ANALYSES OF CHAR AND COAL FEEDS

	<u>Disco Char</u>	<u>Cresap Char</u>	<u>Ireland Coal</u>
Moisture, Wt.%	3.65	1.15	1.30
<u>Proximate Analysis, Dry Basis, Wt.%</u>			
Volatile Matter	20.77	14.34	39.84
Fixed Carbon	66.24	60.99	52.60
Ash (Ex. mineral sulfur)	12.99	24.67	12.67
<u>Elemental Analysis, Dry Basis, Wt.%</u>			
H	3.28	1.65	4.81
C	70.81	63.08	69.25
N	1.42	1.55	1.37
O (Diff.)	10.53	4.60	8.94
S	1.72	6.20	4.15
Btu/lb MF Fuel, Net	11845	10350	12840
<u>Ash Fusion Temp., °F (Oxid. Atm.)</u>			
Initial Deformation	2040	1920	1950
Softening	2120	2020	2020
Hemispheric	2270	2200	2140
Fluid	2360	2360	2320
Screen Size, Tyler Mesh	28 x 150	28 x 200	28 x 150

TABLE IIANALYSIS OF TYMOCHTEE FEED DOLOMITE

	<u>Weight, %</u>
CaO	27.93
MgO	18.56
Fe <sub>2</sub> O <sub>3</sub>	.41
SiO <sub>2</sub>	1.40
Al <sub>2</sub> O <sub>3</sub>	1.64
CO <sub>2</sub>	44.87
Unaccounted for	5.19

SCREEN ANALYSIS, TYLER MESH

On 14	0
16	1.0
20	39.1
24	33.9
28	24.7
35	1.2
-35	0.1

Raw dry stone/fully calcined stone, wt. ratio = 1.814

Ca/Mg, mol ratio - 1.08

TABLE III

RESULTS WITH CHAR FEEDSTOCKS  
AND ONCE-THROUGH DOLOMITE

Acceptor: 16 x 28 mesh raw Tymochtee  
           dolomite  
 Inlet Gas: 100% air  
 Pressure: 8 psig.

Run No.	1	2	3	4	5	6
Fuel	← Disco Char →				← Cresap Char →	
Bed Temperature, °F	1700	1800	1800	1900	1800	1800
Ca/S mol feed ratio	7.3	7.9	8.3	8.0	4.2	2.0
Superficial velocity, fps	1.5	1.5	← 3.0 →			
Stoichiometric air, %	116	118	120	121	125	118
Fuel feed rate, lb/hr	1.27	1.19	2.34	2.23	2.46	2.62
Raw dolomite feed rate, lb/hr	1.00	1.01	2.09	1.90	4.05	1.99
Run length, hr.	.30	.28	.32	.29	.38	.33
Gas residence time, sec.	2.0	2.0	← 1.0 →			

Results

Feed sulfur removed, %	100.0	97.9	98.2	99.0	94.5	90.7
Sulfur in effluent acceptor, Wt. %	3.12	2.70	2.51	3.39	5.27	9.40
Carbon burnout, %	95.8	98.3	94.4	97.1	93.8	93.2
Lb. dust overhead/lb. fuel fed	0.165	0.159	0.284	0.267	0.304	0.278
Dolomite overhead as dust, %	7.3	9.4	23.6	24.5	3.8	1.8

Dry Exit Gas, Mol %

CO <sub>2</sub>	16.3	16.8	19.2	20.6	16.5	16.1
CO	0.00	0.00	0.00	0.00	0.01	0.01
O <sub>2</sub>	4.1	3.7	5.0	4.1	5.2	4.7
N <sub>2</sub> + A	79.6	79.5	75.8	75.3	78.3	79.1
SO <sub>2</sub>	0.0000	0.0031	0.0026	0.0015	0.0290	0.0536
NO <sub>x</sub>	0.024	0.027	0.013	0.027	0.0060	0.0103

TABLE IVRESULTS WITH COAL FEEDSTOCKS  
AND ONCE-THROUGH DOLOMITE

Acceptor:	16 x 28 mesh raw Tymochtee dolomite
Inlet Gas	100% air
Pressure, psig	8.0
Superficial velocity, fps	3.0
Temperature, °F	1800
Superficial gas residence time, sec.	1.0

Run No.	<u>7</u>	<u>8</u>	<u>9</u>	<u>10</u>	<u>11</u>
Ca/S, mol feed ratio	4.03	1.89	1.45	.95	3.68
Stoichiometric air, %	122	115	119	120	120
Coal feed rate, lb/hr	2.15	2.27	2.20	2.18	2.19
Raw dolomite feed rate, lb/hr	2.25	.94	.70	.46	2.09
Run length, hr	36	53	85	113	38

Results

Feed sulfur removed, %	93.6	88.5	87.0	74.1	66.5
Sulfur in effluent acceptor, wt. %	5.00	8.62	10.93	12.59	2.99
Carbon burnout, %	97.5	96.7	96.9	97.1	97.5
Lb total dust overhead/lb feed coal	.254	.162	.157	.136	.258
Dolomite overhead as dust, %	20.9	21.6	14.7	11.4	17.6

Dry Exit Gas, Mol %

CO <sub>2</sub>	15.5	14.8	13.9	14.2	14.8
CO	.02	.01	.00	.00	.08
O <sub>2</sub>	4.3	4.0	4.7	4.6	4.3
N <sub>2</sub> + A	80.2	81.2	81.4	81.1	80.7
SO <sub>2</sub>	.0205	.0334	.0370	.0726	.110
NO <sub>x</sub>	.0116	.0044	.0152	.0090	.034

TABLE V

CONDITIONS AND RESULTS  
OF COMBUSTION RUNS WITH SO<sub>2</sub> ABSORPTION  
IN DOLOMITE LIFE STUDY

---

Bed temperature, °F	1800
Pressure, psig	8
Fuel	-28 mesh Ireland coal
Fuel feed rate, lb/hr	1.79
Dolomite feed	To first cycle: raw, 16 x 28 mesh To succeeding cycles: regenerated material from previous cycle
Superficial inlet gas velocity, fps	3.0
Superficial gas residence time, sec.	1.0
Nominal percent of stoichiometric air	120

<u>Cycle Number</u>	<u>1</u>	<u>2</u>	<u>3</u>	<u>4</u>	<u>5</u>	<u>6</u>	<u>7</u>
Dolomite feed rate, lb/hr	10.2	5.8	5.7	6.0	6.0	5.7	5.6
Dolomite residence time, hr	1.09	1.15	1.14	1.11	1.25	1.21	1.11
<u>Inlet gas composition</u>							
Air, SCFH				3.34			
SO <sub>2</sub> , lb/hr	3.29	2.19	1.56	1.56	1.24	1.26	1.08
CaO/S mol feed ratio	.953	1.38	1.86	1.86	2.25	2.27	2.62

Results

Feed S absorbed, %	79.3	80.4	80.2	78.7	77.6	79.3	80.6
S in effluent acceptor, Wt. %	14.27	11.41	9.02	9.70	8.43	7.64	7.13
Carbon burnout, %	97.1	97.5	96.4	97.1	96.4	96.4	97.0
Acceptor activity, CaSO <sub>4</sub> /(CaO + CaSO <sub>4</sub> )	.770	.540	.382	.400	.306	.313	.284
Feed dolomite overhead as dust, %	1.02	.71	1.50	1.42	.25	.25	.21

Dry Exit Gas, Mol%

CO <sub>2</sub>	18.4	12.6	12.7	12.5	12.2	12.3	13.1
CO	0.40	.16	.29	.35	.10	.14	.18
O <sub>2</sub>	4.4	5.0	5.6	5.7	5.9	5.8	5.2
N <sub>2</sub> + A	75.7	81.2	81.1	80.9	81.2	81.2	81.1
SO <sub>2</sub>	1.21	.89	.66	.70	.61	.57	.44

Balance Closures

Mass	96.7	97.2	97.2	96.6	97.2	96.6	98.4
S	95.5	94.3	92.0	91.1	93.3	95.6	96.2
CaO	109.0	100.0	102.5	103.2	116.6	104.7	109.5

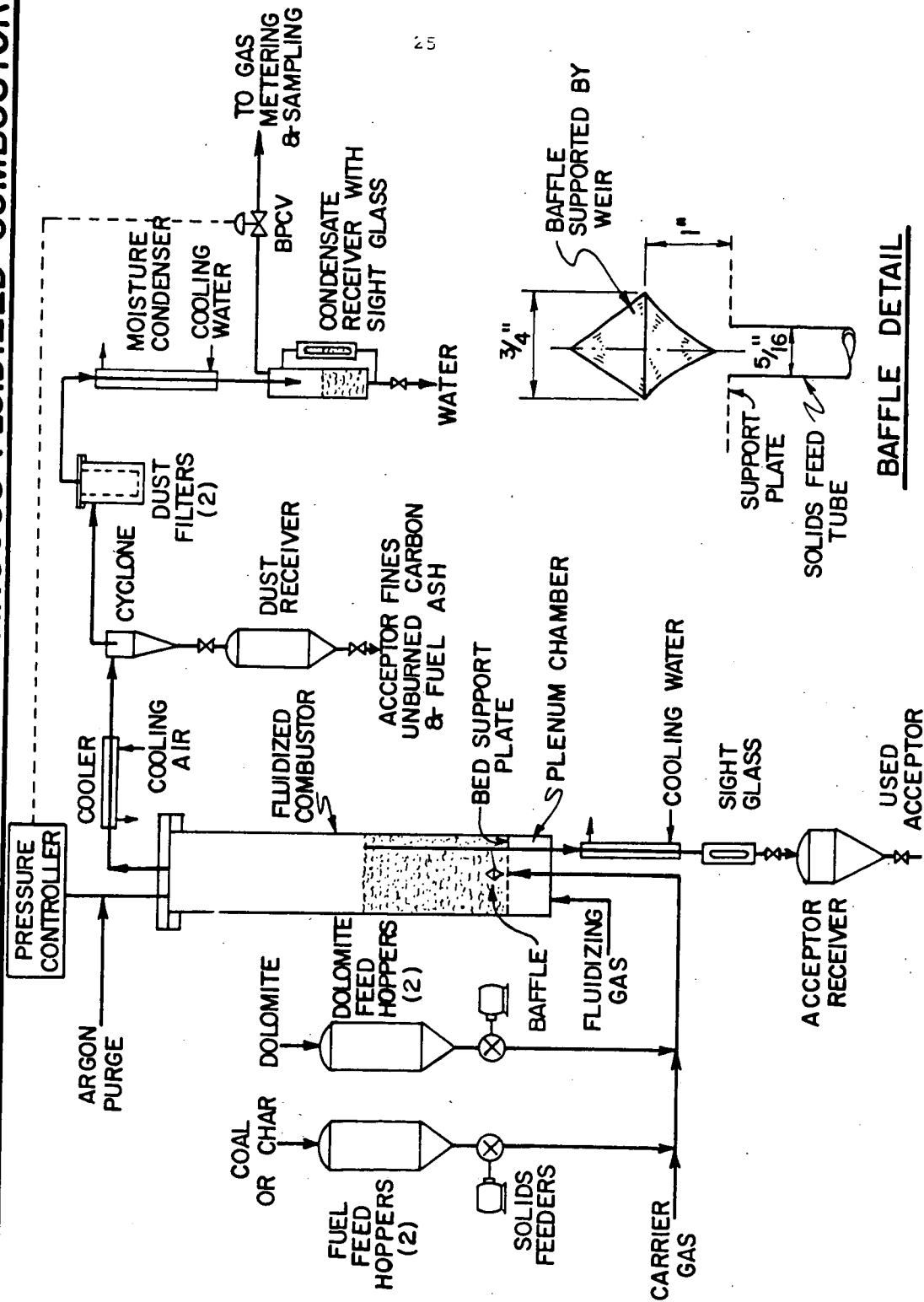
TABLE VI

CONDITIONS AND RESULTS  
OF REGENERATION RUNS  
IN DOLOMITE LIFE STUDY

Bed temperature, °F	1950					
Pressure, psig	8					
Superficial inlet gas velocity, fps	2					
Superficial gas residence time, sec.	1.5					
<u>Cycle Number</u>	<u>1</u>	<u>2</u>	<u>3</u>	<u>4</u>	<u>5</u>	<u>6</u>
Spent dolomite feed rate, lb/hr	8.82	8.20	7.23	6.83	6.98	7.12
Dolomite bed residence time, hr	1.62	1.70	1.78	1.79	1.83	1.78
<u>Inlet gas composition, mol %</u>						
Air	44.6	44.6	44.2	44.2	44.2	44.2
Added N <sub>2</sub>	30.3	31.6	34.3	35.2	34.0	33.9
CO	25.1	23.8	21.5	20.6	21.8	21.9
<u>Excess CO after combustion, mol ratio</u>						
Feed S	.98	.94	.75	.58	.97	1.08
<u>Results</u>						
Fraction of CaSO <sub>4</sub> converted to CaO	.966	.932	.816	.695	.932	.940
Sulfate S in effluent acceptor, Wt.%	.95	.68	2.28	3.53	.56	.51
Sulfide S in effluent acceptor, Wt.%	.03	.40	.00	.00	.20	.07
Feed dolomite overhead as dust, Wt.%	1.86	.75	.33	.25	.38	.50
<u>Dry Exit Gas, Mol %</u>						
CO <sub>2</sub>	23.4	22.2	20.5	19.9	20.9	21.0
CO	.78	.78	.56	.50	.91	.90
O <sub>2</sub>	.09	.13	.15	.42	.27	.33
N <sub>2</sub> + A	68.6	71.6	75.0	76.4	74.3	74.7
SO <sub>2</sub>	7.10	5.12	3.78	2.84	3.53	3.03
COS	.02	.03	.01	.01	.03	.03
<u>Balance Closures, (Out) (100)/In</u>						
Mass	98.1	98.8	99.9	100.1	96.3	101.2
S	104.4	97.5	108.9	105.3	102.2	98.5
CaO	97.6	91.6	100.2	95.0	95.3	99.0

# SIMPLIFIED FLOW DIAGRAM OF CONTINUOUS FLUIDIZED COMBUSTOR

FIGURE 1



BAFFLE DETAIL

FIGURE 2

SULFUR REMOVAL EFFICIENCY VS Ca/S MOL FEED RATIO

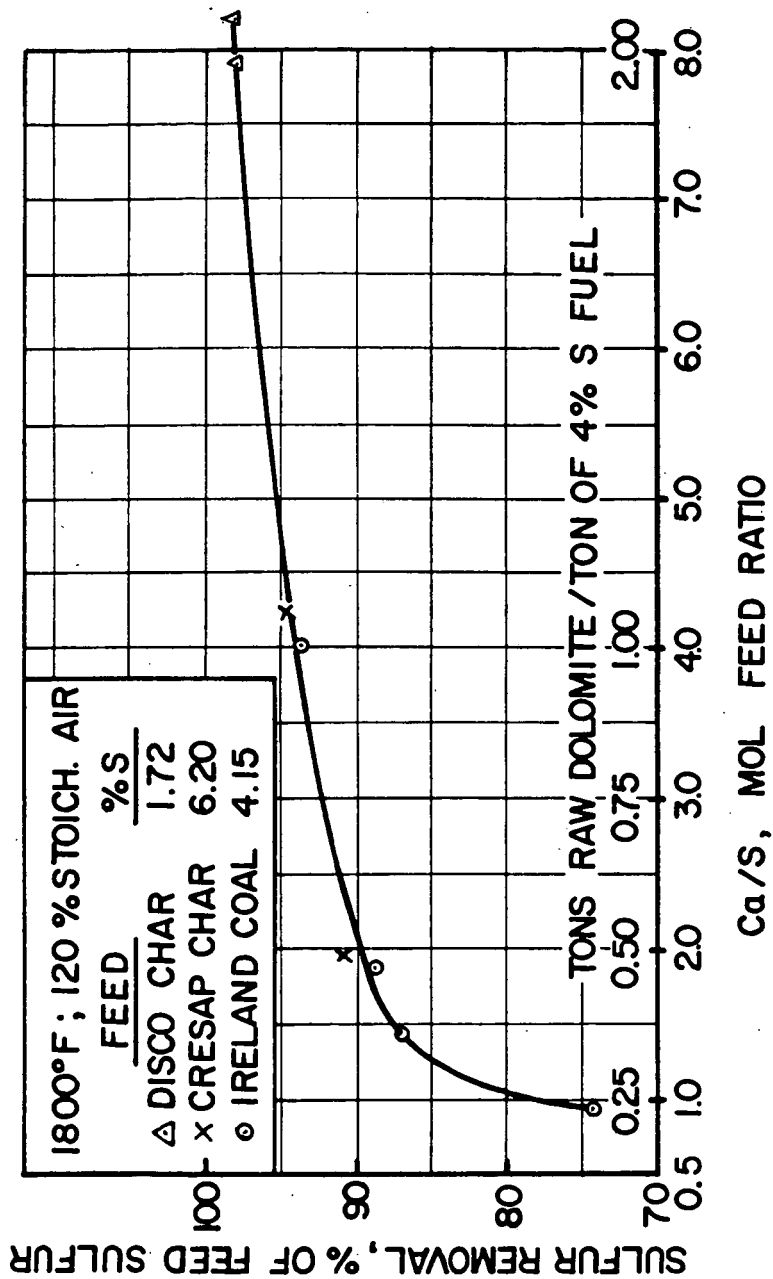


FIGURE 3

# DOLOMITE ATTRITION RATE vs SULFUR CONTENT OF EFFLUENT ACCEPTOR

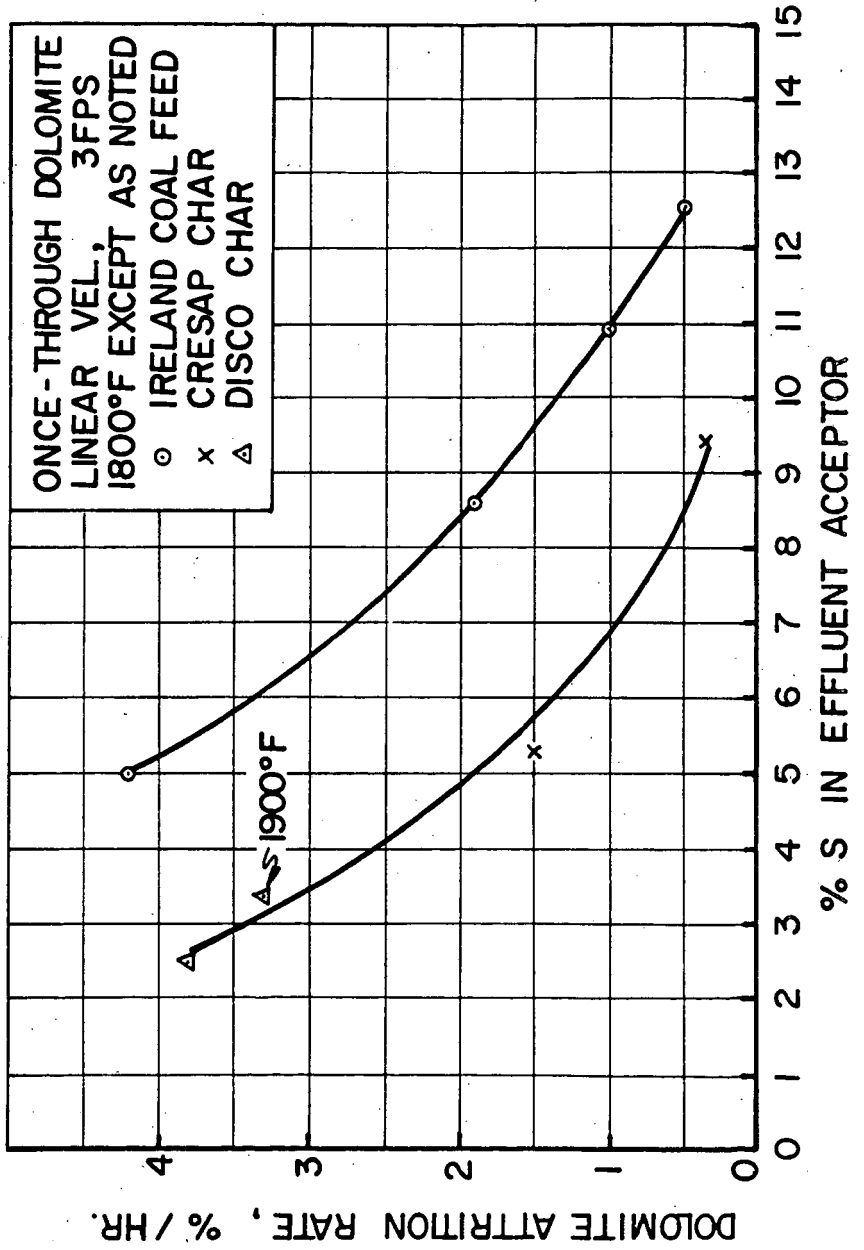


FIGURE 4  
ACTIVITY OF REGENERATED ACCEPTOR

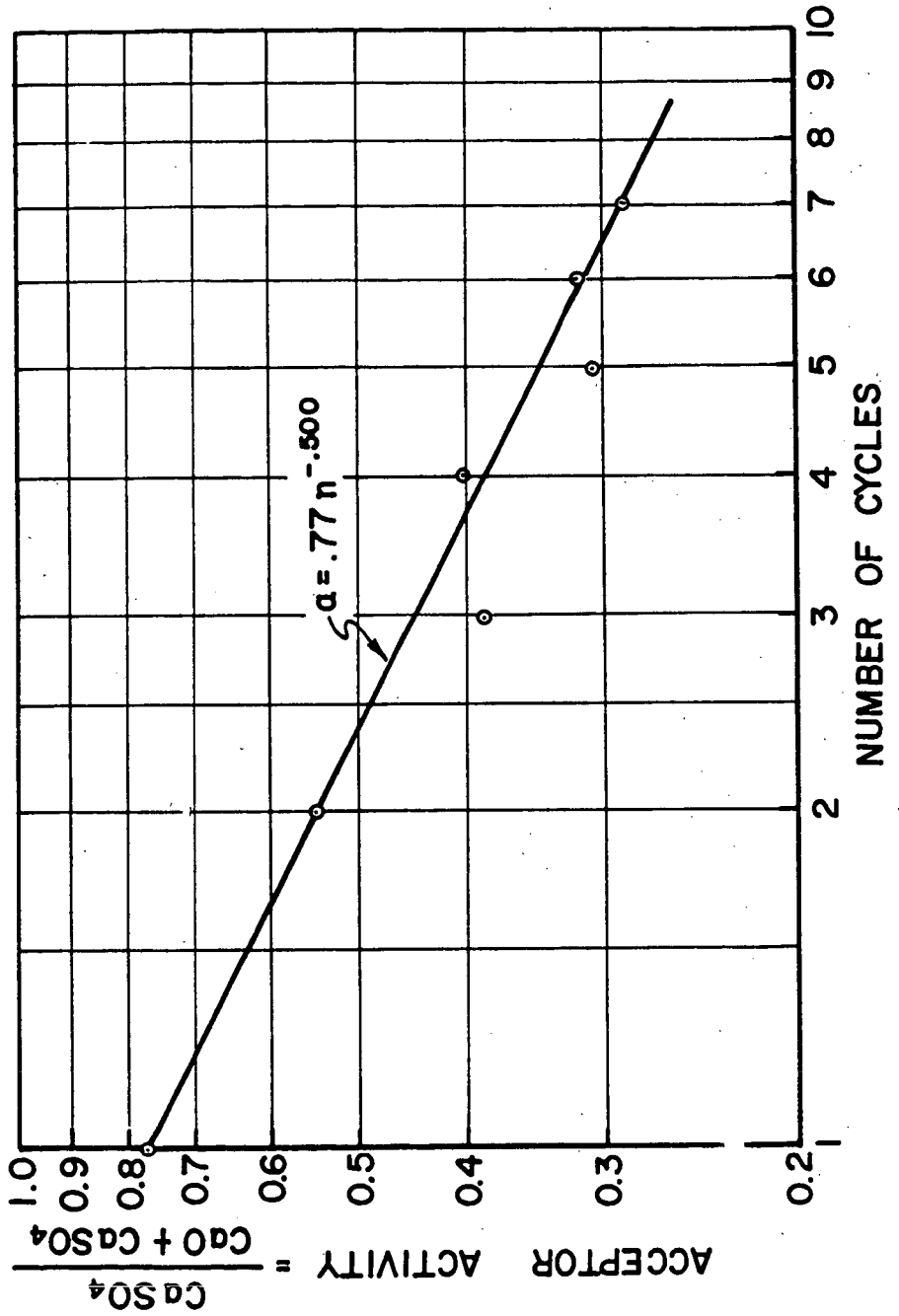
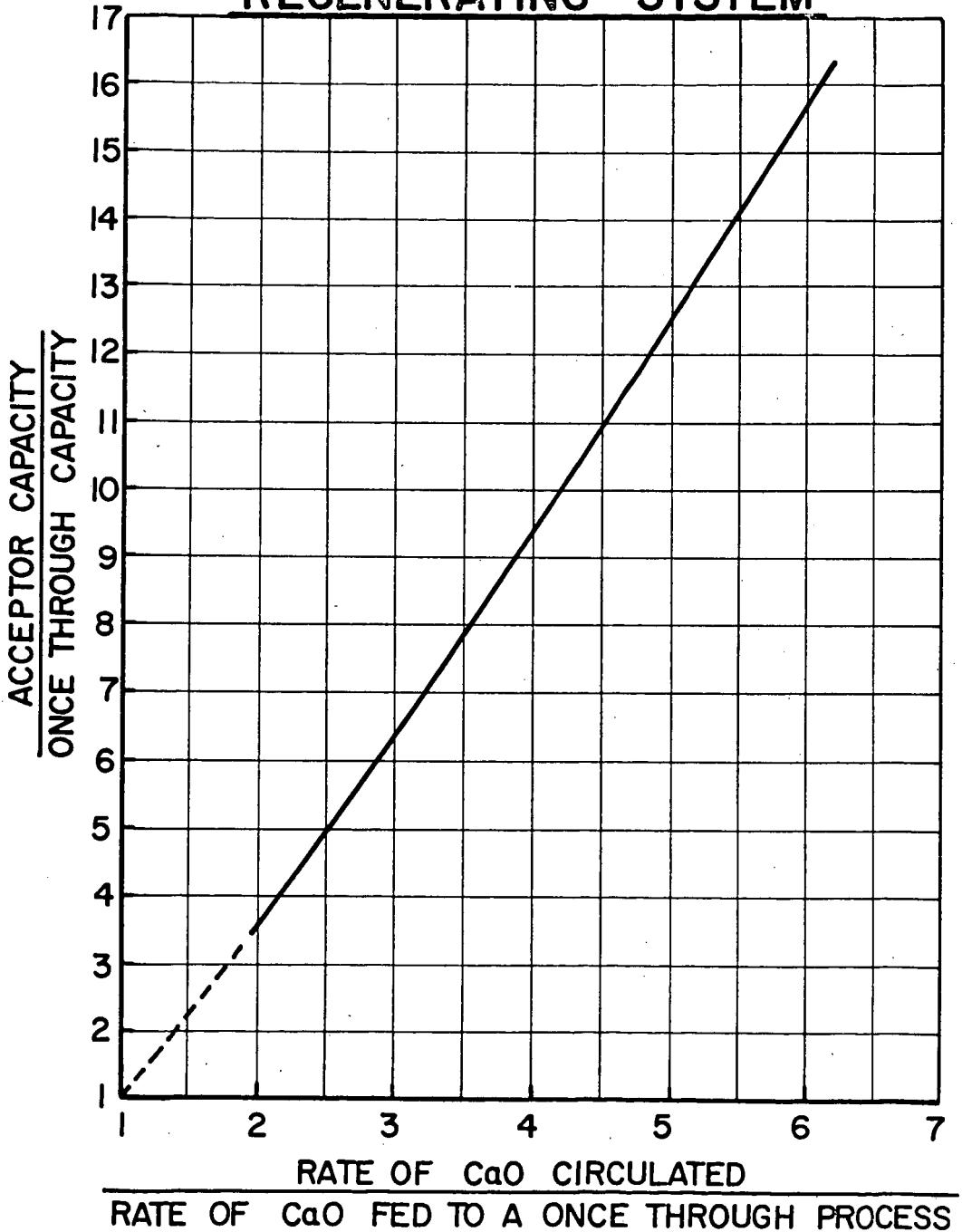


FIGURE 5ACCEPTOR LIFETIME IN A CONTINUOUS  
REGENERATING SYSTEM

## HYDROGEN SULFIDE REMOVAL FROM HOT PRODUCER GAS WITH SINTERED ABSORBENTS

Forrest G. Shultz and John S. Berber

U. S. Department of the Interior, Bureau of Mines,  
Morgantown Coal Research Center, Morgantown, W. Va. 26505

Gas producers have been receiving attention in recent years as a potential source of clean, pressurized gas for a variety of industrial purposes. Removal of  $H_2S$  (hydrogen sulfide) from the hot producer gas is of interest because hydrogen sulfide is an air pollutant, deteriorates equipment, and removal while still hot should be less costly.

Temperature of the producer gas to be treated for  $H_2S$  removal ranges from 1,000° to 1,500° F. To economically utilize the sensible heat of producer gas for power generation, the  $H_2S$  must be removed near the generation temperature of the gas. This precludes the use of liquid absorbents and limits the process to the use of solid absorbents that can react with  $H_2S$  at elevated temperatures. The material should also be regenerable for reuse through several cycles of  $H_2S$  absorption followed by air regeneration.

Literature on producer gas cleanup in the 1,000° to 1,500° F range is quite limited. Information is available on the desulfurization of industrial gases between 68° and 1,292° F with -16 + 100 mesh iron oxide, including data on static and fluidized beds between 617° and 752° F (3). Static beds were tested at a space velocity (gas volume per absorbent volume per hour) of 100 and fluidized beds at 3,000 vol/vol/hr. An absorption capacity of 30% by weight of sulfur per unit weight of absorbent was obtained at higher temperatures and  $H_2S$  removal efficiency was 95 to 99.9%. A full-scale operating plant was built with a capacity for treating 32 million cubic feet of coke oven gas per day (2). Iron oxide was the absorbent in a fluidized bed operating at 680° to 752° F. Although overall operation of the plant was satisfactory, troublesome accumulations of fine oxide dust reportedly were experienced in various parts of the plant.

This paper gives results of a Bureau of Mines investigation of prepared solids for their capacity to remove  $H_2S$  from hot producer gas. Solids utilized were (1) a sintered mixture of ferric oxide ( $Fe_2O_3$ ) plus fly ash; (2) pumice stone coated with fused ferric oxide ( $Fe_2O_3$ ); and (3) sintered pellets prepared from red and brown muds--aluminum refining residues that contain large amounts of  $Fe_2O_3$ .

### APPARATUS AND PROCEDURE

Bench-scale apparatus utilized in this study is shown in Figure 1. Gases from cylinders of nitrogen, hydrogen, hydrogen sulfide, carbon monoxide, and carbon dioxide were metered to form a stream of simulated producer gas devoid of ash and tars and containing approximately 1.5 volume percent  $H_2S$ . The percentage of other constituents is listed on the flowsheet (fig. 1).

Simulated producer gas was passed through a bed of the test absorbent contained in an electrically heated section of 1-inch diameter by 5-foot long, schedule 40 stainless-steel pipe. Alumina spheres in the bottom 22 inches of the pipe extended 10 inches into the hot zone of the furnace. These spheres supported the absorbent bed and preheated the gas. Regeneration facilities, shown in the center right portion of the flow sheet, consisted of an air supply with pressure regulator and flow meter. Purified producer gas and the regeneration gas were vented through a common system. Fifteen-inch depths of absorbent were subjected to a gas flow rate of 15 scfh (7.08 liters per minute), which is equal to a space velocity of 2,000. Hydrogen sulfide concentration in the simulated producer gas was controlled to equal 20.6 to 22.9 mg/l ( $\text{mg/l} \times 43.7 = \text{grams}/100 \text{ cu ft}$ ). Experiments were conducted at 1,000°, 1,250°, and 1,500° F. The runs were terminated when the H<sub>2</sub>S concentration in the effluent gas stream of the test bed, originally near zero, reached 2.3 mg/l. Sulfur capacities of the absorbent were calculated from the product of H<sub>2</sub>S concentration, flow rate, and time duration of the test.

### ANALYTICAL METHODS

Hydrogen sulfide concentration of the gas stream was determined by the Tutwiler method (1) and verified by chemical detection tubes and gas chromatography. Reasonable agreement was found between the different methods. Absorbent was regenerated by passing an air stream through the tube at 1,000° to 1,500° F. During the first several tests, SO<sub>2</sub> liberated during regeneration was absorbed in 2.5 N caustic soda solution, an aliquot was acidified with HCL, and titrated to a starch end point with iodine. The weight of sulfur regenerated was calculated and compared with the calculated weight of sulfur absorbed to determine the error in the sulfur balance. These balances usually checked within 20%. Part of this variance is explained by the fact that during regeneration some of the sulfur was evolved in elemental form and collected in the filter at the effluent end of the reaction tube, and thus was not measurable. Later, SO<sub>2</sub> concentrations were measured by means of impregnated silica gel detection tubes.

### ABSORBENTS

Several commercial absorbents were tested first, but they did not give satisfactory results, all of them disintegrating in the temperature range used. Included among these were chromium-promoted iron oxide, calcined pellets of dolomite, and alkalinized alumina pellets. Seeking more satisfactory absorbents, several other materials were prepared for investigation. The first material consisted of a mixture of fly ash (-4 + 6 mesh) from a bituminous coal-burning power plant (Table 1) and pure Fe<sub>2</sub>O<sub>3</sub>. Fly ash and oxide were thoroughly mixed, water was added, and pellets were formed and sintered at about 1,800° F. Tests were also made with sintered taconite and sintered (pure) Fe<sub>2</sub>O<sub>3</sub>.

The second prepared absorbent consisted of granular pumice stone (-4 + 8 mesh, Table 2) impregnated with 99+% pure Fe<sub>2</sub>O<sub>3</sub>. Pumice stone granules were coated with the oxide as follows: moistened granules were placed in a tumbler, dry oxide was added and the mixer was operated until a fairly uniform coating of the granules was observed. These were then heated at 1,500° F for 2 hours to bond the two materials. Some shrinkage occurred during the heating, but the

granules remained porous and the oxide adhered well to the pumice stone. Excessive shrinkage and loss of porosity occurred when the absorbent was heated at 1,900° F.

The third material consisted of red or brown mud residues from aluminum refining. They were received in powder or lump form, the latter being reduced to powder before use. The powder was moistened with enough water to form a putty-like material that was formed into 1/4-inch spheres, predried at 500° F, then heated at 2,000° F for 10 to 20 minutes to produce a hard pellet. Chemical analyses of the muds are given in Table 3.

### ABSORPTION TESTS

Results of tests with these materials are given in Table 4. The fly ash (75%) and  $\text{Fe}_2\text{O}_3$  (25%) formed a pellet with high sulfur-absorption capacity that did not disintegrate at the test conditions. Tests 1 through 10 give the absorptive capacity of this fly ash- $\text{Fe}_2\text{O}_3$  mixture through nine  $\text{H}_2\text{S}$  absorption-air regeneration cycles. The data show that there is no loss in absorptive capacity nor any attrition of the pellets. Absorbents with more than 37%  $\text{Fe}_2\text{O}_3$  were difficult to test because the pellets either disintegrated or the materials fused.

Compositions and results obtained with pumice stone coated with ferric oxide are listed in Table 5 and Figure 2. This material did not exhibit any tendency to disintegrate, and showed some tendency to fuse into larger particles.

Results obtained with the muds are listed in Table 6. Red mud No. 1 formed a very durable pellet and had the highest capacity of any material tested.

Figure 3 shows sulfur capacities of the materials that did not disintegrate or fuse and appeared suitable as  $\text{H}_2\text{S}$  absorbents.

### REGENERATION OF ABSORBENTS

During regeneration of absorbents, all at space velocities of 2,000 calculated at standard conditions (68° F and 1 atmosphere pressure), instantaneous  $\text{SO}_2$  concentrations were measured by chemical detection tubes. Error in the sulfur balance amounted to about 15% or less when the regeneration temperature was 1,000° or 1,250° F. When regeneration was attempted at 1,500° F, the material fused into a mass that could not be regenerated. About 1,000° appeared to be the optimum temperature for regeneration of these types of absorbents. Release of heat from the exothermic regeneration reaction is sufficient to increase the bed temperature about 400° F.

Complete regeneration of absorbents appears impractical; a few parts per million of  $\text{SO}_2$  were measurable even after 80 hours of regeneration. Regeneration proceeds at a high rate (6 to 10 volume percent  $\text{SO}_2$ ) for the first 30 to 50 minutes of regeneration, drops to about 1% by volume after 1 hour, then rapidly decreases and slowly approaches zero. Figure 4 is a plot of  $\text{SO}_2$  concentrations versus time for tests in which the absorption temperatures were 1,000°, 1,250°, and 1,500° F, and the regeneration temperature was 1,000° F. The weight of sulfur regenerated in any of these three tests during the first hour was at least 80% of the total that was regenerated. Tests 18 and 19 (Table 4) were conducted

with a regeneration temperature of 800° F. This temperature was adequate to rapidly regenerate the pellets of test 18 with a low sulfur content of 8.1 wt-pct, but did not achieve a fast regeneration in test 19 in which the pellets had a high sulfur content, 34%. Pellets with a low sulfur content (10% or less) appeared to regenerate more quickly than pellets with a sulfur content of 30% or more, indicating that regeneration should be started before the absorption capacity limit is attained.

## DISCUSSION

Mixtures of 75% fly ash-25%  $\text{Fe}_2\text{O}_3$  gave absorption capacities ranging from 8.1% by weight of sulfur at 1,000° F to 42.7% at 1,500° F. Pellets containing 40% pumice and 60%  $\text{Fe}_2\text{O}_3$  showed sulfur capacities of 23.3% at 1,000° F to 30.6% at 1,500° F. The most effective absorbent was a red mud having capacities ranging from 16.0% at 1,000° F to 45.1% at 1,500° F.

Spectrographic analysis of reaction products revealed the formation of troilite ( $\text{FeS}$ ). Stoichiometric calculations indicate the formation of ferric sulfide ( $\text{Fe}_2\text{S}_3$ ) and pyrite ( $\text{FeS}_2$ ) as products of the reaction. No attempt was made to define precisely the stoichiometry because of the numerous forms in which iron sulfide can occur. The reaction is complicated further by the existence of other metal oxides in the absorbent that may or may not absorb  $\text{H}_2\text{S}$  under the test conditions investigated.

Possible methods of recovering the sulfur contained in the  $\text{SO}_2$  during regeneration are the catalytic conversion to  $\text{SO}_3$  with subsequent production of sulfuric acid, or the reaction of the  $\text{SO}_2$  with some of the producer gas over a suitable catalyst to form elemental sulfur.

Gas chromatographic analyses of both influent and effluent gas streams were made (when using sintered fly ash-ferric oxide) to determine if rearrangement of the gas composition occurs and to determine if gaseous sulfur compounds are formed which are not detected by titration for  $\text{H}_2\text{S}$ . At 1,500° F, water vapor and a small concentration of methane (0.4%) were formed, but no other gases were detected that were not present in the influent gas. The influent gas contained the impurities  $\text{SO}_2$  and methyl mercaptan in low concentrations (45 and 16 ppm, respectively), but these are not found in the effluent.

## CONCLUSIONS

Hydrogen sulfide can be removed from hot producer gas in the 1,000° to 1,500° F temperature range by reaction with a metallic oxide, such as  $\text{Fe}_2\text{O}_3$  (a material which has long been used to absorb  $\text{H}_2\text{S}$  from producer-type gases at low temperatures), but the material must be incorporated into a semifused porous matrix of other metallic oxides to prevent dust formation and loss of absorption material. This research shows that such a material can be made by mixing  $\text{Fe}_2\text{O}_3$  with fly ash and sintering the mixture, or by sintering red mud residues from aluminum refining. In all cases, the mixture contains alumina and silica, which may act as matrix formers, and alkali metal oxides which could act as fluxes to reduce temperature required to sinter the materials.

Absorbents were regenerated to an essentially fresh condition by passing air through the bed at a temperature of 1,000° to 1,200° F. Sulfur dioxide was liberated and the reactive metallic oxides were re-formed. Small quantities of elemental sulfur and sulfuric acid were formed during regeneration.

#### LITERATURE CITED

1. Altieri, V. J., "Gas Analysis and Testing of Gaseous Materials," American Gas Association, Inc., New York, 1945, pp. 339-342.
2. Bureau, A. C., Olden, M. J. F., Chem. Eng. 49, CE55 (1967).
3. Reeve, L., J. Inst. Fuel 31, 319 (1958).

Table 1. - Chemical composition of sintered fly ash used for H<sub>2</sub>S absorption

<u>Constituent</u>	<u>Percent</u>
SiO <sub>2</sub> . . . . .	47.9
Al <sub>2</sub> O <sub>3</sub> . . . . .	23.8
Fe <sub>2</sub> O <sub>3</sub> . . . . .	15.7
P <sub>2</sub> O <sub>5</sub> . . . . .	0.6
TiO <sub>2</sub> . . . . .	2.8
CaO . . . . .	3.6
MgO . . . . .	1.5
Na <sub>2</sub> O . . . . .	1.9
K <sub>2</sub> O . . . . .	2.2

Table 2. - Chemical composition of the granular pumice stone

<u>Constituent</u>	<u>Percent</u>
SiO <sub>2</sub> . . . . .	72.49
Al <sub>2</sub> O <sub>3</sub> . . . . .	13.55
Fe <sub>2</sub> O <sub>3</sub> . . . . .	1.51
Na <sub>2</sub> O and K <sub>2</sub> O . . . . .	8.06
CaO and MgO . . . . .	2.93

Table 3. - Chemical analyses of muds

Mud No.	L. O. I. <sup>1</sup>	Fe <sub>2</sub> O <sub>3</sub>	SiO <sub>2</sub>	TiO <sub>2</sub>	Al <sub>2</sub> O <sub>3</sub>	CaO	Na <sub>2</sub> O
1 <sup>2</sup>	11.2	42.4	8.1	4.4	18.8	5.3	5.6
2 <sup>3</sup>	5.6	7.5	23.3	3.7	6.9	46.4	3.5
3 <sup>4</sup>	11.5	53.2	3.6	7.2	12.8	7.3	2.1
4 <sup>5</sup>	11.2	34.7	13.9	9.0	19.4	5.8	6.0

<sup>1</sup> Loss on ignition at 1, 100° C.

<sup>2</sup> Red mud from Alcoa's Point Comfort operations.

<sup>3</sup> Brown mud from Alcoa's Arkansas operations.

<sup>4</sup> Field dried red mud from Reynolds Metals Co. Sherwin plant.

<sup>5</sup> Mobile red mud from Alcoa.

Table 4. - H<sub>2</sub>S absorbing capacities of sintered materials at 2,000 space velocity

Test No.	Absorption temp., ° F	Capacity, g sulfur / 100 g material
<u>75% Fly ash - 25% Fe<sub>2</sub>O<sub>3</sub></u>		
1	1,000	8.7
2	1,000	8.2
3	1,000	8.1
4	1,250	16.4
5	1,250	21.1
6	1,250	16.5
7	1,250	13.3
8	1,250	15.8
9	1,500	41.1
10	1,500	42.7
<u>Taconite</u>		
11	1,000	3.5
12	1,250	4.8
13	1,500	Disintegrated
<u>Fe<sub>2</sub>O<sub>3</sub></u>		
14	1,000	22.0
15	1,250	20.0
16	1,500	Disintegrated
<u>63% Fly ash - 37% Fe<sub>2</sub>O<sub>3</sub></u>		
17	1,000	6.1
18	1,250	8.1
19	1,500	34.0
20	1,500	26.0
<u>87% Fly ash - 13% Fe<sub>2</sub>O<sub>3</sub></u>		
21	1,000	4.4
22	1,250	9.8
23	1,500	22.0

Table 5. -  $H_2S$  absorbing capacities of sintered pumice stone

Test No.	Temp., ° F	Capacity, g sulfur / 100 g absorbent
Pumice, granular, -4 + 8 mesh		
24	1,000	0
25	1,250	1.4
26	1,500	3.7
87% Pumice, 13% $Fe_2O_3$		
27	1,000	4.7
28	1,250	6.3
29	1,500	8.5
66% Pumice - 34% $Fe_2O_3$		
30	1,000	7.2
31	1,250	8.4
32	1,500	12.3
33	1,500	13.3
40% Pumice - 60% $Fe_2O_3$		
34	1,000	23.3
35	1,000	20.4
36	1,250	26.8
37	1,500	27.6
38	1,500	30.6

Table 6. -  $H_2S$  absorbing capacities of brown and red mud

Test No.	Temp., ° F	Capacity from quantity $H_2S$ absorbed	g of sulfur / 100 g absorbent from quantity $SO_2$ evolved	Percent error in sulfur balance
Mud No. 1				
39	1,000	16.2	16.0	1.2
40	1,250	25.6	24.0	6.0
41	1,500	52.7	45.1	14.4
Mud No. 2				
42	1,000	1.6	1.5	6.0
43	1,250	6.1	6.6	7.6
44	1,500	28.2	26.4	6.6
Mud No. 3				
45	1,000	13.7	12.2	11.0
46	1,250	14.9	13.7	8.1
47	1,500	34.0	37.6	9.6
Mud No. 4				
48	1,000	5.9	6.6	10.6
49	1,250	14.6	13.2	9.6

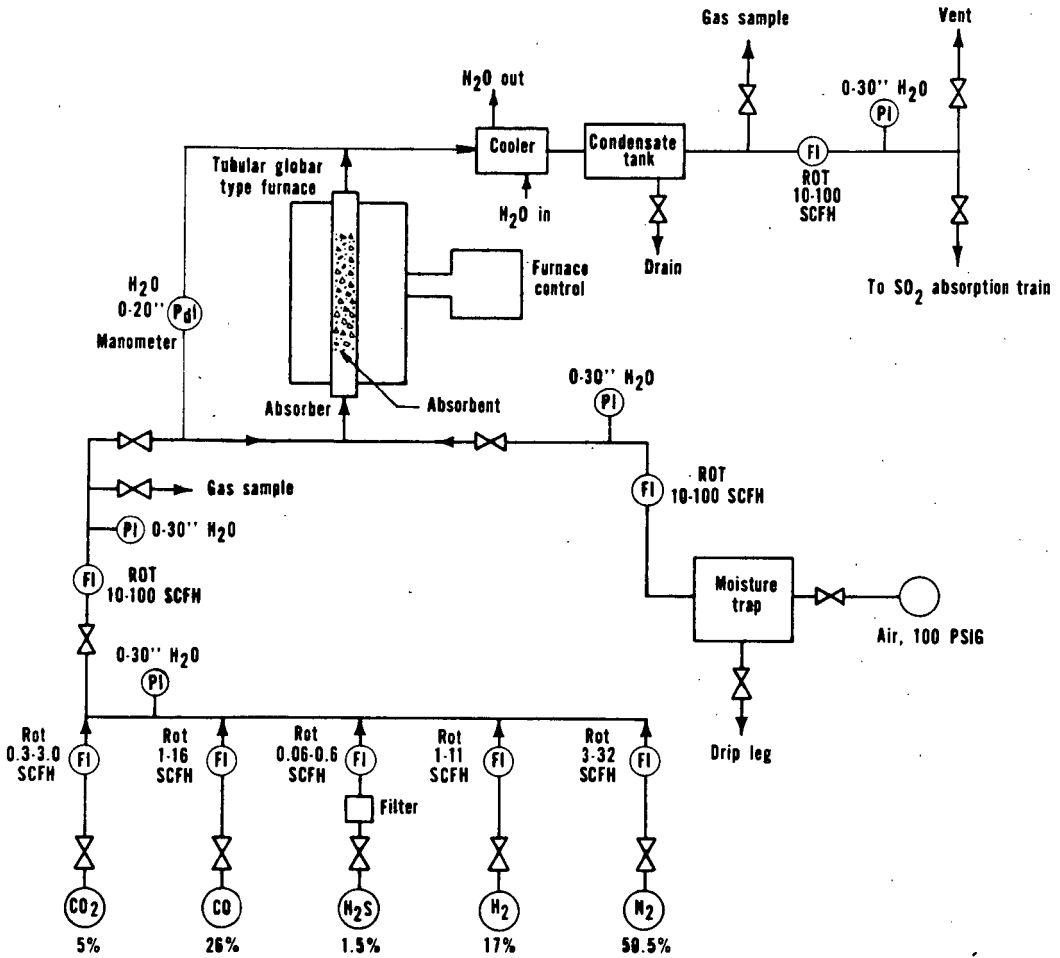


Figure 1. - Flowsheet for Removal of Sulfur from Hot Producer Gas.

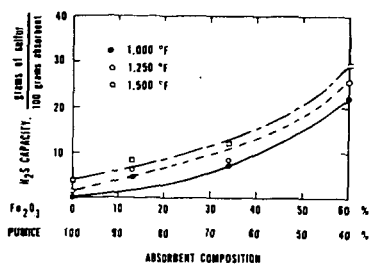


Figure 2. - H<sub>2</sub>S Absorption Capacity of Sintered Pumice Stone.

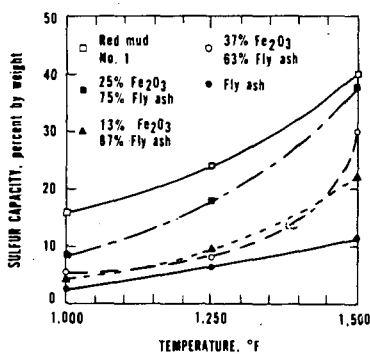


Figure 3. - Sulfur Capacities of Absorbents at 1,000° F to 1,500° F.

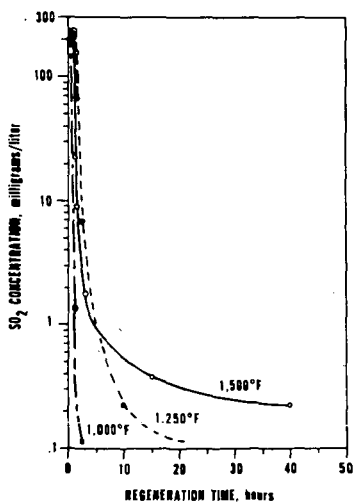


Figure 4. - Typical SO<sub>2</sub> Concentration Versus Regeneration Time.

DISSIMILAR BEHAVIOR OF CARBON MONOXIDE PLUS WATER  
AND OF HYDROGEN IN HYDROGENATION

Herbert R. Appell, Irving Wender, and Ronald D. Miller

Pittsburgh Coal Research Center, U. S. Bureau of Mines,  
4800 Forbes Avenue, Pittsburgh, Pa. 15213

Under certain conditions the conversion of lignite, subbituminous and some bituminous coals to benzene-soluble oils proceeds more readily in the presence of carbon monoxide and water than in the presence of hydrogen (1-4).

The purpose of the work described here was to compare the behavior of carbon monoxide plus water with that of hydrogen under mild coal hydrogenation conditions. Pure compounds and materials having structures resembling those that might exist in coal were the objects of the hydrogenations.

The experimental work was conducted in a 500 ml rocking stainless steel autoclave. Analysis of the pure compounds was by gas chromatography and mass spectrometry. Conversions of lignite, lignin, and cellulose were measured by extracting the products with hot benzene and then weighing and analyzing the benzene-insoluble residues. Pressures referred to in the tables are initial pressures. The maximum pressures were about three times the initial pressure. The time at temperature did not include the time required to reach operating temperature or the cooling off period. The reactants were thus exposed to temperatures where a significant amount of reaction was occurring for approximately an additional hour.

RESULTS AND DISCUSSION

The effectiveness of carbon monoxide and water in solubilizing low rank coal may be due to a number of reasons, including (1) hydrogenation with activated hydrogen produced by the water-gas shift reaction, (2) the introduction of alkyl groups, and (3) the unique ability of carbon monoxide to cleave certain types of bonds or to inhibit condensation reactions leading to benzene-insoluble materials.

Mass spectrometric analysis of the benzene-soluble products from a fresh lignite and a less reactive, rapidly aged lignite, revealed that a major difference in composition was an increase in methylated aromatic compounds in the product from the more reactive lignite. This is in agreement with the observation of Sternberg and Delle Donne of our laboratory that coal may be solubilized by the introduction of alkyl groups (5). The relatively high methyl content of the products suggested that the effectiveness of CO and water in lignite solubilization might be due in part to the introduction of methyl groups.

Table 1 lists the relative peak heights of several of the more prevalent compounds in the products. Inasmuch as the solvent used consisted of equal weights of  $\alpha$ -naphthol and phenanthrene, the compounds present in largest concentration were the solvent and products derived from the relatively reactive  $\alpha$ -naphthol. (In a solvent free system the cresols usually show the highest mass peaks.) Not only are the aromatic compounds from fresh lignite present in higher concentration, but the methylated derivatives of the parent aromatic compound are also consistently and significantly higher. The large content of methyl-naphthol, in both products, indicates that methyl groups are being picked up, either from the lignite, from the carbon oxides, or from traces of formaldehyde. The probable reactions are

carbonylation, carboxylation, and hydroxymethylation, followed by reduction. The presence of relatively large amounts of dinaphthylmethanes suggest that naphthoic acid, hydroxymethylnaphthalene and naphthylmethyl radical may be intermediates in the route from naphthol to methylnaphthalene.

TABLE 1. - Methyl groups in benzene soluble material from hydrogenated lignite  
(30 g. lignite, 15 min. at 380°C, 1500 psig CO pressure,  
1:1:1 = water:lignite:solvent<sup>a</sup>)

Compound	Relative peak heights by M.S. analysis	
	North Dakota lignite (89% conversion)	Aged North Dakota lignite <sup>b</sup> (54% conversion)
Phenol	12	8
Cresols	18	11
Xylenols	14	5
Naphthalene	50	27
Methylnaphthalene	80	24
Naphthol	900	1070
Methylnaphthol	340	240
Phenanthrene	2500	2500
Methylphenanthrene	14	10
Dinaphthylmethane, dinaphthofuran	60	43
Methylnaphthylmethane )	57	26
Methylnaphthonaphthofuran )		

<sup>a</sup> Equal parts of  $\alpha$ -naphthol and phenanthrene.

<sup>b</sup> Heated 24 hr. in air at 105°C, 54% conversion.

Although treatment with hydrogen, with or without water present, gave a smaller total yield of benzene-soluble product, the ratio of methylated to parent aromatic structures were the same, within experimental error, as those obtained in the presence of carbon monoxide and water (4). This result implies that carbon monoxide or dioxide liberated during lignite hydrogenation was reentering the reaction. In the presence of the alkaline lignite ash, carbon dioxide would be expected to add to phenolic materials readily via a Kolbe type carboxylation. One advantage of the reaction with hydrogen is that in the absence of large quantities of water, the carboxylation reaction may proceed rapidly. Reduction of the carboxyl group to a methyl group also occurs more readily with hydrogen than with carbon monoxide and water.

Although methylation may be a factor serving to increase the solubility of lignite, the effect is similar for carbon monoxide plus water and for hydrogen. Methyl group introduction, therefore, does not appear to be a major reason for the greater effectiveness of carbon monoxide and water in lignite solubilization.

The presence of methoxyl groups in lignite prompted several experiments probing the behavior of anisole at mild coal hydrogenation conditions (approximately 4500 psig maximum pressure at 380°C using low activity catalysts). Table 2 shows that in addition to demethylation to phenol, a significant portion of the anisole is converted to benzene and toluene. The highest yield of benzene was obtained with hydrogen. This demonstrates the greater effectiveness of hydrogen in hydrocracking reactions. The absence of dimethylated products suggests that ring methylation proceeds predominantly by an intramolecular shift. It does not appear likely that methoxy or methyl transalkylation occurs to a major extent during coal hydrogenation.

TABLE 2. - Hydrogenolysis of anisole

(20 ml. anisole, 15 ml. water, 1 g. catalyst, 1500 psig, 2 hr. 380°C)

Catalyst	Gas	Wt. pct. of total products			
		Benzene	Toluene	Phenol	Anisole
None	CO	1.9	7.4	6.5	84
Lignite ash	CO	1.5	4.2	18	76
Charcoal	CO	2.0	7.8	6.5	83
Fe	CO	2.6	8.5	10	77
Fe <sub>3</sub> O <sub>4</sub>	CO	2.9	8.4	8.3	80
Fe <sub>3</sub> O <sub>4</sub> <sup>a</sup>	H <sub>2</sub>	6.8	7.7	11	74
Fe <sub>3</sub> O <sub>4</sub>	H <sub>2</sub>	4.5	8.2	16.5	70

<sup>a</sup> No water present.

The possibility that methyl groups could be introduced via CO, CO<sub>2</sub>, or methyl alcohol was evaluated by treating phenol under mild coal hydrogenation conditions. Table 3 shows that in the presence of iron oxide, methylation occurs to a significant extent with CO<sub>2</sub> and with methyl alcohol. Although small amounts of the latter might be formed by a Fischer-Tropsch reaction, it appears more likely that either formaldehyde or CO<sub>2</sub> adds to reactive phenolic rings and the compound formed is then reduced by the carbon monoxide or by the hydrogen. Even in the absence of added catalysts, small amounts of cresol, toluene, and xylene were obtained with CO<sub>2</sub> plus either CO or H<sub>2</sub>. More reactive phenolic materials can be expected to methylate to a greater extent. The formation of dinaphthylmethanes indicated in table 1 is perhaps a result of carboxylation or hydroxymethylation of the  $\alpha$ -naphthol followed by condensation with a molecule of naphthol or methylnaphthol. The condensed product apparently loses phenolic OH groups easily; not more than traces of masses corresponding to oxygen containing dinaphthylmethanes were observed. This mechanism may account for the formation of some high molecular weight materials during coal hydrogenation.

TABLE 3. - Methylation of phenol

(20 g. phenol, 1 g. catalyst, 2 hr. 380°C, 1500 psig)

Catalyst	Gas	Water, g.	Reagent, g.	Wt. pct. of total products
CoCO <sub>3</sub>	CO	15	None	Trace o-cresol
None	CO	15	MeOH, 10	No reaction
Fe <sub>3</sub> O <sub>4</sub>	CO	15	MeOH, 10	o-Cresol, 6%; anisole, 1.3%; xylenol, trace
None	CO	15	CO <sub>2</sub> , 15	Traces of o-cresol, toluene, xylene
None	H <sub>2</sub>	None	CO <sub>2</sub> , 15	o-Cresol, 0.7%; traces of benzene, toluene, xylenol
Fe <sub>3</sub> O <sub>4</sub>	H <sub>2</sub>	None	CO <sub>2</sub> , 15	o-Cresol, 6%; benzene, 2.5%; toluene, trace
Lignite ash	H <sub>2</sub>	None	CO <sub>2</sub> , 15	o-Cresol, 0.4%; benzene, 0.2%

Although not more than traces of formaldehyde can be expected to be present at operating conditions, the high reactivity of formaldehyde with phenols suggests that the small amounts formed are continuously scavenged from the system by reaction with the phenols.

The major high molecular weight oxygen containing compound appeared to be dinaphthofuran. This is probably formed by cyclization of dinaphthyl ether; but oddly, not more than very small amounts of the mass corresponding to this ether was found by mass spectrometry.

A number of compounds were tested for their ease of hydrogenation with carbon monoxide and water and with hydrogen. The hydrogenation of 1-octene proceeded more rapidly with hydrogen than with carbon monoxide and water at the same total pressure (table 4). However, the rate with carbon monoxide and water was four times as fast as expected based on the partial pressure of hydrogen in the autoclave in the absence of a catalyst. In the presence of potassium carbonate, more hydrogen was formed by the water-gas shift reaction but the rate of hydrogenation was only three times that expected. The rate, however, was approaching that obtained with high pressure hydrogen. It thus appears that hydrogen formed by the water-gas shift reaction is activated and has a beneficial effect on the rate of hydrogenation. The lower total extent of hydrogenation, in this system at least, makes it clear that the hydrogen is not activated sufficiently to reach or surpass the hydrogenation rates obtainable with high pressure hydrogen. It may be that, with the proper choice of catalyst, reactants and operating conditions, the hydrogenation rate with carbon monoxide and water could equal or exceed that obtained with hydrogen.

TABLE 4. - Hydrogenation of octene-1  
(1 hr. 400°C, 1000 psig, water:hydrocarbon = 1.5:1)

	H <sub>2</sub>	CO <sup>a</sup>	CO-K <sub>2</sub> CO <sub>3</sub> <sup>b</sup>	H <sub>2</sub> <sup>c</sup>
Product (mole pct.)				
Below C <sub>8</sub>	8	9	11	8
n-Octane	61	36	50	26
n-Octene-1	21	41	22	49
n-Octene-2	9	11	13	15
Above C <sub>8</sub>	1	3.5	4	2.5

<sup>a</sup> 14.6 Mole pct. H<sub>2</sub> in final gas; 36.5% water-gas shift reaction.

<sup>b</sup> 27 Mole pct. H<sub>2</sub> in final gas; 66% water-gas shift reaction.

<sup>c</sup> 400 psig initial pressure.

The reduction of p-methylbenzaldehyde to xylene also proceeded at a more rapid rate with hydrogen than carbon monoxide and water (table 5). The yield of condensation products (tolylxylmethanes) was also higher when hydrogen was used.

TABLE 5. - Reduction of p-methylbenzaldehyde  
(20 ml. aldehyde, 1 g. Fe<sub>3</sub>O<sub>4</sub>, 2 hr. at 380°C, 1500 psig)

Gas	Water	Conversion	Products, percent (wt.)			
			Toluene	Xylene	Methylbenzylalcohol	Diaryls
CO	15 ml.	50	25	14	6	4
H <sub>2</sub>	None	94	14	70	3	7

The possibility that carbon monoxide plus water has a unique ability to cleave certain types of bonds in coal was explored by subjecting a variety of compounds to coal hydrogenation conditions (table 6). Very little hydrogenolysis occurred

except with phenyl sulfide; but here again hydrogen was more effective than carbon monoxide and water. The considerable reduction of sulfur in lignite with carbon monoxide and water (4), and the stability of thiophene at these conditions suggests that thiophenic sulfur is not common in lignites.

TABLE 6. - Conversions of miscellaneous compounds  
(20 g. compound, 15 ml. water, 1 g. catalyst, 2 hr. 400°C, 1500 psig)

Compound	Catalyst	Gas	Products, percent (wt.)
Phenyl ether	Na <sub>2</sub> CO <sub>3</sub>	CO	Very little reaction
3-Methylthiophene	Na <sub>2</sub> CO <sub>3</sub>	CO	Very little reaction
3-Methylthiophene	Charcoal	CO	Very little reaction
Diphenylmethane	Na <sub>2</sub> CO <sub>3</sub>	CO	Very little reaction
Diphenylmethane	Charcoal	CO	Benzene 1.0, toluene 1.4
Diphenylmethane	Charcoal	H <sub>2</sub>	Benzene 3.1, toluene 3.8
Phenyl sulfide	Charcoal	CO	Benzene 3.6, toluene 2.0
Phenyl Sulfide	Charcoal	H <sub>2</sub>	Benzene 61

Lignin and cellulose, the generally accepted coal precursors, were found to be, like coal, more reactive with CO and water than with hydrogen (table 7). Glucose and presumably certain other carbohydrates share this property. Surprisingly, cellulose is most reactive. This order of reactivity is probably caused by the relatively large number of stable aromatic units in lignin and the ease of pyrolysis of glucose. A carbonyl group appears to be necessary for low temperature charring. Glucose and other carbohydrates that contain a carbonyl group or an incipient carbonyl group form chars on being heated at 250 to 300°C with the liberation of considerable quantities of water. Sorbitol and sorbic acid do not form chars at these conditions.

TABLE 7. - Conversion of lignin and carbohydrates to benzene-soluble material  
(1500 psig, 40 ml. water, 2 hr. at temperature)

Material, g.	Gas	Temp., °C	Catalyst, g.	Conversion, % of feed (maf) <sup>a</sup>	Benzene soluble product, wt. % <sup>a</sup>
Lignin, 10	CO	250	None	77	29
Lignin, 10	H <sub>2</sub>	350	None	33	9
Lignin, 10	CO	380	None	80	N.A.
Lignin, 10	CO	380	Na <sub>2</sub> CO <sub>3</sub> , 1	92	N.A.
Glucose, 20	CO	350	None	64	6.5
Glucose, 20	H <sub>2</sub>	350	None	60	3
Glucose, 20	CO	350	Na <sub>2</sub> CO <sub>3</sub> , 1	93	35
Cellulose <sup>b</sup> , 20	CO	350	None	90	40
Cellulose <sup>c</sup> , 20	CO	350	None	63	17
Cellulose <sup>b</sup> , 20	H <sub>2</sub>	350	None	60	20
Cellulose <sup>c</sup> , 20	CO	350	Na <sub>2</sub> CO <sub>3</sub> , 1	94	46
Cellulose <sup>c</sup> , 20	H <sub>2</sub>	350	Na <sub>2</sub> CO <sub>3</sub> , 1	90	27

<sup>a</sup> Based on charge.

<sup>b</sup> Crude cellulose.

<sup>c</sup> Ash free cellulose.

The advantage of carbon monoxide and water over hydrogen in liquefying carbohydrates is reflected not only in the higher yields of benzene-soluble product but also in the composition of the residues (table 8). The atomic ratio of

hydrogen to carbon in the residue from hydrogenation with carbon monoxide and water is close to 1:1, whereas the much larger residue obtained in the presence of hydrogen is only 0.73:1.

TABLE 8. - Composition of benzene-soluble products and residues from cellulose  
(2 hr. at 350°C, 1500 psig)

	Benzene soluble product (CO + H <sub>2</sub> O) (40% yield) <sup>a</sup>	Residue (CO + H <sub>2</sub> O) (10% yield) <sup>a</sup>	Residue (H <sub>2</sub> ) (40% yield)
C (%)	83.3	71.4	74.9
H (%)	7.8	5.9	4.6
H/C	1.11	.98	0.73

<sup>a</sup> The remaining 50% yield is largely water plus some carbon dioxide.

Sodium carbonate is an effective catalyst for liquefying cellulose, glucose, or lignin in the presence of carbon monoxide and water. Benzene-insoluble residues of less than 5% of the original weight of cellulose and less than 10% of the original weight lignin have been obtained at relatively mild conditions. The product is similar in elemental analysis to that obtained from lignite but is less aromatic.

The ease of conversion of cellulose and glucose to benzene-soluble products with carbon monoxide and water suggests that structural units derived from those found in carbohydrates exist in low rank coals. The reactivity of coals with CO and water may be indicative of the number of carbohydrate-derived structures in the coal. The structure of low rank coals is even less certain than that of high rank coals and it is hoped that this approach will assist in improving our knowledge of low rank coal structure.

#### REFERENCES

1. F. Fischer and H. Schrader, *Brennstoff-Chem.*, **2**, 257 (1921).
2. H. I. Waterman and F. Kortland, *Rec. trav. Chim.*, **43**, 258, 691 (1924).
3. H. I. Waterman and J. N. J. Perquin, *Proc. Acad. Sci. Amsterdam*, **27**, 132 (1924); *CA*, **18**, 1903 (1924).
4. H. R. Appell and I. Wender, 156th National Meeting, American Chemical Society, Fuel Division Preprints, vol. 12, No. 3, 220 (1968).
5. H. W. Sternberg and C. L. Delle Donne, 156th National Meeting, American Chemical Society, Fuel Division Preprints, vol. 12, No. 4, 13 (1968).

## HYDROCRACKING IN STATIC AND EBULATING BED REACTOR SYSTEMS

S. A. Qader, W. H. Wiser, and G. R. Hill

Department of Mineral Engineering

University of Utah, Salt Lake City, Utah 84112

Abstract

The results of hydrocracking of coal and petroleum oils in static and ebulating bed reactors are presented. The static bed system was found to be more efficient at low space velocities, while the efficiency of both the systems was almost the same at higher space velocities with respect to the yield of naphtha. The gas oil and coal oil hydrocracking severities, respectively, varied from 0.03 to 0.4 and 0.08 to 0.45 in the case of the static bed system and 0.03 to 0.31 and 0.07 to 0.32 in the case of the ebulating bed system. The static bed system affected more desulfurization, denitrogenation, and deoxygenation at lower space velocities, while the ebulating bed system was more efficient at higher space velocities. The static bed system appears to be more suitable for operations designed for the production of naphtha and for the complete removal of heterocyclic compounds.

Introduction

Hydrocracking of fuel oils is mostly carried out in static bed reactor systems which are very versatile for the processing of distillate oils. They, however, pose some problems in the treatment of heavy and residual oils. The residual oils may give rise to excessive deposits in the bed leading to catalyst deactivation, reactor plugging, and pressure drop in the bed. This necessitates frequent regeneration and changing of the catalyst which is an expensive and tedious problem. The heavy feed stocks can easily be processed in an ebulating bed type of reactor system as incorporated in the H-oil process (1, 2). In the ebulating bed system, the catalyst bed expands in excess of the true volume of the catalyst and the catalyst remains always in a state of random motion caused by the velocity of the feed oil, hydrogen, and some internal circulation of the oil. This system has several advantages and can be employed for the processing of different types of feed stocks ranging from vacuum residues to light gas oils (3, 4). It is, thus, evident that the ebulating bed system has the advantage of processing heavy and residual oils over the static system, while both the systems can be employed for the treatment of distillate oils of medium and low viscosities such as some gas oils and coal oils. There are no data available at this time in the open literature on the relative efficiencies of these two reactor systems for the processing of either petroleum or coal oil and is, therefore, difficult to select the proper system for practical adaptation. This communication describes the results of our investigation on the evaluation of the relative efficiencies of the static and ebulating bed reactor systems in the hydrocracking of petroleum and coal oil distillates.

## Experimental

### Materials.

The gas oil was prepared from a mixed base petroleum crude and the coal oil was obtained by the carbonization of a high volatile, bituminous coal from Utah at 650°C in a laboratory oven (Table I). A dual-functional catalyst containing sulfides of nickel and tungsten on silica-alumina in 1/16th-inch size pellets was used as the hydrocracking catalyst.

### Equipment.

The static bed reactor system (Figure 1) contained a tubular 316-stainless steel reactor of 0.75-inch diameter and 40-inch length. One hundred c.c of the catalyst was used in the reactor. The ebulating bed reactor system (Figures 2 and 3) contained a reactor of 3-inch internal diameter and 9-inch height. The ebulation of the catalyst was mainly caused by a magnetic drive stirrer of 1800 r.p.m. The total volume of the catalyst bed was 500 c.c and 250 c.c of the catalyst was used for the experimental work.

### Hydrocracking procedure.

Both systems were first flushed and pressurized with hydrogen and heated to the reaction temperature. The pressure was then adjusted to the experimental value and the oil was fed at the desired rate. The hydrocracking reactions were carried out at a constant pressure of 2000 p.s.i. and the hydrogen to oil feed ratio was maintained at about 1000. The data presented were obtained at a reaction temperature of 450°C unless otherwise mentioned. The values of space velocities varied in the range of  $\pm 10\%$  and were rounded off. In the case of the static bed reactor, the experiments were carried out at 1 to 6 space velocities (V. of oil/hr./V. of catalyst). In the ebulating bed reactor system, experiments were carried out at 2.5 to 6 space velocities and the results were extrapolated down to 1-space velocity. Experiments could not be carried out at space velocities lower than 2.5 due to practical difficulties. In this system, the catalyst (250 c.c) expands to a total volume of 500 c.c (catalyst bed volume) and, hence, the space velocities were calculated on the basis of 500 c.c of the catalyst volume. The product was cooled in the condenser and the liquid product was collected in the separator. The gaseous product containing some uncondensed oil was passed through an active carbon tower to adsorb the oil and a gas meter to measure the rate and total volume passed. The liquid product was distilled and the fraction boiling up to 200°C was designated as naphtha and the residue as middle distillate. The yield of gas was calculated from the total gas and its composition. All products were obtained in single pass operations. The ratio of naphtha plus gas to the feed is designated as cracking severity. The analyses of the products were done by standard methods.

### Results and Discussion

Selection of a suitable processing system mainly depends upon the type of feed stock to be processed and the nature of products desired. Due to the anticipated development of synthetic oil industry in the near future, feed stocks widely varying in physical and chemical properties will be available and

different types of processing systems may have to be employed for their treatment. It is, therefore, necessary to consider the different types of reactor systems available and evaluate their relative efficiencies for the processing of different feed stocks. A realistic evaluation can only be made by processing the same feed stock under similar reaction conditions in different systems. The gas oil and the coal oil used in this work were distillates of medium viscosity and can be easily processed in either static or ebulating bed system without problems, so that a reasonably good evaluation of the two processing systems can be made. The product distribution data obtained in the hydrocracking of gas oil (Figure 4) illustrated that both systems are almost equally efficient at space velocities greater than 4. They yielded almost the same amounts of naphtha and middle distillate at 430° and 450°C. The yield of naphtha, however, was very low and varied between 2 and 3%. Both systems exhibited different efficiencies at lower space velocities with respect to the yields of naphtha and middle distillate. At space velocities between 1.0 and 4.0, the static system yielded more naphtha and, correspondingly, less middle distillate when compared to the ebulating bed system. There was no significant difference in the yield of the gaseous product. The results obtained under the experimental conditions employed, indicate that the static bed system is more suitable for hydrocracking operations mainly designed for naphtha production, while both systems are equally suitable if middle distillate production is desired. This is further illustrated by the similar data obtained in the hydrocracking of a coal oil (Figure 5) which, however, yielded relatively more naphtha and less gas. The latter probably is due to the differences in the boiling ranges and the composition of the two feed stocks. The static bed system exhibited higher cracking severities when compared to the ebulating bed system at lower space velocities (Figure 6). The gas oil and coal oil hydrocracking severities, respectively, varied from 0.03 to 0.4 and 0.08 to 0.45 in the case of the static bed system and 0.03 to 0.31 and 0.07 to 0.32 in the case of the ebulating bed system. The results indicate that the product distribution obtained in the static bed system is being influenced very much by the space velocity, while the latter is not very critical in the case of the ebulating bed system. In any system the efficiency of contact between the catalyst and the reactants is mainly affected by the size of the catalyst and the space velocity. It appears that the space velocity is a more critical factor in the operation of the static bed system, while the size of the catalyst is probably more critical in the case of the ebulating bed system.

The product distribution at different levels of naphtha formation (Figures 7 and 8) indicates that both systems affect the product yields in a similar manner. The actual quantities, however, depend upon the nature of the feed stock. The properties of the naphtha and middle distillate produced by the two systems were found to be quite similar (Tables II and III). The coal oil naphtha was, however, more aromatic in nature than the gas oil naphtha. The composition of the gaseous product was somewhat different and the static system product from gas oil contained more C<sub>4</sub> hydrocarbons while the ebulating system product contained more C<sub>1</sub> and C<sub>2</sub> hydrocarbons. The static system product from coal oil contained more C<sub>3</sub> hydrocarbons, while the ebulating system product contained more C<sub>1</sub> and C<sub>2</sub> hydrocarbons. The production of more C<sub>1</sub> and C<sub>2</sub> gases in the ebulating bed system is indicative of the occurrence of more thermal cracking reactions in this system.

Removal of heterocyclic compounds from fuel oils is one of the major functions of hydrocracking and the extent of such hydroremoval depends upon the nature of the feed stocks, the catalyst, and the experimental conditions. The type of processing system may also have some influence. In gas oil hydrocracking, desulfurization and denitrogenation varied linearly with space velocity in the static bed system, while it was not the case in the ebulating bed system where the desulfurization and denitrogenation leveled off from a space velocity of 2 and down (Figure 9). The static bed system was more efficient for the removal of sulfur and nitrogen compounds at lower space velocities ranging from 1.0 to 3.0, while the ebulating bed system was more effective at higher space velocities ranging from 4.0 to 6.0. The efficiencies were almost the same in the range of 3 to 4 space velocities. Maximum desulfurization of 96% and denitrogenation of 83% were obtained in the static bed system at a space velocity of 1.0. In the case of the ebulating bed system, a maximum desulfurization of about 75% and denitrogenation of about 64% were obtained at a space velocity of 2.0. At space velocities lower than 2, there was no further removal of sulfur and nitrogen from the gas oil. It appears that the ebulating bed system is not very suitable for operations designed for complete removal of sulfur and nitrogen from fuel oils, though it can remove about 70 to 80%. The obvious choice, then, will be to employ the static bed system for such operations. Analogous results were obtained in the hydrocracking of the coal oil (Figure 10) wherein maximum desulfurization and denitrogenation of 97% and 87% were respectively affected by the static system and about 82% and 72% by the ebulating bed system. Oxygen removal from coal oil also followed the same pattern as the removal of sulfur and nitrogen. The rates of hydrocracking of sulfur, nitrogen, and oxygen compounds of gas oil and coal oil appear to be almost the same under conditions of high severities, irrespective of the type of processing system employed. The rates, however, were different under less severe conditions of hydrocracking (Figure 11). The material balance obtained in the two systems with gas oil and coal oil is given in Table IV. A total product recovery of about 102 to 103% was obtained, indicating 2 to 3% of hydrogen consumption in the process. The gas yield was approximated to about 0.5%. The yields of hydrogen sulfide, ammonia, and water were calculated from the extent of removal of sulfur, nitrogen, and oxygen during the process.

#### Acknowledgement

Research work was supported by the Office of Coal Research and the University of Utah.

Literature Cited

1. Hellwig, K. C., Feigelman, S., Alpert, S. B., Chem. Eng. Progress, 62, No. 8, 71 (1966).
2. Rapp, L. M., Van Driensen, R. P., Hydrocarbon Processing, 44, No. 12, 103 (1965).
3. Chervenak, M. C., Johanson, E. S., Johnson, C. A., Schuman, S. C., Sze, M., The Oil and Gas J., 58, No. 35, 80 (1960).
4. Chervenak, M. C., Johnson, C. A., Schuman, S. C., Petrol. Refiner, 39, No. 10, 151 (1960).

Table I. Analysis of the feed materials.

	<u>Coal oil</u>	<u>Petroleum oil</u>
Gravity, °API	11.5	31.80
Sulfur, wt. %	0.84	0.94
Nitrogen, wt. %	0.92	0.80
Oxygen, wt. %	6.84	-
Distillation data		
I.B.P., °C	200	300
50% distillate, °C	305	340
F.B.P., °C	395	440
Hydrocarbon types, vol. % (neutral oil)		
Aromatics + olefins	68.0	29.0
Saturates	32.0	71.0

Table II. Properties of products of gas oil.  
 Temperature: 450°C, pressure: 2000 p.s.i.,  
 sp. vel.: 4.0

<u>Products</u>	<u>Static bed</u>	<u>Ebulating bed</u>
Naphtha		
Aromatics, vol. %	31.0	30.0
Saturates, vol. %	66.0	66.0
Olefins, vol. %	3.0	4.0
Sulfur, wt. %	0.14	0.21
Nitrogen, wt. %	0.18	0.26
Middle distillate		
Aromatics + olefins, vol. %	30.0	31.0
Saturates, vol. %	70.0	69.0
Diesel index	51.0	50.0
Gas, vol. %		
C <sub>1</sub>	10.0	15.0
C <sub>2</sub>	12.0	14.0
C <sub>3</sub>	29.0	28.0
C <sub>4</sub>	49.0	43.0

Table III. Properties of products of coal oil.  
 Temperature: 450°C, pressure: 2000 p.s.i.,  
 sp. vel.: 4.0

<u>Products</u>	<u>Static bed</u>	<u>Ebulating bed</u>
Naphtha		
Aromatics, vol. %	42.0	44.0
Saturates, vol. %	54.0	53.0
Olefins, vol. %	4.0	3.0
Sulfur, wt. %	0.11	0.13
Nitrogen, wt. %	0.21	0.28
Middle distillate		
Acids, vol. %	8.5	11.0
Bases, vol. %	1.0	1.7
Neutral oil, vol. %	90.0	89.0
Middle distillate (neutral)		
Aromatics + olefins, vol. %	61.0	60.0
Saturates, vol. %	39.0	40.0
Diesel index	41.0	41.0
Gas, vol. %		
C <sub>1</sub>	13.0	16.0
C <sub>2</sub>	15.0	19.0
C <sub>3</sub>	33.0	25.0
C <sub>4</sub>	39.0	40.0

Table IV. Material balance.  
 Temperature: 450°C, pressure: 2000 p.s.i.,  
 sp. vel.: 4.0

<u>Product yield,</u> <u>wt. %</u>	<u>Static bed system</u>		<u>Ebulating bed system</u>	
	<u>Gas oil</u>	<u>Coal oil</u>	<u>Gas oil</u>	<u>Coal oil</u>
Naphtha	5.0	10.0	4.0	9.0
Middle distillate	96.0	91.0	97.0	92.0
Gas	0.5	0.5	0.5	0.5
Water	-	1.0	-	1.0
Hydrogen sulfide	0.5	0.5	0.5	0.5
Ammonia	0.5	0.5	0.5	0.5

## THE DIRECT METHANATION OF COAL

R. L. Zahradnik\* and R. A. Glenn

Bituminous Coal Research, Inc.  
350 Hochberg Road  
Monroeville, PennsylvaniaIntroduction

The fact that coal is composed of various fractions with widely varying properties has long been realized. Recent attention to this fact has resulted in a number of proposed staged gasification schemes. In particular, research at BCR has led to the concept of a two-stage super-pressure gasifier to take specific advantage of the varied nature of coal in the production of a gas rich in methane and amenable to conversion to a high Btu pipeline gas. The two-stage super-pressure gasifier utilizes synthesis gas and heat generated in a high temperature stage to convert a portion of fresh coal in a lower temperature stage into a methane-rich gas.(5)

A study of the methane formation occurring at short gas-coal contact times in the low temperature stage is being carried out at Bituminous Coal Research, Inc., for the Office of Coal Research. This program has included batch tests in rocking autoclaves and continuous flow experiments in an externally-heated 5 lb/hr continuous flow reactor (CFR).(8) Tests in this unit have been carried out under a wide variety of conditions using North Dakota lignite, Elkol subbituminous "C" and Pittsburgh high volatile "A" bituminous coals. The program has produced considerable data on the methanation step and has led to the design and construction of an internally-fired 100 lb/hr process and equipment development unit now being placed in operation.(9)

This paper presents a method of analysis of the short contact time methanation step, based on the premise that rapid heating of coal in the presence of hydrogen produces, in addition to gaseous pyrolysis products, an active but transient species which undergoes rapid reaction with hydrogen to produce additional methane. A simplified rate expression is used to derive a relationship between methane yield and hydrogen partial pressure which fits the experimental data obtained by others.(8,13,16)

Background

Until recently, studies of the coal-hydrogen reaction were generally carried out with long gas-coal contact times, and the results are not directly applicable to short contact time methanation. Von Fredersdorf and Elliott (17) have provided an excellent review of the many such investigations through 1963. Although various methods of contacting were tried and a number of mechanisms for the reaction proposed, the general consensus based on these investigations was that the rate of methane production from coal or char is approximately proportional to hydrogen partial pressure, with the constant of proportionality dependent upon temperature, coal type, and percent carbon burnoff.

\* Professor, Chemical Engineering Department,  
Carnegie-Mellon University, Pittsburgh, Pa.

Recent investigations have indicated that the rate of methane production varies with gas-coal reaction time. In experiments carried out at the U.S. Bureau of Mines, Hiteshue *et al.*, studied the hydrogasification of bituminous coals, lignite, anthracite, and char (10) and high volatile "A" bituminous coal. A packed bed of coal was used in these studies, but because of heating capacity limitations, two minutes were required to raise the system temperature to 800 C. Nevertheless, the Bureau of Mines group was able to demonstrate that the test coals reacted with hydrogen in the initial period at a rate much higher than that observed at longer contact times.

Further indication of the rapid gasification rates during the initial contact period was obtained by Feldkirchner and Linden in their study of high-pressure gasification with hydrogen and steam.(6)

In 1965, Moseley and Paterson (14,15) demonstrated this rapid initial rate more conclusively and reported the results of their experiments on the high-temperature hydrogenation of coal chars at hydrogen partial pressures up to 1000 atmospheres. By means of a specially constructed reactor heating device, Moseley and Paterson obtained rate data for methane production in 15-second intervals. With this resolution, they observed a rapid initial rate, which decreased with time until a final steady value was obtained. The steady-state methane production rate had many of the characteristics of rate data as reported earlier by others, i.e., it was roughly proportional to hydrogen partial pressure and depended on char type. However, the rapid initial rate necessitated a new explanation and prompted Moseley and Paterson to suggest a three-step mechanism for the solid phase hydrogenation of coal.

The first step is the devolatilization of coal by a process which is activated by hydrogen but whose rate is not affected by hydrogen. In addition to volatile products, a char is produced in this first step with exposed or labile carbon atoms, which is particularly susceptible to reaction with hydrogen. The second step in the proposed mechanism involves the reactions of the labile carbon atoms, either with hydrogen to form methane or with each other in a cross-linking polymerization to form an inactive char. The third step involves the slow reaction of hydrogen with the inactive char.

Blackwood and McCarthy (3) have discounted the three-step process, offering instead a two-step mechanism consisting of a rapid reaction of hydrogen with groupings in the coal which are associated with oxygen followed by a more sedate attack on the residual carbon structure. Blackwood and McCarthy cited their own data (2,3) as well as Hiteshue's data (10,11) to support their claim, but, in fact, the poor initial time resolution of these data makes it difficult to distinguish between a two- or three-step process.

On the basis of their three-step model, Moseley and Paterson (15) projected that contact times in excess of 0.5 second were unlikely to lead to significant gains in the extent of carbon conversion to methane, and

that complete conversion of the carbon in coal to methane should be possible at 1000 C and 500 atm hydrogen partial pressure. In 1967, they published results of rapid high-temperature hydrogenation of bituminous coal, virtually substantiating their claim.(16) The carbon in the coal was gasified to completion at 500 atm and 900 C.

In point of fact, for contact times of a few seconds, only the first two steps of the three-step model are significant, and a satisfactory accounting of the direct methanation of coal may be obtained on this basis. Moseley and Paterson have presented mathematical relationships between methane yield and gasifier parameters, derived on the assumptions that the decomposition of structures in coal to give the active intermediate is a first-order process, and that the intermediate is simultaneously removed by a first-order process. Methane formation is assumed to give no net consumption of the active species. In this paper, alternate rate expressions are proposed for the first two steps, which result in a simple methane yield expression that properly extrapolates to low and high conversion.

#### The Initial Reaction

Studies of the thermal decomposition of coal have been carried out at BCURA, largely because of the importance of devolatilization in the ignition process of coal particles in pulverized fuel firing.(1,7) Although a large number of complex chemical reactions and physical changes are known to make up the devolatilization process, workers at BCURA were able to represent the grams of carbon lost as methane per gram of starting carbon,  $\Delta W_I$ , for twelve coals tested as a function of absolute temperature, T, and time of residence at this temperature, t:

$$\Delta W_I = VM (1-C)Q \left\{ (1 - \exp - A [\exp - (B/T)] t) \right\} \quad (1)$$

where VM = volatile matter in coal on daf basis

Q = ratio of weight loss to change in volatile matter

ABC = empirical constants

Their results were obtained for 20 $\mu$  coal particles heated at rates of  $2.5 \times 10^4$  to  $5 \times 10^4$  C/sec. Since the mechanism for thermal decomposition depends upon the rate of heating of the coal particles, the quantitative results of this research may not apply directly to the initial reactions occurring in the direct methanation of coal. However, many of the aspects will undoubtedly remain the same--particularly the rapidity of the overall process.

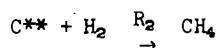
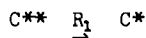
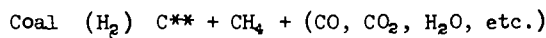
By using typical values reported for the constants in Equation 1,  $A = 1 \times 10^6$  sec;  $B = 8900$  K, a time constant for the devolatilization process of 14 milliseconds is obtained at a temperature of 1750 F.

The significance of this value is its indication that the initial reaction per se should be essentially complete as soon as hot hydrogen-containing gas contacts the coal feed.

The amount of carbon,  $\Delta W_I$ , released as methane to the gas phase during this initial step may be dependent on temperature and coal type, but should be independent of other gasifier parameters such as residence time and gas composition.

As indicated by Moseley and Paterson, the presence of hydrogen does, without a doubt, activate the initial "breakdown" of the basic coal "molecule" during thermal depolymerization. Because of the rapidity of these reactions, little experimental evidence has been accumulated to indicate the degree to which the presence of hydrogen affects the rate of this initial "breakdown."

It is apparent, however, both from the work data of Moseley and Paterson and of Glenn and co-workers, that a highly active species or intermediate appears to be the principal primary product of this initial breakdown. This may be shown schematically as:



where,

$\text{C}^{**}$  = active intermediate produced directly from coal when coal is thermally depolymerized; and

$\text{C}^*$  = inactive char produced by reaction of the active intermediate with itself.

#### The Active Intermediate

The specific chemical processes involving the active intermediate are very complex; any attempt to model them must be viewed, as approximate. The approach taken by the present authors, as opposed to that proposed by Moseley and Paterson, is to consider explicitly the competition between the methanation reaction and the inactive char-forming reaction for the active intermediate.

To this end, consider that coal particles containing one gram of carbon are introduced into a reactor, maintained at a constant temperature,  $T$ , together with a gas whose hydrogen partial pressure is  $P_{\text{H}_2}$ . Consider that there is a sufficient supply of hydrogen so that  $P_{\text{H}_2}$  does not change as methanation proceeds and that the total gas-coal contact time in the reactor is  $\tau$ . Assume that upon completion of the initial reaction  $W_0^*$  gram of active intermediate has been formed;  $W_0^*$  may in general be some fraction,  $f$ , of the ungasified carbon and that  $W_0^*$  may be represented by  $f(1 - \Delta W_I)$ .

The rate of reaction of hydrogen with carbon is generally taken as a linear function of hydrogen partial pressure and expressed per unit of surface area available for reaction.(4) If then, the rate at which the

active intermediate is removed by the char-forming mechanism is assumed to be a first-order process, a similar behavior may be postulated for the active intermediate, and the net rate of change of  $W^*$ , the grams of active intermediate per gram of carbon fed, will be given by the following:

$$\frac{dW^*}{dt} = k_1^1 (P_{H_2}) A^* - k_2 W^* \quad (2)$$

where  $A^*$  = area associated with active intermediate

$k_1^1$ ,  $k_2$  = rate constants of methane formation and deactivation reactions respectively

There are ways in which  $A^*$  may be related to  $W^*$ ; however, at the temperatures and rates under which methanation proceeds, it is reasonable to assume that the methane formation reaction proceeds in a topochemical fashion at a shell-like reaction surface surrounding the active species. In this case  $A^*$  is proportional to  $(W^*)^{2/3}$ , so that Equation 2 may be written as follows:

$$\frac{dW^*}{dt} = -k_1 (P_{H_2}) (W^*)^{2/3} - k_2 W^* \quad (3)$$

where the rate constant  $k_1^1$  and the proportionality constant relating  $A^*$  to  $(W^*)^{2/3}$  have been confined together in the symbol  $k_1$ .

The boundary condition on Equation 3 is that of the completion of the initial reaction (essentially  $t = 0$ ),  $W^* = W_0^*$ . Equation 3 may be integrated to find  $W^*$  at any time  $t$ .

$$\int_{W_0^*}^{W^*} \frac{dW^*}{k_1 (P_{H_2}) (W^*)^{2/3} + k_2 W^*} = - \int_0^t dt$$

or

$$\ln \left[ \frac{k_1 (P_{H_2}) + k_2 (W^*)^{1/3}}{k_1 (P_{H_2}) + k_2 (W_0^*)^{1/3}} \right] = - \frac{k_2 t}{3} \quad (4)$$

Of particular interest is the time  $t^*$  when all of the active intermediate will have disappeared; i.e., at  $t = t^*$ ,  $W^* = 0$ . From Equation 4

$$t^* = \frac{3}{k_2} \ln \left[ 1 + \frac{1}{S} \right] \quad (5)$$

where  $S = \frac{k_1 (P_{H_2})}{k_2 (W_0^*)^{1/3}} = \frac{k_1 (P_{H_2}) (W_0^*)^{2/3}}{k_2 W_0^*} = \frac{\text{Initial rate of Methanation}}{\text{Initial rate of Deactivation}}$

Notice that  $S$  represents a selectivity for the reacting system.

If  $t^*$  is less than  $\tau$ , the gas-coal contact time, then all of the available intermediate will be consumed in the reactor and methane yield will be independent of  $\tau$ .

In order to compute the methane produced during this process, it is necessary to integrate the rate expression for the reaction of hydrogen with the active intermediate. If  $W_c$  denotes the weight fraction of carbon in coal which has appeared as methane, the rate expression for  $W_c$  is:

$$\frac{dW_c}{dt} = k_1 (P_{H_2}) (W^*)^{2/3} \quad (6)$$

where  $t = 0$  corresponds to the end of the initial reaction and where  $W_c = \Delta W_I$ . Since the expression for  $W^*$  as a function of time is known from Equation 4, Equation 6 may be integrated to  $t = t^*$ , at which point the active intermediate has been completely consumed and  $W_c = \Delta W_c$ , the total yield of methane from the short time methanation process. Continued exposure of the inactive char to hydrogen will result in further methane production, but at a much reduced rate. The expression for  $\Delta W_c$  is obtained from the integral

$$\int_{\Delta W_I}^{\Delta W_c} dW_c = 3W_0^* S \int_0^{t^*} [(1 + S) e^{-\frac{k_2 t}{3}} - S]^2 \frac{k_2}{3} dt$$

When the right hand side of this equation is integrated and the expression for  $t^*$  substituted from Equation 5, the resultant expression is:

$$\Delta W_c = \Delta W_I + 3W_0^* S^3 \left[ \ln\left(1 + \frac{1}{S}\right) - \left(\frac{1}{S} - \frac{1}{2S^2}\right) \right] \quad (7)$$

If the series expansion for  $\ln\left(1 + \frac{1}{S}\right)$  is invoked, the square bracketed term in Equation 7 becomes equal to

$$\frac{1}{3S^3} \left[ 1 - \frac{3}{4S} + \frac{3}{5S} - \dots \right]$$

which is closely approximated by the rational fraction

$$\frac{1}{3S^3} \left[ \frac{1}{1 + \frac{3}{4S}} \right]$$

hence, Equation 7 becomes

$$\Delta W_c = \Delta W_I + \frac{\frac{4}{3} W_o^* S}{1 + \frac{4}{3} S}$$

Again, if  $W_o^*$  and  $S$  are replaced by their equivalent expressions, the final relationship between methane yield and gasifier parameters is

$$\Delta W_c = \Delta W_I + \frac{\frac{4 F (1 - \Delta W_I) k_1 (P_{H_2})}{3 k_2 (W_o^*)^{1/3}}}{1 + \frac{4 k_1 (P_{H_2})}{3 k_2 (W_o^*)^{1/3}}} \quad (8)$$

Equation 8 predicts that in the absence of hydrogen, methane yield is due only to the thermally induced decomposition. At small hydrogen partial pressures, the denominator is approximately one, and methane yield is proportional to hydrogen partial pressure. At high hydrogen partial pressures, methane yield again becomes constant, being given by the expression  $\Delta W_c = \Delta W_I + f (1 - \Delta W_I)$ . If  $f = 1$ , complete methanation of the carbon in coal is possible.

#### Correlation of Experimental Data

Equation 8 indicates that the methane yield resulting from the direct methanation of coal by gases containing large excesses of hydrogen should be correlated by an equation of the form

$$\Delta W_c = b_1 + \frac{b_2 (P_{H_2})}{1 + b_3 (P_{H_2})} \quad (9)$$

where  $b_1$ ,  $b_2$ , and  $b_3$  are correlation constants related to the kinetic parameters for the process.

The methane rate data for lignite and Elkol coal previously reported by Glenn and co-workers (8) were obtained in continuous flow experiments which did not employ large excesses of hydrogen. However, the presence of CO and H<sub>2</sub>O in the feed gas permitted replacement of consumed hydrogen via the water-gas shift reaction. Comparison of inlet and outlet gas compositions for these continuous flow experiments shows only slight variations in hydrogen partial pressure values, so that the constancy of  $P_{H_2}$  is considered a reasonably valid assumption.

Equation 9 was fitted to the CFR data by a non-linear least squares curve fitting routine.(12) The results of the correlation were:

$$\text{Lignite: } \Delta W_c = 0.07 + \frac{0.0062 (P_{H_2})}{1 + 0.0067 (P_{H_2})} \quad (10)$$

$$\text{Elkol coal: } \Delta W_c = 0.08 + \frac{0.0054 (P_{H_2})}{1 + 0.006 (P_{H_2})} \quad (11)$$

Equation 10 explains 63 percent of the variance in the lignite data; equation 11 explains 52 percent of that in the Elkol coal data. The effect of changes in  $P_{H_2}$  on  $\Delta W_c$  for the two coals is shown in Figure 1. In the operating region for the continuous flow reactor, the hydrogen partial pressures were low enough so that the predicted curve is approximately linear in hydrogen partial pressure.

If the proposed methane-hydrogen relationship is valid, Equations 10 and 11 should extrapolate correctly for methanation experiments carried out at similar temperatures and higher hydrogen partial pressures. In a study of the rapid high-temperature, high-pressure hydrogenation of bituminous coal, Moseley and Paterson gasified coal in pure hydrogen at temperatures of 950 C and pressures as high as 500 atm. (16) Figure 2 presents their experimental data together with typical data points from the CFR experiments of Glenn and co-workers. The curve through the data is Equation 11; the agreement is good over the entire pressure range.

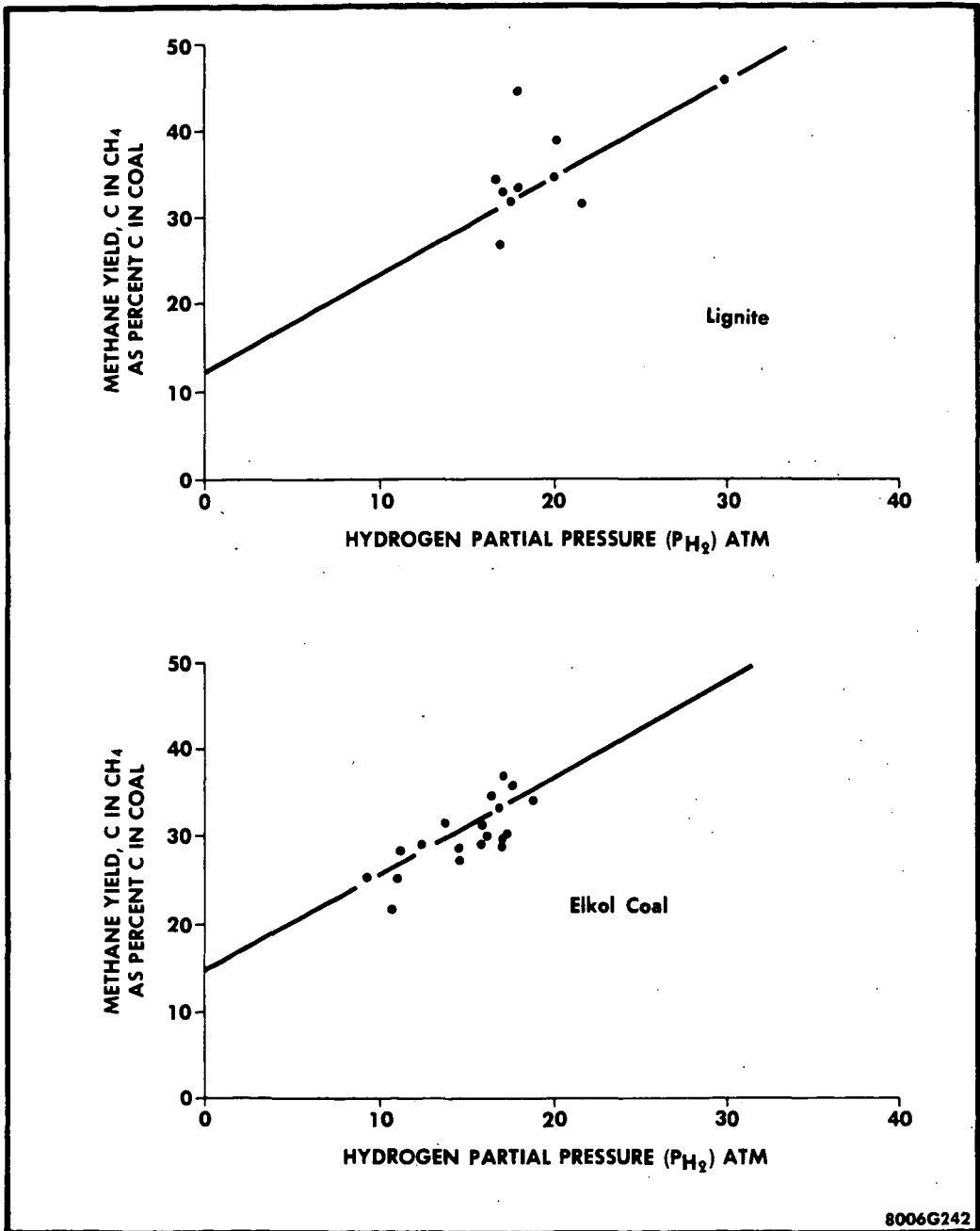
Moseley and Paterson also reported data from a few experiments at 850 C. Since the parameters in the correlating equation depend upon temperature, Equation 11 cannot be applied directly to these lower temperature results. However, an equation of the form of Equation 9 does fit the data quite well, provided the constants are adjusted as indicated in the following equation:

$$\Delta W_c = 0.07 + \frac{0.0033(P_{H_2})}{1 + 0.0035(P_{H_2})} \quad (12)$$

The 850 C data points and Equation 12 are presented in Figure 3.

Lewis, Friedman, and Hiteshue (13) reported data on the direct conversion of untreated bituminous coal into high Btu gas in a dilute-phase concurrent flow apparatus similar to that used by Glenn and co-workers in the CFR experiments, and by Moseley and Paterson in their later work. The residence times used by Lewis *et al* were somewhat longer than those used by Glenn and co-workers and their operating temperature was lower, i.e., 725 C. The data of Lewis *et al* shown in Figure 4 may be correlated by the following equation:

$$\Delta W_c = 0.09 + \frac{0.0016(P_{H_2})}{1 + 0.0017(P_{H_2})} \quad (13)$$



8006G242

Figure 1. Correlation of Methane Yield with Hydrogen Partial Pressure

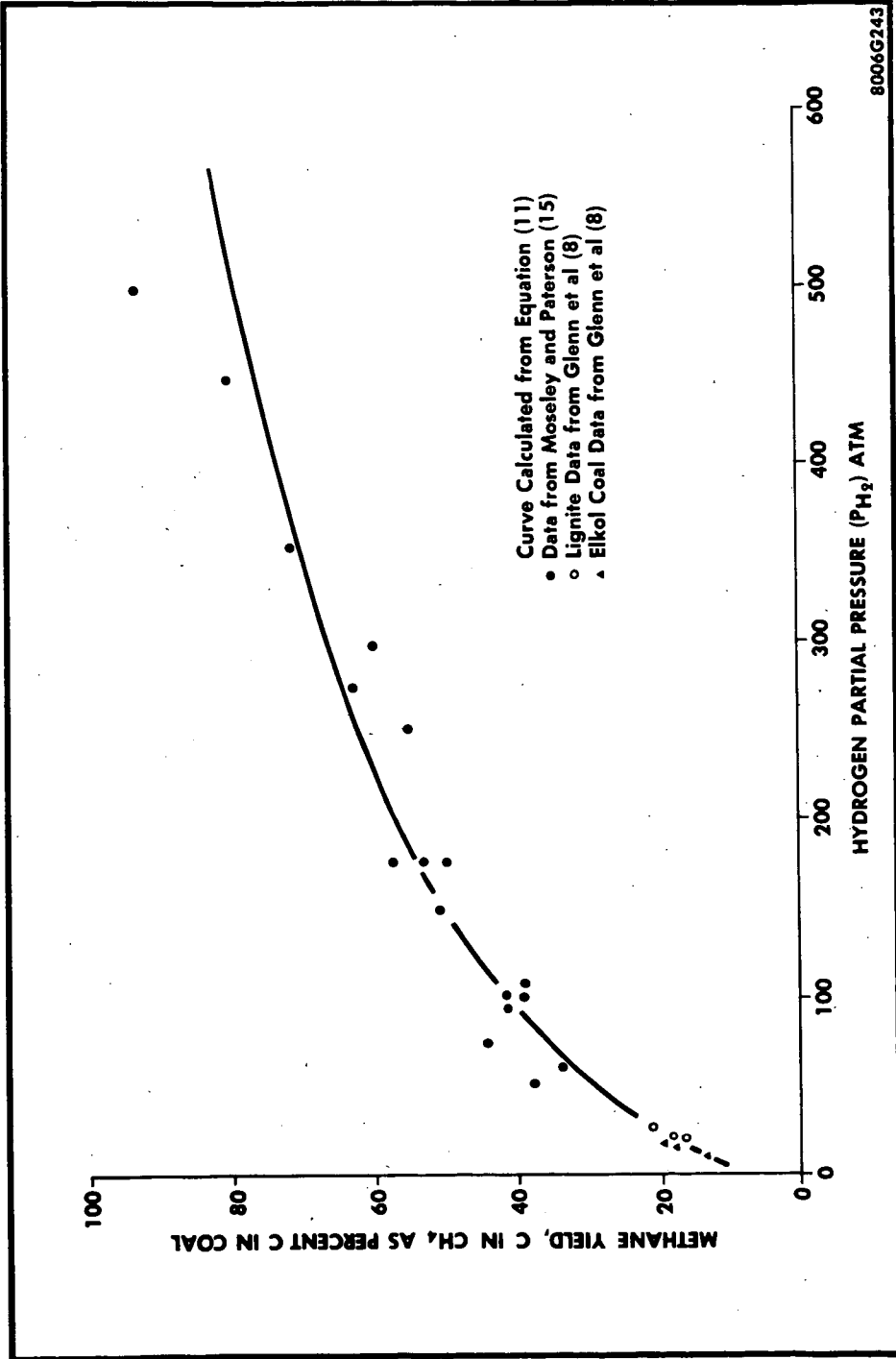


Figure 2. Correlation of Methane Yield with Hydrogen Partial Pressure at 950° C

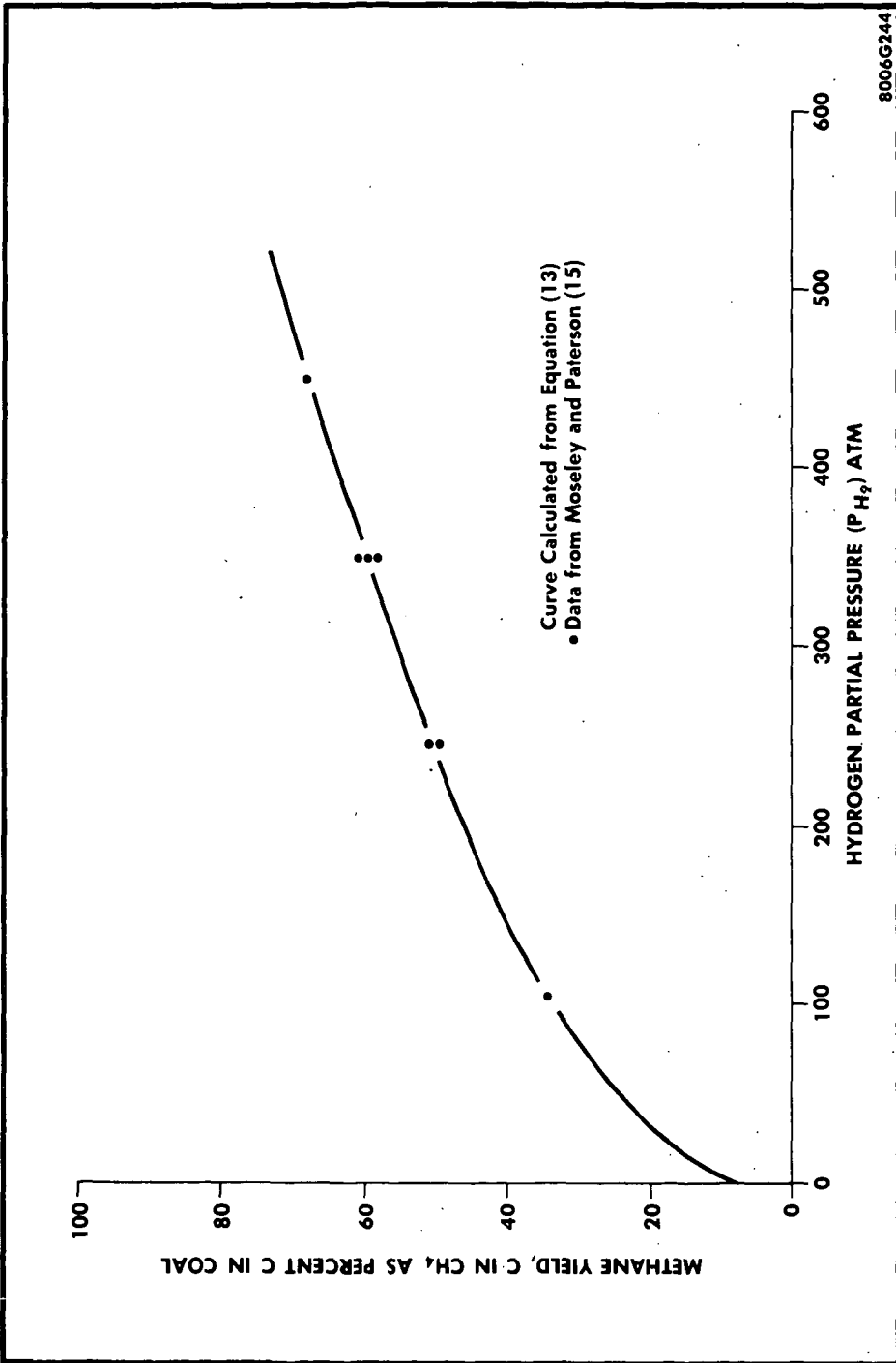


Figure 3. Correlation of Methane Yield with Hydrogen Partial Pressure at 850° C

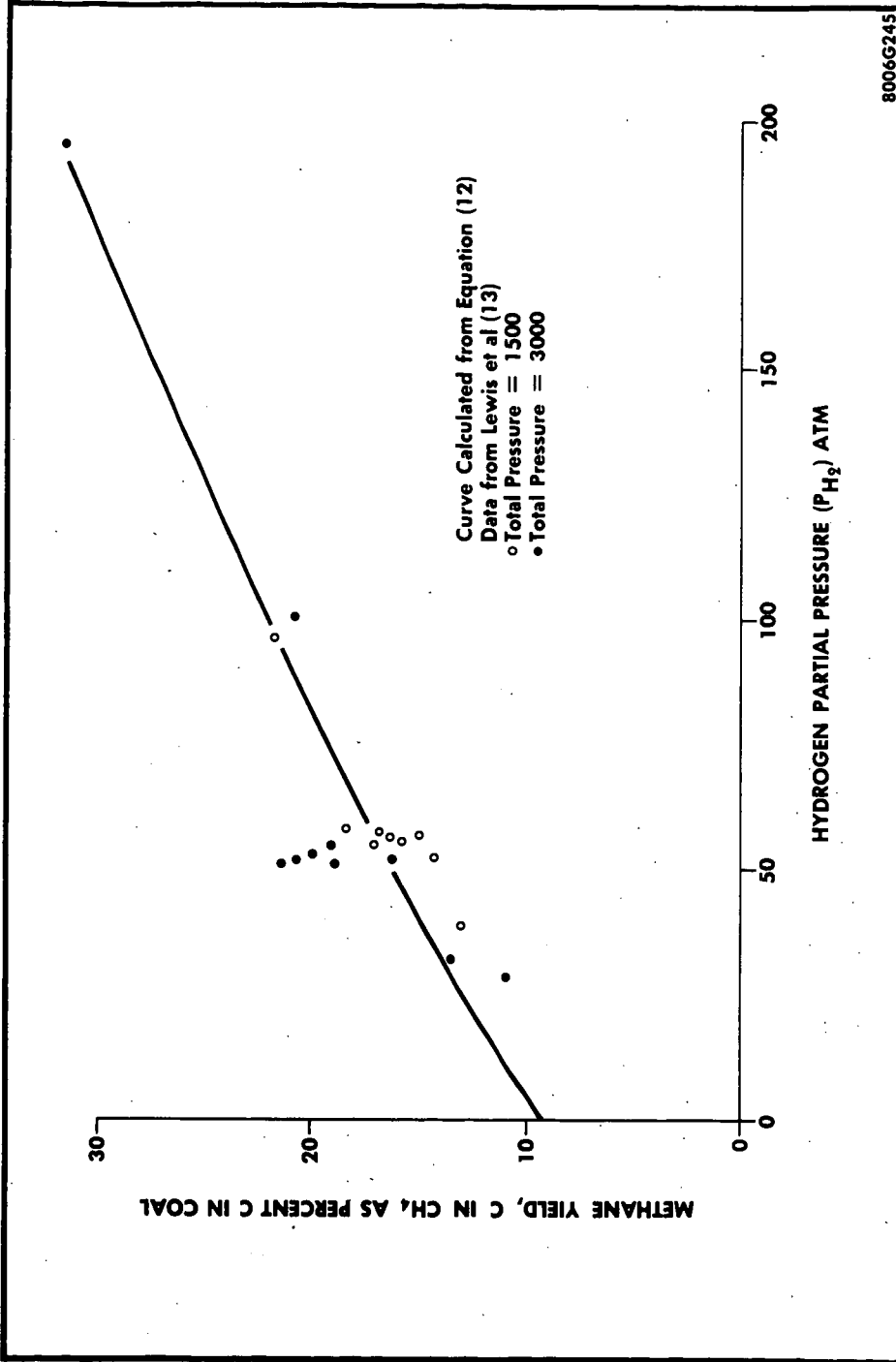


Figure 4. Correlation of Methane Yield with Hydrogen Partial Pressure at 725° C

All of these correlations indicate that methane yield values of one are possible if high enough hydrogen partial pressures are used. Furthermore, it is interesting that an Arrhenius plot of the parameter  $b_2$  (or  $b_3$ ) gives a reasonably straight line. (See Figure 5.) Since  $b_2$  represents the ratio of  $k_1$  to  $k_2$ , one would expect such a fit, and the observed activation energy of 15 Kcal indicates the difference in activation energy between the methanation and the deactivation processes.

The expression for methane yield, as represented by Equation 8, provides a framework for unifying and correlating data on the direct methanation of coal with hydrogen. The fact that the behavior of a variety of coals is consistent with this expression lends support to the hypothesis of the formation of an active intermediate. The fact that the postulated ratio of rate constants for the reactions involving this active intermediate exhibits an Arrhenius behavior further supports this claim and indicates the general validity of the derivation.

It should be pointed out, however, that the rate expressions used to obtain Equation 8 are by no means unique. The unique concept in the analysis is the treatment of the methanation and deactivation steps as being competitive reactions which essentially consume the entire supply of active intermediate in a finite time. For example, if both reactions are assumed to be zero-order with respect to the active intermediate, or if the intermediate concentration at the reaction sites is assumed to be a constant, the equation for the rate of change of  $W^*$  would be as follows:

$$\frac{dW^*}{dt} = -\hat{k}_1(P_{H_2}) - \hat{k}_2 \quad (14)$$

where  $\hat{k}_1$  and  $\hat{k}_2$  are the rate constants associated with the methane formation and deactivation reactions, now considered zero-order with respect to intermediate concentration.

Integration of Equation 9 in the same manner as before, defines the time to consume the intermediate entirely,  $t^*$ , to be in this case

$$t^* = \frac{1}{\hat{k}_2} \frac{W_0^*}{1 + \hat{S}}$$

where  $\hat{S} = \frac{\hat{k}_1(P_{H_2})}{\hat{k}_2}$  = selectivity for zero-order assumption.

The methane yield under this condition,  $\Delta W_C$ , is given as follows

$$\Delta W_C = \Delta W_I + \hat{k}_1 P_{H_2} t^* = \Delta W_I + \frac{f(1 - \Delta W_I) \frac{\hat{k}_1(P_{H_2})}{\hat{k}_2}}{1 + \frac{\hat{k}_1(P_{H_2})}{\hat{k}_2}} \quad (15)$$

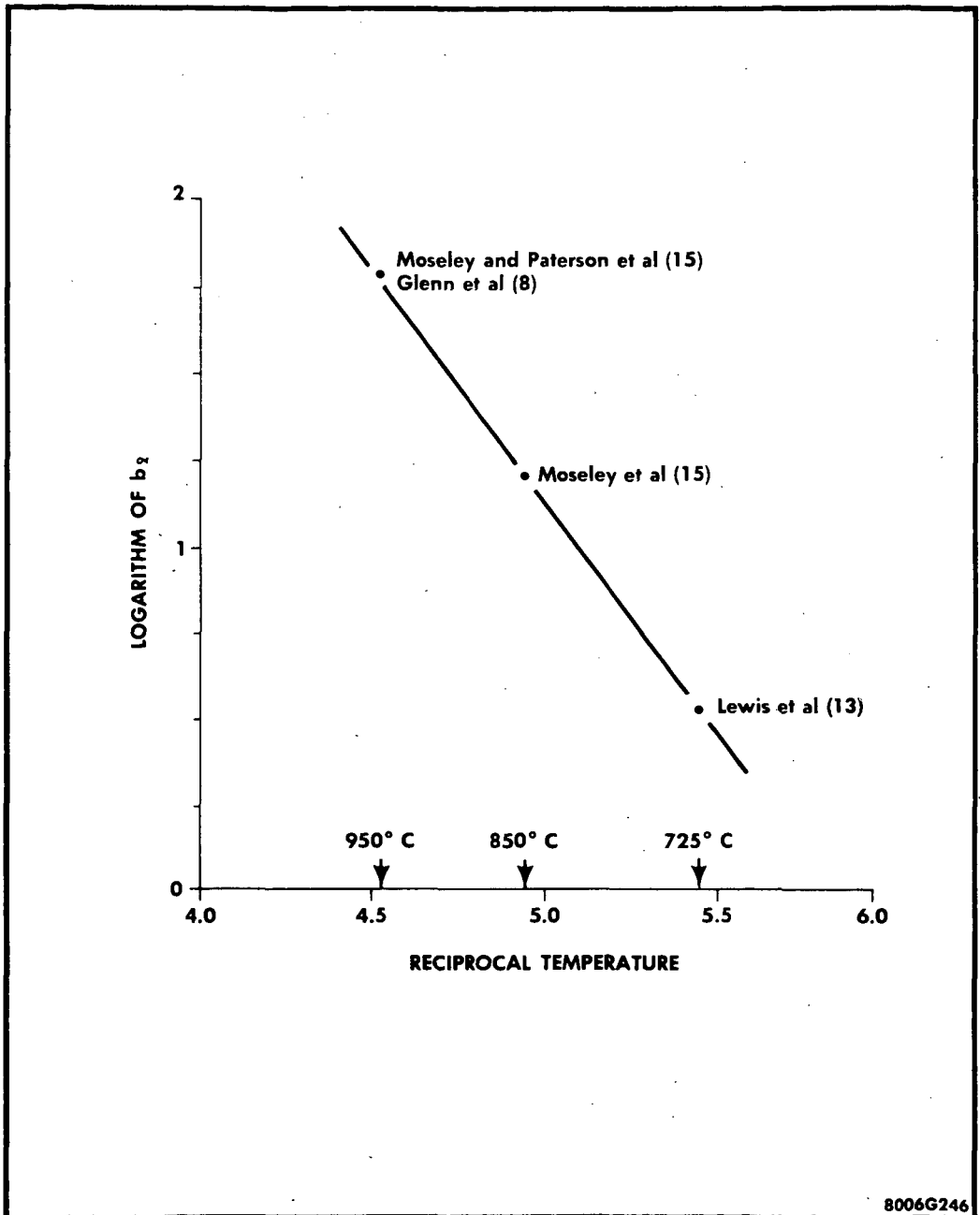


Figure 5. Arrhenius Plot of Parameter  $b_2$

Equation 15 is identical in form to Equation 8 and indicates that there are a number of ways of obtaining the expression which correlates methane yield with hydrogen partial pressure. Thus, even though Equation 8 successfully fits the available data, the nature of the exact mechanism of the reactions involving the active intermediate is still unresolved.

This does not detract from the utility or significance of the yield expression, however. The important point is that the rapid rate of methanation of coal, observed by Moseley and Paterson (16) at high hydrogen partial pressures, has also been shown to be achieved at lower hydrogen partial pressures and in the presence of other gaseous species. Moreover, both conditions are explained by a single equation. The implication, then, is that synthesis gas and steam can be effectively used in a short-contact-time reactor to take advantage of the high activity imparted to coal by rapid heating in the presence of hydrogen. This feature, of course, is the essence of the BCR two-stage super-pressure gasifier.

The specific equations for methane yield, because of their simplicity and independence of most gasifier parameters, can be utilized in the design and engineering evaluation of integrated, multistage gasifiers. This is being done for the BCR two-stage gasifier in order to make better predictions of its ultimate capability as well as to assess effects of process variables and novel operating practices.

Acknowledgment

This paper is based on work carried out at Bituminous Coal Research, Inc., with support from the Office of Coal Research, U.S. Department of the Interior, under Contract No. 14-01-0001-324. Also, the stimulating comments of Dr. E. E. Donath regarding the work are most gratefully acknowledged.

REFERENCES

1. "BCURA annual report 1966," Brit. Coal Util. Res. Assoc., Leatherhead, England, 1967.
2. Birch, T. J., Hall, K. R., and Urie, R., "Gasification of brown coal with hydrogen in a continuous fluidized-bed reactor," J. Inst. Fuel 33, 422-35 (1960).
3. Blackwood, J. D. and McCarthy, D. J., "The mechanism of the hydrogenation of coal to methane," Australian J. Chem. 19, 797-813 (1966).
4. Blackwood, J. D., "The reaction of carbon with hydrogen at high pressure," Australian J. Chem. 12, 14 (1959).
5. Donath, E. E. and Glenn, R. A., "Pipeline gas from coal by two-stage entrained gasification," in "Operating Section Proceedings," New York: Am. Gas Assoc., 1965. pp 65-P-147--151.
6. Feldkirchner, H. L. and Linden, H. R., "Reactivity of coals in high pressure gasification with hydrogen and steam," Ind. Eng. Chem., Process Design Develop. 2 (2), 153-62 (1963).
7. Field, M. A., Gill, D. W., Morgan, B. B., Hawksley, P. G. W., "Combustion of Pulverised Coal." Leatherhead, England: Brit. Coal Util. Res. Assoc., 1967.
8. Glenn, R. A., Donath, E. E., and Grace, R. J., "Gasification of coal under conditions simulating stage 2 of the BCR two-stage super-pressure gasifier," in "Fuel Gasification," Washington: Am. Chem. Soc., 1967. pp 81-103.
9. Glenn, R. A. and Grace, R. J., "An internally-fired process and development unit for gasification of coal under conditions simulating stage two of the BCR two-stage super-pressure process," Am. Gas Assoc., Synthetic Pipeline Gas Symp., Pittsburgh, Pa., 1968.
10. Hiteshue, R. W., Friedman, S., and Madden, R., "Hydrogasification of bituminous coals, lignite, anthracite, and char," U.S. Bur. Mines, Rept. Invest. 6125 (1962).
11. Hiteshue, R. W., Friedman, S., and Madden, R., "Hydrogasification of high-volatile A bituminous coal," U.S. Bur. Mines, Rept. Invest. 6376 (1964).
12. Marquardt, D. W., "Least-squares estimation of nonlinear parameters," Computer Program in Fortran IV Language, IBM Share Library, Distribution No. 3094 (1964).
13. Lewis, S., Friedman, S., and Hiteshue, R. W., "High Btu gas by the direct conversion of coal," in "Fuel Gasification," Washington: American Chemical Society, 1967. pp 50-63.

14. Moseley, F. and Paterson, D., "The rapid high-temperature hydrogenation of coal chars. Part 1: Hydrogen pressures up to 100 atmospheres," J. Ins. Fuel 38 (288), 13-23 (1965).
15. Moseley, F. and Paterson, D., "The rapid high-temperature hydrogenation of coal chars. Part 2: Hydrogen pressures up to 1000 atmospheres," J. Inst. Fuel 38 (296), 378-91 (1965).
16. Moseley, F. and Paterson, D., "The rapid high-temperature high pressure hydrogenation of bituminous coal," J. Inst. Fuel 40, 523-30 (1967).
17. Von Federsdorff, C. G. and Elliot, M. A., "Coal Gasification," in "Chemistry of Coal Utilization," New York: John Wiley & Sons, Inc., 1963. pp 892-1022.

NOMENCLATURE

A*	area associated with active intermediate, $\text{cm}^2$
A, B, C	empirical constants in devolatilization yield equation
$b_1, b_2, b_3$	empirical constants in methane yield correlation equation
C**	active intermediate
C*	inactive char
$k_1^{\dagger}, k_1, k_2$	kinetic parameters in methanation reactions
$P_{\text{H}_2}$	partial pressure of hydrogen, atm
Q	constant in devolatilization equation representing the ratio of unit change in coal weight per unit change in volatile matter content
S	reaction selectivity
T	reactor temperature, $^{\circ}\text{K}$
t	time of reaction, sec
t*	time required to deplete active intermediate, sec
$\tau$	residence time of coal particles in reactor, sec
VM	volatile matter in coal, daf basis, percent
W*	weight of active intermediate per gram of carbon fed at any time
$W_0^*$	weight of active intermediate per gram of carbon fed at time zero
$\Delta W_I$	weight of carbon lost by initial devolatilization per gram of carbon fed
$W_C$	total weight of carbon appearing as methane at any time per gram of carbon fed

EFFECT OF INCREASING FREE SPACE ABOVE THE CHARGE ON THE COMPOSITION  
AND YIELD OF THE VOLATILE PRODUCTS FROM COAL CARBONIZATION

C. Ortuglio, J. G. Walters, and D. E. Wolfson

U. S. Department of the Interior, Bureau of Mines  
Pittsburgh Coal Research Center, Pittsburgh, Pa. 15213

ABSTRACT

The effect of increasing the free space above the charge on the composition and yields of the volatile products from the carbonization of Pittsburgh-bed coal and one industrially used blend from the eastern United States and one from western United States was investigated with the BM-AGA carbonization apparatus.

Increasing the free space above the charge from 1 inch to 3 inches, to 6 inches and to 9 inches resulted in lower tar yields and increased gas and light oil yields. Anthracene and naphthalene yields were increased, quinoline and benzene insoluble fractions of both the tar and pitch increased considerably with increased free space, although the carbon content of the tars and pitches increased only slightly.

Increased cracking, a result of the increase in free space, caused a decrease in the yields of tar acids, tar bases, neutral oils, olefins, aromatics, and paraffins and naphthenes. Gas composition was relatively constant; hydrogen and methane tended to increase and ethane decrease.

Results of the investigation are being used to design a unit to upgrade the volatile products of carbonization by cracking the hot products as they leave the carbonization chamber.

INTRODUCTION

The Bureau of Mines, in cooperation with the American Gas Association, jointly developed a pilot-scale carbonization test apparatus (BM-AGA) to determine the carbonization characteristics of coals and to evaluate the byproduct yields (5).

Although the BM-AGA test apparatus is used primarily to determine the coking characteristics of coals for metallurgical use, the objective of this investigation was to determine the effect of cracking on the quality of carbonization products by varying the free space above the coal charge when the temperature is kept constant.

Carbonization yields are influenced by the rank of coal carbonized, whereas their composition is primarily a function of the temperature and contact time of the evolved vapors with the heated surfaces within the retort or ovens. Decomposition of vapors proceeds in two steps: Primary decomposition of gaseous vapors as they are evolved from the plastic layer at moderate temperatures and then pass through the hot coke surfaces, and secondary decomposition as the vapors pass through the free space above the coal charge with less contact surface. Porter (4) in a study of coal carbonizing equipment has found that the variance of contact time of the gases and vapors passing through the heated spaces in approved industrial ovens may be 100 percent or more.

EXPERIMENTAL PROCEDURES

Procedure and apparatus for BM-AGA carbonization tests have been described in detail in a previous publication (5). Basically, the apparatus consists of a cylindrical steel retort, electrically controlled resistance-type furnace, product

recovery train, gas scrubbers, meters, and sampler. The standard retort used throughout this investigation is 26 inches high and 18 inches in diameter. The results from previous carbonization tests, using standard retorts and 900°C carbonization temperatures have been correlated with industrial (7) and experimental oven (6, 8) data. The coal charges were adjusted in height so as to leave 1-, 3-, 6-, and 9-inches of free space above the coal charge. Duplicate carbonization tests were made at 900°C and the results reported are averages of two determinations.

A single coal (1166) and two commercial coal blends (1161 and 1167A) were used in this investigation. Coal 1161 was carbonized as received so that the size consist would be comparable to that charged at the coke plant. Coals for tests 1166 and 1167A were received separately in lump form and were crushed in the hammer-mill and blended.

In computing yields from BM-AGA carbonization tests, the quantitative yields are based on U. S. gallons (231 cubic inches) and short tons (2,000 pounds). Coke yields are reported as dry coke, weight-percent of coal carbonized. The yield, specific gravity (determined), and gross heating value of the gas are reported as stripped of light oil and saturated with water vapor at 60°F and under a pressure equivalent to 30 inches of mercury. Light oil refers to the crude product stripped from the gas. Liquor includes the fixed ammonia and absorbed free ammonia. Ammonium sulfate is reported in pounds per ton of coal and includes the total free and fixed ammonia. The tar yield, properties, and constituents are reported on a dry basis and includes only that light oil which condenses with the tar, and the specific gravity of the tar is reported at 15.5°C/15.5°C.

The yields of carbonization products are given on the as-carbonized basis (table 1). The latter basis is used to compare coals when the moisture and ash contents differ significantly. Comparisons lose their significance because a high percentage of ash or moisture makes the yield of coke or liquor artificially high and those of other products correspondingly low. The calculation of moisture- and ash-free basis assumes that all ash remains in the coke and that all moisture in the coal is recovered as liquor.

#### Properties of Tar

The tar yields are affected by coal rank, temperature of carbonization and free space above the coal charge. The temperature of carbonization is the most significant contributing factor in determining tar quality. Increased free space permits the vapors to remain longer at the higher temperature resulting in considerable variations in tar quality.

The effect of free space on tar quality is presented in table 2. Cracking of tar due to increased free space resulted in progressive increases in its specific gravity, naphthalene yield, anthracene yield, except for the 9-inch free space and a reduction in tar acids, bases, and neutral oils. It is interesting to note that unlike naphthalene, the anthracene yield was slightly less at the 9-inch free space for all tests. There was no significant change in the residue yield.

The chemical composition of tars and pitches is presented in table 3. As expected, the carbon content increased and the hydrogen content decreased with progressive increases in the free space.

Quinoline (1) and benzene (free carbon) (5) insoluble values for the tars and pitches, as well as the softening point of the pitches were determined. These are critical factors, commercially important, in determining the suitability of coal tar pitches as electrode binders. The tar values were determined on the whole tar and the pitch values were determined on the +350°C fraction of the tar. The cube-in-air method was used to determine the softening point of the pitches. The results are presented in table 4.

Table 1. - Yields of carbonization products, as-carbonized basis

Coal number	Free space inches	Yields, weight-percent										Yields per ton of coal		
		Coke	Gas	Tar	Light oil	Liquor	Free ammonia	Total	Gas	Tar	Light oil in gas	Ammonium sulfate, pounds		
1161	1	65.9	18.2	5.8	1.13	8.8	0.160	100.0	10,450	11.9	2.81	21.3		
	3	65.6	16.5	5.5	1.17	10.2	.177	99.1	10,640	11.2	3.25	23.6		
	6	65.7	16.2	5.5	1.23	10.3	.180	99.1	10,770	11.1	3.42	22.8		
	9	65.5	16.3	5.3	1.13	10.0	.209	98.4	10,790	10.2	3.16	23.1		
1166	1	66.3	14.9	7.6	1.28	8.8	.166	99.0	10,400	15.8	3.57	25.3		
	3	66.3	15.3	8.1	1.24	8.0	.168	99.1	10,750	16.5	3.45	23.7		
	6	66.4	15.3	7.7	1.31	7.6	.173	98.5	10,700	15.2	3.64	22.6		
	9	66.4	15.2	7.5	1.37	7.7	.174	98.3	10,850	14.8	3.81	22.1		
1167A	1	70.8	13.6	6.7	1.16	7.0	.163	99.4	10,140	13.7	3.23	23.2		
	3	70.7	13.9	6.4	1.15	6.2	.161	98.5	10,290	12.9	3.20	20.8		
	6	70.7	13.9	6.2	1.24	6.1	.164	98.3	10,350	12.1	3.47	20.0		
	9	70.7	14.1	6.1	1.21	6.3	.149	98.6	10,490	11.9	3.36	18.8		

Table 2. - Specific gravity and component tar yields

Coal number	Void space inches	Specific gravity of tar	Yields, gallons per ton										Yields, pounds per ton			
			Acids	Bases	Neutral oils	Residue	Olefins	Aromatics	Maphthalenes	Naphthalene	Anthracene	Paraffins and	Maphthalenes	Naphthalene	Anthracene	
1161	1	1.17	0.52	0.33	3.50	6.82	0.39	2.95	0.16	5.36	2.81					
	3	1.19	.35	.27	2.89	6.60	.31	2.52	.06	7.42	3.58					
	6	1.20	.20	.22	2.31	7.10	.25	2.04	.02	8.70	5.25					
	9	1.23	.11	.15	1.63	7.03	.17	1.45	<.01	9.55	4.71					
1166	1	1.16	.78	.32	3.95	10.26	.33	3.52	.10	3.57	1.36					
	3	1.18	.55	.28	3.69	10.87	.32	3.33	.04	7.20	2.34					
	6	1.20	.25	.24	2.57	10.89	.29	2.26	.02	10.32	3.27					
	9	1.21	.20	.22	2.20	10.86	.24	1.95	.01	11.59	2.52					
1167A	1	1.17	.69	.27	3.50	8.68	.31	3.14	.09	4.14	1.92					
	3	1.19	.37	.26	2.41	8.82	.20	2.19	.03	7.53	3.12					
	6	1.22	.21	.18	1.98	8.54	.21	1.76	.01	8.97	3.31					
	9	1.22	.17	.17	1.78	8.57	.21	1.57	.01	9.92	2.95					

Table 3. - Effect of free space on the chemical composition of tar and pitch

Void space, inches	Tar				Pitch			
	1	3	6	9	1	3	6	9
Coal 1161								
Hydrogen.....	5.7	5.2	5.0	4.7	4.8	4.4	4.3	3.9
Carbon.....	90.5	91.4	92.7	93.1	92.3	92.8	93.8	94.2
Nitrogen.....	1.1	1.2	1.1	1.0	1.4	1.3	1.2	1.0
Oxygen.....	2.2	1.7	0.7	0.7	1.1	1.1	0.3	0.4
Sulfur.....	0.4	0.4	.4	.4	0.3	0.3	.3	.3
Ash.....	.1	.1	.1	.1	.1	.1	.1	.2
Coal 1166								
Hydrogen.....	5.4	5.0	4.8	4.7	4.9	4.7	4.6	4.2
Carbon.....	89.7	90.4	90.8	91.1	90.5	91.0	91.9	92.1
Nitrogen.....	1.3	1.3	1.2	1.1	1.5	1.4	1.3	1.3
Oxygen.....	2.5	2.2	2.1	2.0	2.1	2.0	1.3	1.6
Sulfur.....	1.0	1.0	1.0	1.0	0.8	0.7	0.7	0.7
Ash.....	0.1	0.1	0.1	0.1	.2	.2	.2	.1
Coal 1167A								
Hydrogen.....	5.8	5.4	5.1	5.0	4.9	4.7	4.6	4.4
Carbon.....	90.3	92.0	91.5	92.0	91.1	91.6	92.0	92.2
Nitrogen.....	1.3	1.3	1.3	1.3	1.5	1.4	1.4	1.3
Oxygen.....	1.4	0.4	1.0	0.6	1.7	1.5	1.2	1.3
Sulfur.....	1.0	.8	1.0	1.0	0.7	0.7	0.7	0.7
Ash.....	0.2	.1	0.1	0.1	.1	.1	.1	.1

Table 4. - Effect of free space above coal charge on quinoline and benzene insolubles

Coal number	Void space, inches	Tar <sup>1</sup>		Pitch <sup>1</sup>		Softening point, °C
		Quinoline insolubles	Benzene insolubles	Quinoline insolubles	Benzene insolubles	
1161	1	1.70	6.61	3.85	25.95	119.0
	3	2.73	8.17	3.96	24.25	105.0
	6	4.84	11.29	8.87	28.33	110.0
	9	11.07	17.42	22.03	32.55	138.0
1166	1	2.26	8.64	2.82	22.55	96.8
	3	4.13	11.60	4.78	26.55	101.0
	6	7.29	14.26	9.14	28.33	94.0
	9	11.15	18.76	14.34	30.87	85.8
1167A	1	2.57	7.66	2.86	21.75	94.0
	3	3.87	10.34	4.73	23.70	94.3
	6	6.39	12.47	7.60	25.15	82.3
	9	9.50	15.46	12.15	27.85	85.0

<sup>1</sup>Weight-percent for tar and pitch.

The insolubility values for all tars and pitches increased with increasing free space. There were marked increases at the 9-inch free space for all tests, indicating the formation of insoluble high boiling hydrocarbons.

#### Properties of Gas

Properties of byproduct gas vary with carbonizing conditions as well as with coal characteristics. An investigation (9) of the gas yielded by coals carbonized by the BM-AGA method at 900°C showed that the physical and chemical properties of the gas depend on the rank of coal.

The yield of carbonization gas increases with increased carbonization temperature; similarly, maintaining the effluent vapors at elevated temperatures by increasing the free space above the coal charge exposes the vapors to high temperatures for a longer time resulting in degradation of the volatile material with a still greater increase in the gas yield. Davis and Auvil (3) have attributed this increase to greater cracking of hydrocarbons in the enlarged free space. Table 1, confirms these results, in that the gas yield increases with increased free space.

The chemical and physical properties of the gas are presented in table 5. Two important properties of gas are its heating value and hydrogen sulfide content. The heating value, generally considered to be the most important property of byproduct gas, is presented on both the cubic foot and pound-of-coal basis. The greatest heat recovery for the longest exposure time of gas in the retort was 112 Btu per pound of coal (1167A) or a gain of 224,000 Btu per ton of coal. Coal 1161 showed a steady decline in heating value with increased exposure time.

The hydrogen sulfide content of the gas, calculated to grains per 100 cubic feet of gas, is becoming increasingly important because of air pollution restrictions, and must be reduced to limited concentrations before disposal. Results indicate that the formation of hydrogen sulfide is related to exposure time; however, the concentration of hydrogen sulfide in the byproduct gas is dependent on the sulfur content of the coal and is not related to coal rank. Although the sulfur content for coal 1167A (1.4 percent) was higher than that for coal 1161 (0.6 percent), the net increase in hydrogen sulfide, attributed to free-space cracking, was only 14.8 percent, compared with 26.0 percent for coal 1161.

#### Light Oil

The composition of light oil, like the tar, is a function of the carbonizing conditions of which temperature, free space above the coal charge, and the contact time of the gas in the hot free space are the most important; however, the total yield of light oil under normal carbonizing conditions is dependent largely upon the rank of the coal.

Benzene, the principal constituent of the light oil, is a decomposition product whose formation is accelerated under conditions favorable to cracking effluent vapors.

The percent composition of benzene in the light oil, as presented in table 6, progressively increased with an increase in free space, whereas all other constituents of light oil were adversely affected by the free space increases.

The total light oil yield reached a maximum at the 6-inch free space for the coal blends and at the 9-inch free space for the straight coal.

Table 5. - Chemical and physical properties of gas

Coal number	Void space, inches	Composition, dry, volume-percent					Heating value		Hydrogen sulfide grains per 100 cu.ft.
		Hydrogen	Carbon monoxide	Methane	Ethane	Ethylene	Btu per cu.ft.	Btu per lb.coal	
1161	1	60.87	5.98	25.78	2.43	5.03	618	3,235	131
	3	62.13	6.07	24.51	2.15	5.14	608	3,231	157
	6	64.01	5.07	23.79	1.60	5.53	600	3,180	157
	9	63.29	5.91	27.40	1.08	2.32	576	3,121	165
1166	1	59.38	6.49	30.08	1.42	2.63	603	3,133	638
	3	59.37	6.13	30.11	1.56	2.83	608	3,268	714
	6	59.09	6.45	30.97	0.92	2.57	601	3,221	707
	9	61.87	4.52	29.85	.75	2.96	596	3,189	828
1167A	1	63.91	4.31	28.81	1.30	1.67	583	2,956	561
	3	61.94	5.12	30.05	0.85	2.04	587	3,020	600
	6	61.98	5.15	30.08	.70	1.29	581	3,007	606
	9	61.91	4.85	30.94	.56	1.74	585	3,068	644

Table 6. - Composition of light oil, gallons per ton

Coal number	Void space, inches	Composition, dry, volume-percent				
		Benzene	Toluene	m,p-xylene	o-xylene	Ethylbenzene
1161	1	2.24	0.38	0.12	0.05	0.01
	3	2.65	.42	.14	.04	.006
	6	2.91	.40	.09	.01	.004
	9	2.89	.22	.04	.01	-
1166	1	2.77	.64	.13	.02	.004
	3	2.79	.55	.08	.02	.003
	6	3.13	.45	.05	.01	.001
	9	3.34	.42	.04	.01	.001
1167A	1	3.05	.06	.10	.02	.013
	3	3.05	.05	.07	.02	.003
	6	3.39	.04	.03	.01	.001
	9	3.30	.03	.03	.01	.001

### Properties of Coke

The physical properties of the cokes were determined by standard methods of the American Society for Testing Materials (2). The tumbler indices, 1-inch stability and 1/4-inch hardness, are the only coke properties reported as these parameters are most commonly used in evaluating metallurgical coke.

Variations of free space had no effect on the coke yield. The only significant change in the coking properties was for coal 1166 in which the 1-inch stability index was progressively lowered from 33 for the 1-inch free space to 28 for the 9-inch free space. The stability and hardness indices for both coal blends remained essentially the same.

### CONCLUSIONS

The yields of carbonization products are influenced by the rank of coal used and the temperature of carbonization. The primary decomposition is influenced by the rate of heating and the secondary decomposition by the time of contact of the vapors while in the hot retort and is dependent on the volume of free space per unit volume of charge.

The cracking of tar due to increased free space resulted in progressive increases in specific gravity, naphthalene yield, anthracene yield (except for the 9-inch free space test) and a reduction in tar acids, bases, and neutral oils.

Free space increases had no effect on the coke yield or coke properties except for the 1-inch tumbler stability for coal (1166) which was progressively lowered with increased free space.

The light oil yield was increased and reached a maximum at the 6-inch free space for the coal blends, and the 9-inch free space for the straight coal.

There was a progressive increase in gas yield, with the greatest variation of 500 cubic feet per ton of coal and the heat recovery for the longest exposure of gas in the retort was 112 Btu per pound of coal.

Increased free space above the coal charge during carbonization, permitted longer residence time of the vapors at a specific temperature and improved the quality of the byproducts. However, since coke is the major and most valuable product of coal carbonization, it would be economically infeasible to decrease the capacity of commercial ovens. In recognition of this, the Bureau of Mines is investigating the upgrading of volatile materials, in a separate cracking unit, outside of the coking furnace. Results of this investigation will be published in a subsequent report.

## REFERENCES

1. American Society for Testing Materials. Bituminous Materials, Soils, Skid Resistance, Part II, March 1969, pp. 701-704.
2. American Society for Testing Materials, ASTM Standards on Coal and Coke, 1954, 155 pp.
3. Davis, J. D. and S. Auvil. High Temperature Carbonization of Coal. Ind. & Eng. Chem., vol. 27, April 1935, p. 459.
4. Porter, H. C. Improvement of Design of Coal Carbonization Equipment. Ind. & Eng. Chem., vol. 24, 1932, pp. 1363-1368.
5. Reynolds, D. A., and C. R. Holmes. Procedure and Apparatus for Determining Carbonizing Properties of American Coals by the Bureau of Mines-American Gas Association Method. BuMines Tech. Paper 685, 1946, 35 pp.
6. Staff, Division of Bituminous Coal. Comparative Evaluation of Coking Properties of Four Coals. BuMines Inf. Cir. 8010, 1961, 22 pp.
7. Walters, J. G., and G. W. Birge. Duplicability Studies of the BM-AGA Test Method and Correlation with Industrial Coking. BuMines Rept. of Inv. 5467, 1959, 16 pp.
8. Wolfson, D. E., G. W. Birge, and J. G. Walters. Comparison of Properties of Coke Produced by BM-AGA and Industrial Methods. BuMines Rept. of Inv. 6354, 1964, 19 pp.
9. Wolfson, D. E., and D. A. Reynolds. Yields and Properties of Gases From BM-AGA Carbonization Tests at 900°C. BuMines Tech. Paper 693, 1946, 12 pp.

**LIGHT-INDUCED CHEMILUMINESCENCE IN DERIVATIVES OF COAL AND PETROLEUM**

Raymond E. Markby, R. A. Friedel, Sidney Friedman, and Heinz W. Sternberg

Pittsburgh Coal Research Center, U. S. Bureau of Mines,  
4800 Forbes Avenue, Pittsburgh, Pa. 15213

**INTRODUCTION**

In connection with work requiring the use of a liquid scintillation spectrometer for the determination of radioactive methyl groups introduced into coal, we discovered that solutions of alkylated coal exhibited chemiluminescence when exposed to light in the presence of air. We subsequently found that solutions of other products derived from coal and petroleum also exhibited chemiluminescence. In this paper we report our observations and suggest a mechanism for this light-induced chemiluminescence in products derived from coal and petroleum.

**EXPERIMENTAL**

Materials Investigated — The materials investigated are described in table 1.

**TABLE 1. - Materials Tested**

<u>Material</u>	<u>Description</u>
Coal tar I	High temperature coal tar from Pocahontas No. 3 (lvb) coal prepared in 1% yield by Bm-AGA method. <sup>a/</sup>
Coal tar II	Commercial high temperature coal tar.
Coal asphaltenes	Obtained by combining samples from several coal hydrogenation runs carried out at Pittsburgh Coal Research Center.
Methylated coal Ethylated coal Butylated coal	Prepared by reductive alkylation of Pocahontas No. 3 (lvb) vitrain. <sup>b/</sup>
Petrolenes I	Pentane soluble portion of straight run residual asphalt (Venezuelean crude) 85/100.
Asphaltenes I	Pentane insoluble, benzene soluble portion (20%) of above asphalt.
Petrolenes II	Pentane soluble portion of straight run residual asphalt (Californian crude) 85/100.
Asphaltenes II	Pentane insoluble, benzene soluble portion (21%) of above asphalt.

<sup>a/</sup> Technical Paper 685, U. S. Government Printing Office, Washington, D. C., 1946.

<sup>b/</sup> H. W. Sternberg and C. L. Delle Donne, "Solvation and Reductive Alkylation of Coal via a Coal Anion Intermediate." Preprints of Papers presented at the Division of Fuel Chemistry, Atlantic City, N. J., September 8-13, 1968.

**Apparatus** — A tensor\* lamp with a GE 1133 bulb (rated 32 candle power at 6 V. and 3.9 A.) was used as a light source and a liquid scintillation spectrometer, model 2101 by Packard Instruments Company was used to detect light emission. The quantum efficiency of the instrument was 16% at 3800 Å, 4% at 5500 Å, 1% at 6000 Å, and 0% at 6500 Å.

**Procedure** — One-tenth to 5 milligrams of the material dissolved in 20 ml. of toluene was placed in a 22 ml. counting vial provided with a screw cap. The vial was irradiated by a tensor lamp at a distance of 1 cm. between light bulb and wall of vial for a period of one minute. The vial was then placed in the cavity of the liquid scintillation spectrometer and counting was started 30 seconds after the irradiation had been completed. To obtain chemiluminescence decay curves, the intensity of light emission (in counts per 0.1 minute) was recorded at 30 second intervals.

## RESULTS

**Chemiluminescence Decay Rates** — The count rate of a sample as determined by the liquid scintillation spectrometer is proportional to the intensity,  $I$ , of the emitted light. The decay of chemiluminescence intensity,  $I$ , with time was determined for the materials listed in table 1. In all cases straight line relationships were obtained when  $I^{-1/2}$  was plotted vs. time. In all cases the straight line relationship held up to at least 85% completion. A typical chemiluminescence decay curve as obtained for butylated coal is shown in figure 1. The arrow marks 92% completion.

**Spectral Region of Chemiluminescence** — Qualitative information on the spectral region of the light emitted was obtained by wrapping the sample vial after irradiation in various Kodak Wratten Gelatin filters of known transmittance and recording the count rate. A zero count rate indicated complete absorption, a normal count rate no absorption. By this method we established that the light emitted during chemiluminescence was in the 4800-5200 Å region.

**Wavelength of Irradiating Light** — We were interested in determining whether irradiation with red light, i.e., light in the lower energy region of the visible spectrum is capable of inducing chemiluminescence. A solution of 10 mg. of Petrolenes I (see table 1) in 20 ml. toluene was irradiated for 1 minute with a red filter (transmission in the 6500 Å region) placed between tensor lamp and sample. The irradiated sample emitted light in the same spectral region as a sample irradiated with white light.

**Intensity of Chemiluminescence** — The chemiluminescence intensities of the various materials listed in table 1 were obtained by determining count rates after irradiation. The results are summarized in table 2.

The chemiluminescence of irradiated solutions can be detected by visual observation. A vial containing 20 mg. of petrolenes I in 20 ml. of toluene emits a greenish-blue light which is clearly visible to the dark-adapted eye. The intensity of the light emitted immediately after irradiation of this sample corresponded to about  $10^6$  counts per minute. The light remained visible for about 20 minutes after which time the count had dropped to approximately  $2 \times 10^4$  counts per minute.

\* Reference to a company or product name is made to facilitate understanding and does not imply endorsement by the U. S. Bureau of Mines.

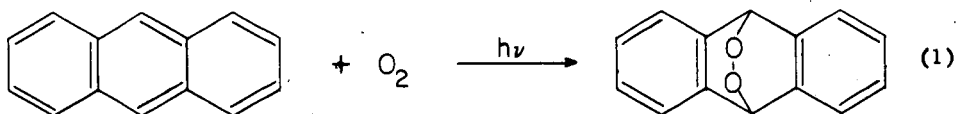
TABLE 2. - Intensity of chemiluminescence in products derived from coal and petroleum

<u>Material</u>	<u>Intensity, counts/min./mg.</u>	<u>Relative intensity</u>
Coal tar I	$1.6 \times 10^3$	1.0
Coal tar II	$6.2 \times 10^3$	3.9
Coal asphaltenes	$7.1 \times 10^4$	$4.4 \times 10$
Methylated coal	$3.8 \times 10^6$	$2.4 \times 10^3$
Ethylated coal	$3.8 \times 10^5$	$2.4 \times 10^2$
Butylated coal	$2.0 \times 10^5$	$1.3 \times 10^2$
Petrolenes I	$7.9 \times 10^3$	4.9
Petroleum asphaltenes I	$9.0 \times 10^3$	5.6
Petrolenes II	$4.3 \times 10^4$	$2.7 \times 10$
Petroleum asphaltenes II	$6.5 \times 10^4$	$4.1 \times 10$

### DISCUSSION

We believe that the light-induced chemiluminescence we observed involves photo-sensitized addition of oxygen to acene-type ring systems to form labile endoperoxides followed by decomposition of these endoperoxides with emission of light. This view is consistent with the experimental evidence and is based on the following considerations.

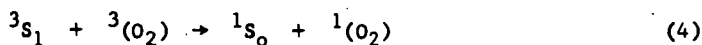
Moureau, Dufraisse and their co-workers<sup>1/</sup> have shown that acene-type hydrocarbons such as anthracene react with oxygen under the influence of sunlight or artificial white light to form endoperoxides:



The mechanism<sup>2/</sup> of this light-induced endoperoxide formation involves excitation of ground state triplet  $\text{O}_2(^3\Sigma_g^-)$  to excited singlet  $^1\text{O}_2(^1\Delta_g \text{ or } ^1\Sigma_g^+)$  by a sensitizer S. The sensitizer  $^3\text{S}_0$  absorbs light energy to give an excited singlet state ( $^1\text{S}_1$ ) which is converted by intersystem crossing to a triplet state



The sensitizer in its triplet state exchanges energy with triplet ground state oxygen to give singlet oxygen which adds to anthracene (A) to form the endoperoxide ( $\text{AO}_2$ ):



Decomposition of the acene-type endoperoxides formed in coal and petroleum derived products with emission of light



explains the observed chemiluminescence. Rubrene endoperoxide, for example, decomposes at elevated temperature with emission of greenish-yellow light,<sup>3)</sup> visible to the dark-adapted eye, to give oxygen and rubrene. On the basis of recent work<sup>4,5)</sup> the emission of light observed during the decomposition of peroxides is attributed to transition of excited van der Waals type "double molecules" [ $^1O_2 + ^1O_2$ ] to ground state oxygen  $^3O_2$ . Depending on the state of the  $(^1O_2)_2$  double molecule, light of different wavelengths can be emitted. The transition  $(^1\Delta_g + ^1\Delta_g) \rightarrow 2\ ^3\Sigma_g^-$  produces light of 6335 Å (orange-red),  $(^1\Delta_g + ^1\Sigma_g^+) \rightarrow 2\ ^3\Sigma_g^-$  light of 4780 Å (blue) and  $(^1\Sigma_g^+ + ^1\Sigma_g^+) \rightarrow 2\ ^3\Sigma_g^-$  light of 3800 Å (ultraviolet) wavelength. The light observed in our experiments was in the 5000 Å region, corresponding to a  $(^1\Delta_g + ^1\Sigma_g^+) \rightarrow 2\ ^3\Sigma_g^-$  transition.

The formation of an excited double molecule,  $(^1O_2)_2$ , resulting from the interaction of two endoperoxide molecules,  $AO_2$



followed by rapid transition of  $(^1O_2)_2$  to ground state with emission of light



is consistent with the observed decay rate, i.e., with a straight line relationship between  $1/I^{1/2}$  and time. According to (6) and (7), the rate of light emission,  $I$ , is proportional to the  $[AO_2]^2$  concentration and consequently  $I^{1/2}$  may be substituted for the  $[AO_2]$  concentration. In the integrated rate equation

$$1/c = 1/c_0 + kt \quad (6a)$$

the instantaneous concentration  $c$  is replaced by  $I^{1/2}$  and the initial concentration by  $I_0^{1/2}$ . This leads to the observed straight line relationship between  $1/I^{1/2}$  and time

$$1/I^{1/2} = 1/I_0^{1/2} + kt. \quad (6b)$$

According to equation (5), singlet oxygen (in either the  $^1\Delta_g$  or  $^1\Sigma_g^+$  state) is required for the formation of endoperoxide, a fact which determines the minimum of irradiating energy required to excite ground state triplet oxygen to excited singlet oxygen. The excitation energies for ground state oxygen ( $^3\Sigma_g^-$ ) to singlet oxygen ( $^1\Delta_g$ ) is 22.5 kcal (12,700 Å) and to singlet oxygen ( $^1\Sigma_g^+$ ) is 37.5 kcal (7620 Å).<sup>8</sup> Consequently, light in the red region (44 kcal, 6500 Å), should contain sufficient energy for the excitation of ground state triplet to excited singlet oxygen, provided that sensitizers are present capable of absorbing this energy (equation 2) and of intersystem crossing (equation 3) to a triplet level whose energy lies above the energy (22.5 resp. 37.5 kcal) required for the  $^3O_2$  to  $^1O_2$  excitation. That sensitizers meeting these requirements are present in products derived from coal and petroleum follows from the observation that irradiating light in the red region (6500 Å) produces chemiluminescence in the blue-green (5000 Å) region. The formation of endoperoxide by irradiation in the presence of a sensitizer (methylene blue) absorbing in the red (6400 Å) region was recently demonstrated<sup>6)</sup> in the case of rubrene. That singlet oxygen is involved in our light-induced chemiluminescence reaction is supported by the fact that addition of an excess of tetramethylethylene (TME) prior to irradiation reduces the chemiluminescence intensity by 98%. TME was shown to act as a captor for singlet oxygen and as an inhibitor in the photosensitized oxidation of rubrene.<sup>8)</sup>

Normal acene endoperoxides, containing a 9,10 bridge, are stable at room temperature, while the endoperoxides observed in coal and petroleum derivatives decompose with chemiluminescence at room temperature. This behavior is similar to that reported for the 1,4-endoperoxides formed by certain 1,4-dimethoxyanthracenes,<sup>7/</sup> and suggests that the chemiluminescent endoperoxides in coal and petroleum derivatives are also of the 1,4 type and consequently contain activating substituents in the 1,4 positions. These substituents may be ethers present in the starting material, or in the case of alkylated coal, formed from OH groups during the alkylation. Moreover, the substituents undoubtedly need not be ethers, but probably could be any sufficiently electron-releasing groups, such as alkyl groups. This effect is illustrated by the 100-fold greater rate of formation of endoperoxide from 9,10-dimethylanthracene and singlet oxygen than from anthracene and singlet oxygen.<sup>8/</sup> The activating effect of alkyl groups is undoubtedly the reason why alkylated coal exhibits chemiluminescence which is 2 to 3 orders of magnitude higher in intensity than that of the other materials examined (table 2).

#### CONCLUSIONS

Solutions of coal tar, coal asphaltene and alkylated coal as well as petroleum asphalt exhibit chemiluminescence when exposed to oxygen and light. This chemiluminescence is believed to be due to decomposition of endoperoxides formed by photooxidation of acene-type compounds present in products derived from coal and petroleum.

#### REFERENCES

1. For a comprehensive review of their work, see W. Bergmann and M. J. McLean, *Chem. Rev.* 28, 367 (1941) and Yn. A. Arbuzov, *Russian Chemical Reviews* 34, 558 (1965).
2. Foote, C. S., Wexler, S., Ando, W., and Higgins, R., *J. Am. Chem. Soc.*, 90, 975 (1968).
3. Moureau, C., Dufraisse, C., and Butler, C. L., *Compt. Rend.*, 183, 101 (1926).
4. Khan, A. U. and Kasha, M., *J. Am. Chem. Soc.*, 88, 1574 (1966).
5. Stauff, J. and Schmidkunz, H., *Z. Physik. Chem. (Frankfurt)*, 35, 295 (1962).
6. Wilson, T., *J. Am. Chem. Soc.*, 88, 2898 (1966).
7. Dufraisse, C., Rigaudy, J., Basselier, J., and Cuong, N. K., *Compt. Rend.*, 260, 5031 (1965).
8. Corey, E. J. and Taylor, W. C., *J. Am. Chem. Soc.*, 86, 3881 (1964).

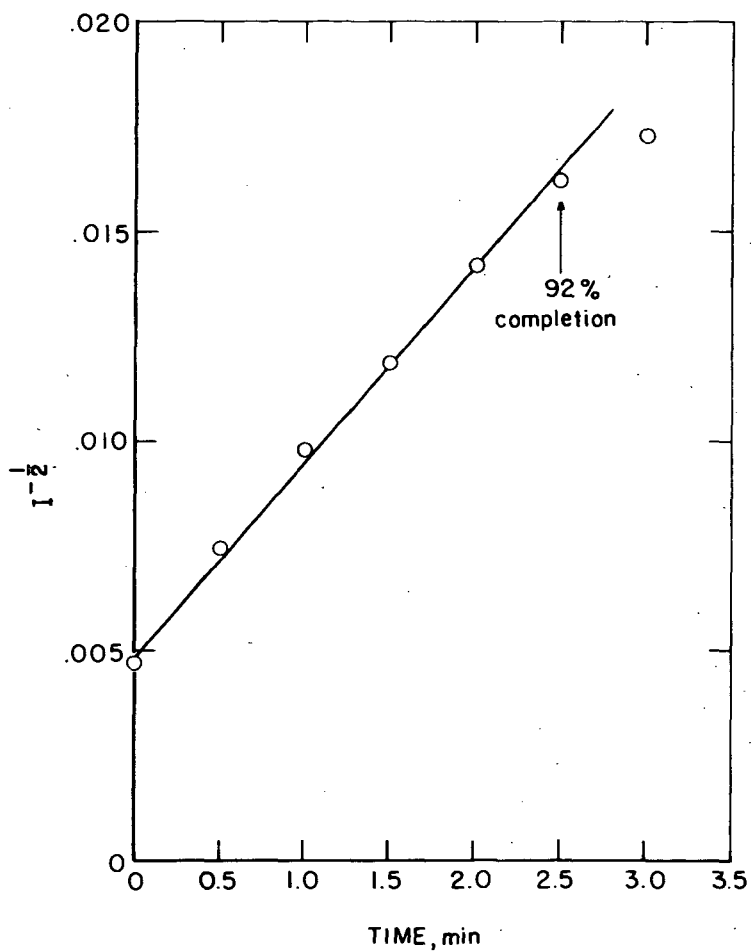


Figure 1-  $I^{-1/2}$  vs time curve of chemiluminescence  
decay for butylated coal.

L-11223

# The Carbonization of Aromatic Hydrocarbons

I. C. Lewis and L. S. Singer

Union Carbide Corporation  
Carbon Products Division  
Parma Technical Center  
Cleveland, Ohio 44101

## I. Introduction

Carbonization is the thermal conversion of organic materials to carbon and graphite. The overall transformation involves a complex series of chemical reactions and diffusion processes in both the liquid and solid state. The reaction sequence consists of the elimination of substituent atoms and groups from the organic molecule, aromatization, and subsequent polymerization to a large aromatic carbon framework.

Any organic material can be converted to carbon. Commercially, synthetic carbon and graphite are prepared from aromatic starting materials such as coal tar pitch and heavy petroleum residues. These raw materials consist largely of mixtures of compounds containing aromatic hydrocarbon and heterocyclic structures. We have found that the carbonization behavior of complex raw materials can be understood on the basis of the thermal reactions of relatively few, representative aromatic hydrocarbons. This paper reviews previous work and also presents results of our recent studies of the carbonization of several pure aromatic hydrocarbons.

## II. Chemical Constitution of Pitch

The carbonization of an organic material proceeds through an initial aromatic stage. Coal tar pitch is an example of such an aromatic stage formed during the pyrolysis of coal. There have been numerous compilations of the chemical constituents of coal tar pitch.<sup>(1, 2)</sup> These compilations include several hundred aromatic hydrocarbon and heterocyclic compounds. Table I lists the major aromatic hydrocarbon components that have been quantitatively determined in a typical coal tar pitch. The 13 structures shown constitute 13.6 percent of the entire pitch. The remainder of the material is composed of small amounts of hundreds of other aromatic compounds.

## III. Thermal Reactivity and Aromatic Structure

The aromatic hydrocarbon components of pitch vary widely in thermal reactivity. This thermal reactivity is directly related to molecular structure. Table II compares the effect of chemical structure on the thermal reactivity of a number of hydrocarbons. The thermal reactivity is indicated by the lowest temperature at which an initial reaction is observed. Also listed are the corresponding ionization potentials derived from the optical absorption frequencies of the longest wavelength p-bands.<sup>(3)</sup> It is apparent that thermal reactivity increases with decreasing ionization potential. The presence of substituent groups on the aromatic ring can significantly alter these thermal reactivities either by providing a reaction site, or by altering the relative bond strengths in the molecule.<sup>(4)</sup>

Table I

Some Aromatic Hydrocarbon Components of Coal Tar Pitch  
and their Occurrence in Weight Percent

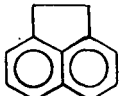
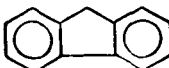
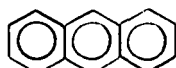
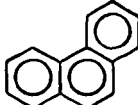
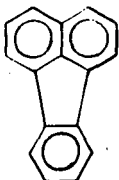
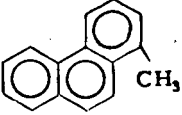
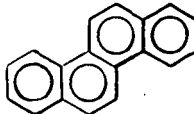
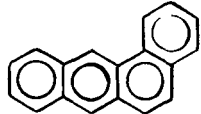
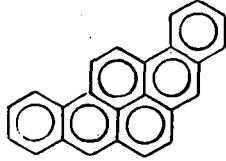
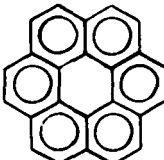
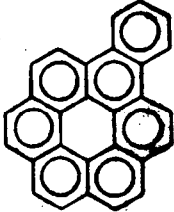
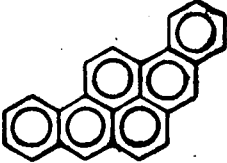
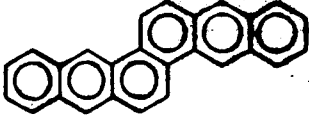
			
Acenaphthene 0.3	Fluorene 0.1	Anthracene	+ Phenanthrene 1.2
			
Fluoranthene 1.5	Pyrene 1.3	Methylphenanthrene 0.3	Chrysene 2.7
			
Benz-(a)-anthracene 0.7	Benzo-(a)-pyrene 3.6	3,4,9,10-Dibenzopyrene 1.5	
			
Coronene	Picene		

Table II

Relation of Thermal Reactivity to Aromatic Structure

Aromatic Hydrocarbon	Reaction Temp. °C	Ionization Potential (eV)
	637	7.24
	560	7.07
	535	6.86
	480	6.64
	411	6.23

#### IV. Effects of Chemical Structure on the Nature of the Final Graphite

The heat treatment of organic materials to 3,000°C results in carbons possessing basically the graphite structure. The degree of graphitization and the properties of synthetic carbons obtained at 3,000°C are determined largely by the structure of the starting material. This effect is illustrated by the data in Tables III and IV which give the X-ray semilattice spacings for 3,000°C carbons prepared from a variety of aromatic hydrocarbons:

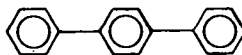
Table III includes well-graphitizing compounds which possess c-spacings between 3.354 and 3.363Å. Natural graphite has a c-spacing of 3.354Å. Table IV lists some poorly graphitizing materials. The high c-spacings, 3.370 to 3.44, obtained for these materials indicate a much more disordered carbon structure. It is not generally obvious from the initial chemical structures in Tables III and IV how well a given aromatic hydrocarbon will graphitize. For example, the 5-membered ring aromatic hydrocarbon acenaphthylene yields a well-ordered graphite, while the highly symmetrical molecule coronene gives rise to a poorly ordered graphite. However, sterically overcrowded and nonplanar molecules generally lead to more disordered graphite structures. <sup>(5)</sup>

#### V. Carbonization of Acenaphthylene and Terphenyl

The chemical transformations which occur during carbonization can be aptly demonstrated by the coking behavior of two representative aromatic hydrocarbons, acenaphthylene (I) and p-terphenyl (II). Acenaphthylene produces an extremely well-graphitizing carbon, while p-terphenyl yields a disordered, nongraphitizing carbon.



Acenaphthylene  
(I)



p-Terphenyl  
(II)

As with all organic materials, the carbonization of these hydrocarbons involves the removal of substituent hydrogen and the polymerization of the aromatic carbon residue. Three methods which we have found particularly useful for following these processes are: elementary analysis, X-ray, and diamagnetic susceptibility.

Figure 1 shows a plot of hydrogen content for acenaphthylene and p-terphenyl cokes versus heat-treatment temperature. The terphenyl does not react at all below 500°C. Between 500°C and 700°C the decrease in hydrogen content is more rapid for the terphenyl, while above 700°C the acenaphthylene dehydrogenation proceeds faster.

Figure 2 presents some X-ray data obtained by Ruland<sup>(6,7)</sup> for the same series of samples. The growth of average aromatic layer size,  $L_a$ , is plotted versus temperature. The terphenyl shows an extremely rapid growth of  $L_a$  to 800°C, followed by a much slower growth rate at higher temperatures. For acenaphthylene, the polymerization of aromatic layers is much more gradual below 700°C but eventually surpasses the terphenyl. <sup>(7)</sup>

Table III

Effects of Aromatic Structure on the  
c-Spacings of 3,000°C Carbons

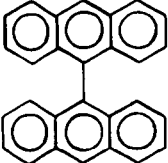
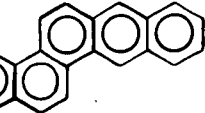
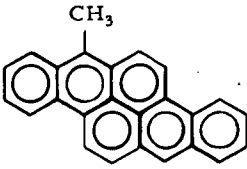
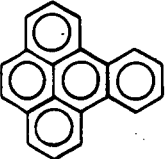
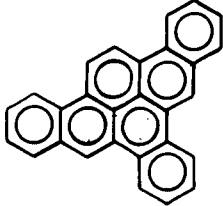
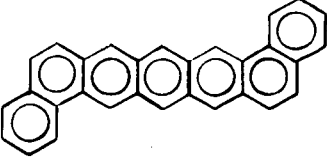
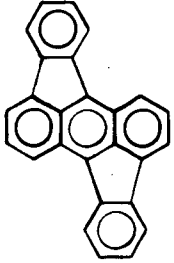
Structure	002, Å	Structure	002, Å
	3.354		3.357
	3.354		3.358
	3.356		3.358
	3.356		3.358
	3.356		3.363

Table IV

Effects of Aromatic Structure on the  
c-Spacings of 3,000°C Carbons

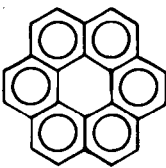
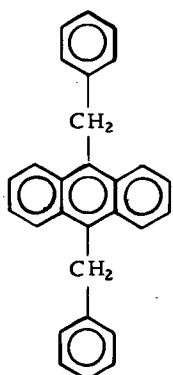
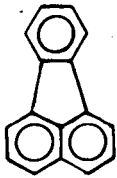
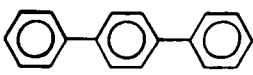
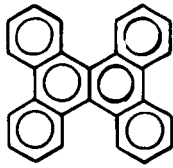
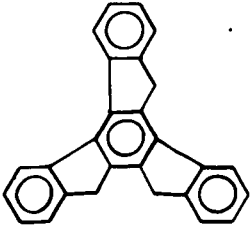
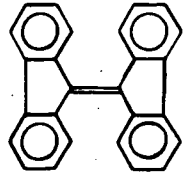
Structure	002, Å	Structure	002, Å
	3.370		3.41
	3.371		3.44
	3.373		
	3.385		3.44

Figure 3 contains a plot of magnetic susceptibility data obtained by Wagoner<sup>(8)</sup> for these two compounds heat treated to 3,000°C. The terphenyl shows a slight decrease in  $\chi$  between 500° and 700°C, and then an increase with temperature to a maximum at 3,000°C. The acenaphthylene shows a more pronounced dip in  $\chi$  between 500° and 800°C than observed for terphenyl. This decrease in susceptibility is presumably due to a paramagnetic contribution from free radicals. The acenaphthylene exhibits a lower diamagnetic susceptibility than terphenyl up to about 1,600°C, while above this temperature the aromatic layer growth is much more rapid for acenaphthylene.

All these data indicate that the aromatic polymerization process is much more rapid at low temperature for the more disordered terphenyl system. However, the initially-formed polymers from terphenyl are structurally not as suitable for continued aromatic growth to graphite as the much smaller polymers initially produced from acenaphthylene.

The dehydrogenation-polymerization process which leads to the formation of carbon is still poorly understood. This point is illustrated by the data plotted in Figure 4. From elementary analysis and X-ray data, the number of carbon and hydrogen atoms per fused aromatic molecule have been estimated and plotted as a function of temperature for both acenaphthylene and terphenyl cokes. Also included in Figure 4 is a theoretical plot of carbon versus hydrogen content for the most highly condensed aromatic hydrocarbon molecule. Up to about 600°C the acenaphthylene and terphenyl curves fall close to the theoretical line. The reactions occurring in this region appear to involve the removal of a hydrogen atom from the aromatic ring to form a simple free radical. At 700°C and above, multiple hydrogen atoms are eliminated leaving aromatic molecules with many unsubstituted edge sites. This process appears to proceed more readily for acenaphthylene than for terphenyl.

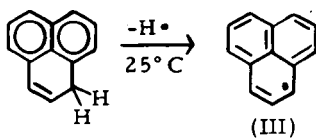
The nature of the bonding of the free electrons in these molecules is not clear. The interpretation of electron spin resonance measurements of materials in this region<sup>(9)</sup> is complicated by the onset of electrical conductivity and magnetic anisotropy.

## VI. Chemical Reactions of Carbonization

We can delineate the kinds of chemical reactions which occur during the early stages of coking by studying the carbonization of several aromatic hydrocarbons. Their initial reactions lead to the intermediates which control the subsequent course of carbonization. There are three types of thermal reaction processes which are important. (1) dehydrogenation, (2) rearrangement, and (3) polymerization. These reactions do not proceed in distinct steps, but occur continuously throughout the coking process. Several examples of these reactions follow.

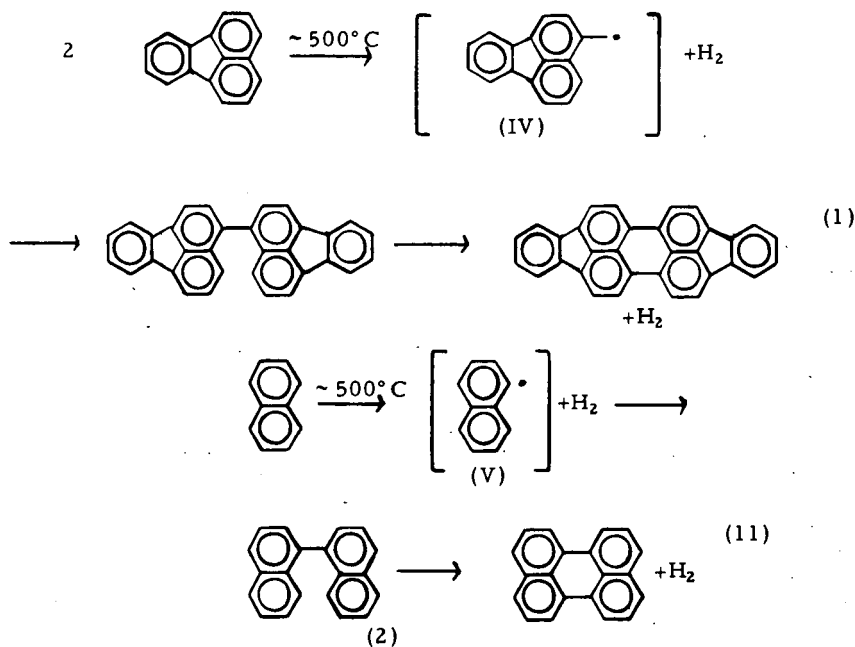
### A. Dehydrogenation

The initial reaction in carbonization involves the loss of a hydrogen atom from an aromatic hydrocarbon and leads to the formation of an aromatic free radical intermediate. If the free radical intermediate is stable, it can then be detected by electron spin resonance. In the liquid state, usually all but the most stable free radicals will rearrange or polymerize. The phenalenyl radical (III) is an example of an extremely stable free radical produced by simple hydrogen dissociation reaction at room temperature.

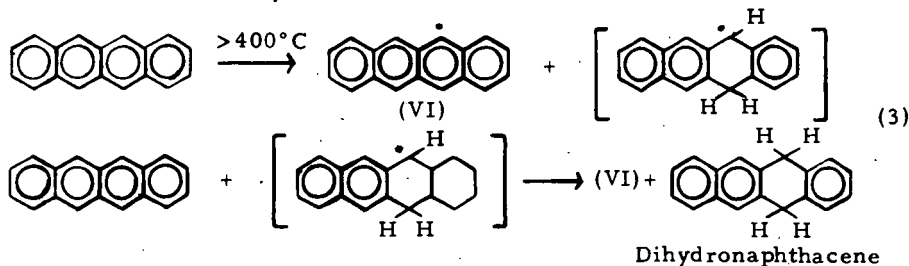


It can be well characterized by its simple ESR spectrum. <sup>(10)</sup>

The hydrocarbons fluoranthene and naphthalene polymerize directly with the direct loss of hydrogen. The unstable free radicals (IV) and (V) can be postulated as intermediates in these reactions.

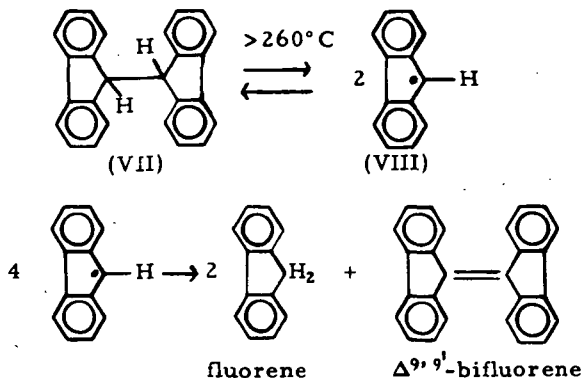


In many instances the dehydrogenation of aromatic hydrocarbons appears to involve bimolecular hydrogen transfer reactions. Hydrogenated aromatic hydrocarbons are often identified in the volatile products of carbonization. <sup>(4)</sup> These reactions usually occur at the most reactive site on the aromatic molecule. A typical hydrogen transfer sequence is illustrated for the hydrocarbon naphthacene:



The volatile 5,12-dihydronaphthacene is a major reaction product during the initial stages of reaction. It is not clear whether the intense but unresolved ESR signal observed during the onset of pyrolysis of naphthacene is due to the radical (VI).<sup>(12)</sup>

It should be pointed out that if there is a carbon-carbon single bond available, thermal cleavage will occur at this site. The thermally produced free radical can then participate in hydrogen transfer reactions. This reaction is illustrated in the pyrolysis of 9,9'-bifluorene (VII).

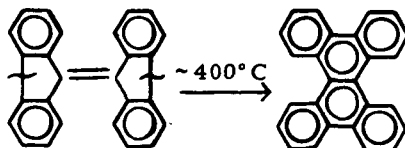


At about 260°C (VII) dissociates to produce the fluorenyl radical (VIII). This species has been detected by ESR.<sup>(12)</sup> At higher temperatures a hydrogen transfer reaction leads to fluorene and Δ<sup>9,9'</sup>-bifluorene as the major products. The reactive phenyl radicals produced from the pyrolysis of terphenyl also undergo hydrogen transfer processes, since benzene and biphenyl are among the reaction products.

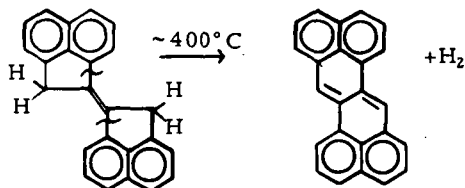
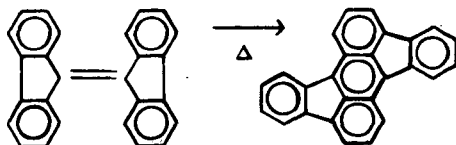
## B. Rearrangement Reactions

Perhaps the most complicating features of the early stages of carbonization are the thermal rearrangement reactions. They often make it impossible to predict from the starting structure whether a given compound will produce a well-graphitizing or a disordered carbon. Thermal rearrangement usually leads to a more stabilized aromatic ring system which can then become the building block for graphite growth. Several examples of the thermal rearrangement of aromatic hydrocarbons follows.

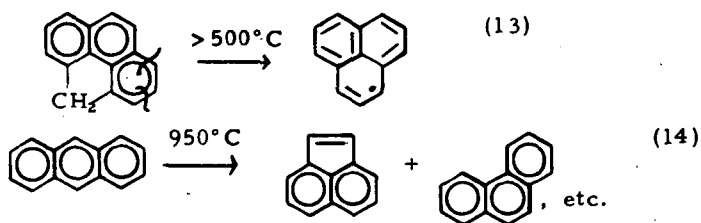
### 1. Conversion of Δ<sup>9,9'</sup>-bifluorene to tetrabenzonaphthalene:



## 2. Conversion of biacenaphthylidene to zethrene.

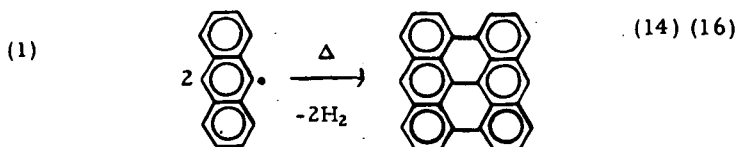
3. Formation of rubicene from  $\Delta^{9,9}$ -bifluorene.

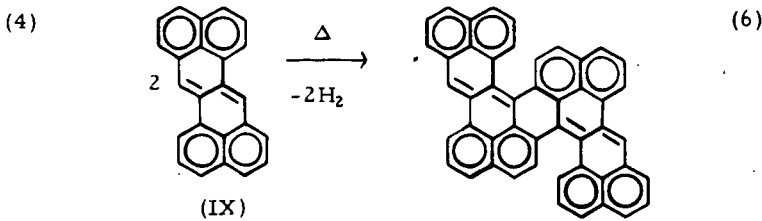
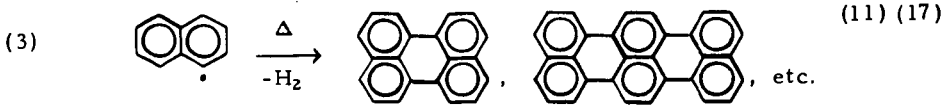
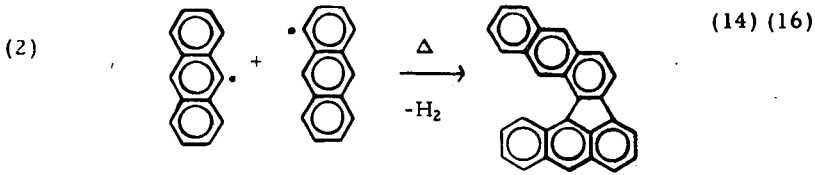
In some instances thermal rearrangement can involve a carbon-carbon bond cleavage within a condensed aromatic ring. These reactions are higher energy processes and are usually observed at very high temperatures, as in vapor phase pyrolysis.

C. Polymerization of Aromatic Radicals

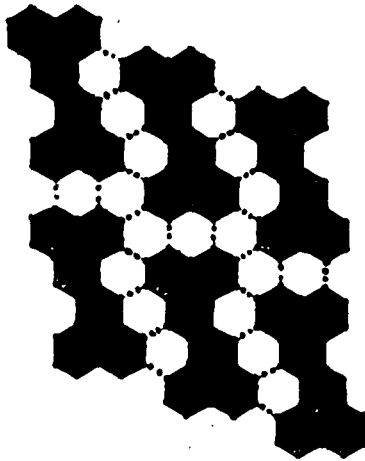
The formation of carbon involves the polymerization of aromatic free radicals. These polymerizations usually initiate in the liquid phase and lead to solid aromatic polymers. This step is an important stage in the graphitization process. <sup>(15)</sup>

Unlike conventional polymerization reactions which rapidly increase the molecular size, the aromatic polymerization appears to proceed in steps. <sup>(6)</sup> The following examples show the formation of dimers and trimers during the first stages of polymerization of aromatic radicals.





The most important criterion for obtaining a well-ordered graphite is to have the right "building blocks" from the standpoint of reactivity and steric configuration.<sup>18</sup> A molecule such as zethrene meets these requirements since it can polymerize at its most reactive positions and give rise to a condensed aromatic polymer without vacancies (see X). Nonplanar radical intermediates, such as those produced from  $\Delta^{9,9}$ -bifluorene or p-terphenyl, lead to disordered aromatic polymers which never truly graphitize.



(X)

## VII. Conclusions

The formation of synthetic carbon and graphite involves the thermal dehydrogenation and polymerization of aromatic hydrocarbons. The thermal reactivity and the course of carbonization are controlled by the structure of the starting aromatic molecule. More rapid reaction during the early stages of carbonization usually leads to a more disordered graphite structure.

Chemical studies on the pyrolysis of representative individual aromatic hydrocarbons show the importance of 3 types of thermal chemical reactions: (1) dehydrogenation, (2) rearrangement, and (3) polymerization. The nature of the final graphite and the course of carbonization appear to be related to the structure and reactivity of the aromatic free radical intermediates, which are the building blocks for subsequent carbonization and graphitization.

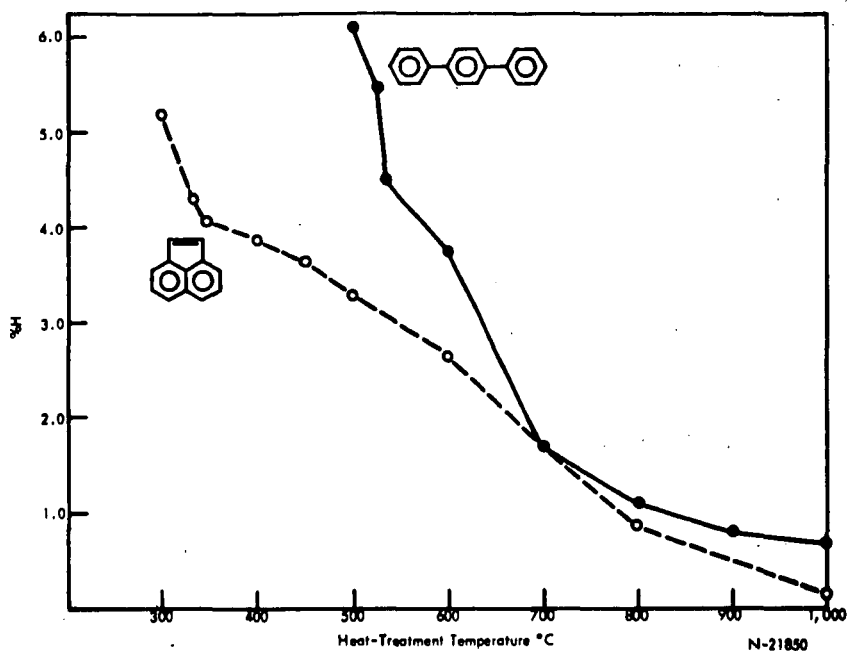


Figure 1. Elementary Analysis of the Products of Carbonization of Acenaphthylene and p-Terphenyl; Weight Percent Hydrogen vs. Heat Treatment Temperature

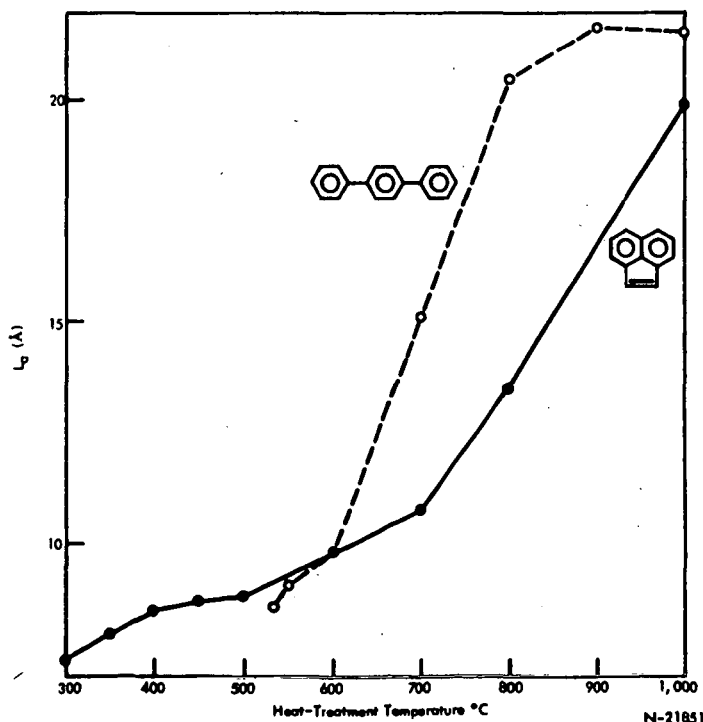


Figure 2. Aromatic Layer Growth in the Carbonization of Acenaphthylene and p-Terphenyl;  $L_p$  (Å) vs. Heat-Treatment Temperature.

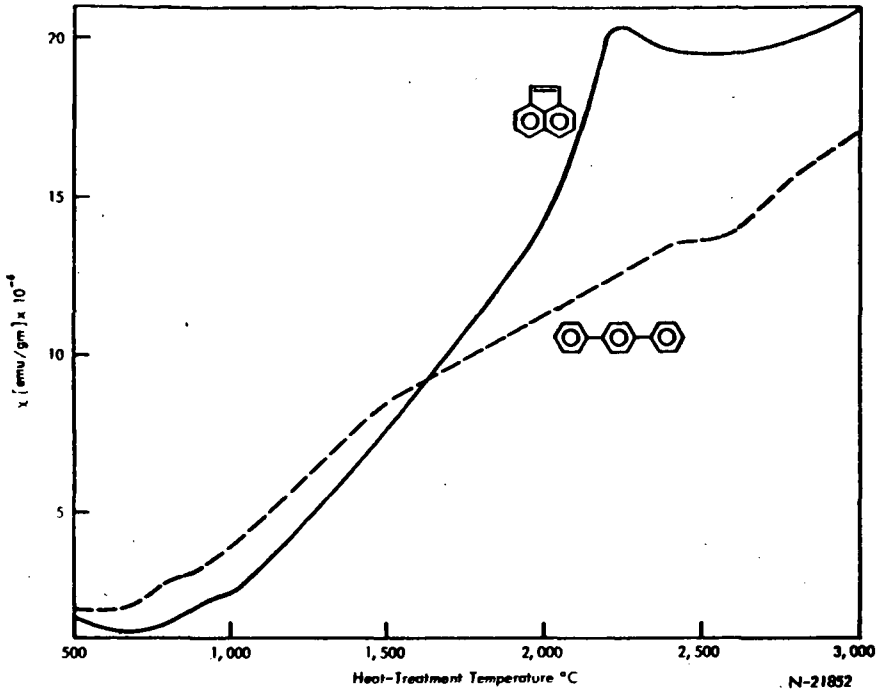


Figure 3. Static Magnetic Susceptibility of Acenaphthylene and p-Terphenyl as a Function of Heat-Treatment Temperature

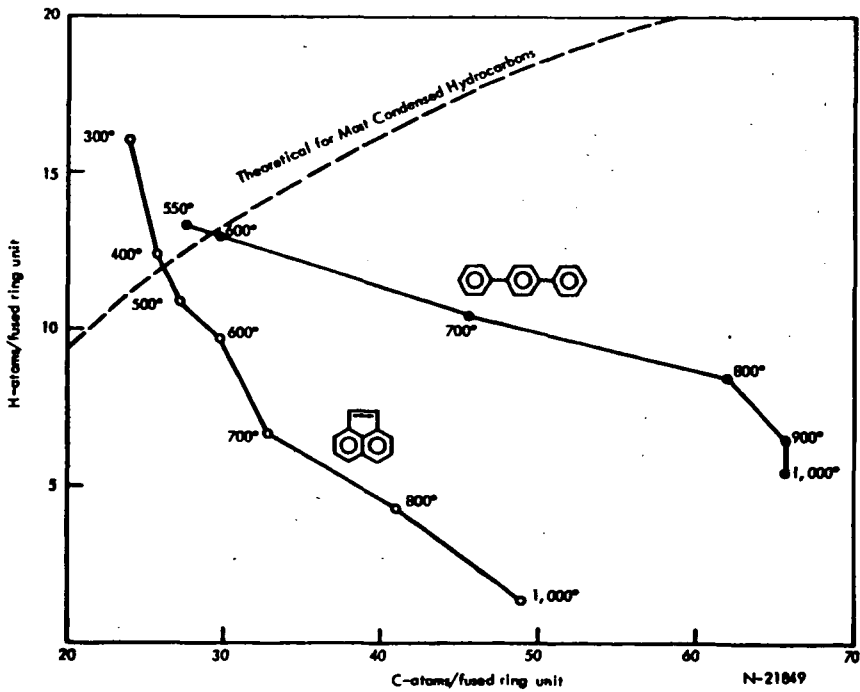


Figure 4. Dehydrogenation-Polymerization Diagram for Heat-Treated Acenaphthylene and p-Terphenyl

References

- (1) "The Coal Tar Data Book," Coal Tar Research Association, Oxford Road, Gomersal, Nr. Leeds, Percyland, Humphries and Co. Ltd., London 1963.
- (2) "Bituminous Materials: Asphalts, Tars, and Pitches," Vol. III, Interscience Publishers, New York, N. Y., (1966), pp. 139-216.
- (3) F. A. Matsen, *J. Chem. Phys.*, 24, 602 (1956).
- (4) I. C. Lewis and T. Edstrom, *J. Org. Chem.*, 28, 2050 (1963).
- (5) T. Edstrom and I. C. Lewis, *Carbon* 7, 85 (1969).
- (6) W. Ruland, *Carbon* 2, 365 (1965).
- (7) W. Ruland, unpublished results.
- (8) G. Wagoner, unpublished results.
- (9) L. S. Singer and A. R. Cherry, Abstracts of the 9th Carbon Conference, Boston, (1969).
- (10) For a review of ESR measurements of phenalenyl, cf., I. C. Lewis and L. S. Singer, *J. Phys. Chem.*, 73, 215 (1969).
- (11) K. F. Lang, H. Buffleb and J. Kalowy, *Chem. Ber.*, 90, 2888 (1957).
- (12) I. C. Lewis and L. S. Singer, *Carbon* 5, 373 (1967).
- (13) L. S. Singer and I. C. Lewis, *Carbon* 2, 115 (1964).
- (14) G. M. Badger, J. K. Donnelly, and T. M. Spotswood, *Aust. J. Chem.*, 17, 1147 (1964).
- (15) J. D. Brooks and G. H. Taylor, "Chemistry and Physics of Carbon," Volume 4, Marcel Dekker, Inc., New York, 1968, pp. 243-286.
- (16) K. F. Lang, and H. Buffleb, *Chem. Ber.*, 94, 1075 (1961).
- (17) G. H. Badger, "Progress in Physical Organic Chemistry," Vol. 3, 1 (1965).
- (18) I. C. Lewis and L. S. Singer, *Carbon* 7, 93 (1969).

STRUCTURAL CHANGES ACCOMPANYING  
COKE CALCINATION

M. P. Whittaker, F. C. Miller and H. C. Fritz

Great Lakes Research Corporation

INTRODUCTION

Although a voluminous number of articles have been published on the structural changes occurring in carbons upon heat treatment over a wide 1200°C-2800°C temperature range, similar information for the narrow 500°C-1200°C calcination range is rather sparse. A few articles<sup>1-4</sup> have been written in which properties such as density, electrical resistivity and pore structure have been correlated with temperature of calcination and time at maximum temperature. It is, however, difficult to relate the various experimental results and conclusions reported. In this study the progression of structural changes occurring during the calcination of four raw coke samples from different sources was followed using high temperature microscopy techniques. Concurrent with the examination of the topographical features, the transformation of the microstructure of the carbons was studied by means of x-ray diffraction and mercury porosimetry.

EXPERIMENTAL

The high temperature microscopic examinations were performed using a Leitz Ortholux microscope equipped with a Leitz vacuum heating stage. Thin polished sections (≈0.03" thick) of the cokes were placed on a hollow graphite cylinder encompassing a Pt + 10% Rh vs. Pt thermocouple which had been calibrated against the melting points of several pure compounds. The sample and sample holder were then radiantly heated at a rate of ca. 30°C/minute in an inert atmosphere. A holding time of 5-10 minutes was allowed at each temperature to establish thermal equilibrium. Two representative areas were selected from each sample and photographed at a magnification of 35X with parallel and crossed nicols in the raw state, 300°C and at increments of 100°C to 1000°C. The dimensional and structural changes were obtained from 100X photographic enlargements.

In a complementary microscopic study relatively large lumps of the raw cokes were polished, and suitable areas were selected and photographed at 10X. These samples were then successively heated from 500°C to 1200°C in 100°C increments at a rate of 5°C/minute.

A 15,000 psi Aminco mercury porosimeter was used to obtain micro-pore volume distribution in representative samples of each coke as a function of heat treatment. The samples were crushed to 10/20 mesh particle size and duplicate measurements made on 0.5 g. samples.

X-ray diffraction studies were carried out employing a recording diffractometer using monochromatic Cu K $\alpha$  radiation. Crystallite size values were obtained using the Scherrer formula with KCl as an internal standard.

102  
RESULTS

A total of four cokes was studied in this investigation. As indicated by the characteristics of the four cokes listed in Table I, these samples are representative of an anisotropic coke (sample A&B) and an isotropic coke (sample C&D). The ash and sulfur contents and real densities of the raw cokes represent the range of values generally encountered with commercial cokes.

The type of changes in topographical features which the cokes underwent during calcination as revealed under the hot stage microscope are illustrated in Figure 1. The structure of the raw coke could be determined only with the aid of polarized light. Heating to 700°C produced very little change in the appearance of the polished surface of the samples except, perhaps, a slight increase in the width of existing cracks. Suddenly at 800°C, the detailed structure of the coke could be observed under parallel nicols. Further increase in temperature resulted in progressive opening of existing cracks, apparent creation of a few small cracks, and an obvious overall shrinkage. However, the basic macrostructure of the calcined coke was essentially the same as observed in the raw coke under polarized light. The two isotropic cokes had areas of pitch and mesophase which melted upon heating above 500°C producing voids lined with highly anisotropic carbon.

The magnitude of the dimensional changes observed as a function of temperature are illustrated in Figure 2 representing results typical of an anisotropic coke and in Figure 3 for a coke with an isotropic structure. The curves were plotted from data obtained with the hot stage (micro) and from ambient temperature measurements on the coke lump samples (macro). Considering the high temperature microscopy experiments, it should be noted that the dimensional changes recorded include the reversible thermal expansion of the carbon as well as shrinkage. The 1.0% to 2.5% linear expansion observed in all of the coke samples upon heating to 500°C is a manifestation of the reversible expansion. Contraction of the coke begins after 500°C with the maximum rate of dimensional change occurring between 700°C and 800°C. It is also significant to note in this same temperature range the marked shrinkage in the direction perpendicular to the needle structure as compared to that occurring parallel to the needle structure for the anisotropic cokes.

The information derived from the larger samples at room temperature correlates well with the high temperature measurements. The two sets of curves are similar in shape and the cross-over point of the shrinkage perpendicular and parallel to the flow structure occurs, within experimental error, at the same temperature. The weight losses calculated from these experiments suggest, as one would expect, a general direct relationship with the volatile content. Of more interest is the change in slope observed in the curves representing weight loss as a function of temperature which occurs in the 700°C to 800°C temperature range. This information for the two anisotropic and two isotropic cokes is given in Figure 4.

Mercury porosimetry measurements of 10/20M fractions were used to determine the accessible pore volume at each of the heat treatment temperatures. Pore volumes were determined in two pore size ranges,  $V_2$  for pore diameters between 65 and 12 $\mu$  and  $V_1$  for diameters between 12 and 0.015 $\mu$ . Although a gradual increase in  $V_2$  with increasing

temperature was noted for all of the cokes, the results were usually erratic and appeared to reflect gross, non-uniform structural changes. The  $V_1$  porosity behavior, as illustrated in Figure 5, is generally the same for both types of cokes. There is an overall increase in accessible porosity with increasing temperature. This increase in porosity is considered to be due to the formation of shrinkage cracks resulting primarily from loss of volatiles during calcination. As shown in Figure 5, three of the four cokes exhibited a relatively abrupt increase in porosity beginning at about 900°C, which would appear to be indicative of a significant structural change.

Changes in apparent density measured by mercury displacement were also determined concurrent with the porosity measurements. Figure 6 displays the trends in density change vs. temperature for the two types of coke studied. The A. D.'s of the cokes were observed to remain constant until 700°C-800°C at which point a sudden increase in density occurred. These results correlate well with the hot stage microscopy measurements where a significant linear shrinkage of the samples was observed to occur in this temperature range.

The (002) x-ray diffraction peak intensities were measured on the four cokes and plotted as a function of temperature. The peak intensity measurements reflect the progressive ordering of the graphitic planes during calcination. Figure 7 illustrates the extreme cases of the anisotropic cokes compared with the isotropic cokes. In all cases the peak intensity appears to increase at a logarithmic rate with temperature; however the anisotropic cokes maintain peak intensities of a higher magnitude throughout the calcination range than the isotropic cokes.

The d-spacing, which is classically a measure of the graphitic nature of carbon, was obtained for all samples as a function of temperature. As might be expected, d-spacings were found to decrease with increasing temperature. This is illustrated in Figure 8, where it is of interest to note that while the isotropic cokes have large d-spacings at the outset, the d-spacings of the anisotropic and isotropic cokes are essentially equivalent by 1100°C. The low initial d-spacings of the isotropic cokes are believed to be due to the amorphous material contributing mainly to the background of the diffraction curve. Only the highly graphitic portions of the sample are detectable, which result in low d-spacing values not truly representative of the entire sample. On the other hand, less amorphous material is present in the anisotropic cokes, and a broader spectrum of crystallite perfection is detectable. Therefore, the total value of the d-spacings appears large. Other experiments conducted beyond the 1200°C range have shown that the d-spacings of isotropic cokes maintain higher values than the anisotropic cokes, which is in agreement with the cross-over point at 1100°C in Figure 8.

The change in crystallite size along the c crystallographic axis as a function of temperature was very similar for all cokes. This relationship, presented in Figure 9 for the four cokes, is characterized by a significant decrease in size between 500°C and 900°C; after which a steady increase is observed up to 1200°C. Since the  $L_c$  values represent an average of all detectable crystallites for a given sample, it is believed that the initial decrease in  $L_c$  is due to the appearance of a large number of extremely small crystallites which have grown to a detectable size. This pronounced decrease in

Lc values at 600°C-700°C corresponds with the onset of the rapid shrinkage of the coke samples. It seems reasonable, therefore, to presume that the coke structure shrinkage is in part a result of its conversion to a more compact crystalline structure.

#### CONCLUSIONS

With only minor exceptions, the general overall structure of the calcined coke is predetermined in the raw state. With respect to microstructure, the dominant recurring theme running through our experimental data is the sudden changes which occur in the 600°C to 900°C temperature range. The sharp observed increase in dimensional shrinkage results from the loss of volatile constituents as well as ordering and growth of the polycrystalline structure. The increased microporosity represents the creation of shrinkage cracks as well as pores formed due to the escape of volatile components.

REFERENCES

1. P. L. Walker, Jr., F. Rusinko, Jr., J. F. Rakszawski, and L. M. Liggett. Proceedings of the Third Conference on Carbon, University of Buffalo (1957) p. 643.
2. C. F. Stout, M. Janes, and J. A. Biehl: WADD Technical Report 61-72, Vol. 36 (1964).
3. E. Barrillon, Carbon, 5, 167-171 (1967).
4. P. Rhedey, Transactions of the Metallurgical Society of AIME, 239 1084 (1967).

TABLE I  
CHARACTERIZATION OF THE RAW COKES

Sample	Volatile Matter (%)	Ash (%)	Sulfur (%)	Real Density (g/cc)	002 Peak Intensity (c/s)	d-Spacing (Å)	X'tal Size LC (Å)
Coke A	5.90	0.110	0.72	1.437	115	3.5131	25.6
Coke B	6.43	0.085	0.70	1.397	178	3.7745	23.6
Coke C	15.71	0.086	1.32	1.345	111	3.5186	30.1
Coke D	21.46	0.281	1.28	1.314	117	3.5118	32.6

FIGURE 1  
STRUCTURAL CHANGES ACCOMPANYING  
COKE CALCINATION



RAW (PARALLEL NICOLS)



RAW (CROSSED NICOLS)



700°C (PARALLEL NICOLS)



800°C (PARALLEL NICOLS)



1000°C (PARALLEL NICOLS)



1000°C (CROSSED NICOLS)

100  $\mu$

**FIGURE 2**  
**DIMENSIONAL CHANGES OF AN ANISOTROPIC COKE**

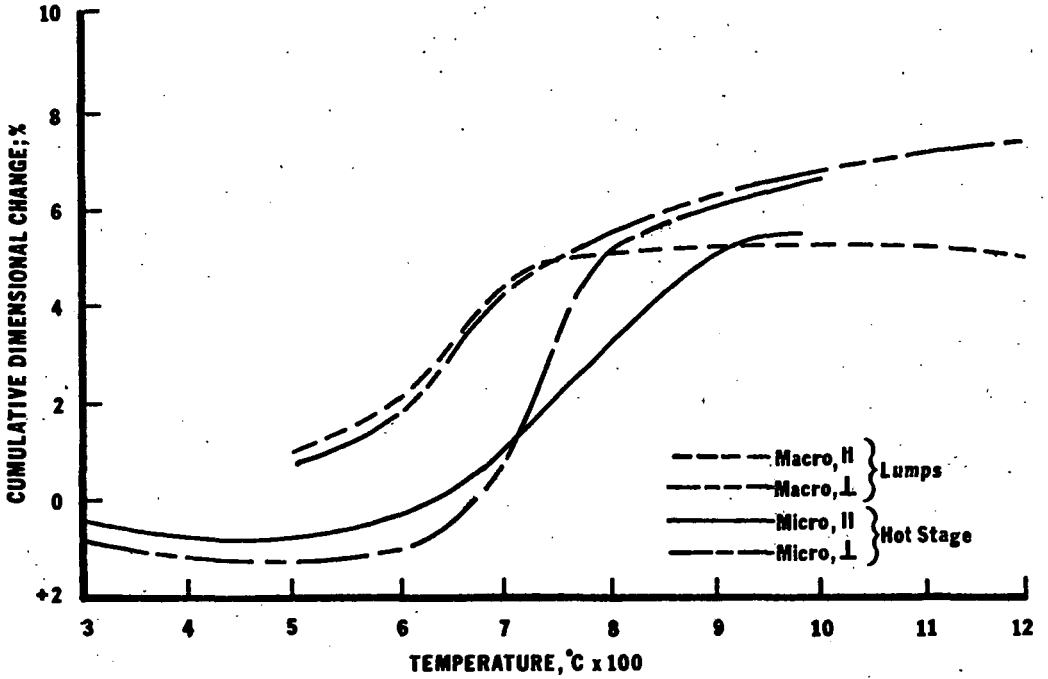


**FIGURE 3**  
**DIMENSIONAL CHANGES OF AN ISOTROPIC COKE**

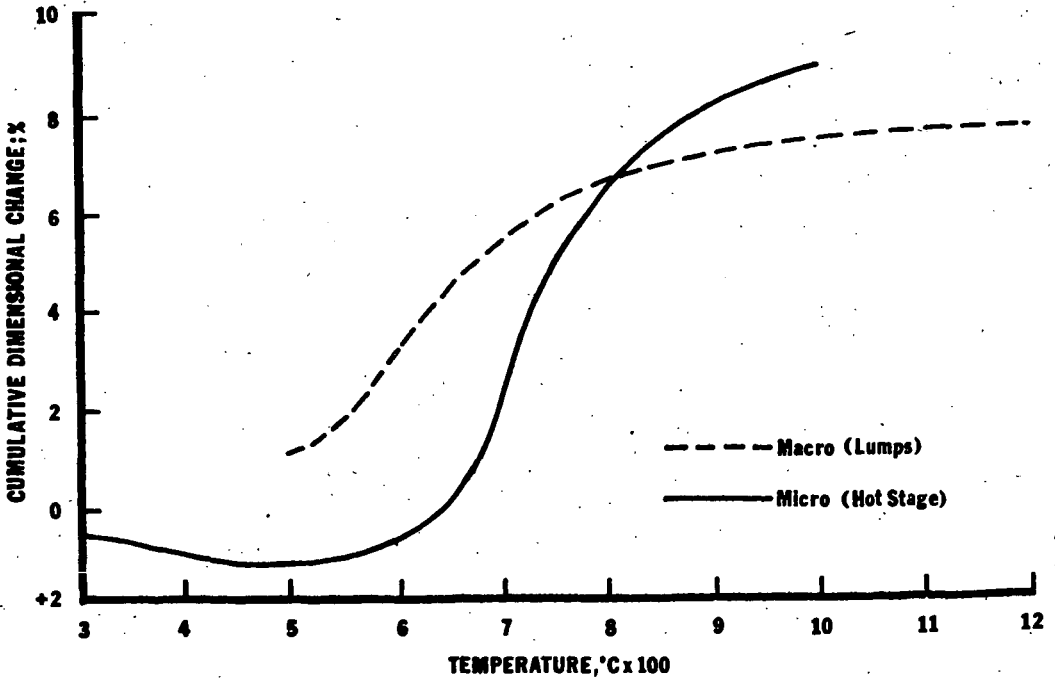


**FIGURE 4**  
**WEIGHT LOSSES vs TEMPERATURE**

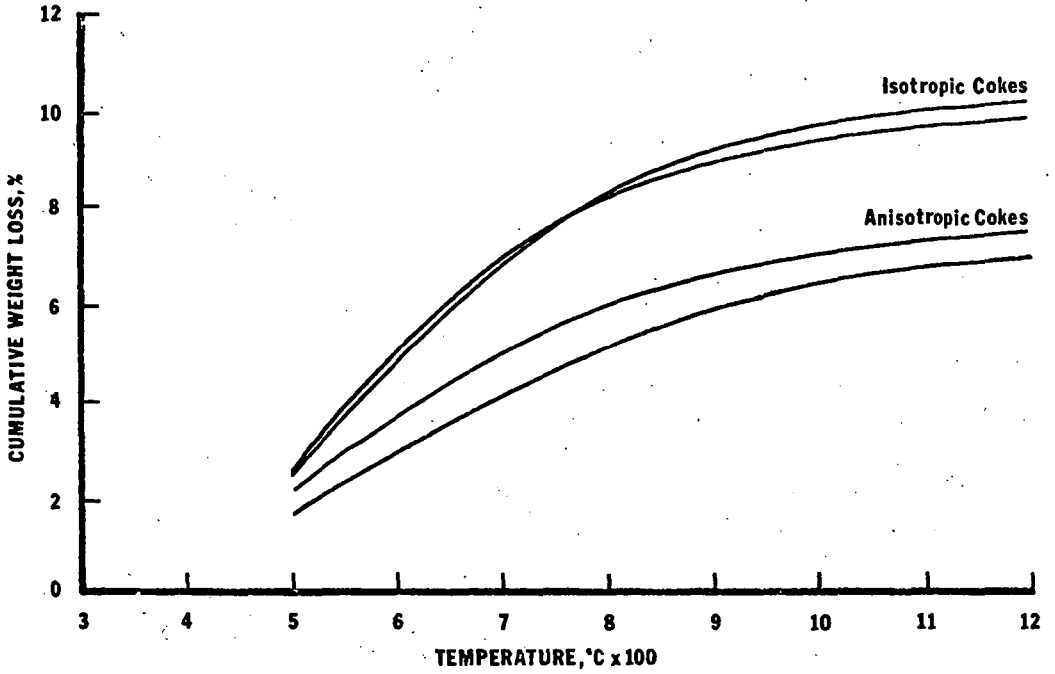


**FIGURE 5**  
**POROSITY vs TEMPERATURE OF VARIOUS COKES**

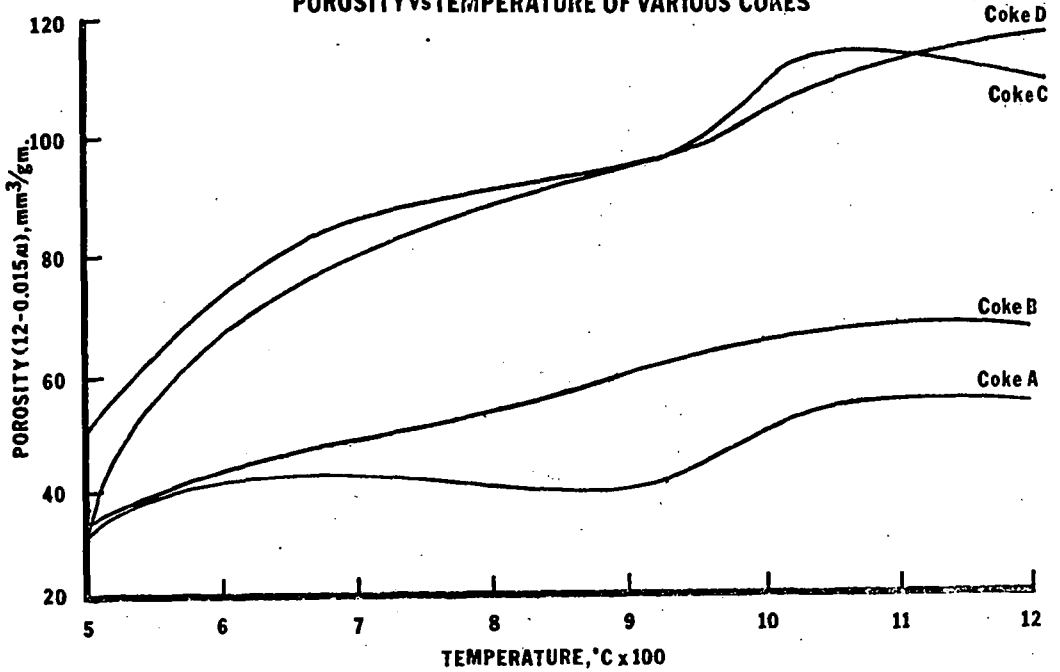


FIGURE 6  
DENSITY vs TEMPERATURE

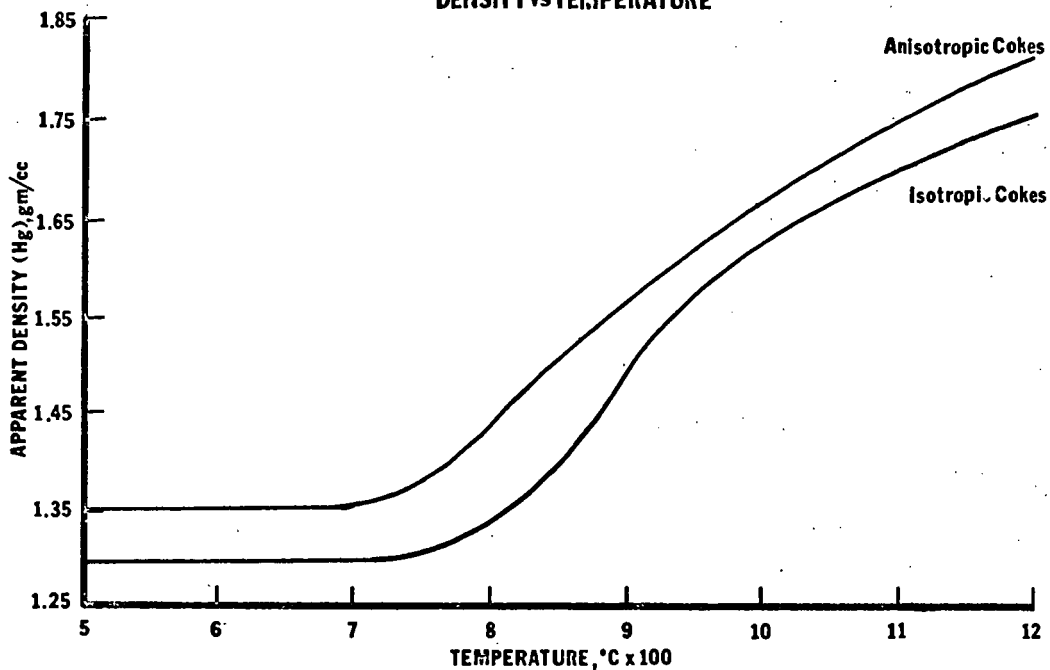


FIGURE 7  
PEAK INTENSITY vs TEMPERATURE

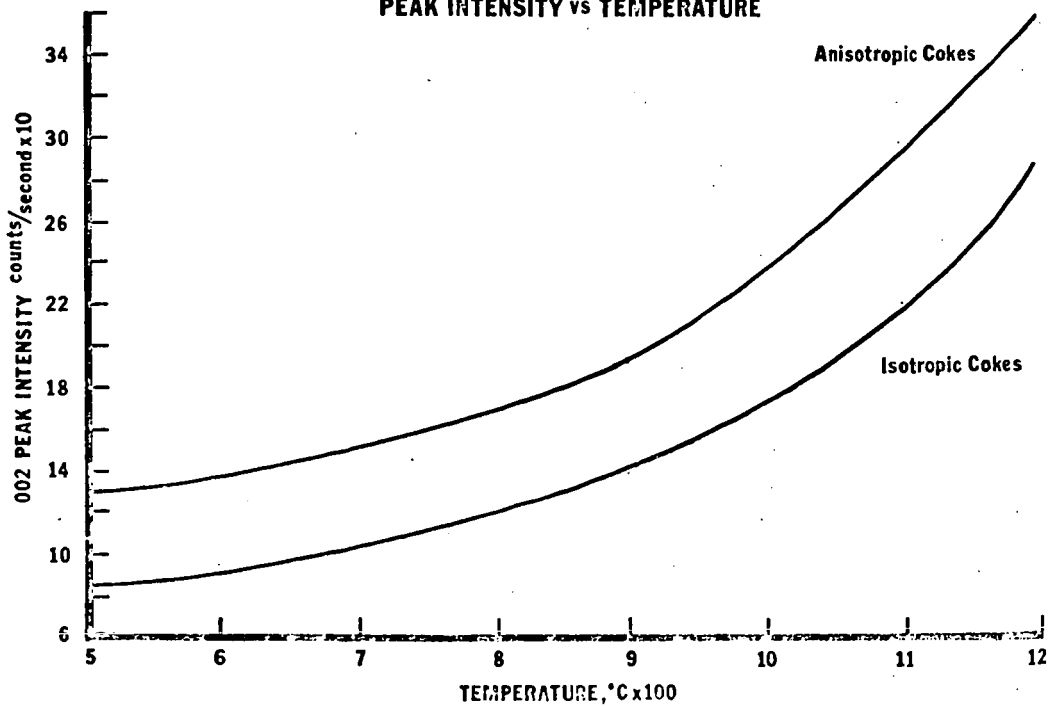


FIGURE 8  
D-SPACING vs TEMPERATURE

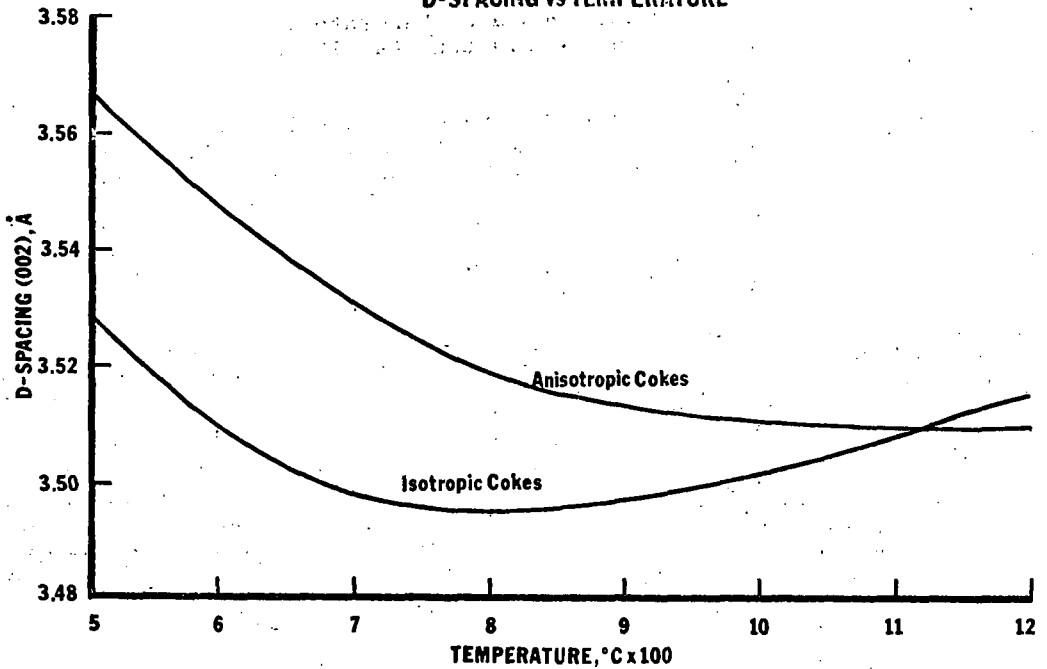
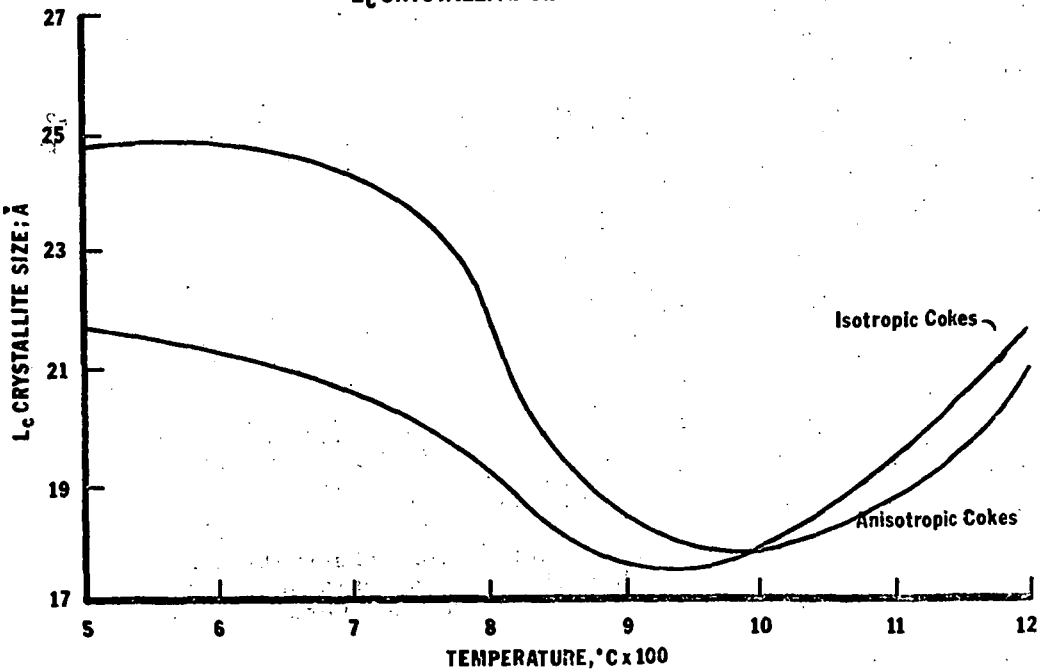


FIGURE 9  
 $L_c$  CRYSTALLITE SIZE vs TEMPERATURE



WETTABILITY OF PETROLEUM COKES BY PITCH

M.L. Dell, R.W. Peterson

Alcoa Research Laboratories  
New Kensington, Pa. 15068

In 1968 well over a million tons of petroleum coke were used in the United States in manufacturing carbon and graphite. For carbon anodes in aluminum smelting, delayed petroleum coke mixed with coke-oven pitch and subsequently baked has been used almost exclusively. While many investigations have been made on the properties required in binder pitches for carbon electrodes (1), there are no data on the characteristics of cokes other than impurity content and real density that relate to anode properties.

Microstructures of a variety of cokes and carbons were reported by Martin and Shea (2). In a petroleum coke, Kusakin et al, 1965 (3), observed two different types of particles: "spherulitic" particles, which are isotropic and relatively non-graphitizing, and a "streak" type, which is softer and graphitizing. Abramski and Mackowsky have developed methods for measuring in the microscope characteristic parameters for coke pores and walls (4). Other coke properties such as microporosity, macroporosity, and surface area have been measured. Rhedey (5) obtained a correlation between aggregate porosity and binder requirement of Soderberg paste for constant flowability. However, in none of the work is a correlation shown with baked anode properties.

A measurement related to porosity but more useful in assessing the effect of widely different calcined cokes on Soderberg anodes is the "wettability" by pitch. For the investigation reported here, an empirical procedure for measuring wettability was adapted from the elongation test used by Bowitz et al (6).

Procedure

In the modified elongation test, a mixture of 100 g -140 +200 mesh (Tyler) calcined coke and 120 g standard pitch (softening point 110°C, cube-in-air) was stirred in a small can at 160°C for 20 minutes with a spatula. Cylindrical specimens 45-50 mm long and 9 mm diameter were molded and cooled. The specimens were placed on the inclined board in an oven at 160°C for one hour. After cooling, the change in length (elongation) of the specimen was measured and the percent elongation calculated. The less an aggregate was wet by the standard pitch used in these tests, the greater was the elongation. The increased elongation was caused by the greater amount of pitch available in the space between coke particles because of decreased absorption into the pores.

Real densities were determined using a pycnometer with kerosene as the confining fluid (Alcoa Analytical Procedure 424). Microporosity was calculated as 100 times the difference between real density and the density with mercury as the confining fluid divided by the real density.

Samples were mounted for microscopic observation by impregnating at 29 in. hg vacuum with Maraglas Type A resin and Maraglas hardener 555 (7). After standing overnight, samples were cured at 70°C for 16

hours. They were ground successively on 320, 2/0 and 4/0 grit papers on a glass plate, polished on a wheel with Metaul 6 mu (Duhler, Ltd.), with alpha alumina, and finally with gamma alumina.

For preparing baked anodes, an aggregate particle size distribution was used having the greatest dry bulk density as determined in a series of settling experiments on a vibrating table. Cokes G and W were used as 46.5 percent of the total aggregate in the coarse fraction without crushing. The sizing of coke P was then adjusted for maximum dry bulk density of the blend. Similarly, coke A was used in the fines, as received, and the sizing of coke P was adjusted for maximum dry bulk density. Anodes were made with about 27 percent pitch (softening point 105°C cube-in-air). The amount of pitch was adjusted so that all mixes had the same elongation as determined on a specimen 2-1/2 in. long x 1 in. diameter molded from the green paste. Anodes 3 in. diameter x 4 in. tall were baked to 1000°C under 3.7 psi pressure. Baked apparent density (EAD) and electrical resistivity were determined on the baked samples.

### Results

The elongation test procedure of Bowitz et al (6) specified 80 percent coke passing through a 200 mesh sieve. Lack of a lower limit permitted a wide range in particle size and surface area of the sample. In addition, the fine grinding could destroy much of the pore volume. Preliminary tests demonstrated greater reproducibility when using five fractions between 100 and 325 mesh (Tyler). The sizing finally chosen, -140 +200 mesh, gave even better reproducibility. To increase ability of the test to discriminate among cokes, the pitch content was increased to 54.5 percent. Typical results are shown in Table 1 for two successive mixes of coke P, with 18 specimens molded from each mix and tested in the oven, six at a time.

Table 1  
Reproducibility of Elongation Test for Coke P

Test	Elongation, %					
	Mix 1			Mix 2		
	1	2	3	1	2	3
	60.0	56.0	63.8	64.2	61.5	56.7
	58.1	57.6	63.2	64.0	64.3	59.3
	56.9	55.4	63.2	66.1	61.8	60.1
	53.4	54.0	60.1	61.9	59.5	62.2
	53.8	61.2	-	68.3	64.5	58.7
	61.2	58.7	-	63.7	65.8	64.7
Average	57.2	57.2	62.6	64.7	62.9	60.3
Std. deviation	3.99	2.58	1.66	2.21	2.35	2.34
Average for Mix 1	58.5%					
Average for Mix 2	62.6%					

For the particle size chosen, -140 +200 mesh, the accessible porosity appeared completely filled with pitch because increasing mixing temperature to 200°C and 230°C did not change the amount of elongation. However, the degree to which pores in larger particles were penetrated by pitch was affected by mixing temperature. For example, with a typical anode aggregate (-4 mesh +pan) molded into 1-in.

diameter 2-in. long cylinders there was a marked decrease in elongation with increased mixing temperature (Figure 1). At the lower mixing temperature, viscosity of the pitch prevented substantial penetration into the remote pores of the larger particles.

Three calcined delayed cokes had elongations from 61 to 227 percent (Table 2), and the calcined fluid coke had an elongation of 355 percent. Anode properties, as measured by baked density and resistivity, varied with elongation and seemed to optimize at the intermediate values of 186 and 227 percent. Anode properties did not correlate with real density or the microporosity measurement of the calcined cokes.

Table 2

Properties of Calcined Cokes and Laboratory Anodes  
Made from Mixtures with Coke P in the Aggregate

Coke	P	G	W	F
Process	Delayed	Delayed	Delayed	Fluid
Real Density	2.02	1.96	2.03	1.98
Microporosity	10.9	8.2	13.3	3.5
Elongation, %	61	186	227	355
<u>Anode Properties</u>				
Amount of Coke P in Aggregate	100	53.5	53.5	57.5
Baked app. density	1.39	1.44	1.43	1.41
$\rho$ , ohm-in.	.0028	.0025	.0025	.0032

Microscopic examination showed that green delayed petroleum coke (Figure 2) had the incipient pore structure of calcined coke (Figure 3). In green coke the pores were filled, probably with a hardened residuum from the coker feed, which distilled off during calcination and exposed the pores and typical lamellar structure of calcined coke.

Although cokes P, G, and W were made by the delayed coking process, each had a distinctive microstructure. Coke P (Figure 3) had the lamellar and pore structure typical of many delayed cokes. Coke W (Figure 4) had in addition a characteristic mottled structure. Coke G (Figure 5) consisted of fused spherules, each having an onion-like structure. Each spherule had a microporous surface coating.

The fluid Coke F (Figure 6) consisted of spherical particles, each in turn frequently being made up of clusters of small spherules of isotropic coke. Some of the larger particles had the onion-like structure.

#### Discussion

The wide range of microstructures indicates the difficulty in trying to find a single characterization factor for cokes in carbon anodes. The wettability test, however, largely overcomes this objection since it is a direct measure of how the pore structure affects the relationship between coke and binder. For example, the fluid coke

F, with its limited amount of surface accessible pores had poor wettability as judged by elongation. Because of the poor bond between coke and binder, fluid coke produced anodes with high resistivity. This poor bond in anodes was clearly discernible in the microscope (Figure 7). Attempts were made to alter the surface of Coke F to improve the bond with binder pitch. Neither crushing to expose fresh surface nor chemical etching with oxygen was successful (Table 3).

Table 3

Effect of Treatment of Coke F on Properties of  
Anodes Containing 20% of Coke F

<u>Treatment</u>	<u>Baked App. Density</u>	<u>Resistivity ohm-in.</u>
Untreated	1.41	.0029
Crushed to -100 mesh	1.40	.0030
Oxidized at 1050° to 6% wt loss	1.38	.0031

This was consistent with the explanation that pores in the aggregate accessible to the binder are necessary to produce a good bond. After coking of the binder, the binder coke and aggregate coke are kept from separating by the mechanical action of binder coke formed within the pore system of the aggregate. Coke G formed an excellent bond with the binder coke (Figure 8), probably because the binder was able to penetrate the porous layer characteristically on the surface of this coke (Figure 4).

Because coke P had a high wettability by binder, the green mix required a high pitch content, and this may have been a factor in the high resistivity. The large pores and laminations in Coke P may also have contributed to the high resistivity by presenting a tortuous path for current flow.

The cause of differences in microstructure of the delayed cokes is not known. Since all were made by the same process, operating variables such as recycle ratio could be a factor. The presence of nuclei seems to favor isotropic coke. For example, needle coke, a non-isotropic coke is made by a 2-step process in which the nuclei present in the feed stock are first removed and the needle coke is prepared from the clarified feed (8). Even more important for Coke G may be the chemical nature of the feed to the delayed coker. It has been reported (9,10) that heterocyclic structures tend to produce isotropic cokes and the feed for Coke G had a relatively high nitrogen content.

For carbon manufacture the wettability test can be used to predict behavior in anodes of cokes having a wide variety of microstructures. Low wettability indicates a poor bond may be expected between baked binder and coke, and this will cause high electrical resistivity. On the other extreme, high wettability may indicate an extremely porous coke whose interior pores unfilled with binder can cause high electrical resistivity.

#### References

1. Weiler, J.F., "Chemistry of Coal Utilization" H.H. Lowry ed, John Wiley & sons, Inc., New York; Supplementary Vol. p 627 (1963)

2. Martin, S.F. and Shea, F.L. Jr., *Ind. Eng. Chem.* 50, 41 (1958)
3. Kusakin, N.D., Vyatkin, S.E. and Averina, M.V., *Tsvetnye Metally* 38, 65 (No. 10, 1965)
4. Abramski, C. and Mackowsky, Marie-Therese in "Handbuch der Mikroskopie in der Technik," Hugo Freund, ed, Umschah Verlag, Frankfort am Main (1959) 2, Part 1, p 311
5. Rhedey, P., *Trans AIME* 239, 1084 (1967)
6. Bowitz, D., Eftestol, T. and Selvik, R.A., "Extractive Metallurgy of Aluminum," Gary Gerard, ed. Interscience Publishers, New York (1963) 2, p 331
7. The Marblette Corporation, Long Island City, New York
8. Shea, F.L., U.S. Patent 2,775,549 - December 25, 1956
9. Blyden, H.E., Gibson, J., and Riley, H.L., *J. Inst. Fuel, Wartime bulletin*, pp 117-129 (1945)
10. Hutcheson, J.M. and Jenkins, H.L., "Second Conference on Industrial Carbon and Graphite," The Society of Chemical Industry (1966) p. 433

Large pore filled with mounting plastic.

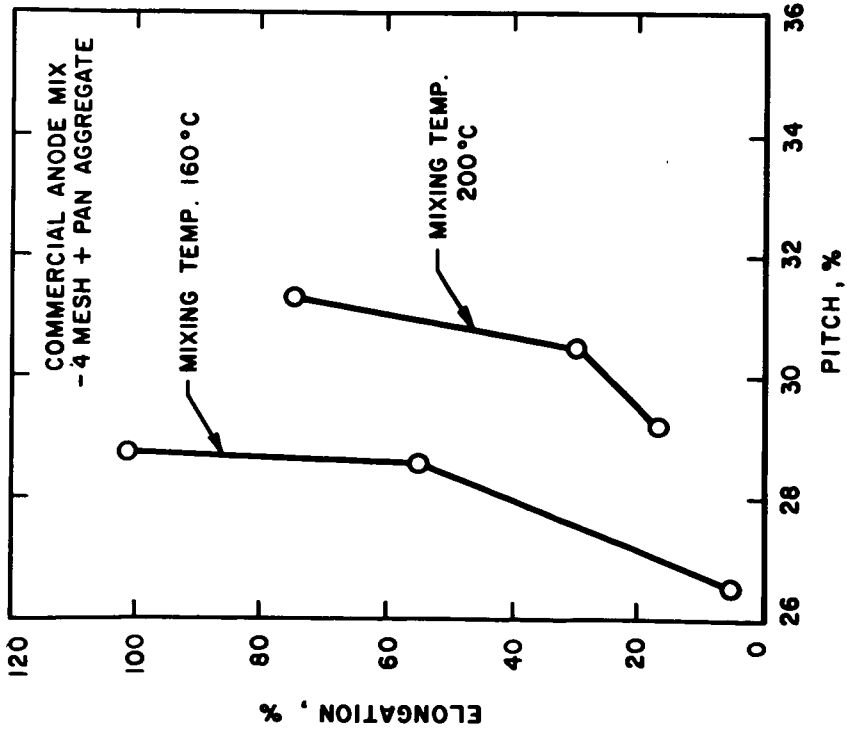
Incipient lamellar structure

Coke



Filled pores

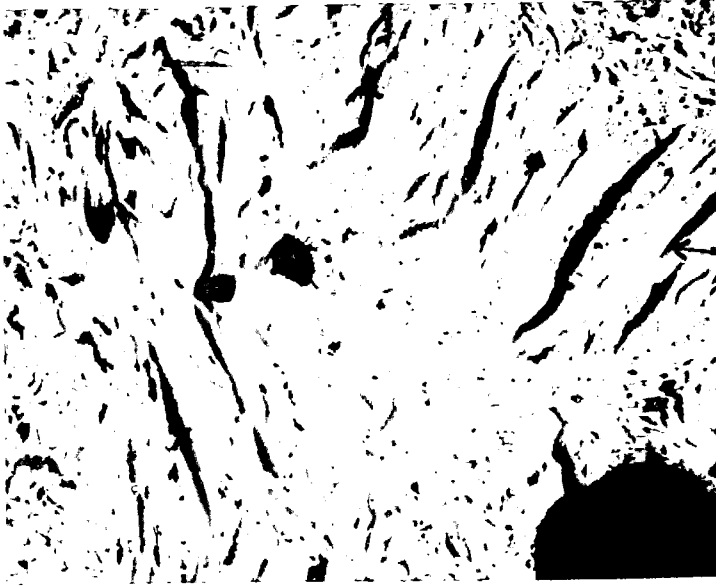
Vague lamellar structure



EFFECT OF MIXING TEMPERATURE ON ELONGATION

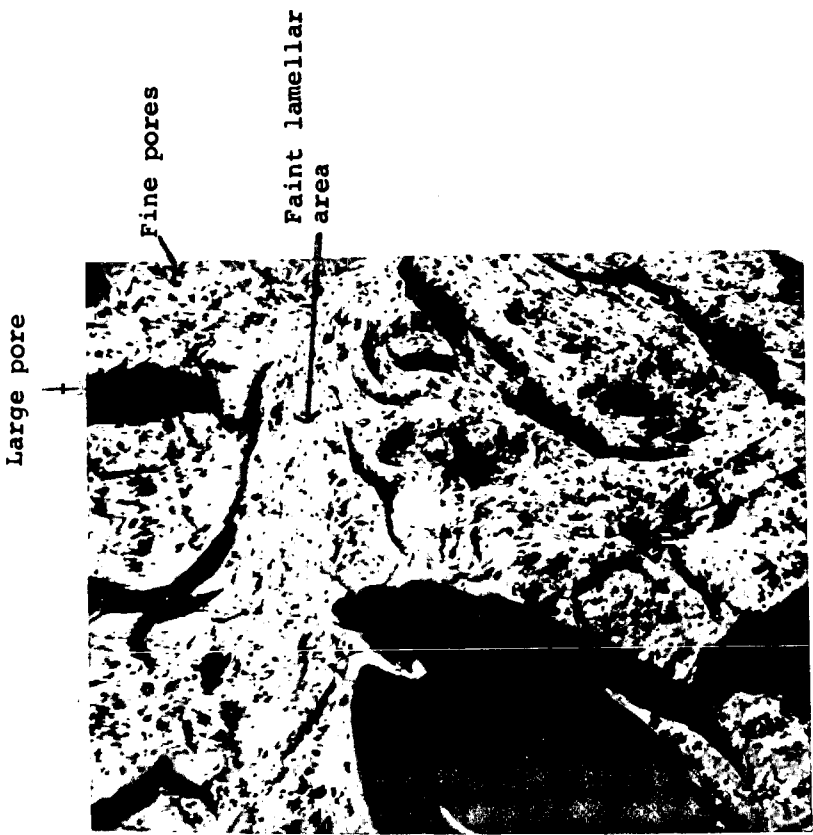
FIG. 1

Figure 2  
Green Delayed Coke P  
100X



Mottled area  
Lamellar area  
Mottled area around pore

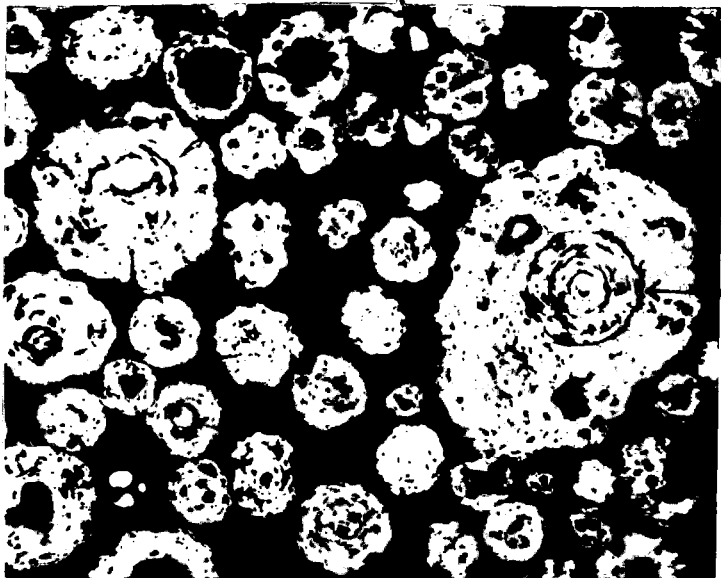
Figure 4  
Calcined Delayed Coke W  
100X



Large pore  
Fine pores  
Faint lamellar area

Figure 3  
Calcined Delayed Coke P  
100X

Cluster of  
spherules



Onion structure

Figure 6  
Fluid Coke F Baked in Laboratory  
100X

Surface  
coating

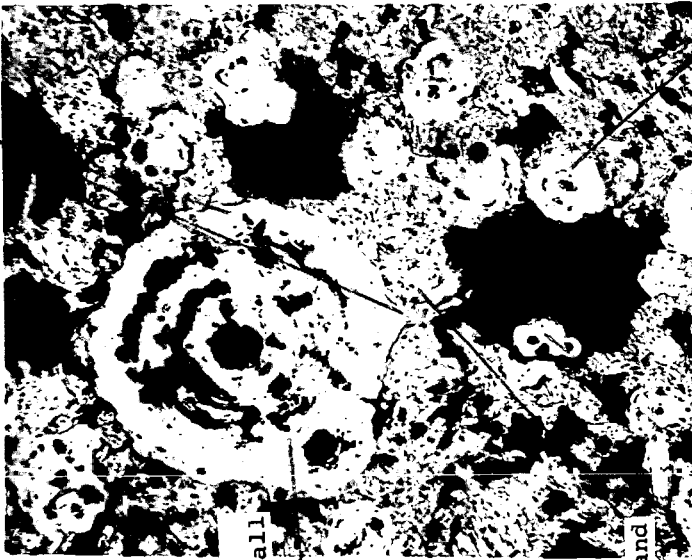


Spheres  
with onion  
structures

"Binder"  
coke

Figure 5  
Calcined Delayed Coke G  
100X

Separation between Coke F and binder



Coke F no binder coating

Binder and Coke P  
Fines

Coke F - half coated with binder

Figure 7 - Laboratory Soderberg Anode Containing 20% Coke F (100X)



Interface between Coke G and binder coke.

Figure 8 - Laboratory Soderberg Anode Containing 46-1/2% of Coke G (100C)

## PETROLEUM COKE HANDLING PROBLEMS

H. W. Nelson

GREAT LAKES CARBON CORPORATION  
Carbon Division  
New York, N. Y.INTRODUCTION

Calcined petroleum coke is an industrial carbon which is used as a raw material in the Aluminum Industry and the Graphite Industry. From the time it is first formed as a by-product of petroleum refining until it is finally processed into elemental carbon it is handled many times. Extreme care must be exercised at each point of handling in order to preserve the desired physical structure and maintain the required degree of purity. This paper reviews the steps used in the carbon industry to achieve these objectives.

Quality Considerations

Calcined petroleum coke is a commodity which must be delivered to the ultimate consumer in a size range which will permit an adequate proportion of coarse particles. This is necessary in order to meet the formulation requirements in a carbon paste mix. It must also be free from contamination.

Formation of Petroleum Coke

Raw petroleum coke is a by-product from refining of petroleum residuals. One of the procedures by which this is accomplished is known as the delayed coking process. This gives a coke with a sponge-like structure. Other methods such as the fluid coking process are also used but the product from this operation does not have the structural properties required for use in the Aluminum Industry or Graphite Electrode Industry.

Figure 1 shows a cross section of a coke drum and illustrates how the coke is formed in the delayed coking operation. The drum is a large insulated vessel about 20 feet in diameter and 70 feet high. The coke is formed at the rate of about 2 feet per hour and proceeds to build up during a 24 hour cycle. The material at the bottom is fully polymerized and develops a porous structure through which gases and liquids can pass. The top layer in the coke drum is not fully polymerized until it is subjected to heat for a prolonged period of time.

At the very top, some foam occurs. This foam subsides during the steaming and cooling cycle. It is important in filling the coke drum to avoid any carry over of foam or pitchy material into the vapor lines. Foam depressants are used to minimize the amount of foam (1). Level indicators are used to establish the position of the liquid or foam in the drum (2). These are operated by transmitting a beam from a radioactive source to an instrument mounted near the top of the drum. When the liquid reaches a predetermined level the feed to the drum is switched to an empty drum. At this time the full drum is steamed to remove light hydrocarbons and finally cooled by introducing water at the bottom of the drum.

#### Factors affecting Sizing of Coke

The coke is removed from the drum by means of high pressure water jets which operate on the principle used in hydraulic mining of coal (3). The procedure used in cutting the coke from the drum is extremely important. If it is not carried out properly the physical structure of the coke will be destroyed and the ultimate consumer would not have enough coarse particles to balance out their carbon aggregate formulation. The recommended procedure for cutting the coke is illustrated in Figure 2. This series of diagrams shows the steps which should be taken in order to get the maximum amount of lump coke needed for further processing.

The first step is to bore a pilot hole. During this operation the fine cuttings are held in the upper section of the drum until the hole is completely through the bottom. At this time, all of the center cuttings fall out of the drum together with the water used in cutting.

The drill stem is raised to the top and the bit is changed to a cutting head which has nozzles directed in a horizontal manner. The pilot hole is enlarged so that lumps of dislodged coke can fall freely through the opening. This avoids the danger of a coke build up around the drill stem which would prevent the rotation of the cutting head.

Once the pilot hole is enlarged the stem is raised to the level of the coke in the drum. The operator can tell by the sound of the water hitting the metal walls when the top is reached. At this time the stem is lowered 3 - 4 feet below the top. It is held in this position for several minutes until the coke is undercut. Then the stem is raised and lowered rapidly within this section until the coke is all cut from this layer. This action causes the coke to collapse from the drum walls resulting in large pieces which fall through the pilot hole. This operation is repeated until the drum is completely empty. In general, the decoking operation requires about 3 to 4 hours depending on the hardness of the coke. The harder

the coke the more time required.

Lump coke in the size range of baseballs to footballs can be handled easily in conventional conveying systems. At the calcining plant all coke is run through a roll crusher set at an opening of 4 inches before it is fed to the kiln. The tumbling action in the kiln results in further degradation so that the final product all passes a 1 inch screen with approximately 35 to 40% retained on a  $\frac{1}{4}$  inch screen.

#### Procedures to avoid Contamination

There are several systems used in handling coke after it is discharged from the drum. These are as follows:

- A. The coker is mounted over a railroad track so that coke can be discharged directly into open hopper cars or gondola cars.
- B. A roll crusher is placed below the drum on small tracks. This breaks up the large lumps to a size which will permit a coke slurry to be transported by pumping through a pipe line.
- C. The coke is directed to a ramp which leads to a pit. The pit may or may not contain water for further cooling of the coke.

In each of the above systems it is necessary to provide for the recovery of water used in cutting. The areas around the coking unit should be paved. Curbs and retaining walls should be provided to contain any coke spillage. The drainage around the coker must be carefully planned to avoid sand, clay and gravel from entering the system. Drainage from rainstorms should be directed away from the coking unit.

#### Transporting and Conveying Coke

The freight cars used to transport the coke should be clean. Any sand, gravel or iron rust will contaminate the coke. The cars should be carefully inspected before loading.

When coke is unloaded at the calcining plant, it is either conveyed directly to a storage silo or to an outdoor storage. When outdoor storage is necessary, it is preferable to provide paved areas to minimize contamination. The activities in the surrounding area can also affect the purity of the coke. For example, unloading of iron ore in the vicinity will contaminate the coke pile under

certain wind conditions.

Magnetic separators are used at the calcining plants. These will remove scrap iron from green coke, but will not remove iron rust, since the latter is non-magnetic. During calcining any iron oxide (rust) will be reduced to iron which can be removed from the calcined petroleum coke with magnets.

#### Chemical Composition of Petroleum Coke

Green petroleum coke from the delayed coking process is essentially a hydrocarbon. The chemical composition as obtained by an ultimate analysis is given in Table I. Before it can be used as a carbon aggregate it is necessary to convert the green coke into elemental carbon by a petrochemical process. This is carried out by a pyrolytic treatment at temperatures around 2300°F. In this operation the carbon is not developed until hydrogen is chemically removed by thermal decomposition. In the trade this process is referred to as calcination, but it is essentially a dehydrogenation reaction which converts a hydrocarbon into elemental carbon as indicated in Table I.

A number of changes in basic properties and structure are brought about by the removal of chemically bound hydrogen from the hydrocarbons in order to produce elemental carbon. Some of these are as follows:

- A. The real density of green petroleum coke is 1.30. After calcining the real density is 2.07.
- B. Green petroleum coke is an electrical insulator whereas elemental carbon (calcined petroleum coke) is an electrical conductor. For example:

Electrical Resistivity of Green Petroleum coke is  $9 \times 10^6$  ohm-inches.

Electrical Resistivity of Calcined Petroleum coke is .035 ohm-inches.

- C. There are corresponding changes in the X-ray diffraction pattern.

While there are profound changes occurring during the chemical conversion of green petroleum coke to elemental carbon, the mineral matter as indicated by the ash content remains essentially unchanged. The composition of the ash is important as this will affect the type of aluminum metal which can be produced.

The metallic components which are present in the crude oil will be carried over into the coke. Materials such as vanadium and nickel occur in crude oils in varying amounts depending on the area of origin. There is actually very little if any iron or silicon in crude oil. Iron which is found in petroleum coke comes primarily from corrosion of the pipes and vessels used to process the crude oil. Additional iron finds its way into the coke in the form of rust from rail cars and conveying equipment. Silicon can come from the catalyst used in refining also from sand or gravel contamination.

#### Iron and Silicon in Calcined Petroleum Coke

The iron in calcined petroleum coke will normally range between .01 and .06%. The silicon content will range between .01 and .05. Table II shows the car analysis of iron and silicon in calcined petroleum coke all loaded from the same storage silo. The samples were taken from a conveyor belt with an automatic sampler. In this group of cars, we find some individual cars with iron as low as .019% and silicon as low as .010%. This information is useful to the carbon plant superintendent of a prebaked plant. If he is required to supply anodes which are low in iron or silicon, he can select the cars from a given shipment and segregate the low ash material in a separate area of his storage shed.

Since the iron in calcined coke is magnetic, further removal can be accomplished at the consumers' plant by using magnetic separators. This will be most effective if applied after the grinding operation since iron pick up does take place in equipment such as the ball mill.

Several aluminum plants are now asking for a special grade of carbon with very low silicon. This is a difficult requirement to control at an ordinary calcining plant. However, a substantial improvement can be accomplished by screening the coke and using the coarse fraction for the low silicon application. An example of the degree of improvement which can be achieved by this method is shown in Table III. The silicon bearing material is concentrated in the fines (minus  $\frac{1}{4}$ "). The plus  $\frac{1}{4}$ " fraction contains only 40% of the total silicon or .008%.

SUMMARY

In summarizing the information just presented, we find that a reasonable amount of care should be exercised at each step of handling petroleum coke. It is recognized that some of the physical properties (sizing) of a calcined coke can be destroyed if the cutting operation is not carried out properly. Also sources of contamination should be avoided in order to keep the iron and silicon content within required limits. Where a carbon aggregate with low silicon or low iron is required a selection can be made from a given shipment if the material is delivered in rail cars.

References

1. Trammell, W. D., Glaser, D., Oil and Gas Journal p. 65, June 5, 1961.
2. Wright, P. G., Oil and Gas Journal p. 93 - 94, Aug. 11, 1958.
3. Maas, R., Lauterbach, R. E., Petroleum Engineer p. 110 - 124, Feb. 1947.

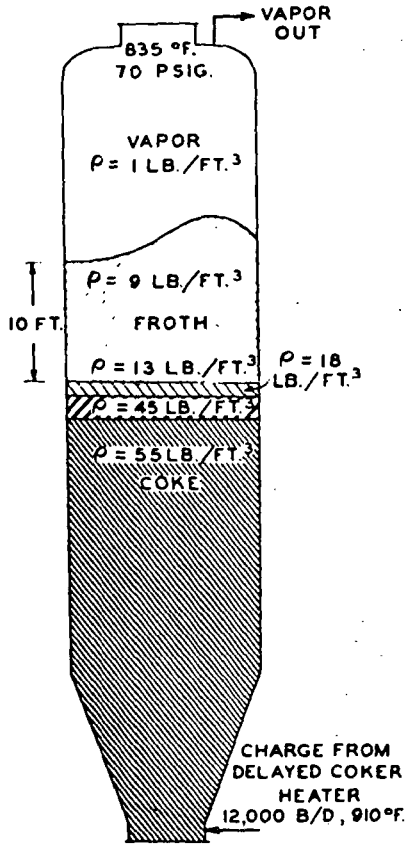
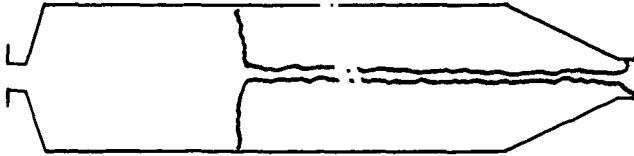


Figure 1.

Figure 2

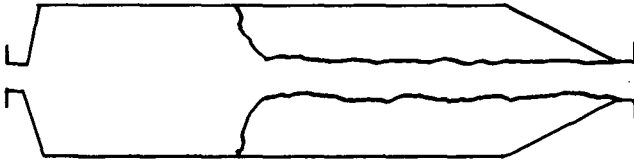
RECOMMENDED DECKING PROCEDURE

STEP 1



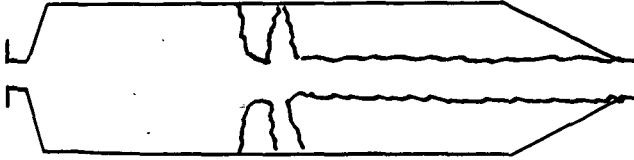
DRILL PILOT HOLE

STEP 2



USE CUTTING BIT TO ENLARGE PILOT HOLE

STEP 3



LOWER BIT 3 FT. BELOW TOP COKE HOLD UNTIL COKE IS UNDERCUT

STEP 4



RAISE AND LOWER BIT RAPIDLY CAUSING COKE TO COLLAPSE FROM WALLS

STEP 5 - REPEAT STEPS 3 AND 4 UNTIL DRUM IS EMPTY

STEP 6 - CLEAN DRUM WALLS

TABLE I

TYPICAL ULTIMATE ANALYSIS OF  
GREEN PETROLEUM COKE AND CALCINED PETROLEUM COKE

	Green Petroleum Coke (Polymerized Residual)	Calcined Petroleum Coke (Pure Carbon)
CARBON	91.80	98.40
HYDROGEN	3.82	0.14
OXYGEN	1.30	0.02
NITROGEN	0.95	0.22
SULFUR	1.29	1.20
ASH	0.35	0.35
CARBON-HYDROGEN RATIO	24	910

TABLE II

ANALYSIS OF CALCINED COKE SHIPMENTS  
CARS LOADED FROM PRODUCT SILO

ORDER OF LOADING CAR NO.	ASH %	IRON %	SILICON %
1	.24	.019	.010
2	.21	.021	.012
3	.40	.065	.028
4	.42	.073	.022
5	.34	.043	.025
6	.24	.030	.010
7	.23	.020	.015
8	.33	.035	.025
9	.41	.065	.015
10	.26	.041	.021

TABLE III

EFFECT OF SCREENING  
ON SILICON CONTENT OF  
CALCINED PETROLEUM COKE

SIZE	% SILICON
Run of Kiln	.021
Plus ¼ Inch Fraction	.008
Minus ¼ Inch Fraction	.022

COKING OF COAL SOLUTIONS IN A  
LABORATORY COKE OVENV. L. Bullough, L. O. Daley and W. R. JohnsonReynolds Metals Company  
Reduction Research Division  
P. O. Box 191  
Sheffield, Alabama

## INTRODUCTION

The manufacture of aluminum by the Hall-Heroult process requires nearly one-half pound of high-grade carbon for each pound of aluminum produced. This carbon must contain a minimum of metallic impurities to prevent contamination of the aluminum produced in the process. For this reason raw materials used in the anode manufacture for the aluminum industry have stringent purity specifications. Petroleum coke represents a large volume source of relatively pure carbon and is used extensively throughout the aluminum industry as the material of choice for anode manufacture.

Most of the petroleum coke that is used in electrode manufacture is produced in delayed cokers where the product is subsequently calcined in rotary kilns to temperatures of 1200°C — 1430°C<sup>1</sup>. After heat treatment to this temperature the coke has obtained dimensional stability and electrical conductivity suitable for its use as an electrode material. Coke produced by this process usually has a particle size adequate for its use in the manufacture of large monolithic electrodes. A limited amount of petroleum coke produced in fluid bed cokers is used in the manufacture of anodes for the aluminum process. Fluid coke is sometimes used as a supplement to delayed petroleum coke to produce electrodes. The absence of large size particles in fluid coke generally limit its use in large electrodes. A limited amount of coke is produced for electrode use by the delayed coking of Gilsonite<sup>2</sup>. Recently, the Nittetsu Chemical Industry of Japan completed the installation of a delayed coker for the coking of coal tar pitch for electrode use<sup>3,4</sup>. Some coal tar pitch coke is manufactured in Europe to supplement the supply of petroleum coke. This coke is generally produced in coke ovens<sup>5</sup>.

Coke derived from coal had not been used as a general source of anode carbon in alumina reduction cells because of its high ash content. Investigators have studied methods of removing mineral matter from coal,<sup>6-11</sup> and coke from purified coal has been used on a commercial scale in at least two cases<sup>12-14</sup>. These were war-time uses that were discontinued when adequate supplies of high-grade petroleum coke were available.

Because of possible future shortages of electrode grade petroleum coke, we have studied the coking of purified solutions of coal in creosote oil as a process for producing an alternate source of electrode grade coke. A pilot plant was constructed at Reduction Research Laboratory where high-volatile bituminous coal was mixed with heavy residue creosote oil and digested under pressure to give a solution of coal. The solution was treated with a combination

of disc and solid bowl centrifuges to yield a solution of coal that had been freed from its mineral matter and fusain. Most of the solvent oil was removed from the coal by distillation in a continuous still and the pitch-like residue remaining from the distillation was charged as a liquid to a coke oven where the remaining solvent and volatile matter were removed to produce a calcined electrode grade coke<sup>15</sup>. The principal process steps are shown diagrammatically in Figure 1. This paper will be concerned primarily with our experience in operating a laboratory coke oven to produce calcined coke.

While much excellent work has been published on the solubility of coal in different solvents<sup>15-23</sup>, little has been published about coking of such solutions to yield coke. We were aware that most of the petroleum coke was produced in delayed cokers and that Gilsonite was being coked in delayed cokers to produce a high-grade electrode coke, but we were uncertain that a product as aromatic as dissolved coal could be satisfactorily handled in a delayed coker. The Koppers Company in the United States had coked coal tar pitch in coke ovens; coke ovens are being used to coke coal tar pitch in Russia<sup>24</sup> and Germany; and we were aware that the coal solution produced in the Pott-Broche process in Germany during World War II had been coked in slot ovens<sup>13</sup>.

The product of a delayed coker is not satisfactory for use in an alumina reduction cell without further heat treatment to remove the residual volatile matter, obtain proper electrical conductivity, and insure dimensional stability of the coke particles at high temperature. Generally, the coke from the delayed coker is heat treated or calcined to a temperature of about 1300°C before use in alumina reduction cell anodes. Thus, the use of a delayed coker would also require the use of a calciner. We elected to combine the two steps in our pilot plant and construct the only coker that we knew of capable of operating at temperatures of 1300°C - the coke oven.

## PROCESS DESCRIPTION

The Bureau of Mines had reported<sup>25</sup> on a coke oven heated with silicon carbide glow bars of the approximate size that we needed. We used the general idea of this coke oven as our model, with the exception that the coke oven we constructed was gas fired and the sole of the oven was heated by the passage of hot gas from the flue to the exhaust stack. The oven was fired symmetrically with burners at four corners of the flues, and the flues were baffled to provide uniform heat distribution for the entire surface of the refractory. The coking slot was 17 inches wide by 48 inches long by 48 inches high and was tapered one-quarter inch from the pusher end to the coke end over the length of the slot. The slot walls were silica refractory of the type used in commercial coke ovens while the sole was super-duty fire-clay refractory. The roof and doors were cast with super-duty castable refractory. Tongue and groove construction was used to maintain better seals in the refractory joints. The oven was fired with four 158,000 Btu per hour capacity gas burners. The system was protected against high and low gas pressure and blower failure. Because the refractories were incandescent during operation, flame failure protection was regarded as superfluous. Figures 2 and 3 are diagrammatic sections through the coke oven.

Cokes from the solution of two different coals were studied in the coke oven. Both of these coals were high volatile bituminous coals. One was the Black Creek Seam in Northern Alabama and the other, the No. 9 Seam in Western Kentucky. Typical analysis of these coals are shown in Table I. Prior to each charging, the door faces were cleaned, seated on a strand of asbestos rope and sealed with a refractory cement.

Steam was introduced into the oven slot to reduce the surface temperature of the refractories before charging the dissolved coal to the oven. This was done to minimize the amount of carbon-black formed by cracking of the coal solution on the incandescent refractory surfaces. After passing through the continuous still where part of the solvent was removed by distillation, the dissolved coal solution was fed into the top of the coking slot and the volatile matter and gases that were flash evaporated were passed through a condenser. The condensed vapor was collected in a solvent recovery tank where it was recombined with the solvent fractions removed by the continuous still.

The hot coal solution was charged at a rate of about 2 — 3 gallons per minute into the slot of the coke oven. While this material left the still at about 320°C, it had cooled to about 200°C in the piping by the time it had reached the coke oven. During the first few minutes of the charge the condenser was flushed with a spray of water to wash away the copious quantities of carbon-black that were generated. When the first condensation of oil was observed, the water spray was discontinued in the condenser, and the condensing oil was turned into the solvent recovery tank. At this point the flow rate was reduced to about 1 gallon per minute. At a predetermined volume, usually 300 gallons, the feed rate to the coke oven was decreased to about 0.5 gallon per minute for the remainder of the usual 400 gallon charge. At that point the coke oven was removed from the feed circuit and the lines and still were flushed with recovered oil. The oven was observed for about one hour after the completion of the charge for excessive frothing.

Malfunctions in the operation, such as oven door leakage or excess oven pressure, were corrected as they occurred. If care was taken to clean the condenser and prevent excess pressure from developing in the oven, the carbon-black formed at the beginning of the charge soon sealed the doors and cracks in the flues, and the operation settled down to a relatively smoke-free condition. Figure 4 illustrates typical temperature cycles during the operation of the coke oven.

After completion of the charge, the coke was held in the oven for an additional 8 — 10 hours to permit the coke to obtain a uniform temperature of 1250°C — 1300°C. This temperature was measured with an optical pyrometer on the coke surface through an observation port in the top of the furnace. Before any work was done on the oven, a valve was closed between the condenser and the receiver tank. This was done to prevent hot gases and sparks from the oven from igniting any accumulated combustible gases in the tank.

At the completion of the coking cycle, the doors were lifted and the coke was pushed from the oven with a mechanical ram. During pushing the coke was quenched slightly with water and permitted to evaporate to dryness. As removed from the oven the coke was in large strong, angular lumps with some anisotropic

structure. Properties of the cokes compared with that of a typical petroleum coke are shown in Table II. Use of the coke in anodes of commercial reduction cells showed the coke to be satisfactory in every respect<sup>26</sup>.

## DISCUSSION

As the gases from the coke oven were vented to the atmosphere and the liquid product recombined with the solvent oil removed by distillation, it was not practical to obtain a material balance on the coking operation. However, work done by the Bureau of Mines from the coking of the Black Creek coal in retorts at 1000°<sup>27</sup> provides some insight into the product distribution that could be expected from this coal on carbonization. This information is shown in Table III along with the coke yield from a series of coke oven runs involving some 20 tons of coal from the Black Creek Seam. About 44 percent of the original coal is converted to calcined coke that would be usable in aluminum cell anodes. The coke obtained from coking the purified coal solution, when combined with the coke obtained from coking the centrifuge sludge, agrees within about 2 percent of the amount of coke predicted by the Bureau of Mines for this particular coal. This would indicate that the molecular size distribution of the coal has not been greatly altered by solution.

Normally, when we open the coke oven doors, we found that the coke charge had shrunk and pulled away from the coke oven walls. The charge could be pushed from the oven with very little effort. In some cases when it was necessary to interrupt the charge to the coke oven for any prolonged length of time (two hours) we found that the coke charge was stuck tightly to the oven wall and we were unable to remove the coke with the pusher. In these cases it was necessary to break the coke from the oven with steel bars. We adopted the practice of charging the solution to the oven continuously and if we were forced to interrupt our charge sequence for more than an hour we terminated the charge at that point and coked a partially filled oven.

Our experience has shown that we can produce a satisfactory electrode coke from high-volatile bituminous coal through a solution process followed by coking in a slot-type coke oven.

## ACKNOWLEDGMENT

The permission of Reynolds Metals Company to publish the results of this investigation is gratefully acknowledged.

## REFERENCES

1. Scott, C. B., "Petroleum Coke as a Raw Material for Graphite and Metallurgical Carbon Manufacture," Chemistry and Industry, July 1, 1967, pp 1124-1131.
2. Kretchman, H. F., The Story of Gilsonite, American Gilsonite Company, Salt Lake City, Utah, 1957.

3. Chemical Week, November 30, 1968, pp. 41-45.
4. Gambro, A. J., D. T. Shedd, H. W. Wang and T. Yoshida, "Delayed Coking of Coal Tar Pitch," paper presented to American Institute of Chemical Engineers, New Orleans, La., March, 1969.
5. Osthaus, K. H., "The Production (sic) of Pitch Coke," Journal of Mines, Metals and Fuels (India), 1959 (Special), pp. 334-336.
6. Selvig, W. A., W. H. Ode, and F. H. Gibson, "Coke from Low-Ash Appalachian Coals for Carbon Electrodes in Aluminum Industry," Bureau of Mines Report of Investigations 3731, 1943, 188 pp.
7. Graham, H. G., and L. D. Schmidt, "Methods of Producing Ultra-Clean Coal for Electrode Carbon in Germany," Bureau of Mines Information Circular 7481, 1948, 13 pp.
8. Campbell, R. J., Jr., R. J. Hilton, and C. L. Boyd, "Coal as a Source of Electrode Carbon in Aluminum Production," Bureau of Mines, Report of Investigations 5191, 1956, 53 pp.
9. Klemgard, E. N., "Electrode Carbon from Washington State Coal," Bulletin No. 218, Washington State Institute of Technology, Pullman, Washington, 1953, 37 pp.
10. Bloomer, W. J., and F. L. Shea, "Coal Deashing and High-Purity Coke," American Chemical Society, Division of Fuel Chemistry, Preprints, 11 No. 2, 378-392 (April 1967).
11. Kloepper, Dean L., Thomas F. Rogers, Charles H. Wright, and Willard C. Bull, "Solvent Processing of Coal to Produce a De-ashed Product," Research and Development Report No. 9, Office of Coal Research.
12. Nelson, H., "The Selective Separation of Super Low Ash Coal by Flo-tation," Gas World, Vol. 127, 1947, pp. 125-130-132.
13. Lowry, H. H., and H. J. Rose, "Pett-Broche Coal Extraction Process and Plant of Ruhrol G. M. B. H., Bottrop-Wilhelm, Germany," Bureau of Mines Information Circular 7420, 12 pp.
14. Graham, H. G. and L. D. Schmidt, "Methods of Producing Ultra-Clean Coal for Electrode Carbon in Germany," Bureau of Mines Information Circular 7420, 12 pp.
15. Bullough, V. L. and W. C. Schroeder, U. S. Patent 3,240,566.
16. Dreyden, I. G. C., British Coal Utilization Research Association Monthly Bulletin, Vol. XIII, Nos. 4 and 5, 1949, pp. 113-138.
17. Golombic, C., J. B. Anderson, M. Orchin, and H. H. Storch, "Solvent Extraction of Coal by Aromatic Compounds at Atmospheric Pressure," Bureau of Mines Report of Investigations 4662, 1950, 12 pp.

18. D'yakova, M. K., A. V. Lozoyi, T. G. Slepantsera, and S. A. Senjavin, "Solutions of Coals," Compt. rend. Acad. Sci., U. S. S. R., Vol. 20, 1938, pp. 681-4, (in English.).
19. Kostal, J., "Extraction of Coal Under Pressure," Prace ustavu pro uyzkum a vyuziti paliv 8, pp. 60-85, 1957 (in Czech.).
20. Srinevasan, S. R., N. G. Basak, and A. Lahiri, "Pressure Extraction of Vitrain-rich Coal with Anthracene Oil," J. Sci., Industr. Res. (India), Vol. 19B, Jan., 1960, pp. 10-15.
21. Lahari, A., and A. N. Basu, "Improvements in or Relating to the Solvent Extraction of Coal," Indian Patent No. 49, 729, Dec. 14, 1954.
22. Rose, H. J., and W. H. Hill, "Coal-Treatment Process," U. S. Patent 1,923,005, August 29, 1933.
23. Van Krevelen, D. W. and I. Schuyler, Coal Science, Elsevier, 1957, Chap. 3.
24. Dobrovolski, I. P., M. V. Donde, and N. Kh. Nemirovskii, "Some Problems in the Planning and Running of Pitch Coke Plants," Coke and Chemistry, U. S. S. R., Vol. 1, 1961, pp. 30-33.
25. Gayle, J. B., and H. S. Auvil, "Development of New, Experimental Coke Oven," Bureau of Mines, Report of Investigations 4923, 1952, 17 pp.
26. Bullough, V. L., L. O. Daley, W. R. Johnson and C. J. McMinn, "Electrode Tests of Purified Coke from Coal in Aluminum Manufacture," American Chemical Society, Division of Fuel Chemistry, preprints, 12 No. 4, 73-80 (September, 1968).
27. Fieldner, A. C., J. D. Davis, R. Thiessen, E. B. Keister, W. A. Selvig, D. A. Reynolds, F. W. Jung, and G. C. Sprunk, "Carbonizing Properties and Constitution of Black Creek Bed Coal From Empire Mine, Walker County, Alabama," Bureau of Mines Technical Paper 531, 1932, 67 pp.

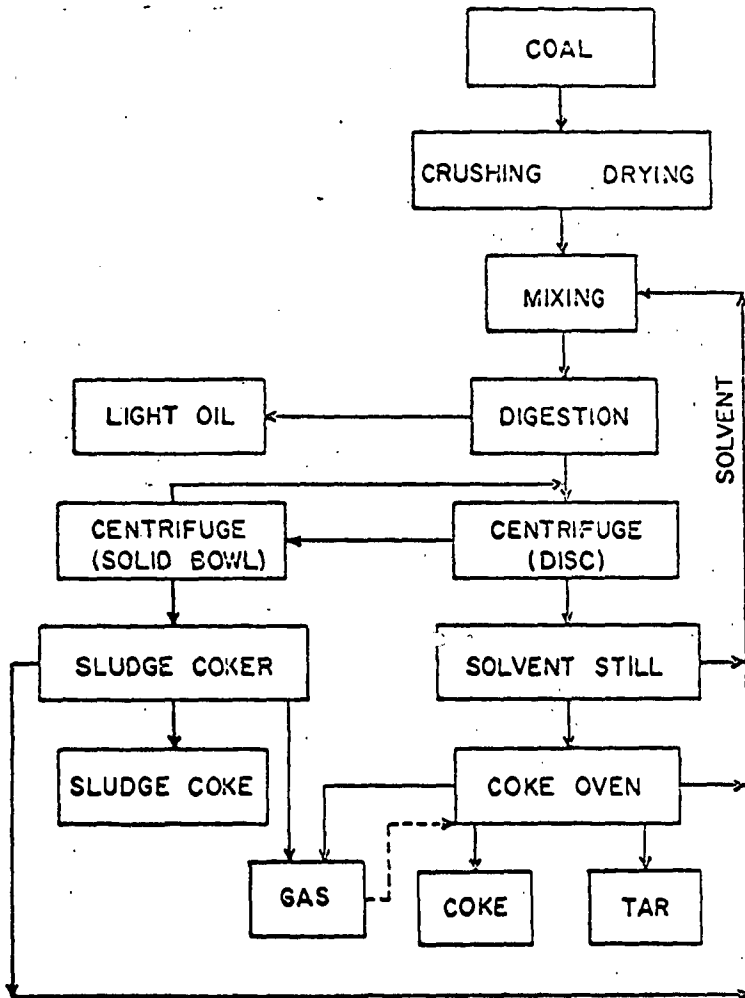


FIGURE 1. DIAGRAM OF A COKE-FROM-COAL PROCESS

TABLE I.  
ANALYSES OF COALS USED IN INVESTIGATION  
OF ELECTRODE COKE FROM COAL

	Black Creek Coal Seam		Kentucky No. 9 Coal Seam	
	As Received	Dry, Ash-Free	As Received	Dry, Ash-Free
Moisture	2.7	----	----	----
V. M.	35.4	37.4	40.5	45.0
Ash	2.8	----	9.9	----
H <sub>2</sub>	5.4	5.4	5.1	5.6
C	79.8	84.4	72.5	80.5
N <sub>2</sub>	1.7	1.8	1.5	1.7
O <sub>2</sub>	9.5	7.6	7.9	8.8
S	.8	.8	3.1	3.4
Anthraxylon		45		65
Trans. Attritus		38		27
Opaque Attritus		7		5
Fusain		10		3
B. t. u.	14,310	15,150	13,060	14,500

Source: Bureau of Mines. Bull. 550.

TABLE II.

PROPERTIES OF COKES FROM KENTUCKY COAL AND  
ALABAMA COAL AFTER CALCINING TO 1340°C

	Alabama Coke	Kentucky Coke	Typical Petroleum Coke
Specific Gravity	2.02	2.01	2.03
Electrical Resistivity, ohm-in.	0.029	0.034	0.034
Hardgrove Grindability Index	22	22.5	37
Sulfur, Percent	0.46	0.67	0.8 - 1.65
Silicon, Percent	0.04	0.09	0.03
Iron, Percent	0.07	0.08	0.05
Aluminum, Percent	0.09	0.09	0.02
Ash, Percent	0.58	0.76	0.34

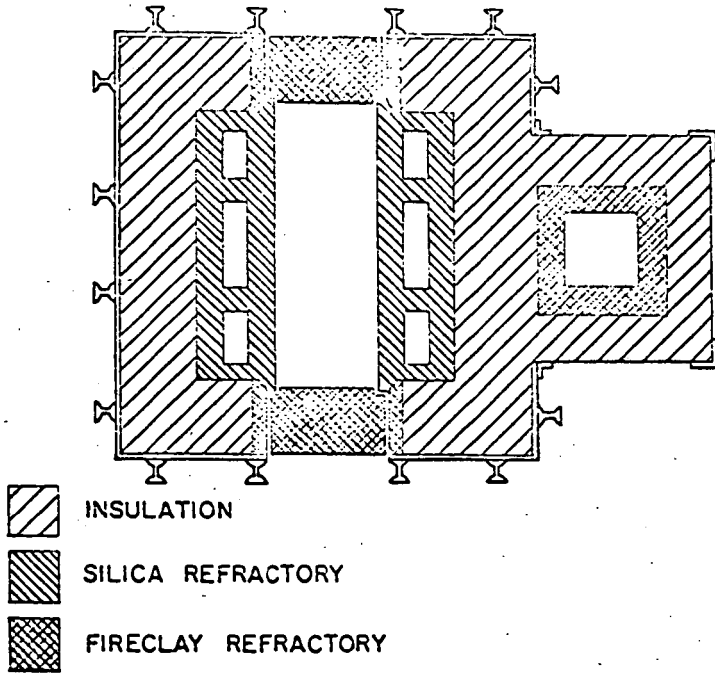


FIGURE 2. EXPERIMENTAL COKE OVEN TYPICAL CROSS SECTION THROUGH FLUES AND COKE CHAMBER (VIEWED FROM ABOVE)

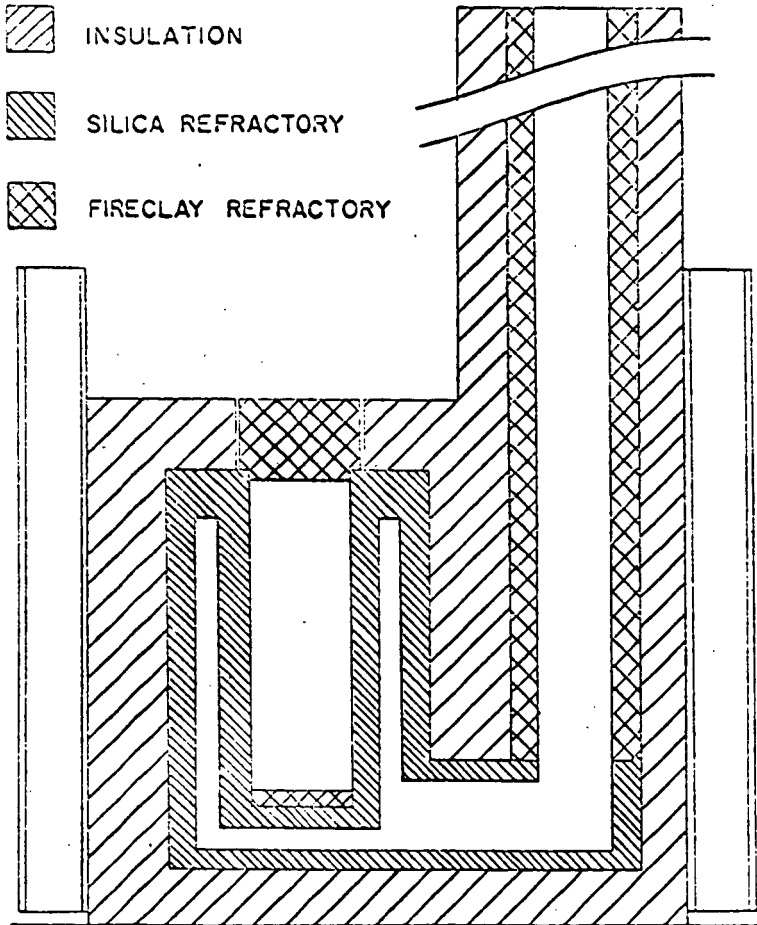


FIGURE 3. EXPERIMENTAL COKE OVEN - TYPICAL CROSS SECTION THROUGH FLUES AND COKE CHAMBER (VIEWED FROM COKE END)

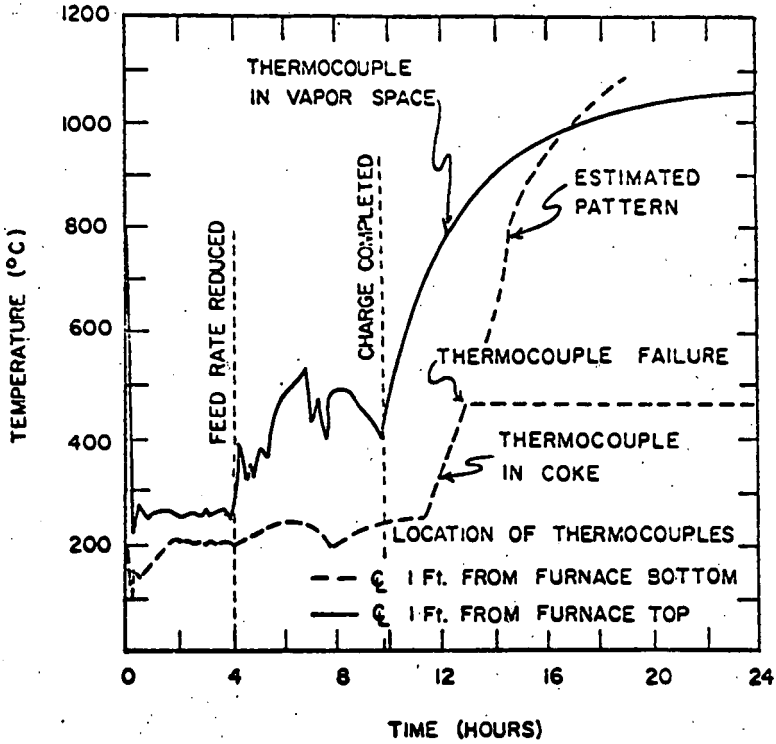


FIGURE 4. TEMPERATURE PATTERN IN COKE SLOT DURING COKING

TABLE III.  
PRODUCT YIELD FROM COKING OF  
BLACK CREEK COAL

	Estimated <sup>1</sup>	Found
COKE	66.6%	44.2%
CENTRIFUGE RESIDUE COKE	-----	24.4%
GAS	17.6%	-----
TAR LIQUOR	6.7%	-----
AMMONIA	0.2%	-----
TAR	6.0%	-----
LIGHT OIL	1.3%	-----

<sup>1</sup>Fieldner, A. C., et. al., Bureau of Mines Technical Paper 531, 1932.

PEABODY CONTINUOUS COKING PROCESS  
VAUGHN MANSFIELD - VICE PRESIDENT - RESEARCH  
PEABODY COAL COMPANY - ST. LOUIS, MISSOURI

ABSTRACT

The paper presents a description of the Peabody Continuous Coking Process which produces coke from coal in a continuous operation. Carbonization is initiated on a moving bed grate carbonizer. A controlled flow of preheated air at 450° F is percolated through the moving bed. Retention time in this pre-treatment furnace is normally about 18 minutes. The product from the moving bed containing 7-10% volatile matter is discharged to a shaft furnace where devolatilization is completed. The hot coke product from the shaft furnace is cooled with inert gas which is generated in the process. By-product gas from the moving bed carbonizer and shaft furnace are combined and used as energy for steam generation or for other purposes. Utilization of the by-product energy is essential to the economics of the process.

INTRODUCTION

The original development work on carbonization of coal on a moving bed furnace was done by Mr. A. H. Andersen of Shawinigan Chemicals, Ltd. at Shawinigan Falls, Quebec in the late 1930's. During the pre-war period, Shawinigan put into operation a number of moving bed carbonizers to produce coke for use in carbide furnaces.

Study of this original work and test reports on a similar installation in South Africa in the middle 1950's indicated certain limitations as to the size of

coal that could be carbonized on a moving bed carbonizer without excessive burning of fixed carbon at the expense of coke yield.

In 1957 Peabody Coal initiated the research and development that resulted in combining a moving bed carbonizer with a shaft furnace. Early test work indicated that to make a totally enclosed continuous system, inert gas cooling or quenching of the product was required to prevent air pollution.

- 
1. Andersen, A. H. and N. R. Fasken  
Carbonization. U. S. Pat. 2,380,930  
August 7, 1945  
Andersen, A. H. and J. E. Renaud  
Coke Production. U. S. Pat. 2,209,255  
July 23, 1940
  2. LaGrange, C. C. Journal of the South African Inst. of Mining  
& Metallurgy  
October, 1956 v 57 No. 3 pp 99-114

## DESCRIPTION OF PROCESS

Figure I shows a flow sheet of the continuous coking process. Coal is fed uniformly by a layer loader onto a moving bed grate carbonizer where the coal is subjected to a furnace environment of 1800<sup>o</sup>F to 2000<sup>o</sup>F. Ignition of the coal is automatic as it enters the furnace on the top layer of the coal bed. Carbonization through the plastic state proceeds downward as a controlled amount of preheated air (450<sup>o</sup>F) is percolated upward through the moving bed. Retention time in this pretreatment furnace is normally 18 minutes and timed to prevent over-carbonization of the top layer of coal.

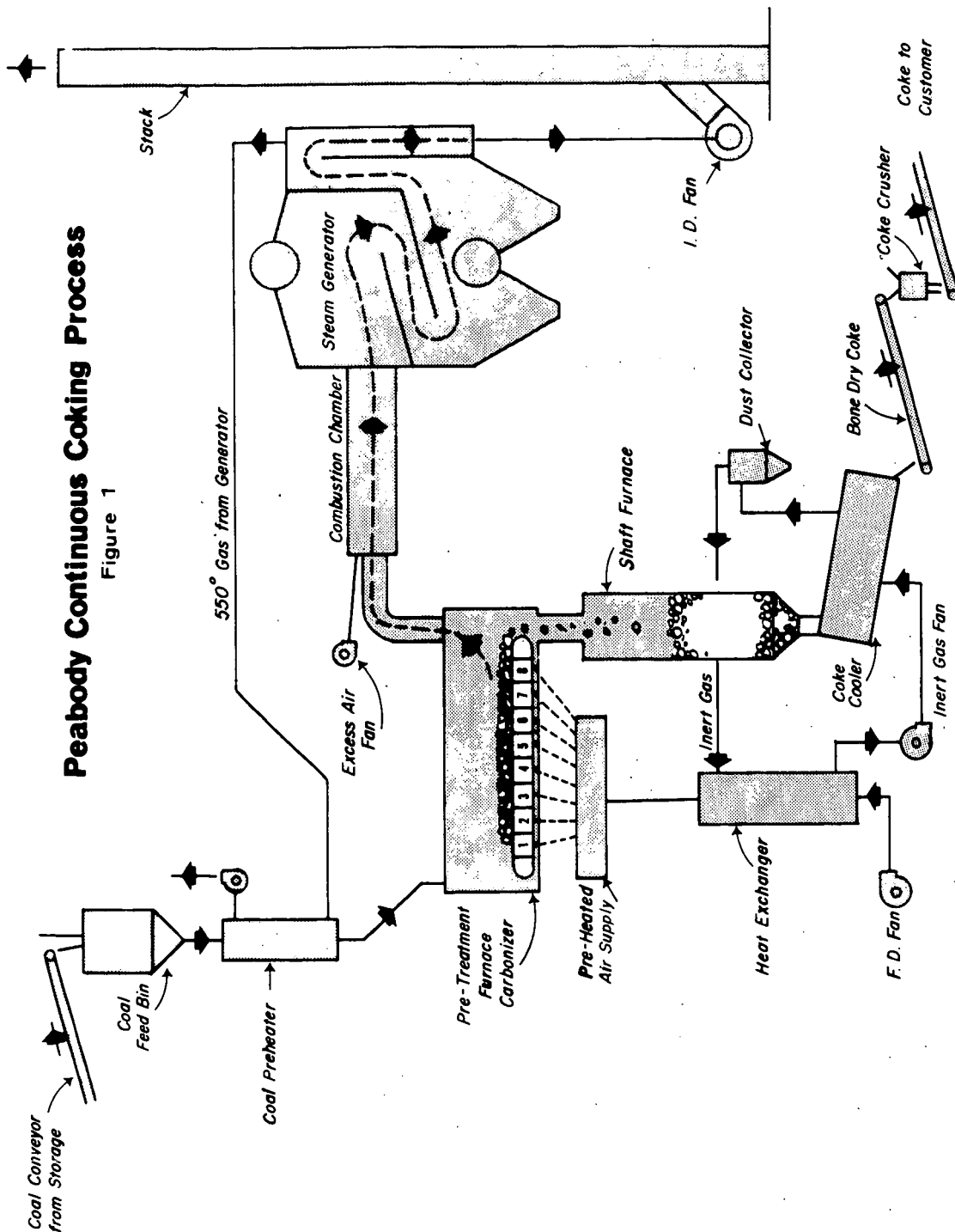
To prevent excessive carbonization of the top layers, the timing and the amount of preheated air is controlled so that 7% to 10% volatile still remains in the product as it is discharged into the shaft furnace. Devolatilization is completed in the shaft furnace without air by retention of the product in the shaft furnace for one hour.

At the bottom end of the shaft furnace the hot coke product (1600<sup>o</sup>F to 1800<sup>o</sup>F) is discharged by gravity into an inert gas cooling unit where the coke product is cooled to a temperature of 250<sup>o</sup>F. The inert gas is self-generated in the combined shaft furnace and cooling system. This system is totally enclosed and prevents air pollution from dust particles or gases.

The by-product gas generated in the moving bed carbonizer and the shaft furnace are combined as an energy supply for steam generation or for other heat-using processes. The use of the by-product gas (approximately equivalent to CO gas) is essential to the economics of the process, particularly with high volatile coals.

# Peabody Continuous Coking Process

Figure 1



TYPICAL ANALYSIS OF PRODUCTFORELECTRIC FURNACES

	<u>Coal Input</u>	<u>Coke Output</u>
	<u>Chemical Analysis</u>	<u>Chemical Analysis</u>
% Fixed Carbon	54.59	89.52
% Ash	4.33	8.76
% Volatile	37.71	1.72
% Moisture	3.37	.00
% B. T. U.	13,965	13,035
% Sulfur	1.03	.90
<u>Size</u>	<u>Screen Analysis</u>	<u>Screen Analysis</u>
	Percent	Percent
1 X 1-1/2	6.9	3.9
5/8 X 1	21.5	11.7
1/2 X 5/8	14.2	23.6
1/4 X 1/2	32.0	53.3
-1/4	25.4	7.5

ENERGY BALANCE OF PEABODY PROCESS

	<u>Input</u>	<u>Output</u>	
	M - B. T. U.	M - B. T. U.	
Energy in Coal	27.92		
Energy Reporting into Coke		15.50	
Energy Reporting into Steam		<u>10.44</u>	
Total Energy Recovered in Products		25.94	
Energy Conversion Efficiency			92.9%

## ECONOMICS OF THE PEABODY COKING PROCESS

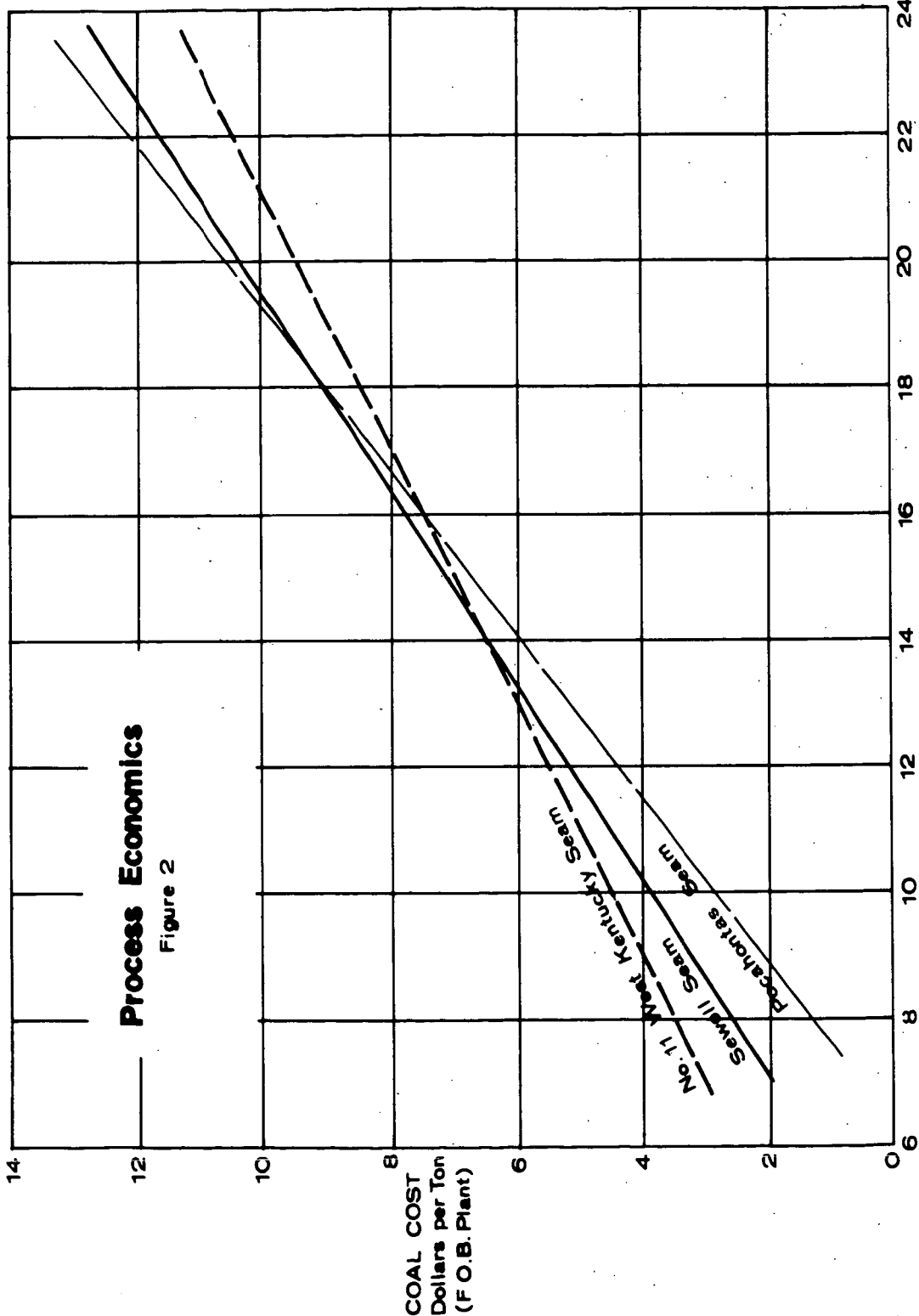
Figure 2 was prepared from extensive tests and operating data obtained at the Columbia, Tennessee plant, which has been in continuous production for the past eight years. Capital cost data was based upon a 500-ton per day coke plant and the return on investment was calculated at 16% before taxes.

## FLEXIBILITY OF THE PROCESS

1. The process variables of temperature, speed of carbonization, air to coal ratio, retention time, can be controlled over such a wide range of environment that practically all classes of coal can be carbonized.
2. The process can produce a bone dry coke product with a density range from 9 pounds per cubic foot to 32 pounds per cubic foot.
3. A blend of coals is not required to produce a suitable coke.
4. The continuous coking system is totally enclosed and can operate without dust or without objectionable air pollution.

# Process Economics

Figure 2



COKE COST (Dollars per Ton, F.O.B. Plant)

COAL COST  
Dollars per Ton  
(F.O.B. Plant)

## CHEMICALS FROM COAL

by

Howard R. Batchelder

Battelle Memorial Institute, Columbus Laboratories  
Columbus, OhioIntroduction

This paper is intended as a review up to 1962 of the history of chemicals from coal, the controlling influences in the past, and what may be expected in the future. The term "chemicals" covers primarily ammonia, the light aromatics (benzene, toluene, and xylene), tar acids, tar bases and tar or pitch, gas, and coke.

In the United States, these chemicals have been derived from coal almost exclusively through high-temperature byproduct carbonization. In England and in Europe, these and other chemicals have been obtained to some extent through various low-temperature carbonization processes and by coal hydrogenation in England and Germany for a few years. No attempt will be made to trace the periodic efforts to establish low-temperature carbonization in the United States. In no case did these result in significant commercial chemical production.

In this country, the production of coke was closely linked to the demands of the iron and steel industry. Up to the time of World War II, in periods of high industrial activity with good markets for steel, coke-oven capacity and output increased and the coal chemicals were in good supply. When demand for steel decreased, oven operation slowed down and the supply of chemicals fell also. Markets for the chemicals other than coke were never strong enough to justify oven operation for these alone.

In 1910, coke-making capacity amounted to about 70 million tons per year--substantially all in beehive ovens with no chemicals recovery. Coal tar derivatives were obtained primarily by importation from Germany. During and immediately after World War I with the German supplies cut off, the markets for chemicals obtainable from coal were strong enough to support the construction of byproduct ovens and start the displacement of beehive ovens. At the end of the war (1919), total carbonizing capacity had risen to 97 million tons per year, of which 40% was in byproduct ovens. At no subsequent time did the total capacity increase above the 97 million tons, but by 1944 almost 90% of the total capacity was in byproduct ovens. In 1962, only 2% of the total coke was produced in beehive ovens.

World War II brought imperative demands for toluene, ammonia, and other chemicals that could not be met by the coke plants. Petroleum and natural gas were used as raw materials, and since that time they have dominated. In a very real sense, the era of significance for chemicals from coal was the period from 1920 to 1940.

Let us consider now some of the most important chemicals to see how the production from coal relates to the production from other raw materials.

### Ammonia

The commercial synthesis of ammonia was well established by 1925, and by 1940 had reached a production rate twice as great as the ammonia recovered from byproduct operations. From that time, byproduct ammonia held in the neighborhood of 200,000 to 250,000 tons per year until 1957. During the next five years, it dropped to about 175,000 tons per year. The production of synthetic ammonia has doubled every five or six years and by 1962 it had reached almost 6 million tons per year.

Figure 1 shows the production rate for each. Figure 2 shows the byproduct ammonia as a percentage of the total. In 1962, this represented only 3% of the total ammonia production in the United States.

### Benzene

Until 1950, benzene was obtained almost exclusively from the products of coal carbonization--either scrubbed from the gas as "light oil" or distilled from the tar stream. By 1940, production had risen from the depression lows to around 150 million gallons per year. During the fifties it reached a peak of almost 200 million gallons per year and has dropped significantly since. In 1950, petroleum benzene was included in the production statistics for the first time at 10 million gallons. By 1962, this had risen to 418 million gallons. Figure 3 shows the dramatic rise of this production and the relation to benzene derived from coal. Actually, much of the benzene formerly derived from coal would not be salable in today's market. It has been only by improved methods of recovery and purification that coke-oven benzene has been able to withstand the competition of petroleum-derived benzene as well as it has.

Most of the benzene produced has been used as intermediate in the manufacture of chemicals that have only come to significance since the time of World War II. Styrene, cyclohexane, and phenol account for almost three-fourths of the benzene consumption. Since 1950, the specific addition of benzene

to gasoline has been negligible in terms of the other uses. Thus it is that the recovery of benzene from petroleum sources has been in response to a demand that did not exist in the earlier days, but which is large enough so that benzene from coal could not have begun to satisfy it.

The economics of the production of benzene from petroleum sources determine the price at which benzene from coal can be sold. The coke-oven benzene production is more or less fixed by the demands of the steel industry for coke. The benzene so produced must be sold, but the production from petroleum can be flexible and can respond in volume to the price situation.

### Toluene

As the demands of the first world war led to the production of toluene from byproduct ovens, so the greater demands of the second world war led to the first significant production from petroleum. During the whole history of coke-oven operation in the United States, the production of toluene from coal did not reach 50 million gallons per year. During the war, the production of toluene from petroleum in only five years rose from nothing to over 160 million gallons per year. At the end of the war, it dropped to less than 10 million gallons, then started a climb that has not yet slowed down. Figure 4 shows the production from coal and from petroleum.

The very dramatic rise during the war and sharp drop in 1946 are evidence of the flexibility of the supply from petroleum. It is this flexibility that lets the coke-oven production set a floor under the price range and the petroleum supply set a ceiling. As price increases, more and more petroleum material will come into the market--to withdraw if the price declines.

Much of the toluene produced is used for the hydrodealkylation to benzene, therefore a significant amount of benzene from petroleum is via toluene. Motor gasoline, solvents, and aviation gasoline are other major uses, and it is probably in these markets that most of the toluene from coal is used.

### Xylenes

Xylenes from coal have not been of great importance in the past. During the fifties, production rose to above 10 million gallons per year for seven years, after which it dropped. Prior to World War II there was no significant production from petroleum. In 1944, almost 50 million gallons was recovered from petroleum. This dropped after the war, but in 1948 started an increase that carried production to almost 350 million gallons in 1962.

This is shown in Figure 5. A substantial part of the production is separated into the isomers for production of phthalic anhydride, isophthalic and terephthalic acids.

### Phenol

The synthesis of phenol was established as a commercial practice many years ago, and by 1940 the synthetic production already amounted to three or four times the amount recovered from coke-oven operations. Phenol from coal stayed in the range of 2 to 3 million gallons per year until 1955 when it rose to 4 to 6 million gallons. Synthetic phenol has increased rather steadily from about 8 million gallons in 1940 to over 80 million gallons in 1962.

These are shown in Figure 6.

### Naphthalene

Coke-oven operations have been the primary or exclusive source of naphthalene through substantially all of the period under consideration. However, some naphthalene was made from petroleum by hydrodealkylation in 1961, and by 1964 this accounted for over 40% of the total production. It has been estimated that the maximum amount available from coal tar would be approximately 650 million pounds per year. The total 1964 production (including petronaphthalene) was 740 million pounds. Obviously, future increases in naphthalene supply will necessarily be of petroleum origin.

### Tar Bases

Of the tar bases, pyridine until the middle fifties was available only from coal tar, as were some of the homologs. The production of synthetic pyridine, the picolones, and others has made for a more stable market and may in the future lead to the development of more widespread uses. It is estimated that the present synthetic pyridine capacity is adequate to supply the total demand. It seems evident that, if the consumption of pyridine and other bases expands, synthetic material will supply this increase--not increased production from coal carbonization.

### Coke-Oven Gas

At one period, gas was a significant byproduct of coal carbonization, too valuable to be used in underfiring the ovens. Blast furnace gas and producer gas were used for underfiring to make the coke-oven gas available for sale. In addition, a significant amount of coke was consumed in the manufacture of carburetted water gas and water gas for ammonia synthesis.

The increased availability of natural gas has substantially eliminated both of these so that coke-oven gas now finds its principal use as a captive plant fuel. Under any normal circumstances, it seems certain that future increases in fuel needs will be supplied by methane whether of natural origin or synthesized.

### Coke

Coke itself, the primary product of carbonization, has experienced also the erosion of its markets by increased utilization of petroleum or natural gas. As stated above, coke for water gas production is no longer necessary to any extent. Even in the blast furnace, the use of oil or gas injection, together with other changes, has reduced the coke required per ton of iron. Many improvements in the blast furnace contributed to the reduction in coke rate, but the overall effect is striking.

In 1962, 66 million tons of pig iron were produced. At the average coke rate of 1920, this would have required over 68 million tons of coke. Actual coke usage in 1962 was only 46 million tons--a difference of 22 million tons.

### Conclusions

From the foregoing, it seems evident that chemicals from coke-oven operation--no matter how important to that operation--cannot be expected to be a significant factor in the future. If chemicals from coal are to be important, they must be derived from some other means of coal conversion on a massive scale.

Work to be reported in this symposium may lead to the establishment of an industry for the conversion of coal to products such as liquid fuels on a major scale. In that case, the simultaneous production of various chemicals may be of a magnitude to challenge the dominance of petroleum and natural gas, and the income from chemicals production may be a significant part of the economic justification of such plants

In making the economic calculations, it must be remembered that in many cases the production of chemicals from petroleum is very flexible, with freedom to enter or withdraw from markets as prices fluctuate. The coal plant, presumably, will not have this freedom, and the projected chemicals income must not be calculated on the basis of a price higher than that which will induce the first petroleum competition into the market.

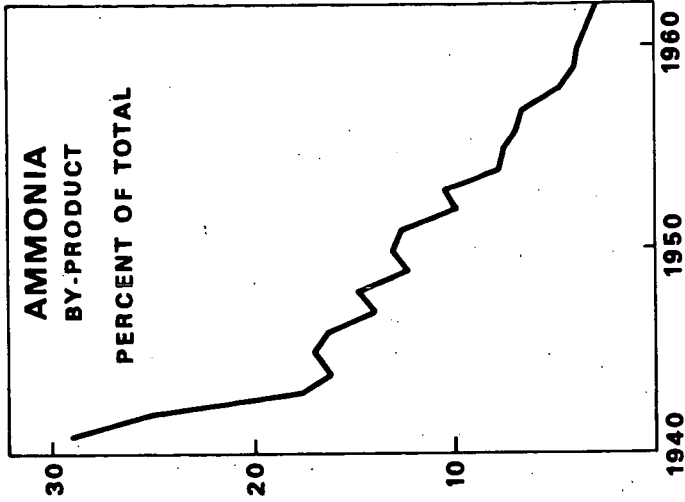


FIG. 2

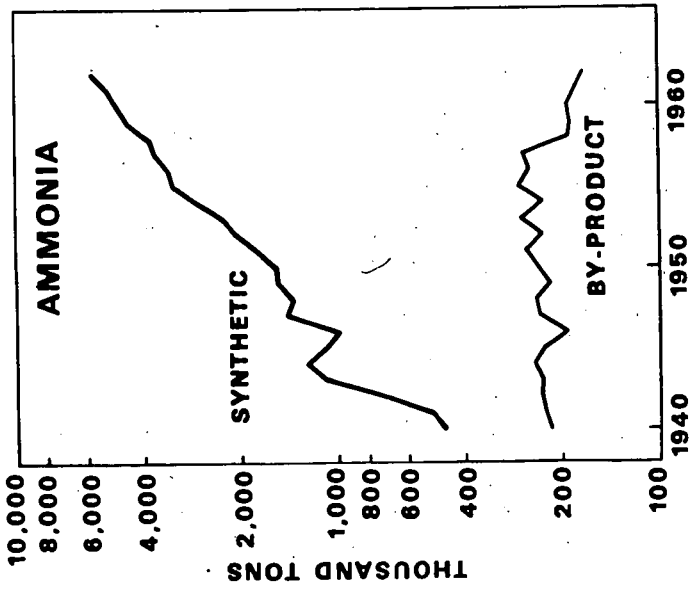


FIG. 1

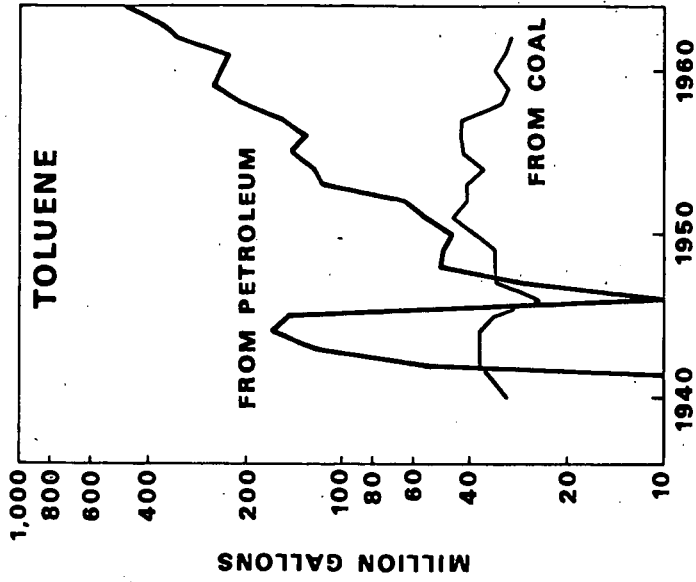


FIG. 4

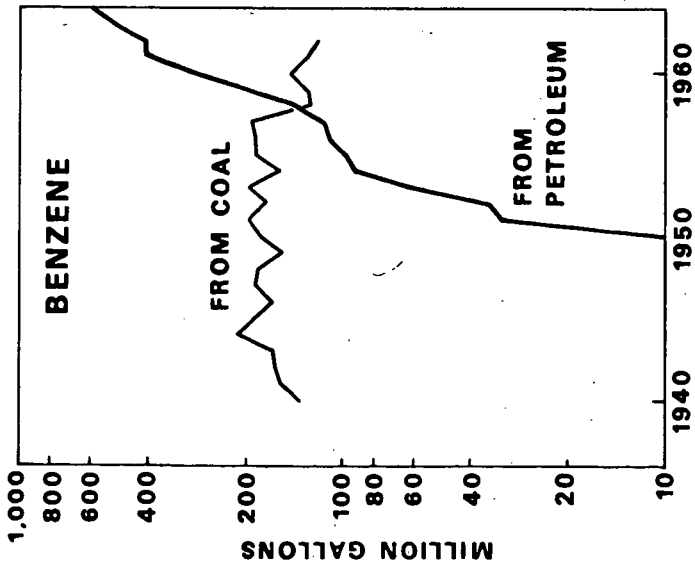


FIG. 3

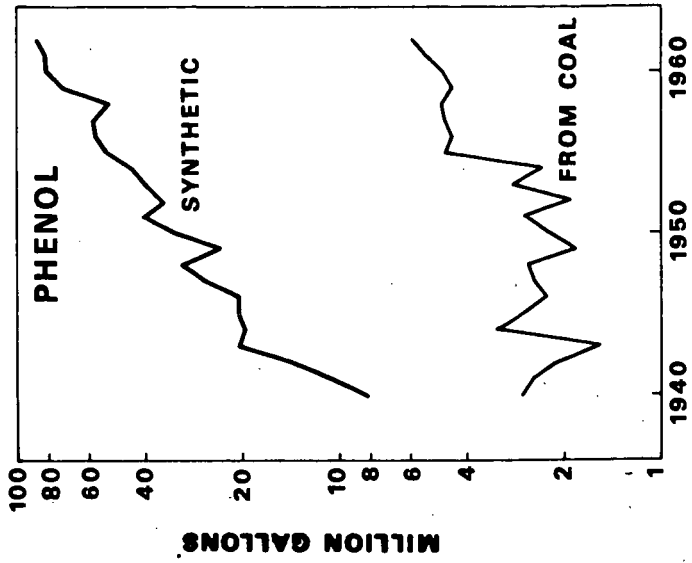


FIG. 6

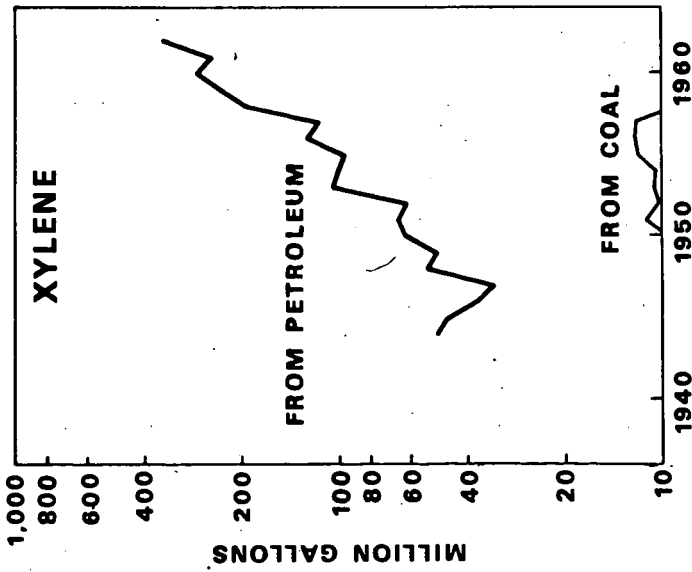


FIG. 5

EFFECT OF COAL RANK ON COMPOSITION OF  
LOW-TEMPERATURE TAR FROM A BENCH-SCALE  
FIXED-BED CARBONIZER

Joseph R. Comberiati, Clarence Karr, Jr., Edward E. Childers,  
Jesse O. Mapstone, Jr., and Patricia A. Estep

U. S. Department of the Interior, Bureau of Mines,  
Morgantown Coal Research Center, Morgantown, W. Va. 26505

The Morgantown Coal Research Center of the U. S. Bureau of Mines has conducted an extensive research program on the effect of changing carbonization conditions on the detailed composition of low-temperature coal tars. Previous publications on the influence of carbonization temperature, carrier gas, and carbonization method have been presented for 10 different low-temperature tars produced from a Colorado subbituminous coal (1, 2), and for 5 different low-temperature tars produced from a Pittsburgh-seam high-volatile A bituminous coal (3).

This report concerns the tars produced in an inert atmosphere at 500° C in fixed beds from seven different coals representing major ranks of humic coals and cannel coals. Analyses were made for the amounts of about 100 compounds, and for several classes of compounds, in each tar and its corresponding light oil, in terms of the coal as it would be charged in a commercial process.

The purpose of this study was to obtain enough detailed information on the amounts of compounds of commercial interest to make an economic evaluation and comparison of the product tars and light oils from coals of various rank carbonized under the same conditions. These relative effects of coal rank are also usable in regard to previous results with commercially feasible processes such as fluidized-bed or entrained-bed methods.

Very little research has been done on the variation of the detailed composition of tars due to coal rank. Recently Maher carbonized two different Australian coals (82 and 89 percent carbon) in a static-bed retort at 500° C (4). Numerical quantitative results were presented for the products from only one of these coals under these conditions, however. Even so, he could draw a few conclusions, mainly that the proportion of aromatic constituents was greater with the higher rank of coal.

## EXPERIMENTAL

The seven different coals used in this work are described in Table 1. Samples sieved from 8 to 42 mesh were used to charge the carbonizer.

The carbonizer and product collecting system are shown in Figure 1. The carbonizer consisted of a vertical 43-in. hinged tubular furnace (4,540 watts, 230 volts) holding a 62-in. by 2-in. OD Vycor tubing reactor. The tubing in turn held a 36-in. long thimble, constructed from fine mesh stainless-steel screen and designed to give an approximately 1/4-in. annular space with the Vycor tubing.

Caking coals swelled sufficiently to block the passage of gas through the annular space, so for these coals the inside of the thimble was lined with pure silica sea sand that had been washed and ignited, and filled with a core of coal. This sand lining was made by inserting a 1-in. ID glass tubing to the bottom of the thimble, placing a 1/4-in. Vycor thermocouple well inside the glass tubing, and adding sand, of particle size retained by a 42-mesh screen, to the space between the thimble and the glass tubing to a depth of about 6 in. Coal was then added through the glass tubing while the tubing was gradually pulled up so that the coal level was always about 1 in. above the bottom of the tubing. When the coal and sand levels were about equal the tubing was tapped gently with a rubber mallet to settle the particles, and the addition of sand and coal then repeated until the thimble was essentially full.

The inside thermocouple well held four chromel-alumel thermocouples (TC 5 through TC 8) for determining the temperature of the coal. The outside thermocouple well, which was inserted between the thimble and the reactor tubing, held four thermocouples (TC 1 through TC 4), for determining the powerstat settings for the four independent heating elements, which consisted of 6-in. sections at the top and bottom of the furnace, and two 14-3/4-in. sections in the central portion. A sectioned furnace was required in order to maintain the same temperature throughout the length of the coal bed.

A tar receiver, consisting of a pot with side arm, was attached to the bottom of the Vycor reactor tubing via a large standard taper joint containing a Teflon sleeve. The No. 1 trap was cooled with ice, No. 2 with powdered Dry Ice, and No. 3 with Dry Ice and trichlorethane, all connecting tapered joints having Teflon sleeves. A column filled with 3- to 8-mesh silica gel was used to recover traces of nongaseous product escaping the traps, followed by a manometer to show that the system was under slight positive pressure, and a gas washing bottle to indicate gas flow.

Coal charges were about 270 g for the cannel coals, 300 g for the bituminous coals, and 560 g for the subbituminous and lignite coals. No sand was used with the latter two in order to obtain enough tar for the assay. The entire system was purged thoroughly with nitrogen, via the nitrogen inlet tube, before each run, and a small, steady stream of nitrogen was used throughout the run. The gas washing bottle was used to confirm the flow of gas. Each run was made at a maximum of 500° C, about 40 minutes being required to reach this temperature. Usually the run was continued at 500° C for about 20 minutes, and then the furnace was turned off because the evolution of yellow aerosol had ceased. Most of the tar was received in the pot, while progressively smaller amounts of tar, light oil, and water were in the three traps.

The contents of the pot and traps were combined, and the water was removed and measured by azeotropic distillation in a Stark and Dean apparatus, using the light oil in the product for the carrier. The light oil was then separated from the tar as a single fraction boiling up to 160° C, and extracted with 10-percent aqueous potassium hydroxide solution to remove any trace of phenols and water that may have been taken over as an azeotrope. The analyses for the individual compounds and classes of compounds in the tars and light oils were made according to a Bureau of Mines procedure (1) based primarily on liquid and gas chromatography. An abridged outline of this procedure has been given (2) and additional information presented (3).

## RESULTS AND DISCUSSION

The yields of individual light oil constituents in pounds per ton of dry coal are shown for the seven different coals in Table II. The yields of the major light oil compound classes are shown in Figure 2, in which the unidentified individual constituents consist almost entirely of nonaromatics such as branched-chain and cyclic aliphatics. Because of the low boiling range of this light oil, only a few benzene aromatics are theoretically possible, and these are all readily identifiable.

As shown in Table II, some of the major aromatic constituents, such as benzene, toluene, and m-xylene, appear to have a general, if not completely consistent, decline in yield with decrease in rank of the normal coals, although the trend for total aromatics is not as clear. The predominant xylene isomer from all seven coals is m-xylene, in the direction of thermodynamic equilibrium. The most striking features of Figure 2 are the high yields of light oil from both cannel coals, due primarily to straight-chain aliphatics, and the large difference in yields of light oil from Pittsburgh coal from two different locations in the seam. The lower yield of 11.40 pounds per ton of coal from Marion County compared to Arkwright coal is in agreement with the 11.20 pounds previously obtained from this same coal in an externally heated 4-in. diameter entrained-bed carbonizer at 538° C (3), and hence cannot necessarily be ascribed to losses.

Table III and Figure 3 show the yields in pounds per ton of dry coal of the fundamental fractions of the total tar, obtained by solvent extractions. The most prominent feature is the extra high yields of tar from the cannel coals, due to the neutral oils. There was a significant difference in the yields of tar from Pittsburgh coal from the two different locations in the seam, the Arkwright coal again giving the higher yield.

Tables IV and V and Figure 4 show the total tar acids and total purified tar bases in pounds per ton of dry coal. The two points emphasized by Figure 4 are the much lower yields of tar bases compared with tar acids for all coals, and the clearly defined decline in yield of total tar acids with decrease in rank of the normal coals. Figure 5, which shows the low-boiling phenols by classes, does not indicate any particular trend with rank; the total cresols, for example, did not vary greatly for the five normal coals. Also, Table V shows that the five lowest boiling phenols totaled about 5 or 6 pounds per ton of each of these five normal coals. Table V also shows that the most prevalent of the six xylenol isomers from all seven coals is 2,4-xylenol, in the direction of thermodynamic equilibrium (5).

Table IV shows that highly alkylated quinolines, such as 2,4-dimethylquinoline which is the most prevalent isomer, make up the bulk of the distillable tar bases. The amounts of pyridines were too small to see by gas-liquid chromatography of the total purified tar bases. In a previous detailed analysis of the tar bases from a 500° C fluidized-bed carbonization of Arkwright mine coal (5), just eight individual alkylated quinolines, especially those alkylated in the 2- and 4- positions, made up fully one-fourth of the total distillable tar bases.

Table VI and Figure 6 show the yields, in pounds per ton of dry coal, of the major classes of compounds making up the high-quality neutral oil, which is an essentially colorless oil containing all the aliphatics (paraffins and olefins) and dinuclear aromatics (naphthalenes and biphenyls) from the entire tar, there having

been no separations by distillation in the recovery of this material. The "other paraffins" and "other olefins" in Table VI consist of the 2-methylalkanes, branched  $\alpha$ -olefins, and trans-internal olefins determined by quantitative infrared analysis. The "not identified" aromatics in Figure 6 include the  $C_{12}$  and  $C_{13}$  biphenyls, which were identified as such, higher alkylated biphenyls, and a variety of compounds containing five-membered rings, such as dibenzofurans. In a previous detailed analysis of the neutral oils from the 500° C fluidized-bed carbonization of Arkwright mine coal (6), a total of nine different classes of polycyclic compounds containing five-membered rings was found.

The most obvious feature shown in Figure 6 is the extra large yield of high-quality neutral oils for both cannel coals, due to every class of compounds except naphthalenes. Table VI shows a definite increase in yield of total olefins with decrease in rank of the normal coals, excluding the subbituminous coal. However, when this same subbituminous coal was carbonized at 500° C in an externally heated entrained-bed, the yield of total olefins was 15.9 pounds per ton of dry coal (2), which is consistent with the trend mentioned above. Total naphthalenes fell in the range of about 4 to 11 pounds per ton of dry coal for the seven different coals. This is compared with the approximately 6 pounds of naphthalene itself obtained from the average coke oven tar.

Naphthalene itself is quite low in all the low-temperature tars, as shown in Figure 7, varying from about 0.04 to 0.85 pound per ton of dry coal. The classes of alkylnaphthalenes, determined by ultraviolet spectroscopy, ran as high as pentamethyl for all seven coals. Figure 7 shows that there was a definite decline in yield of total naphthalenes with decrease in rank of the normal coals. Table VII shows that for six of the seven tars there was substantially more 2-methyl than 1-methylnaphthalene, in the direction of thermodynamic equilibrium at 500° C. The ratio of 2-methyl to 1-methyl for the Arkwright mine coal was 58 to 42, in excellent agreement with the ratio of 57 to 43 for this same coal carbonized at 500° C in a fluidized bed (6).

Figure 8 shows, again, that the yields of aliphatic hydrocarbons from both cannel coals are exceptionally high compared with the normal or humic coals. The yields of "other olefins" alone, which constitute the  $\beta$ - and branched olefins, are greater for each cannel coal than the total aliphatics for each of the normal coals. The "other paraffins" are largely 2-methylalkanes, with lesser amounts of other branched paraffins. The breakdown of the straight-chain paraffins and olefins into individual compounds is shown in Table VIII. Considering the two individual compounds making the highest contributions to the total straight-chain fraction from each tar, these increase from about  $C_{17}$  to  $C_{24}$  n-paraffins with decreasing rank for the first four normal coals. However, the two highest compounds in the lignite tar are olefins, namely 1-heneicosene ( $C_{21}$ ) and 1-docosene ( $C_{22}$ ). No aliphatic hydrocarbons higher than  $C_{36}$  were detected.

Although, as indicated, there are some discernible trends according to rank within the humic coals, the most obvious differences are between the humic and cannel coals. The cannel coals gave extra large yields of paraffins, olefins, and other nonaromatic neutral oil constituents, reflecting the greatly different structure of these coals, which are in the sapropelic deposit series rather than the normal or humic coal series. Cannel, or "candle" coals because of their ready combustibility, are generally made up of the highly "oily" or "waxy" degradation

products of microscopic plant and animal life, such as algae, spores or pollen grains, sporophylls, and plankton (7). Such organic remains when mixed with mud generally produce oil shale. The atomic C-H ratio of cannel coals is generally not greater than about 1.0, similar to oil shales, even though the weight-percent carbon can be as high as that for a high rank bituminous coal in the ASTM classification of humic coals by rank (7).

### CONCLUSIONS

1. There was some evidence of dependence of yield on rank within the humic coals. For example, benzene, toluene, and m-xylene yields generally declined with decrease in rank; yields of total naphthalenes clearly decreased with decrease in rank; yields of total tar acids definitely declined with decrease in rank, although the five lowest boiling phenols totaled about 5 or 6 pounds per ton for all five normal coals; and there was an increase in yield of total olefins with decrease in rank.

2. The cannel coals, which are sapropelic rather than normal or humic coals, gave extra large yields of paraffins, olefins, and other nonaromatic neutral oil and light oil constituents, reflecting the greatly different structure of these coals. For example, the yield of total straight-chain paraffins and olefins in the carbon number range C<sub>5</sub> through C<sub>36</sub> from both cannel coals was around 113 pounds per ton of dry coal.

3. High volatile A bituminous coals from different locations in the Pittsburgh seam gave distinctly different results. For example, the Arkwright mine coal gave higher yields of both light oil and tar than did Consolidation No. 9 mine coal.

4. Total naphthalenes, which included alkylation as high as pentamethyl for all seven coals, fell in the range of about 4 to 11 pounds per ton for all the coals. Highly alkylated quinolines made up the bulk of the distillable tar bases from all seven coals.

5. There was some evidence of a partial approach to thermodynamic equilibrium for the products from all seven coals. For example, the predominant xylene isomer was m-xylene; the most prevalent of the six xylenol isomers was 2,4-xylenol; 2,4-dimethylquinoline was present in the largest amounts; and there was more 2-methylnaphthalene than 1-methylnaphthalene.

### LITERATURE CITED

- (1) Karr, C., Jr., J. R. Comberati, K. B. McCaskill, and P. A. Estep, J. Appl. Chem. 16, 22 (1966).
- (2) Karr, C., Jr., J. R. Comberati, K. B. McCaskill, and P. A. Estep, BuMines Rept. of Inv. 6839, 1966, 9 pp.
- (3) Karr, C., Jr., J. R. Comberati, P. A. Estep, and J. O. Mapstone, J. Inst. Fuel 40, 561 (1967).
- (4) Maher, T. P., Fuel 47, 359 (1968).

- (5) Karr, C., Jr., P. A. Estep, T.-C. L. Chang, and J. R. Comberiat, BuMines Bull. 591, 1961, 228 pp.
- (6) Karr, C., Jr., P. A. Estep, T.-C. L. Chang, and J. R. Comberiat, BuMines Bull. 637, 1967, 198 pp.
- (7) Francis, W., "Coal. Its Formation and Composition," 2nd Ed., Edward Arnold, Publisher, Ltd., London, 1961, 806 pp.

The use of trade names in this article is for identification only and does not constitute endorsement by the Bureau of Mines.

Table I. - Coals Used in the Fixed-Bed Carbonizer

Code	Rank of Coal <sup>a</sup>	Mine	County	State	Carbon, wt-pct <sup>b</sup>	Atomic C-H ratio	Ash, wt-pct
BA	Bituminous (hva) <sup>c</sup>	Arkwright	Monongalia	West Virginia	84.6	1.279	7.9
BC	Bituminous (hva) <sup>c</sup>	Consolidation No. 9	Marion	West Virginia	82.4	1.278	6.4
BS	Bituminous (hvb)	Lower Sunnyside Bed No. 1	Carbon	Utah	82.1	1.214	7.1
SBE	Subbituminous	Eagle	Weid	Colorado	76.1	1.211	6.4
LS	Lignite	Sandow	Milam	Texas	72.9	1.109	13.5
CIC	Cannel	Island Creek No. 13	Logan	West Virginia	86.3	0.989	17.7
CL	Cannel	Leatherwood No. 4	Clay	West Virginia	86.7	0.973	8.7

<sup>a</sup> Cannel coals cannot be included in the ranking of normal coals.

<sup>b</sup> Moisture- and ash-free basis.

<sup>c</sup> These two coals were obtained from the same Pittsburgh seam, but in different counties.

Table II. - Light Oils

Compound	Pounds per ton of dry coal						
	BA	BC	BS	SBE	LS	CIC	CL
<b>Aliphatics</b>							
n-Pentane	0.20	0.08	0.06	----	0.66	3.39	2.89
1-Pentene							
n-Hexane	0.61	0.23	0.30	0.06	0.56	6.63	4.82
1-Hexene	0.31	0.13	0.23	0.03	0.54	6.09	4.34
n-Heptane	0.81	0.41	0.66	0.19	0.58	6.39	6.51
1-Heptene	0.61	0.38	0.49	0.13	0.54	6.09	2.89
n-Octane	1.12	0.36	0.73	0.25	0.54	5.54	3.86
1-Octene	0.71	0.23	0.47	0.14	0.41	4.70	3.13
n-Nonane	1.32	0.19	0.53	0.32	0.46	2.08	1.21
1-Nonene	0.81	0.10	0.41	0.16	0.24	2.00	0.96
n-Decane	0.81	0.07	0.26	0.22	0.19	0.23	0.24
1-Decene	0.20	0.03	0.13	0.08	0.12	0.15	0.12
Total	7.51	2.21	4.27	1.58	4.84	43.29	30.97
<b>Aromatics</b>							
Benzene	1.63	1.03	0.83	0.40	1.44	2.16	2.89
Toluene	7.95	2.88	2.99	2.02	2.53	4.62	4.82
Ethylbenzene	1.22	0.31	0.43	0.42	0.32	0.62	0.48
p-Xylene	1.83	0.34	0.58	0.38	0.17	0.31	0.24
m-Xylene	4.89	1.00	1.11	0.90	0.71	0.77	0.72
o-Xylene	1.94	0.34	0.58	0.52	0.32	0.46	0.24
Isopropylbenzene	0.20	----	----	----	----	----	----
n-Propylbenzene	0.20	0.31	----	0.10	----	----	----
p-Ethyltoluene	2.14	0.17	0.36	0.32	0.07	----	----
m-Ethyltoluene							
1, 3, 5-Trimethylbenzene	0.51	0.06	0.09	0.04	----	----	----
o-Ethyltoluene	0.20	0.03	0.04	0.08	----	----	----
Total	22.71	6.19	7.01	5.18	5.56	8.94	9.39
Total light oils	40.77	11.40	12.80	8.40	13.40	61.60	48.20

Table III. - Fractions Obtained by Solvent Extraction

	Pounds per ton of dry coal						
	BA	BC	BS	SBE	LS	CIC	CL
Resins (cyclohexane insolubles)	54.45	52.48	73.18	19.50	28.75	15.55	35.12
Tar acids	58.35	50.12	44.74	32.56	20.31	18.13	54.13
Tar bases <sup>a</sup>	9.81	6.21	6.61	2.41	4.15	10.27	10.67
High-quality neutral oils	84.70	63.17	70.87	42.47	92.57	292.98	333.29
Other neutral oils	73.54	60.94	45.02	19.49	31.11	204.10	161.38
Resinoids	27.98	13.33	9.53	7.70	26.70	50.11	39.66
Total tar	314.40	246.25	249.95	124.13	204.09	586.80	624.25

<sup>a</sup> All impure; table IV lists tar bases.

Table IV. - Tar Bases (Quinolines)

Compound	Total tar bases, weight percent						
	BA	BC	BS	SBE	LS	CIC	CL
Quinoline	0.03	0.02	0.06	0.16	0.07	0.01	0.51
2-Methylquinoline	0.08	0.07	0.12	0.63	0.40	0.03	0.94
8-Methylquinoline	0.05	0.20	0.24	0.47	0.18	0.02	0.68
7-Methylquinoline	0.18	0.54	0.48	1.02	0.47	0.09	1.54
6-Methylquinoline	0.18	0.42	0.24	0.94	0.91	0.07	0.94
2,6-Dimethylquinoline	0.23	1.13	0.48	1.81	2.03	0.13	1.79
2,4-Dimethylquinoline	0.52	1.81	1.08	2.67	2.25	0.18	4.36
Total tar bases, wt-pct of dry tar	2.28	0.43	0.66	0.38	0.22	0.60	0.98
Total tar bases, lbs/ton of dry coal	7.17	1.06	1.65	0.47	0.45	3.50	6.19

Table V. - Low-Boiling Tar Acids

Compound	Pounds per ton of dry coal						
	BA	BC	BS	SBE	LS	CIC	CL
Phenol	0.83	1.03	0.76	1.07	1.73	----	0.41
o-Cresol	1.90	1.84	1.19	1.01	1.25	0.42	1.01
2,6-Xylenol	0.58	0.61	0.39	0.11	0.17	0.42	0.47
p-Cresol	1.00	1.03	0.96	1.09	1.39	0.27	0.68
m-Cresol	1.65	2.04	1.43	1.65	1.49	0.31	0.58
Total	5.96	6.55	4.73	4.93	6.03	1.42	3.15
o-Ethylphenol	0.48	0.54	0.15	0.16	0.24	0.46	0.33
2,4-Xylenol	1.24	1.53	0.84	0.45	0.55	0.84	1.42
2,5-Xylenol	0.97	1.12	0.67	0.42	0.45	0.69	0.64
2,4,6-Trimethylphenol	0.27	0.35	0.15	0.03	0.07	0.52	0.41
2,3-Xylenol	0.12	0.20	0.13	0.09	0.21	0.21	0.19
p-Ethylphenol	0.19	0.11	0.06	0.09	0.31	0.25	0.19
2,3,6-Trimethylphenol	0.10	0.23	0.10	0.07	0.17	0.15	0.23
m-Ethylphenol	0.22	0.24	0.08	0.09	0.28	0.15	0.21
3,5-Xylenol	0.15	0.29	0.11	0.10	0.24	0.15	0.16
2-n-Propylphenol	0.12	0.17	0.03	0.01	0.03	0.13	0.08
3,4-Xylenol	0.12	0.06	0.03	0.01	0.10	0.15	0.08
Total	3.98	4.84	2.35	1.52	2.65	3.70	3.94
Total tar acids	58.35	50.12	44.74	32.56	20.31	18.13	54.13

Table VI. - High-Quality Neutral Oils

Compound	Pounds per ton of dry coal						
	BA	BC	BS	SBE	LS	CIC	CL
n-Paraffins	9.83	3.92	11.58	7.41	8.25	46.82	42.80
Other paraffins	7.10	8.30	9.97	3.47	9.43	14.11	43.29
Total paraffins	16.93	12.22	21.55	10.88	17.68	60.93	86.09
$\alpha$ -Olefins	3.17	2.65	8.00	4.81	10.88	23.47	37.92
Other olefins	3.20	3.66	7.04	3.77	13.18	69.36	48.38
Total olefins	6.37	6.31	15.04	8.58	24.06	92.83	86.30
Naphthalenes ( $C_{10}$ through $C_{12}$ )	7.28	8.09	4.29	2.19	2.70	5.05	7.06
Total naphthalenes	11.32	10.95	9.19	3.93	5.19	10.55	11.40
Biphenyls ( $C_{12}$ and $C_{13}$ )	0.34	0.64	0.41	0.46	0.48	0.47	1.20
Total high-quality neutral oils	84.70	63.17	70.87	42.47	92.57	292.98	333.29

Table VII. - Low-Boiling Naphthalenes and Biphenyls

Compound	High-Quality Neutral Oils, weight-percent						
	BA	BC	BS	SBE	LS	CIC	CL
Naphthalene	1.00	1.07	0.05	0.46	0.44	0.09	0.04
2-Methylnaphthalene	1.98	4.88	0.13	1.06	0.66	0.27	0.49
1-Methylnaphthalene	1.44	2.94	0.14	0.88	0.36	0.21	0.32
Biphenyl	0.08	0.20	0.12	0.51	0.16	0.05	0.17
1,3-Dimethylnaphthalene	0.55	0.44	0.54	0.41	0.16	0.24	0.28
2-Ethylnaphthalene							
1-Ethylnaphthalene							
2,6-Dimethylnaphthalene	1.14	1.30	0.88	0.61	0.42	0.29	0.32
2,7-Dimethylnaphthalene							
1,6-Dimethylnaphthalene	1.78	1.64	2.47	1.42	0.73	0.43	0.45
1,7-Dimethylnaphthalene							
1,4-Dimethylnaphthalene							
1,5-Dimethylnaphthalene							
1,2-Dimethylnaphthalene	0.71	0.52	1.85	0.30	0.14	0.18	0.22
2,3-Dimethylnaphthalene	0.32	0.81	0.45	0.56	0.36	0.11	0.19
4-Methylbiphenyl							
3-Methylbiphenyl							
Pounds per ton of dry coal							
Naphthalenes (C <sub>10</sub> through C <sub>12</sub> )	7.28	8.09	4.29	2.19	2.70	5.05	7.06
Biphenyls (C <sub>12</sub> and C <sub>13</sub> )	0.34	0.64	0.41	0.34	0.48	0.47	1.20

Table VIII. - Straight-chain Hydrocarbons

Compound	Total straight-chain material, wt-pct						
	BA	BC	BS	SBE	LS	CIC	CL
n-Undecane	0.71	----	0.42	0.68	----	1.28	0.19
1-Undecene	----	----	0.39	0.54	0.07	0.80	0.16
n-Dodecane	1.88	0.46	1.04	1.55	0.27	2.59	0.60
1-Dodecene	----	0.39	0.86	1.06	0.97	1.57	0.58
n-Tridecane	3.39	1.70	1.64	2.21	0.85	3.74	1.23
1-Tridecene	1.34	1.32	1.30	1.44	1.64	2.27	1.07
n-Tetradecane	4.64	2.34	2.10	2.56	1.75	4.54	2.26
1-Tetradecene	2.05	2.01	1.61	1.72	2.54	2.81	1.95
n-Pentadecane	5.45	3.33	2.49	2.80	2.56	5.11	2.88
1-Pentadecene	2.59	2.64	1.92	1.93	3.37	3.29	2.51
n-Hexadecane	5.89	4.03	2.91	2.96	3.19	5.43	3.42
1-Hexadecene	2.95	3.10	2.34	2.12	3.69	3.48	3.12
n-Heptadecane	6.16	4.65	3.22	3.27	3.33	5.46	3.74
1-Heptadecene	3.21	3.64	2.36	2.33	4.00	3.45	3.30
n-Octadecane	6.25	5.35	3.25	3.44	3.42	5.27	3.88
1-Octadecene	3.30	3.95	2.47	2.49	4.13	3.23	3.79
n-Nonadecane	5.89	5.50	3.35	3.65	3.44	4.95	4.12
1-Nonadecene	3.21	4.03	2.55	2.68	4.29	3.07	3.91
n-Eicosane	5.63	5.43	3.51	3.81	3.44	4.54	4.33
1-Eicosene	3.04	3.88	2.65	2.92	4.45	2.78	4.09
n-Heneicosane	5.18	5.35	3.64	4.02	3.44	4.09	4.47

(Continued)

(Page 2 of Table VIII)

1-Heneicosene	2.77	3.49	2.78	3.04	4.63	2.46	4.23
n-Docosane	4.46	4.50	3.84	4.21	3.42	3.64	4.49
1-Docosene	----	3.02	2.99	3.18	4.72	2.20	4.26
n-Tricosane	4.11	4.11	3.97	4.31	3.39	3.23	4.28
1-Tricosene	----	2.71	3.01	3.22	4.58	1.98	4.00
n-Tetracosane	3.57	3.57	4.05	4.28	3.19	2.78	3.93
1-Tetracosene	----	2.56	3.06	3.13	4.08	----	3.70
n-Pentacosane	3.13	2.79	4.00	4.16	2.70	2.33	3.30
1-Pentacosene	----	2.02	2.99	2.94	3.30	----	3.05
n-Hexacosane	2.68	1.94	3.77	3.65	2.16	1.92	2.44
1-Hexacosene	----	1.55	2.80	2.56	2.43	----	1.98
n-Heptacosane	2.23	1.39	3.45	3.18	1.69	1.56	1.53
1-Heptacosene	----	----	2.57	2.05	1.91	----	1.28
n-Octacosane	1.79	1.16	2.93	2.26	0.90	1.25	0.98
1-Octacosene	----	----	2.23	----	0.85	----	----
n-Triacontane	1.34	0.93	2.42	1.81	0.65	1.02	0.56
n-Dotriacontane	0.80	0.70	1.64	1.01	0.45	0.83	0.39
n-Tetratriacontane	0.36	0.46	1.01	0.59	0.25	0.64	----
n-Hexatriacontane	----	----	0.47	0.24	0.04	0.41	----
<hr/> <b>Pounds per ton of dry coal</b> <hr/>							
Paraffins	9.83	3.92	11.58	7.41	8.25	46.82	42.80
Olefins	3.17	2.65	8.00	4.81	10.88	23.47	37.92
Total straight chains	13.00	6.57	19.58	12.22	19.13	70.29	80.72

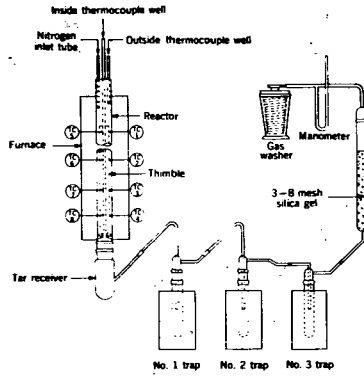


Figure 1. - Schematic Diagram of Carbonizer and Collecting System.

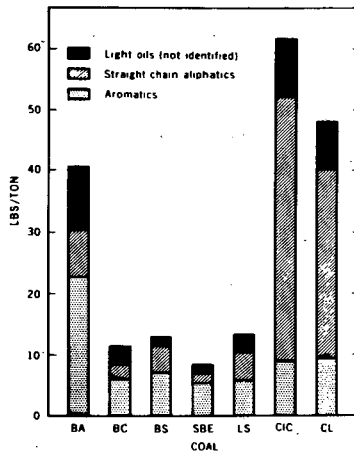


Figure 2. - Light Oils.

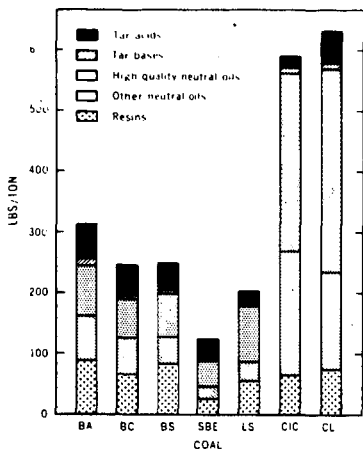


Figure 3. - Fractions Obtained by Solvent Extraction.

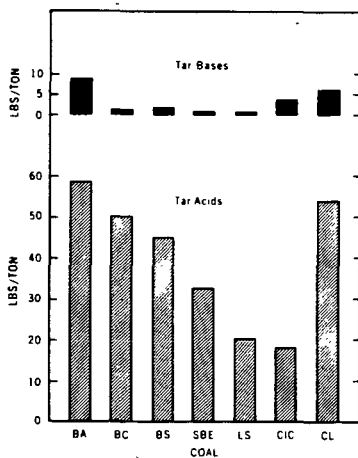


Figure 4. - Total Tar Acids and Pure Tar Bases.

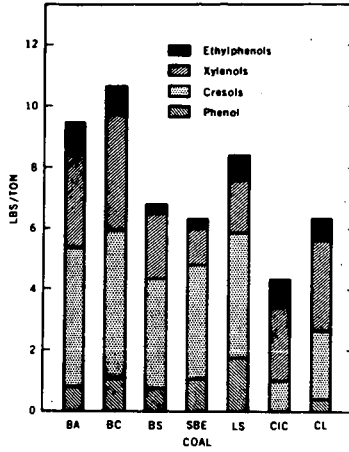


Figure 5. - Low-Boiling Tar Acids.

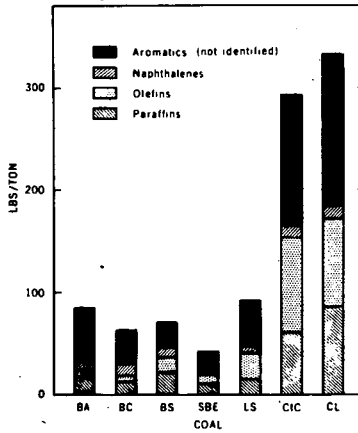


Figure 6. - High-Quality Neutral Oils.

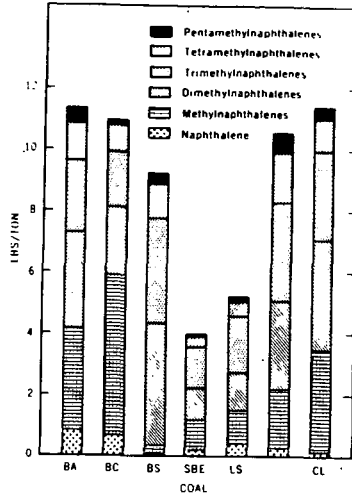


Figure 7. - Totals of All Naphthalene Classes.

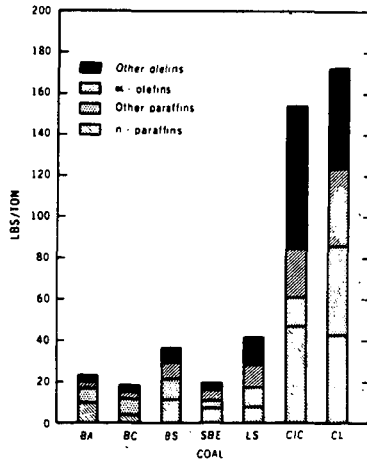


Figure 8. - Classes of Aliphatics.

## PARTIAL DECARBOXYLATION OF COAL AROMATIC ACIDS BY TRANSITION METAL COMPLEXES

Sidney Friedman, Samuel Harris, and Irving Wender

Pittsburgh Coal Research Center, U. S. Bureau of Mines,  
4800 Forbes Avenue, Pittsburgh, Pa. 15213

## INTRODUCTION

Not too many years ago, most of our organic chemical industry depended on coal tar as a source of raw material. Today, petroleum serves this role, and relatively few chemicals are produced from coal. In the foreseeable future, this situation may be again reversed, as petroleum becomes less accessible, and the American energy companies turn to coal as a source of liquid fuels as well as chemicals.

One potential preparation of specific chemicals, directly from coal or coal tar, or from the chars and asphaltenes produced during coal liquefaction, is the result of a combination of two steps, one from traditional coal chemistry, the other from a novel reaction discovered at the Bureau of Mines. This process allows the direct conversion of coal to a mixture of isophthalic and terephthalic acids.

## EXPERIMENTAL PROCEDURES

Preparation of Tributylphosphine Complexes of Dicobalt Octacarbonyl. - Addition of 2 moles of tributylphosphine per mole of  $\text{Co}_2(\text{CO})_8$  in petroleum ether results in evolution of carbon monoxide and precipitation of a yellow solid,  $\text{Co}_2(\text{CO})_7 \cdot 2\text{P}(\text{C}_4\text{H}_9)_3$ , mp 120-121 (dec.) (from  $\text{CH}_3\text{OH}$ ). This compound appears to be stable to air at room temperature when in crystalline form. When in solution, however, decomposition occurs slowly, as evidenced by the formation of a light brown precipitate.

A sample of this catalyst, stored in a refrigerator for 6 months, exhibited no decrease in catalytic activity.

Conversion of  $\text{Co}_2(\text{CO})_7 \cdot 2\text{P}(\text{C}_4\text{H}_9)_3$  to  $\text{Co}_2(\text{CO})_6 \cdot 2\text{P}(\text{C}_4\text{H}_9)_3$  (1). - A solution of 10 g. of yellow  $\text{Co}_2(\text{CO})_7 \cdot 2\text{P}(\text{C}_4\text{H}_9)_3$  in 110 ml. of isooctane was heated to reflux ( $97^\circ\text{C}$ ) under a stream of nitrogen for 3 hours. The solution changed from yellow to dark red-brown in color. The hot solution was filtered, and much of the solvent evaporated from the filtrate under nitrogen. Red-brown crystals appeared upon cooling. These were filtered off to yield 7.7 g. of  $\text{Co}_2(\text{CO})_6 \cdot 2\text{P}(\text{C}_4\text{H}_9)_3$ , mp 120-121 $^\circ\text{C}$ .

Decarboxylation of Benzene Polycarboxylic Acids. - The procedure for carrying out decarboxylations is illustrated by the following example.

A solution of 5 g. of pyromellitic acid and 1 g. of  $\text{Co}_2(\text{CO})_7 \cdot 2\text{P}(\text{C}_4\text{H}_9)_3$  in 110 ml. of dioxane was heated to  $220^\circ$  for 5 hours in a magnetically stirred autoclave under an initial pressure of 2000 psig of 1:1 synthesis gas. The autoclave cooled to room temperature overnight and was vented. The reaction mixture was removed and solvent evaporated under vacuum. The residue was treated with sufficient  $\text{HCl}$  to convert resulting cobalt salts to free acids. An aliquot was

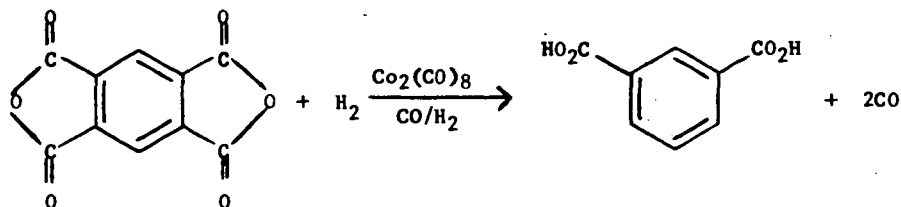
converted to trimethylsilyl esters (2) and analyzed by gas chromatography on a 6 ft. by 1/8-inch-o.d. stainless steel column packed with 3% SE-52\* on 80-100 mesh AW-DMCS Chromosorb G.

#### DISCUSSION AND RESULTS

When coal is carefully air oxidized in the presence of alkali, a mixture consisting largely of aromatic acids is produced (3). This work was originally carried out to obtain product information which could be useful in deducing structure of coal. The product proved to be of sufficient interest in itself for a large chemical company to do bench scale work on oxidizing coal to coal acids (4,5). Unfortunately, the mixed acids, as obtained, found no large markets, largely because of the complexity of the product. Though commercialization did not occur, interest in coal acids has increased, and workers in laboratories scattered around the world have published on this topic in recent years (6-10). Analyses of these fragmentary results indicate that these coal acid mixtures may contain up to 95% (7) benzenepolycarboxylic acid (BPCA), ranging all the way from phthalic acid to mellitic acid.

If it were possible to convert this complex mixture to one with but a few separable components, the oxidation of coal and its derivatives might again become promising. This second step in the process, the conversion of the coal acids to a simple mixture rich in isophthalic and terephthalic acids, is now feasible as a result of a reaction developed at the Bureau of Mines (11,12). In this reaction, a selective decarboxylation of BPCA is effected by  $\text{Co}_2(\text{CO})_8$  and certain of its derivatives.

The reaction was initially carried out on anhydrides, rather than acids, and used  $\text{Co}_2(\text{CO})_8$  as a decarboxylation catalyst. In a typical example, pyromellitic anhydride is decarboxylated to isophthalic acid in 90% yield at 220°C.



This reaction is unique in that a partial, selective decarboxylation occurs. Generally, decarboxylations of aromatic acids are non-specific and drastic (13-15), the products being the parent hydrocarbon.

The reaction has been applied to a number of benzenepolycarboxylic acids and anhydrides, with results shown in tables 1 and 2. For decarboxylation to occur, there must be 2 adjacent carboxyl groups, as in phthalic acid or anhydride, only one of which is eliminated. In anhydrides, the carboxyl which is retained predominantly (12) is the one meta to a ring substituent, such as  $-\text{COOH}$ , which is normally meta-directing in electrophilic substitution. Similarly, ortho-para directing groups ( $-\text{Cl}$ ,  $-\text{CH}_3$ ) result in retention predominantly of a para

\* Reference to a company or product name is made to facilitate understanding and does not imply endorsement by the U. S. Bureau of Mines.

carboxyl. These directional effects are not observed if the substituent is ortho to the two carboxyl groups, when apparently steric effects become important. When both ortho positions are occupied by large groups, as in 3,6-dimethylphthalic anhydride, no decarboxylation takes place. The free acids show less specificity than do the anhydrides. This is illustrated by pyromellitic anhydride, which gives almost exclusively isophthalic acid, while pyromellitic acid goes to a 2:1 mixture of isophthalic and terephthalic acids.

TABLE 1. - Decarboxylation of benzenepolycarboxylic anhydrides with synthesis gas and  $\text{Co}_2(\text{CO})_8^a$

Anhydride	Quantity, $\mu\text{moles}$	$\text{Co}_2(\text{CO})_8$ $\mu\text{moles}$	Product acid or anhydride	Yield, %
Phthalic <sup>b</sup>	176	13	Benzoic	91
Hemimellitic (1,2,3)	26	3	Benzoic	65
			Isophthalic	15
Trimellitic (1,2,4)	26	6	Isophthalic	~ 100
Pyromellitic (1,2,4,5)	23	12	Isophthalic	90
Mellitic (1,2,3,4,5,6)	10	2	Mellitic	80

<sup>a</sup> Standard reaction conditions: 85 ml. toluene, 3500 psig 1  $\text{H}_2$ :1  $\text{CO}$ , 5 hours at 200°C.

<sup>b</sup> Solvent was 175 ml. toluene.

TABLE 2. - Decarboxylation of benzenecarboxylic acids

Acid	Quantity, $\mu\text{moles}$	Catalyst, $\mu\text{moles}$	Product acid	Yield, %
Phthalic	60	3 <sup>a</sup>	Benzoic	95
Hemimellitic	19	6 <sup>a</sup>	Benzoic	40
			Isophthalic	38
Hemimellitic	25	1.5 <sup>b</sup>	Benzoic	56
			Isophthalic	12
Trimesic (1,2,3)	25	1.5 <sup>b</sup>	Trimesic	90
Pyromellitic	12	6 <sup>c</sup>	Terephthalic	15
			Isophthalic	30
			Pyromellitic	55
Pyromellitic	25	1.5 <sup>c</sup>	Terephthalic	35
			Isophthalic	65
Prehnitic (1,2,3,5)	8	3 <sup>c</sup>	Terephthalic	4
			Isophthalic	13
			Trimesic	25
			Prehnitic	58

<sup>a</sup> Reaction conditions:  $\text{Co}_2(\text{CO})_8$ , 85 ml. dioxane, 3500 psig 1  $\text{H}_2$ :1  $\text{CO}$ , 5 hours at 200°C.

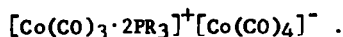
<sup>b</sup> Reaction conditions  $\text{Co}_2(\text{CO})_7 \cdot 2\text{P}(\text{C}_4\text{H}_9)_3$ , 110 ml. dioxane, 2000 psig 1  $\text{H}_2$ :1  $\text{CO}$ , 5 hours at 220°C.

<sup>c</sup> Reaction conditions:  $\text{Co}_2(\text{CO})_8$ , 110 ml. dioxane, 2000 psig 1  $\text{H}_2$ :1  $\text{CO}$ , 5 hours at 220°C.

In the decarboxylation of anhydrides,  $\text{Co}_2(\text{CO})_8$  functions in catalytic amounts; the same is true for phthalic acid. But in reactions involving pyromellitic acid, the  $\text{Co}_2(\text{CO})_8$  is consumed in the course of the decarboxylation, resulting in a mole of product per mole of  $\text{Co}_2(\text{CO})_8$ . Since neither of the products of this reaction, isophthalic and terephthalic acids, react with  $\text{Co}_2(\text{CO})_8$  under normal decarboxylation conditions, deactivation of the catalyst must be the result of direct reaction between it and pyromellitic acid.

It has been found that if one or two of the carbon monoxide groups of  $\text{Co}_2(\text{CO})_8$  are substituted by certain tertiary phosphine ligands, the resulting complexes are excellent decarboxylation catalysts and are no longer destroyed by pyromellitic acid. Though the complex with triphenylphosphine shows no decarboxylative activity, the complex formed by ethyldiphenylphosphine is an active catalyst, as is one from diethylphenylphosphine. Other phosphines which impart catalytic activity are diphenylphosphinoethane and the trialkylphosphines: triethyl-, tripropyl-, tributyl-, trihexyl-, tricyclohexyl-, and trioctylphosphine.

The reaction of  $\text{Co}_2(\text{CO})_8$  with phosphines results in two principal series of complexes. At room temperature, or lower, the usual product is the result of loss of one carbon monoxide and the formation of a yellow, ionic crystalline product insoluble in petroleum ether and soluble in dioxane and acetone. These complexes have the ionic structure (16)



If these complexes are heated, or if the preparation is carried out at elevated temperature, a second carbon monoxide is lost, and a non-ionic complex  $\text{Co}(\text{CO})_6 \cdot 2\text{PR}_3$ , is formed (1). These complexes are red or red-brown and very soluble in petroleum ether.

Either series of complexes may be used for decarboxylation. While the yellow salts appear to be more stable toward long term storage, the red-brown complexes are the stable ones at  $220^\circ$  in the reaction, and are presumed to form in situ from the yellow salts. It is possible to form the complexes themselves in situ, though most of the work reported here was carried out using preformed catalyst.

Solvent plays a critical role in the decarboxylation. Many solvents are too reactive under the conditions used, reacting either by themselves (dimethylsulfoxide, amines) or with the acids or anhydrides (amides, alcohols). The anhydrides are readily decarboxylated in toluene, as well as in other suitable, inert solvents. The acids, being insoluble in toluene, can be reacted in dioxane, acetone, or methyl ethyl ketone. This last solvent is especially convenient, since it is proposed as an extraction solvent for separation of the coal acids (4).

Several complexes of other transition metals have been investigated as decarboxylation catalysts. These include rhodium oxide, iron carbonyl and several phosphine derivatives, manganese carbonyl, bis(triphenylphosphino)palladium dichloride, and chloro-tris(triphenylphosphino)rhodium. Each has been reported to show activity in hydroformylation or carbonylation-decarbonylation reactions. Only rhodium oxide (presumably converted to a rhodium carbonyl) has shown any activity toward decarboxylation, and that activity was poor.

The decarboxylation has been applied to a mixture of acids obtained by oxidation of coal (4). The results of this decarboxylation are shown in the GC analysis of the acids before and after the reaction (table 3). The initial mixture is rich in tri-, tetra-, and pentacarboxylic acids, while the product is mostly

isophthalic and terephthalic acids. Using some of the data scattered in the literature concerning both yields and composition of coal acids, it is possible to speculate on a process that can turn a ton of coal into about 400 lb. of isophthalic and terephthalic acid with a value of five to ten times that of the original coal at today's market price.

TABLE 3. - Analysis of coal acids

Component	Coal acids, weight percent	
	Before decarboxylation	After decarboxylation
Benzoic	--	4
Phthalic	3.3	Trace
Isophthalic	} 0.4	10
Terephthalic		3
Hemimellitic	2.8	--
Trimellitic	5.5	--
Trimesic	--	> 0.5
Pyromellitic	10.1	Trace
Mellophanic (1,2,3,4)	--	a
Prehnitic (1,2,3,5)	--	a
Pentacarboxylic	3.4	Trace
Mellitic	Trace	Trace
Total	25.5	17.5

<sup>a</sup> Traces possibly present; not completely separated from pyromellitic acid.

While the oxidation reaction has been applied only to coal and coke in the past, it is believed that other suitable aromatic sources can be used. These include coal tar, and the chars and asphaltenes currently being produced by the various coal liquefaction processes being investigated. A bench-scale unit to optimize yields of BPCA from various coals and chars is now in operation.

As an alternative to decarboxylation of the total product, a portion of the pyromellitic acid present in the coal acids could be recovered by sublimation before decarboxylation. While this would decrease the overall yields of isophthalic and terephthalic acids, it would furnish a product with considerably higher value.

#### CONCLUSIONS

Controlled air oxidation of coal yields a mixture consisting largely of benzene-polycarboxylic acids. These acids can be partially and selectively decarboxylated to yield a product rich in isophthalic and terephthalic acids by means of catalysts derived from  $\text{Co}_2(\text{CO})_8$  by replacement of carbon monoxide groups by certain tertiary phosphine ligands.

#### REFERENCES

1. F. Piacenti, M. Bianchi, and E. Benedetti, *Chim. Ind. (Milan)*, **49**, 245 (1967).
2. M. L. Kaufman, S. Friedman, and I. Wender, *Anal. Chem.*, **39**, 1011 (1967).
3. R. C. Smith, R. C. Tomarelli, and H. C. Howard, *J. Am. Chem. Soc.*, **61**, 2398 (1939).

4. R. S. Montgomery and R. McMurtrie, Symposium on Technology and Use of Lignite. BuMines Inf. Circ. 8234, pp. 74-98 (1964).
5. W. L. Archer, R. S. Montgomery, K. B. Bozer, and J. B. Louch, Ind. Eng. Chem., 52, 849 (1960).
6. N. W. Franke, M. W. Kiebler, C. H. Ruof, T. R. Savich, and H. C. Howard, Ind. Eng. Chem., 44, 1784 (1952).
7. J. E. Germain and F. Valadon, Bull. Soc. Chim. France 1960, 11.
8. Y. Kamiya, Fuel, 40, 149 (1961).
9. V. Gomez Aranda and F. Gomez Beltran, Combustibles, 22, 147 (1962).
10. A. Benning, Brennstoff-Chemie, 36, 38 (1965).
11. I. Wender, S. Friedman, W. A. Steiner, and R. B. Anderson, Chem. and Ind., 1958, 1694.
12. S. Friedman, M. L. Kaufman, and I. Wender, Ann. N. Y. Acad. Sci., 145, 141 (1967).
13. Y. Kamiya, Fuel, 42, 347 (1963).
14. A. C. McKinnis, U. S. Pat. 2,729,674 (1956).
15. A. C. McKinnis, U. S. Pat. 2,864,854 (1958).
16. L. H. Slaugh and R. D. Mullineaux, J. Organometal Chem., 13, 469 (1968).

CARBON BLACK FEEDSTOCK  
FROM  
LOW TEMPERATURE CARBONIZATION TAR

Donald C. Berkebile, Harold N. Hicks, and W. Sidney Green

Ashland Oil and Refining Company  
1409 Winchester Avenue, Ashland, Kentucky 41101

About three years ago Ashland Oil and Refining Company management initiated a modest coal liquids research program. This program was aimed at accumulating basic technology and at providing a basis for more extensive studies. During the early stages research consisted primarily of literature surveys and scouting experiments. It was concluded from this initial work that low temperature carbonization (LTC) of coal could supply coal liquids at attractive values when considering the current economic conditions.

Discussions with FMC Corporation established their willingness to cooperate in supplying tar from their LTC-pilot plant for experimental work. The FMC unit was constructed under sponsorship of the Office of Coal Research (OCR). This project is designated as Char-Oil-Energy-Development and has the acronym of COED.

The COED process utilizes multiple stage, fluidized-bed pyrolysis with increasing stage temperatures to drive off the volatile matter at controlled rates and temperatures so that a high percentage of the coal is converted to gas and condensable oil products. Coal is crushed and dried and fed to the first stage vessel, where it is fluidized in hot recycle gases generated from combustion of some of the product gas or char. The coal then proceeds from the first stage, which is nominally at 600°F, to the subsequent stages where it is subjected to increasing temperatures of 850, 1000 and 1600°F. Heat for the second and third stages comes from burning some of the char with oxygen in the fourth stage. The gases from the fourth stage flow counter-current to the solids through the third stage to the second stage, from which most of the volatile products are collected. A small percentage of the volatiles comes from the first stage. A small amount of char is recycled to the third and to the second stage to help provide the heat necessary to maintain the vessel temperatures. The volatile products from the pyrolysis are condensed and separated.

The project COED tar that was the feedstock for all work described in this paper was derived from Illinois #6 coal.

Ashland's position as a supplier of refinery products and carbon black--through the United Carbon division--had a significant influence on the selection of the research program goals for processing of LTC tar. The primary objective of this program was to produce carbon black feedstock from all or a portion of the LTC coal liquids. A product of this nature would require a minimum amount of upgrading and would utilize heretofore unmarketable fractions of the coal liquids. Secondly, emphasis was placed on converting the fractions unsuitable for carbon black feedstock into products compatible with normal refinery operations.

Other researchers have tried many techniques to upgrade LTC tar including coking, thermal cracking and hydrogenation. Products ranging from coke to gasoline with some intermediate chemicals are

commonly reported in the literature. Probably the point most common to the work of these various groups was the fact that the processes were uneconomical. Processes to produce chemicals from LTC coal liquids failed because these materials could not be obtained by simple processing schemes.

#### DISCUSSION

An initial quantity of project COED full range coal liquids was obtained from FMC for characterization. A preliminary inspection of the coal liquids showed the following:

Moisture, Volume Percent	4.5-5.0
Benzene Insolubles, Weight Percent	0.5
Quinoline Insolubles, Weight Percent	3.0

This analysis indicated that removal of the particulate matter and moisture would be the minimum treatment for producing carbon black feedstock from the tar.

#### Initial Processing Scheme

The processing scheme used to produce the three initial samples is shown in Figure 1.

The tar was heated until fluid and blended with benzene in a 1:1 volume ratio in order to reduce the tar viscosity sufficiently to permit centrifugation for solids removal and for a subsequent azeotropic distillation to remove the water. Table 1 presents an analysis of the dry, essentially solids-free tar.

The Bureau of Mines Correlation Index (BMCI) is a measure of the quality of a carbon black feedstock. Feedstocks with a BMCI below 70 are unacceptable; feedstocks with a BMCI of 120 and above are considered ideal. The LTC tar physical properties--low gravity and high 50% boiling point--result in a very high, calculated, Bureau of Mines Correlation Index for this liquid. However, subsequent experimental data indicates the BMCI is apparently valid only for materials that are predominantly hydrocarbon; i.e., do not have high percentages of hetero atoms, such as oxygen, nitrogen and sulfur. As shown in Table 1 the COED LTC tar contains significant quantities of O, N and S. A sample of the dry, solids-free LTC tar--sample A in Figure 1--was taken for evaluation as carbon black feedstock.

The dry, solids-free, full range coal liquids were next vacuum fractionated to produce a -530°F overhead cut and a +530°F (at atmospheric pressure) bottoms fraction. The +530°F bottoms material was evaluated as carbon black feedstock; it is designated as sample B in Figure 1. The -530°F overhead was catalytically hydrotreated in a fixed bed 3/4 inch diameter reactor at moderate temperature and pressure. Analytical data revealed a significant change from feed to product. Marked decreases were noted in boiling range and gravity at high volumetric yield. A major reduction in O, N, and S content was observed. The product contained high concentrations of naphthenes and aromatics; this in conjunction with its boiling range, characterized the product as a potential refinery reformer charge stock.

A third sample for carbon black feedstock evaluation--C in

Figure 1--was prepared by solvent extraction (2:1 solvent to oil ratio) of the +530°F coal liquids. The solvent was a typical reformat (°API=53.4) containing about 61% P+N and 38% A. The extraction yielded an insoluble raffinate (275°F S.P. pitch-like material) and the extract fraction. After stripping off the solvent, the extract yield was about 74 weight percent. Ten gallons of this material were evaluated as carbon black feedstock.

An analysis of carbon black feedstock samples B and C is shown in Table 2. Samples A, B and C were evaluated at United Carbon's pilot plant in a 2 inch furnace. All coal derived samples were handled in an identical manner, and a standard carbon black feedstock was also processed in the pilot unit for comparison. The coal liquids carbon black product was compounded into a standard rubber formulation. This formulation was evaluated against rubber compounded from an ISAF control carbon black and the carbon black produced in the pilot plant from the standard feedstock. The full range and vacuum reduced samples (A and B, respectively) produced an inferior carbon black in low yields. The low structure and low modulus exhibited by the rubber formulations were particularly noticeable. The extracted sample (C) produced a low yield of carbon black, but the quality was nearly equal to the standard feedstock, with the exception of having only a slightly lower structure. Yield data is presented in Table 3.

These results indicate the extraction is more of a de-ashing step than a true extraction and that the high oxygen content of the tar suppresses carbon black yield. Carbon black quality is detrimentally affected by sodium, potassium and other metals normally found in coal ash and in low grade feedstocks. These metals cause carbon black structure (chain length) to be low. The yield from +530°F tar was approximately 75% of the standard feedstock and was encouraging from a research standpoint. Nevertheless, the value of the 75% yield feedstock is much less than 75% of the going rate for high quality feedstocks, due to the combination of higher feedstock consumption per pound of carbon black, higher fuel gas consumption per pound of carbon black and reduced reactor capacity.

#### Hydrotreating-Microreactor

Because of the high oxygen content (~8%) of the dry, solids-free tar and its detrimental effect on carbon black yield, it was decided to attempt to selectively hydrotreat the tar with the objective of removing the oxygen, nitrogen and sulfur without ring saturation. Fixed bed, catalytic hydrotreatment of the tar was conducted at a moderate temperature and intermediate pressure in a 3/4 inch diameter reactor. The process was studied by evaluation of composited reactor effluent and off-gas samples from consecutive test periods of 19 to 24 hours duration.

A hydrocarbon liquid yield on feed of about 86 weight percent and an aqueous yield of about 3% were obtained. Hetero atom removal based on the feed and composited effluent samples was over 90% for sulfur, over 60% for oxygen, and nearly 40% for nitrogen. Hydrogen consumption for this level of processing was estimated at 1200 to 1500 SCF/bbl. of feed. Material balance data indicated that hetero atom removal accounted for the largest portion of the hydrogen consumed with most of the remaining hydrogen used appearing as cracked products in the off gas.

The hydrotreated composited product was fractionated into a -600°F refinery feedstock and a +600°F carbon black feedstock. The weight percent yields were about 58% overhead and 42% bottoms.

The +600°F bottoms are characterized below. This table shows a considerable upgrading of the feedstock over that previously produced and indicates that a potential carbon black yield comparable to the standard carbon black feedstock should be obtained from the hydro-treated +600°F bottoms.

#### CARBON BLACK FEEDSTOCK COMPARISON

	Wt. %		Ratio	Carbon Black
	C	H	C/H	Yld. lb/gal.
Standard C.B. Feedstock	90.2	8.2	11.0	3.75
Extract from +530° Fraction	83.7	7.6	11.0	2.74
Hydrotreated +600° Fraction	89.1	8.0	11.1	--

Carbon black yield data on the hydrotreated +600°F tar could not be obtained since the 3/4 inch reactor hydrogenation techniques produced only one gallon of full range hydrotreated tar. Pilot scale carbon black feedstock evaluations require a minimum sample of ten gallons.

The experimental data from the 3/4 inch reactor served as the basis for planning further processing of project COED's LTC tar. It was decided to attempt hydrotreating of the dry, full-range tar in a 4 inch diameter reactor to produce sufficient +600°F material for pilot scale evaluation as carbon black feedstock.

#### Hydrotreating-Four Inch Reactor

As a result of the above work, an additional 150 gallons of full-range COED liquids was obtained for processing through the 4 inch reactor. The coal liquids "as received" contain sufficient particulate matter and water to cause operability problems on a pilot scale. As discussed earlier, the tar was processed initially by centrifugation and azeotropic distillation to remove solids and moisture. The following table shows the results of this processing:

	Tar	Tar
	As Received	Processed
Ash	0.83	0.44
Quinoline, Insolubles	3.6	1.8
Benzene, Insolubles	4.3	7.3

Characterization of the dry, solids-free tar showed it to have essentially the same analysis as shown in Table 1.

After processing to remove water and solids, the full-range LTC tar was hydrotreated in the 4 inch reactor system for hetero atom removal at approximately the same conditions which were used in the 3/4 inch reactor.

Processing in the 4 inch unit represented a feed rate scale up of about 160 over that of the 3/4 inch reactor. Severe temperature control problems resulted from the scaled-up operation due to the exothermic nature of the reactions taking place. The desired isothermal reactor profile for optimum selectivity and hetero atom

removal could not be maintained. Fluctuations between low temperatures (increased naphthene formation) and high temperatures (catalyst deactivation and corresponding reduction in deoxygenation) resulted in more oxygen and hydrogen and less carbon in the reactor effluent than the project goals. Carbon content of the hydrotreated composite was 86.5 weight percent, somewhat below the 87.7 weight percent obtained in the 3/4 inch reactor processing. Figure 2 illustrates the general effects of temperature on product composition.

Overall, considerable difficulty was experienced in obtaining smooth operation of the 4 inch reactor; however, the entire amount of feed available was processed. The liquid hydrocarbon yield was about 89 weight percent on feed, and the aqueous yield was about 3 weight percent. This compares very well with the results from the 3/4 inch reactor.

The table below compares hetero atom removal based on overall feed and composited product data for the 4 inch reactor and 3/4 inch reactor:

HETERO ATOM REMOVAL-WEIGHT PERCENT

	<u>Oxygen</u>	<u>Nitrogen</u>	<u>Sulfur</u>
4 inch Reactor	58	16	83
3/4 inch Reactor	62	38	93

Hydrogen consumption was estimated at 2000 SCF/bbl. based on an overall material balance and hetero atom removal. Hydrogen consumption is thus higher than the 1500 SCF/bbl. obtained in small scale processing. This may be attributed to increased naphthene formation and increased hydrocracking in the 4 inch reactor.

The hydrotreated tar was fractionated to produce a -600°F overhead cut and a +600°F bottoms fraction. The yields on dry, solids-free tar were about 46 volume percent overhead and 54 volume percent bottoms. The -600°F fraction will be discussed later in this paper.

The +600°F Fraction

The +600°F fraction (Table 4) was shipped to the United Carbon laboratories for pilot scale carbon black production. The carbon black produced was then evaluated as described earlier by compounding in a standard rubber formulation. The results of these tests can be summarized as follows:

1. The material handled satisfactorily in the pilot scale reactors.
2. The carbon black produced from the hydrotreated +600°F coal liquids has only a slightly lower modulus with comparable tensile, elongation and abrasion resistance and approximately 10% lower structure as compared to a carbon black which was made from a standard carbon black feedstock.
3. Yield of carbon black from the hydrotreated +600°F tar is only about 80% of the standard feedstock, 3.10 lbs/gal. vs. 3.97 lb/gal., at essentially the same surface area.

4. A 60% reduction in oxygen did not significantly change the carbon black yield. Apparently sufficient naphthene formation had occurred in the 4 inch reactor to counteract the reduction in oxygen. Carbon to hydrogen ration and oxygen content are summarized below:

	<u>% Oxygen</u>	<u>C/H</u>
Standard Feedstock	0	11.0
+530°F Extracted Tar	8	11.0
+600°F Hydrotreated Tar	3	10.2
Raw Tar	9	10.9

In summary, the initial attempt to produce a carbon black feedstock from LTC tar via selective hydrogenation followed by fractionation resulted in an acceptable quality black and demonstrated the technical feasibility for this processing route. Yield was not as high as desired and may be attributed to not achieving process goals for hetero atom removal during hydrotreatment.

#### Further Processing of +600°F Fraction

The original process goal was to achieve a +600°F bottoms material with a 90 weight percent carbon content, since this level is comparable to the standard carbon black feedstock. The following table shows the ultimate analysis of the untreated +600°F tar, the hydrotreated +600°F tar and the standard carbon black feedstock:

<u>Ultimate Analysis, Wt. %</u>	<u>Standard Carbon Black Feedstock</u>	<u>Raw Tar +600°F</u>	<u>Hydrotreated Tar, +600°F</u>
Carbon	90.20	82.6	86.97
Hydrogen	8.20	7.55	8.50
Oxygen	-	8.88	2.97
Nitrogen	-	0.96	0.92
Sulfur	1.60	1.30	0.30

In an effort to achieve 90 weight percent carbon content material, the hydrotreated +600°F tar from the 4 inch reactor was catalytically hydrotreated again at a moderate temperature and pressure in a 2 inch diameter reactor. The second pass hydrotreated +600°F tar is characterized in Table 5. The yield of the material is approximately 35 volume percent of the dry, solids-free COED tar. Note that the project goal of 90 weight percent carbon content was very nearly achieved.

A sample of this second pass hydrotreated +600°F tar was forwarded to the United Carbon division and was processed through their pilot plant to produce carbon black. Performance of this tar in the pilot scale carbon black reactor was practically identical to that of the standard carbon black feedstock.

Data from rubber samples compounded with carbon black from the second pass hydrotreated +600°F tar show the black to be nearly equal to the carbon black produced from the standard feedstock at identical reactor conditions. Some of the pertinent data from these tests are given in Table 6. A carbon black yield of about 90 weight percent of the standard was obtained.

A laboratory inspection of the -600°F fraction from the 4 inch reactor is shown in Table 7. Although the aromatics content of this particular material was not determined, a -600°F cut from the 3/4 inch reactor study, with very similar properties, contained well over 70 volume percent aromatics by FIA analysis. This indicates the -600°F fraction would be a highly desirable refinery feedstock. However, the hetero atom concentration of this cut is too high to permit processing by conventional refinery techniques. For this reason, second pass hydrotreating of the -600°F cut was studied.

Pilot studies indicated a reactor configuration with a fairly high residence time would be required to effectively remove the hetero atoms in the second pass catalytic hydrotreating step. Such a reactor was constructed and successfully operated with the -600°F fraction (Table 7) feed to produce 5.5 weight percent water and a second pass -600°F liquid hydrocarbon product in 92.2 weight percent yield with the following properties:

-600°F SECOND PASS  
HYDROTREATING EFFLUENT

°API	29.5
FIA, LV%	
P + N	33.2
O	1.0
A	65.0
Hetero atoms, ppm	
S	35
N	620
Bromine No.	2.2

Hetero atom concentrations have been reduced sufficiently by this operation to permit processing of the material in conventional refinery units.

The -600°F second pass hydrotreating effluent was fractionated into five fractions: (1) IBP-160°F, 0.9 LV%; (2) 160-360°F, 42.5 LV%; (3) 360-410°F, 12.1 LV%; (4) 410-550°F, 32.5 LV%; (5) 550-600°F, 12.0 LV%, for laboratory and pilot scale evaluation as refinery feedstock. The IBP-160°F cut was not processed further since in practice this would probably be included in the reformer charge because of its small quantity and its composition. The 160-360°F fraction was characterized as reformer chargestock on the basis of its naphthene content and boiling range. Results of the pilot scale reforming are shown in Table 8. Note specifically the very high blending value of the reformat, its high aromatic (90+%) content and the high gas make which is estimated to be 92% hydrogen in a recycle operation.

Laboratory evaluation of the 360-410°F and 410-550°F fractions indicated they should be combined and subjected to a relatively severe hydrotreating step, then fractionated to a 410°F cut point. The -410°F portion with a 98.5 F-1 clear octane would then be blended into gasoline, and the highly aromatic (12.0 °API) 410-525°F bottoms would be an excellent hydrodealkylation feedstock since it has a naphthene potential of over 57 weight percent on feed.

The 550-600°F fraction could be marketed as #2 fuel oil.

### ECONOMICS

The preliminary economics of a commercial scale LTC tar processing facility have been estimated based on a pilot plant and laboratory data. The economics assume a 10,000 ton/day coal carbonization unit is located adjacent to the tar processing facility. This unit, while not directly included in the economics, supplies a low cost source of 11,906 bbl/day of full-range LTC tar. Figure 3 is a block flow diagram of the proposed processing scheme starting with the full-range LTC tar.

A capital investment of \$13,100,000 has been estimated for the processing units shown in Figure 3, with the exception of the carbon black facility, which is not included in the economics. A discounted cash flow of 20% can be realized on this investment with full-range LTC tar valued at \$1.62/bbl. and the following values placed on the various products:

Carbon Black Feedstock	-	7¢/gallon
#2 Fuel Oil	-	9¢/gallon
Gasoline Blending Stock	-	14¢/gallon (102+ Octane No.)
Benzene	-	23¢/gallon
Naphthalene	-	4.5¢/lb.
H <sub>2</sub> Consumed or Generated	-	30¢/1000 SCF

### SUMMARY

The technical feasibility of hydrotreating full-range LTC tar to produce a highly aromatic residue boiling above 600°F, with low hetero atom content, has been demonstrated. The hydrotreated +600°F fraction has been processed on a pilot scale to an acceptable quality carbon black in good yield.

The lower boiling material (-600°F fraction from hydrotreating full-range LTC tar) when nearly free of hetero atoms is a highly aromatic material ideally suited for processing in conventional refinery equipment to yield valuable products.

Preliminary economics, based on pilot plant data, indicate the overall LTC tar processing scheme can realize a good DCF rate of return on investment, when reasonable product values are assumed.

### ACKNOWLEDGMENT

The authors wish to thank Ivan Ceresna and the United Carbon laboratories for their cooperation and excellent work in preparing and evaluating all carbon black samples discussed in this paper.

193  
**FIGURE 1**

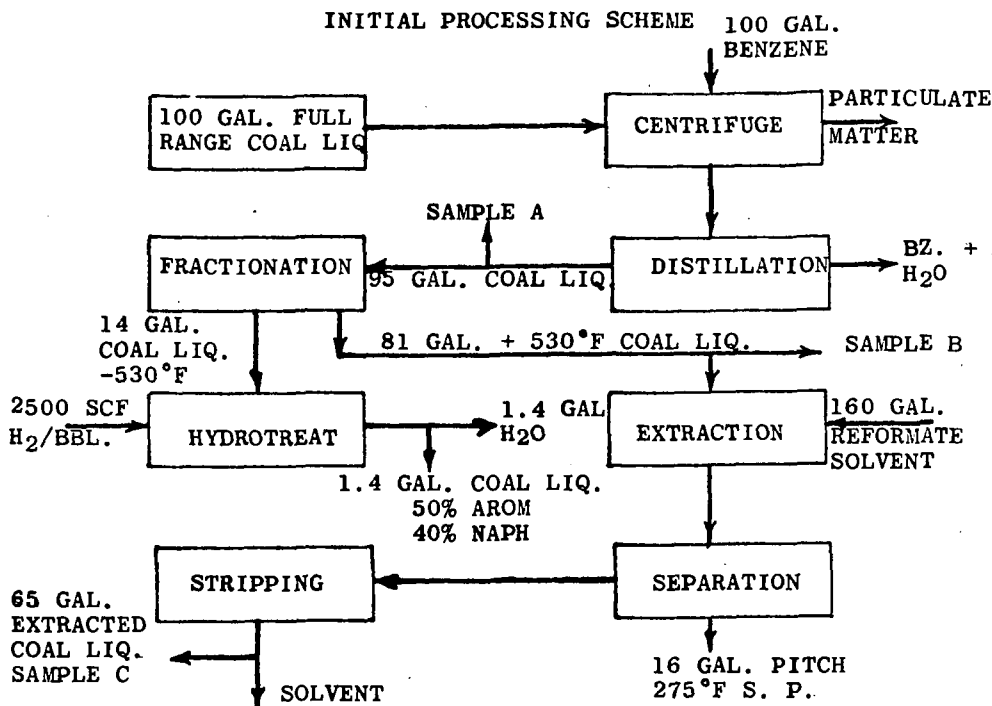


**TABLE 1**

PROJECT COED FULL RANGE COAL LIQUIDS  
 (DRY, SOLIDS-FREE)

SAMPLE	A
DISTILLATION, °F	
5%	457
10%	486
30%	701
50%	831
70%	932
80%	Cracking
QUINOLINE INSOLUBLE, WT. %	0.33
°API AT 60°F	-6.1
ASH, WT. %	0.13
CONRADSON CARBON, WT. %	18.4
CORRELATION INDEX	140
ULTIMATE ANALYSIS, %	
CARBON	82.42
HYDROGEN	7.55
OXYGEN	8.74
NITROGEN	1.10
SULFUR	0.9

TABLE 2

## PROCESSED PROJECT COED COAL LIQUIDS

SAMPLE DISTILLATION, °F	B	C
	+530°F CUT	EXTRACTED +530°F CUT
IBP	-	450
5%	525	521
10%	581	571
20%	680	672
30%	742	741
40%	794	Cracking
50%	836	
60%	Cracking	
BENZENE INSOLUBLE, WT. %	12.0	0.013
°API AT 60°F	-8.7	-7.2
ASH, WT. %	0.18	0.022
CONRADSON CARBON, %	21.7	14.96
CORRELATION INDEX	157	150
ULTIMATE ANALYSIS, %		
CARBON	82.71	82.61
HYDROGEN	7.89	7.55
OXYGEN	8.90	8.88
NITROGEN	1.16	0.96
SULFUR	1.00	1.30
POTASSIUM, PPM		4.7
SODIUM, PPM		8.0

TABLE 3

## CARBON BLACK YIELD DATA

<u>FEED</u>	<u>YIELD (POUNDS/GALLON)</u>
STANDARD C. B. FEEDSTOCK	3.75
FULL RANGE COAL LIQUIDS -- A	2.70
+530°F FRACTION OF FULL RANGE COAL LIQUIDS -- B	2.64
EXTRACT FROM +530°F FRACTION -- C	2.74

FIGURE 2. EFFECT OF TEMPERATURE ON PRODUCT COMPOSITION

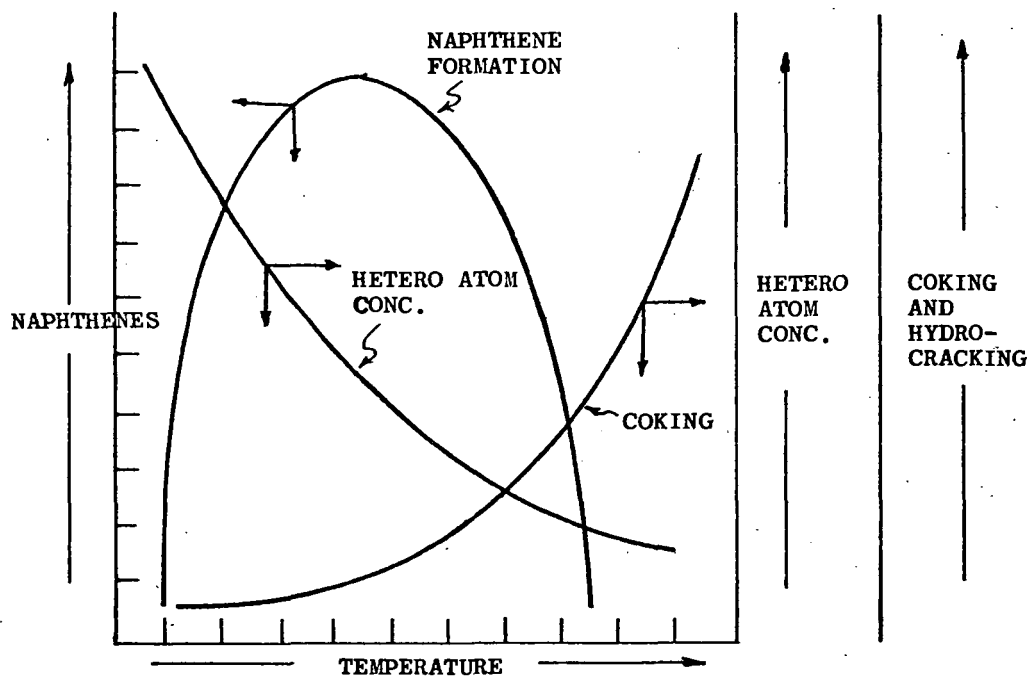


TABLE 4

+600°F HYDROTREATED FRACTION OF  
PROJECT COED COAL LIQUIDS

DISTILLATION, °F	
10%	655
30%	708
50%	781
70%	866
90%	Cracking
GRAVITY, °API AT 60°F	0.4
RAMSBOTTOM CARBON, WT. %	3.8
CORRELATION INDEX	121.9
ULTIMATE ANALYSIS, WT. %	
CARBON	86.97
HYDROGEN	8.50
OXYGEN	2.97
NITROGEN	0.92
SULFUR	0.30
ASH	0.07

TABLE 5

LABORATORY INSPECTION OF SECOND  
PASS HYDROTREATED +600°F FRACTION

DISTILLATION, °F	<u>+600°F BOTTOMS</u>
5%	615
10%	629
30%	668
50%	714
70%	767
90%	866
95%	912
GRAVITY, °API AT 60°F	4.2
BENZENE INSOLUBLE, WT. %	0.094
QUINOLINE INSOLUBLE, WT. %	0.018
RAMSBOTTOM CARBON, WT. %	2.74
CORRELATION INDEX	111.7
ULTIMATE ANALYSIS, WT. %	
CARBON	89.38
HYDROGEN	8.48
OXYGEN	1.54
NITROGEN	0.60
SULFUR	0.04
ASH	0.02

TABLE 6

LABORATORY EVALUATION OF RUBBER SAMPLES

<u>SAMPLE</u>	<u>ISAF</u>	<u>COAL</u>	<u>COAL</u>	<u>COAL</u>	<u>COAL</u>	<u>COAL</u>	<u>COAL</u>
	CONT.C	LIQUIDS	STANDARD	LIQUIDS	STANDARD	LIQUIDS	LIQUIDS
CURED AT 293°F MIN.							
MODULUS AT 300% (PSI)	120	2100	2280	2380	2330	2320	2300
COLLECTED YIELD #/GAL.		3.83	4.23	3.82	3.97	3.51	
TENSILE STRENGTH (PSI)	120	4300	3740	4130	4270	3770	4300
% ELONGATION AT BREAK	120	510	420	435	450	420	445
SURFACE AREA, (M <sup>2</sup> /GM)		126	112	112	139	137	
ANGLE ABRASION GMS LOSS/HR.	90	10.4	12.4	12.5	10.3	10.6	10.1
% SWELL EXT.D.STK		92.1	105.6	102.0	109.3	105.6	109.3
DBP ABRASION		114.8	138.6	138.5	140.1	139.8	141.4

TABLE 7

-600°F FRACTION OF HYDROTREATED  
PROJECT COED COAL LIQUIDS

ASTM DISTILLATION, °F	
IBP	280
10%	370
30%	416
50%	452
70%	492
90%	546
95%	Cracking
GRAVITY, °API AT 60°F	
	17.6
BROMINE NUMBER	
	65.7
ULTIMATE ANALYSIS, WT. %	
CARBON	83.48
HYDROGEN	10.27
OXYGEN	5.38
NITROGEN	0.88
SULFUR	0.13
ASH	0.002

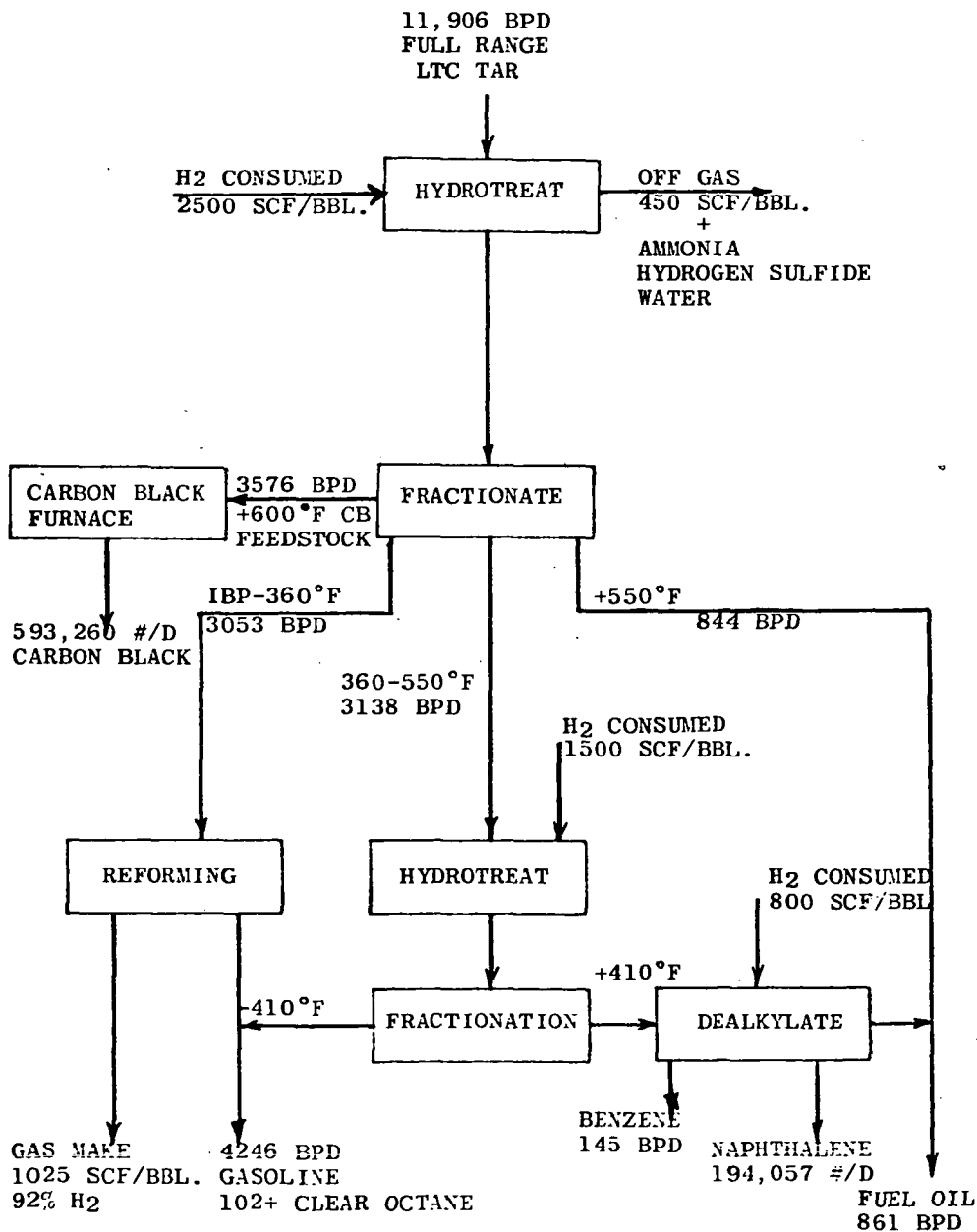
TABLE 8

REFORMATE FROM 160-360°F FRACTION OF SECOND  
PASS HYDROTREATED -600°F COAL LIQUIDS

LIQUID YIELD ON FEED	90.1 VOL. %
GAS MAKE, SCF/BBL. FEED	1025
GRAVITY, °API	33.5
ASTM DISTILLATION, °F	
IBP	168
5%	208
10%	220
30%	244
50%	266
70%	288
95%	232
E.P.	368
OCTANE NUMBERS	
F-1 CLEAR	101.4
F-1 + 3 G. TML.	105.9
BLENDING OCTANE NUMBER	114.7

FIGURE 3

CARBON BLACK FEEDSTOCK  
FROM  
LOW TEMPERATURE CARBONIZATION TAR  
ESTIMATED MATERIAL BALANCE



## CARBON BLACK PREPARATION FROM LOW-TEMPERATURE LIGNITE PITCH

Richard L. Rice, Robert E. Lynch, and John S. Berber

U. S. Department of the Interior, Bureau of Mines,  
Morgantown Coal Research Center, Morgantown, W. Va. 26505

Carbon black consists essentially of finely divided particles of carbon produced by incomplete combustion of carbonaceous fuels, both liquid and gaseous. Carbon black frequently is identified by designating the method of preparation, e. g. channel black, lamp black, furnace black, oil black, and thermal black. Carbon black from the channel, gas, and oil furnace processes is produced by controlled combustion. In the thermal process, carbon black is produced by thermal decomposition of hydrocarbons in the absence of air or flame. Channel black, produced from natural gas, was the main type at the beginning of the carbon black industry (Bond, 1968), but gradual increase in natural gas price impelled the carbon black industry to look for new feedstocks. Now, most carbon black is produced from petroleum-derived feedstock (Drogin, 1968). The carbon industry in the United States is about 100 years old, and more than 135 marketable grades of carbon black meet a wide range of industry specifications (Drogin, 1954).

This paper discusses the preparation, characteristics, and properties of carbon black produced by the thermal decomposition of low-temperature lignite tar pitch. A variety of other carbonaceous materials have been evaluated as carbon black feedstock via thermal decomposition (Kulik, 1961; Williams, 1953; Johnson, 1969).

### EQUIPMENT AND MATERIALS

A 13-inch-long section of 6-inch pipe equipped with external electric heaters served as pitch feed tank. A gear pump fed the pitch to the production furnace. The latter was constructed of 10-gauge carbon steel and had two main parts, the firebox and production zone. The firebox was 9 inches in diameter and 9 inches long overall, with downstream end tapered 45° to 3 inches in diameter. Refractory and insulation made the outside dimensions 27 inches in diameter by 18 inches long. The production zone consisted of silicon carbide tube 4 inches in diameter by 36 inches long surrounded by insulating brick. Outside diameter of the production zone was 21 inches.

Two natural gas burners entering the firebox tangentially preheated the furnace and supplied heat during a run.

Attached directly to the discharge end of the furnace was a quenching chamber, 12 inches in diameter and 42 inches long. Initially it was constructed of 12-inch carbon steel pipe, but its corrosion contaminated the product, so it was rebuilt using stainless steel. A water spray quenched the gases and carbon leaving the furnace.

Carbon black was removed by a 12-inch diameter by 42-inch-long knock-out tank made from stainless steel and equipped on the inside with a water spray. Tangential entry of the gas gave cyclone-type action that assisted in removal of carbon black.

The 2-foot-square wet filter was separated into two compartments by a screen which supported filter paper. Both the box and screen were made of stainless steel. The dry filter was a wool-bag type, 4-1/2 inches in diameter by 4 feet long.

Feed material for the study was pitch obtained from tar produced by the Texas Power & Light Company from the carbonization of Texas lignite at 900° F in a fluidized bed by the Parry process (Parry, 1955). The tar was distilled under vacuum to an atmospheric boiling point of 630° F, and the resulting residue amounted to 45% of the tar. Chemical and physical properties of the pitch are given in Table 1.

## PROCEDURE

Pitch was placed in the feed tank (Figure 1), melted, heated to about 400° F, and pumped into the preheated furnace. Carbon black formed in the production zone, passed into the quenching chamber where it was cooled by the water spray, and dropped to the bottom. Carbon black remaining in the products of combustion was carried to the knock-out tank for removal by the water spray and cyclonic action. Gas carrying unremoved carbon black then went to the dry wool-bag filter for final cleaning up of the gas, after which the gas was metered, sampled, and vented. Carbon black from the quenching chamber and knock-out tank was collected on a wet filter, from which it was removed, washed, dried, and prepared for testing.

## RESULTS

Maximum yields of carbon black at temperatures ranging from 1,800° to 2,500° F are given in Table II and presented in Figure 2. Yields increased from 16.5% at 1,800° F to 37.0% at 2,500° F. Hydrogen content, on the other hand, decreased with increase in temperature. In the 1,800° and 2,000° F runs, corrosion of the carbon steel quenching chamber contaminated the product, as revealed by the high ash and iron content. Ash and iron values dropped significantly in subsequent runs utilizing a stainless-steel chamber. Sulfur content remained relatively constant at 0.7%. A yield of 37% represents 40 pounds of carbon black per ton of lignite carbonized.

Electron micrographs of the carbon black are shown in Figures 3 and 4. These blacks were produced at about 2,300° F. The particles appear spherical in shape, range from 200 to 3,000 Å in diameter, and have a tendency toward arrangement into chainlike structures. Blacks in which this effect is prominent are generally referred to as structure blacks. A high degree of structure is usually indicative of high electrical conductance. These electron micrographs look much like those from a typical SRF material (Kirk and Othmer, 1949). The tendency to form chains also indicates that the particles will bind well with the matrix in compounding.

Results of tests and compounding of the carbon black compared with a commercial-type SRF carbon black, are given in Table III. CB-12 designates a carbon black produced at 2,450° F; CB-13A at 2,250° F; and CB-3, at 2,000° F. Carbon blacks from lignite pitch were intermediate in fineness to thermal and SRF type carbons, but of higher chain structure. They also differed in tinting strength, but this estimate of fineness correlated only roughly with tensile strength of the vulcanizates. Oil absorption (shape factor) of the carbon black was much higher than for furnace black, indicating nonspherical particles. Vulcanizate viscosity and modulus data agreed directionally with oil absorption when related to furnace black data.

The lignite-derived carbon black was high in ash and very high in iodine number. Iodine number does not appear to be a measure of surface area for these samples. Both the high iodine number and oil absorption could be influenced by the high volatile content of the samples and not be a true indication of surface area and particle shape.

The samples dispersed well in rubber. The tensile strength was equivalent to or lower than for furnace black. The CB-13A run appears to be coarsest and gave lowest tensile. The blend of CB-12 and CB-3 was intermediate. Two of the samples produced compounds higher in tensile modulus, dynamic modulus, and hardness than furnace black. This indicates nonspherical particles as confirmed by the higher oil absorption. The mechanical properties of the experimental compounds were similar to those of furnace black. Run CB-12 compound was highest in damping and heat buildup and lowest in resilience.

The compounds differed only slightly in scorch time. The coal derived samples resulted in compounds of a faster cure rate than furnace black.

#### ACKNOWLEDGMENTS

Appreciation is expressed to K. A. Burgess, director, and C. E. Scott, assistant director, Pigments and Elastomers Research Div., The Columbian Carbon Company, and to J. T. McCartney, Pittsburgh Coal Research Center, Bureau of Mines, for help in analyzing the carbon black samples.

#### LITERATURE CITED

- Bond, R. L., Brit. Coal Util. Res. Assoc., Gaz. 65, 6 (1968).
- Drogin, I., Proc. Rubber Technol. Conf., 3rd, London, 1954.
- Drogin, I., J. Air Pollution Control Assoc. 18, 216 (1968).
- Johnson, G. E., U. S. Pat. 3,424,556, (Jan. 8, 1969).
- Kirk, R. E., and D. F. Othmer, eds., Encyclopedia of Chemical Technology, v. 3, The Interscience Encyclopedia, Inc., New York, 1949, pp. 48-49.
- Kulik, Metro (to Consolidation Coal Co.), U. S. Pat. 2,989,458 (June 20, 1961).
- Williams, Ira (to J. M. Huber Corp.), U. S. Pat. 2,625,466 (Jan. 13, 1953).

Table I. Properties of Lignite Pitch

Flash point, ° F . . . . .	510
Softening point (r&b) glycerol, ° F . . . . .	194
Softening point (cube in glycerol), ° F . . . . .	221
Penetration at 77° F, 100 grams, 5 seconds . . . . .	0
Specific gravity, 25° C/25° C . . . . .	1.128
Ash . . . . .	0.35
Water . . . . .	0.00
Ductility, cm at 77° F . . . . .	0
Bitumen, soluble in CS <sub>2</sub> . . . . .	78.80
Free carbon . . . . .	20.85
Conradson carbon . . . . .	20.81
Distillation to 572° F (ASTM D2569-67) . . . . .	6.40
Softening point of residue (r&b), ° F . . . . .	194
Sulfonation index of distillate to 572° F . . . . .	0

---

Ultimate analysis	<u>Percent</u>
Carbon . . . . .	84.72
Hydrogen . . . . .	8.53
Nitrogen . . . . .	0.87
Oxygen . . . . .	4.62
Sulfur . . . . .	0.90
Chlorine . . . . .	0.01
Moisture . . . . .	0.00

Table II. Carbon Black Yields and Composition

Temp., ° F	Carbon Black Yield		Carbon black composition (wt-%) and properties									
	Pitch fed, lb	Weight, lb	Proportion of feed, %	Carbon	H <sub>2</sub>	Ash	Fe	S	Oil absorption, ml/g	Iodine number	Particle size, microns	
1800	0.8	0.13	16.3	85.77	1.80	6.2	1.55	0.8		32	0.02-0.20	
2000	2.0	0.5	25.0	89.42	1.73	2.3	0.66	0.6			0.02-0.15	
2250	5.6	1.6	28.6	95.47	1.00	0.4	0.07	0.7	0.53	18		
2350	8.2	2.7	33.0	95.25	1.27	0.6	0.07	0.7	0.81	20	0.02-0.30	
2500	4.6	1.7	37.0	94.96	0.89	0.7	0.07	0.7	0.56	19	0.02-0.15	

Table III. Carbon Black and Rubber Properties

Carbon	Run CB-12	Run CB-12 + CB-3	Run CB-13A	Commercial furnace black
Carbon Black Properties				
Tinting strength	33	16	12	24
Oil absorption, gal/100 lb	12.8	15.8	10.2	4.4
Iodine number, mg/g	32	12	45	10
Volatile content, wt % at 1750°	7.9	13.4	14.5	0.1
Ash, wt %	0.89	2.4	0.74	0.03
Rubber Properties				
20' L-300	110	90	40	50
20' Tensile	530	520	210	300
60' L-300	700	640	390	410
60' Tensile	1770	1450	1180	1510
60' Elongation	720	600	740	700
60' Shore hardness	55	53	48	47
100' tensile	1580	1320	940	1380
Max. tensile	1780	1580	1180	1710
Visual dispersion	4.0	4.5	3.9	4.5
Dynamic Properties				
Complex modulus	93.0	88.2	76.8	75.0
Viscous modulus	15.0	12.8	12.0	11.0
Phase angle	9.3	8.3	9.0	8.5
Resilience, %	59.7	63.1	60.8	62.4
Goodrich heat buildup	97	89	82	88
Rheometer Cure Properties				
Minimum torque	2.6	2.2	2.0	2.0
Maximum torque	63.0	62.1	52.0	52.9
Time to 7# rise	10.8	10.7	11.2	10.7
Time to 90% max. torque	31.4	31.8	28.2	36.3
Cure rate	7.4	7.1	6.4	4.8

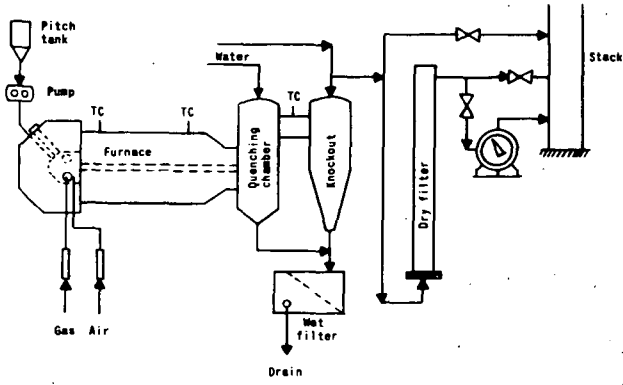


Figure 1. - Carbon Black System.

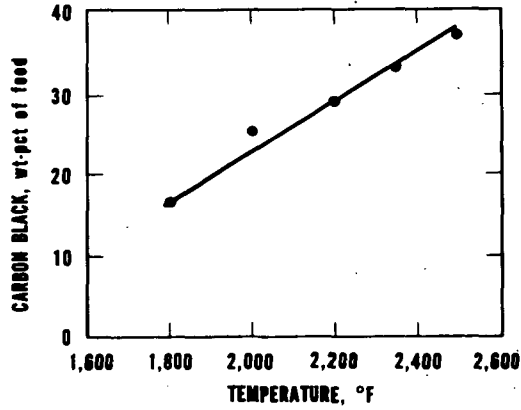


Figure 2. - Carbon Black Yields Versus Temperature.

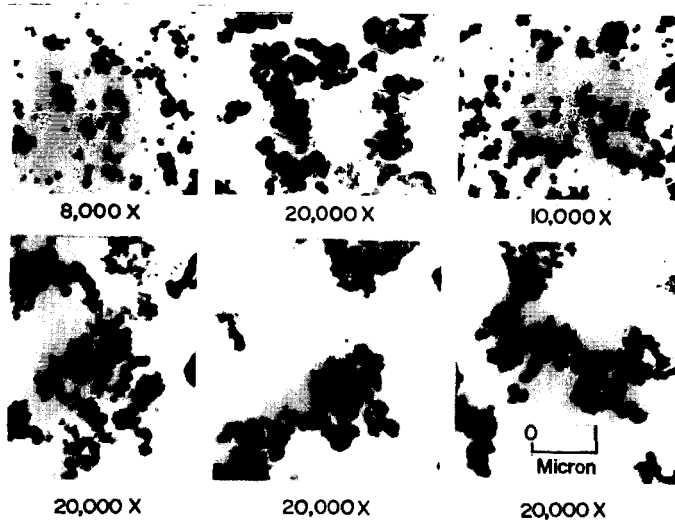


Figure 3. - Electron Micrographs of Carbon Black from Low-Temperature Lignite Pitch.



Figure 4. - Electron Micrograph of Carbon Black.

Not for Publication  
CARBON BLACK PRODUCED BY THE PYROLYSIS OF COAL

G. E. Johnson, W. A. Decker, A. J. Forney, and J. H. Field

U.S. Bureau of Mines, 4800 Forbes Avenue  
Pittsburgh, Pennsylvania 15213

INTRODUCTION

In 1968 the total production of carbon black in the United States was 2838 million pounds, a 12.5% increase over that of 1967.<sup>1/</sup> Production has increased steadily since 1942, averaging more than 5% annually. Figure 1 lists the annual production of carbon black since 1942 and illustrates its growth. The growth of the carbon black industry has closely paralleled that of the automotive industry.

The largest user of carbon black is the rubber industry which accounts for about 94% of domestic use with the remainder divided principally among the ink, paint, paper, and plastic industries. Of the carbon black used by the rubber industry, roughly 90% is used for motor vehicle tires and the rest for mechanical goods. Increasing ratios of carbon black to rubber in tire treads--currently about 50 parts of black to 100 parts of rubber--accounts for some of the increased carbon black demand. Rising sales of motor vehicles have also contributed to the increased demand for black.

Until 1945 almost all carbon black was made by the channel, gas-furnace and thermal processes from natural gas.<sup>2/</sup> Since the introduction of the oil-furnace process in 1945, three-fourths of the carbon black is made from liquid hydrocarbons.

Although the channel process has been almost replaced by the more efficient oil-furnace process as the principal source of rubber grades of carbon black, it still remains the principal source of the premium grades of blacks used in the paint and lacquer and printing ink industries.

The thermal process produces coarser blacks giving softer rubber stocks more desirable for tire carcasses in contrast to the narrow range of fine particle blacks produced by the channel process. In the thermal process natural gas is heated to 1350°-1650° C. where it decomposes to hydrogen and carbon.

Currently furnace black plants account for about 85% of domestic carbon black capacity, channel plants about 5%, and thermal plants 10%. Of the three types, use of thermal black is increasing most rapidly, its sales increasing an average of 8.1% per year from 1956 to 1966.

The U.S. Bureau of Mines in their search for new uses for coal has been investigating the production of carbon black from coal. A thermal-type black has been produced by pyrolysis of coal at 1250°-1350° C.

DESCRIPTION OF EQUIPMENT

A flow sheet of the experimental unit is shown in Figure 2. Coal sized to 70% minus 200 mesh is dropped in free-fall through a preheat zone (850° C.) and then the reaction zone in the presence of a carrier gas, generally bottled nitrogen. Ammonia, argon, and air have also been used.<sup>3/</sup>

Partial decomposition of the coal occurs at the elevated reactor temperature (1250°-1350° C.). The char and heavier solids are collected at the bottom of the vertical reactor while the carbon black is carried by the gas stream (consisting

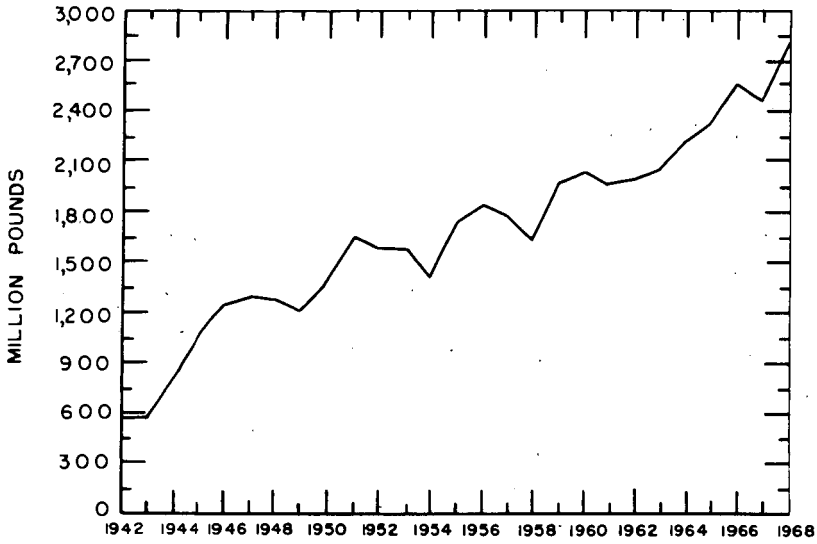


Figure 1 - United States production of carbon black 1942-1968.

L-11227

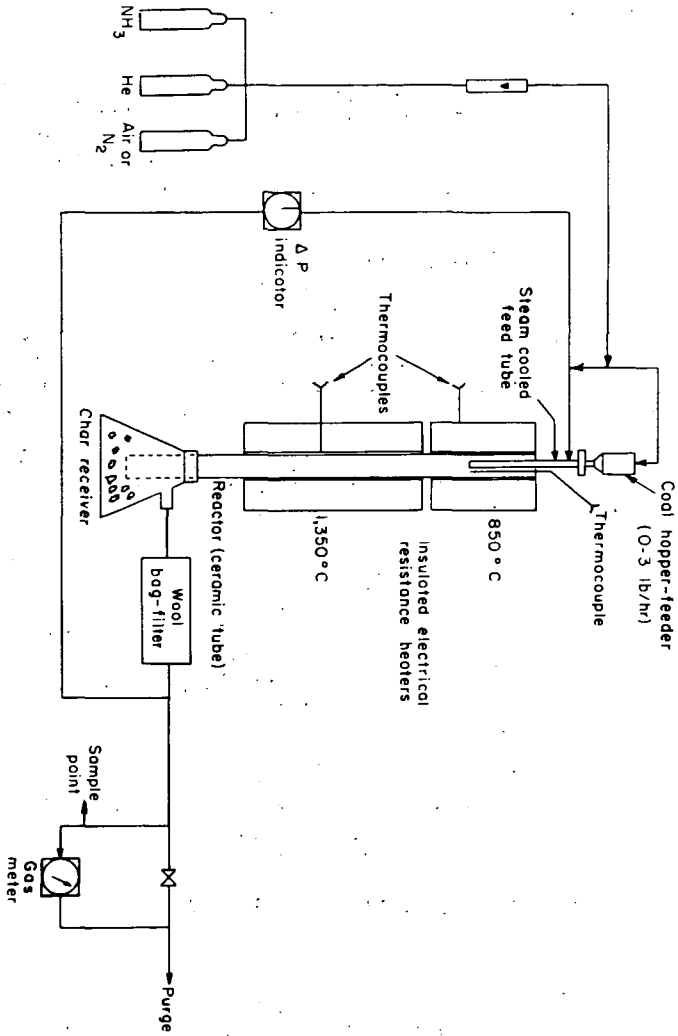


Figure 2.—Flow sheet of experimental unit for producing carbon block from coal.

of product gas and carrier gas) to a bag filter where it is collected. The coal discussed in this report (unless otherwise noted) was high-volatile A bituminous (hvab) Pittsburgh seam from Bruceton, Pennsylvania, containing about 37% volatile matter.

Part of the carrier gas enters the reactor with the coal adding greater velocity to the falling coal. The remainder of the carrier gas enters the top of the reactor adjacent to the cooled feed tube where it flushes away tar vapors which could adhere to walls and cause plugging.

The reactor (Figure 3), a 4-foot length of vitreous refractory mullite (3-1/4-inch i.d. and 3-1/2-inch o.d.), is jacketed with two electrical resistance heaters. The top heater serves as a preheater for the coal and gas (maximum temperature 850° C.), is 12 inches long, and is wound with nichrome wire. A Kanthal\* heater (Al-Cr-Co-Fe alloy) with a maximum temperature rating of 1350° C. encloses the center 20 inches of the tube or the reaction zone.

The bottom section of the reactor tube, which is exposed to the atmosphere for rapid cooling of the products, fits into a side-arm flask or char receiver in which the heavier solids are collected. The light, fluffy solids (carbon black) are carried by the product gas stream to a wool-felt bag filter where they are collected. Clean product gas is then metered, sampled, and flared. Since the unit was originally designed for making hydrogen cyanide from coal and ammonia, the piping and vessels are of stainless steel and glass, and the unit is completely enclosed and ventilated to prevent accumulation of escaped gases. Figure 4 is a view of the panel board and external structure. A special coal-feed system (Figure 5) was designed to prevent agglomeration and possible plugging of the reactor by heating the coal rapidly through its plastic stage of about 400° C.

The finely ground coal is fed through a steam-jacketed tube (1-inch o.d.) which extends into the preheat zone of the reactor. The coal leaves the end of the feed tube, which is at the temperature of the steam (about 200° C.) to enter the preheat zone. The temperature rise of the coal to 850° C. is very sudden because of the high heat transfer rate to the small particles in dilute phase. The carrier gas fed with the coal keeps the particles in motion and helps prevent agglomeration as the coal rapidly passes through its plastic stage.

Chromatographic analyses were made of spot samples of the product gas. Proximate and ultimate analyses<sup>4,5</sup> were made of the char and heavier solids collected in the char receiver, and the carbon black collected in the bag filter. Oil absorption values of the carbon black were determined; particle size was measured by electron microscope, and BET surface area was determined.

## EXPERIMENTAL RESULTS AND DISCUSSION

### Typical Test Data

Typical data from tests for carbon black from coal are shown in Table I which is the averaged data for ten 2-hour tests. The coal feed rate was 676 g./hr. (1.5 pounds per hour), and 10 cubic feet per hour of nitrogen was used as carrier gas. Although the reactor temperature was leveled off at 1252° C. before the introduction of coal, when coal feed was initiated, the reactor temperature increased to 1332° C. after one hour of operation, increasing to a maximum of 1366° C. after two

\*The trade name of this product is given for identification only and does not imply endorsement by the Bureau of Mines.

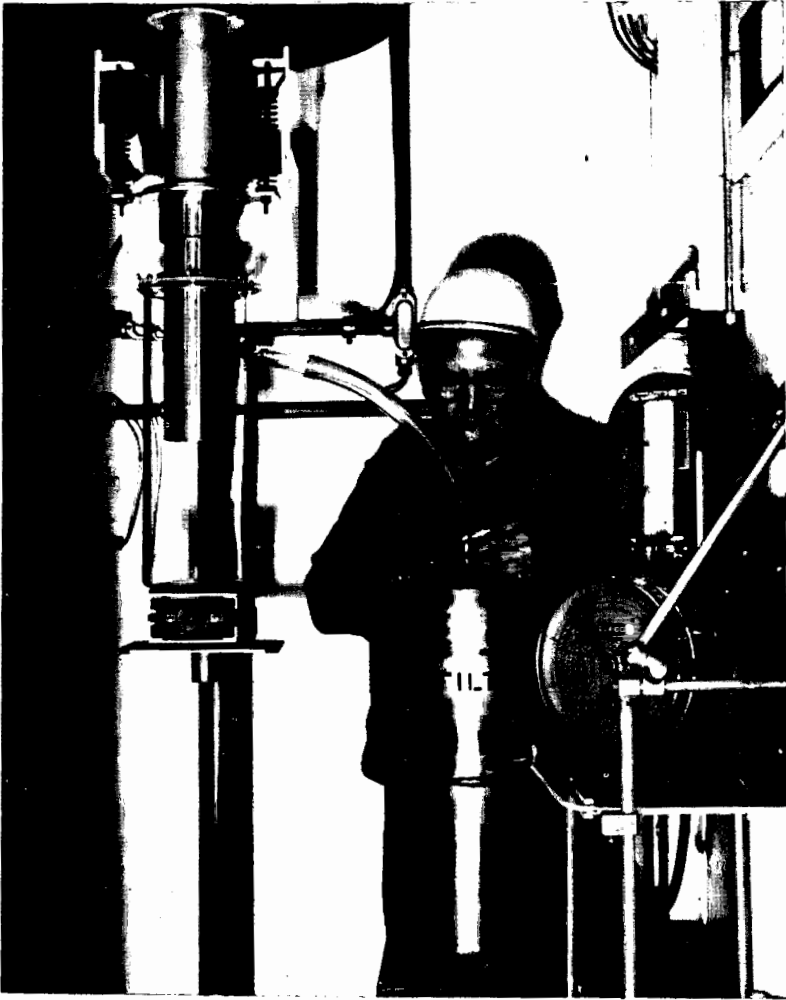


Figure 3 - Carbon black reactor and recovery unit.

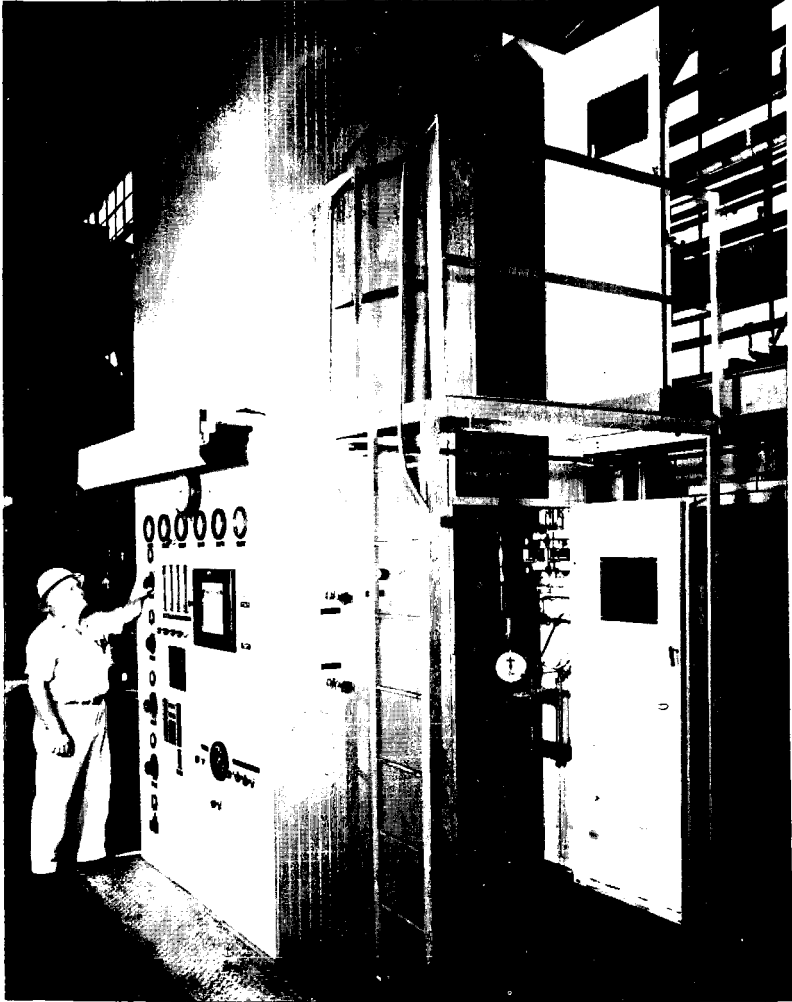


Figure 4-Panel board and external structure of carbon black unit.

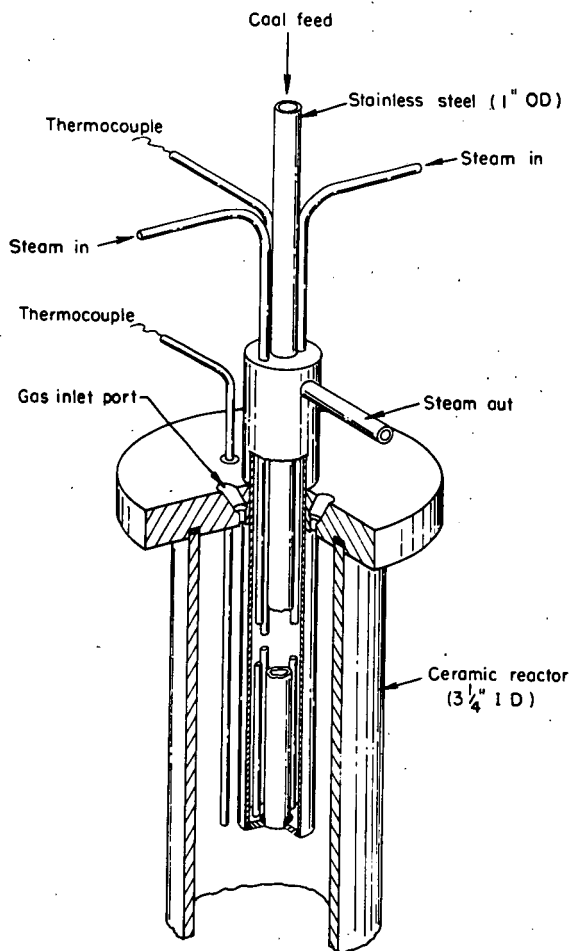
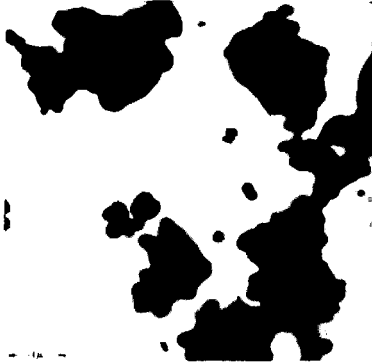


Figure 5.—Steam cooled cool feed system.



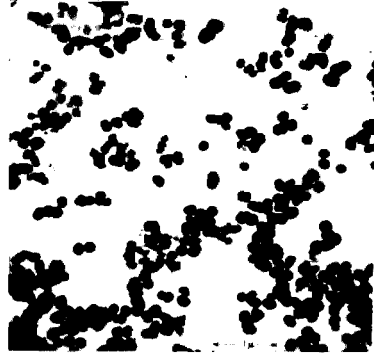
900° C



1,000° C



1,100° C



1,250° C

Figure 6.—Electron micrographs of carbon black from hvab coal.

TABLE I. DATA FROM TYPICAL 2-HOUR TEST FOR PRODUCING CARBON BLACK FROM COAL

Coal Feed Rate, g./Hr. <sup>a/</sup>	N <sub>2</sub> Flow, Cu.Ft./Hr.	Starting Temp., ° C.	Max. Temp., ° C.	Off Gas (Less N <sub>2</sub> ) Cu.Ft./Hr.	Yield		Char, g.
					Carbon Black	Percent of Feed	
Conditions First Hour							
676	10.21	1252	1332	13.42	121	17.9	Not Measured
Conditions Second Hour							
676	10.21	1317	1366	13.81	136	20.2	700

	Solids Analyses, %										Surface Area, m. <sup>2</sup> /g.
	Proximate					Ultimate					
	M.	V.M.	F.C.	Ash	H <sub>2</sub>	C	N <sub>2</sub>	O <sub>2</sub>	S	Ash	
Coal.....	1.4	36.8	54.8	7.0	5.3	77.4	1.6	6.9	1.8	7.0	----
Char.....	.4	8.1	79.5	12.0	1.5	81.7	1.4	1.8	1.6	12.0	1.5
Carbon Black	.5	0.7	98.4	0.4	0.6	96.6	0.8	0.6	1.0	0.4	8.4

Product Gas Analyses, % (Nitrogen-Free Basis)

H <sub>2</sub>	-	80.1	CO <sub>2</sub>	-	0.5
CO	-	14.1	HCN	-	0.5
CH <sub>4</sub>	-	3.5	H <sub>2</sub> S	-	0.4
C <sub>2</sub> H <sub>4</sub>	-	0.8	O <sub>2</sub>	-	0.1

<sup>a/</sup> Particle size, 70% through 200 mesh.

hours of operating time. The yields of carbon black were different for the two-hour test periods, averaging 17.9% for the first hour and 20.2% for the second hour. The yield percentages are based on the weight of carbon black collected per weight of raw coal fed. The char produced was not measured for the first hour, but the total collected for two hours was 700 grams.

Proximate and ultimate analyses of the raw coal, char, and carbon black are shown in Table I. The volatile matter remaining in the char was 8.1% which should be sufficiently high to permit its use as fuel (although it may have to be mixed with coal for satisfactory combustion). The ash content of the carbon black was 0.4%, which is well below the 1% maximum preferred by the rubber industry. The sulfur content of the carbon black, 1.0%, would not be harmful for use in rubber as sulfur is added when the black is compounded with rubber.

The product gas generated amounted to about 10 cubic feet per pound of coal and consisted mainly of hydrogen--80%--and carbon monoxide--14%--with small amounts of hydrocarbons and other gases.

#### Effect of Temperature

To determine the quantity and quality of carbon black produced, tests were made at 900, 1000, 1100, 1250, and 1350° C (Table II). In the first four tests the coal feed rate was 180 g./hr. (-325 mesh) and the nitrogen flow 4 cubic feet per hour, while in the test at 1350° C, the coal feed rate was 676 g./hr. (70% -200 mesh) and the nitrogen flow 10 cubic feet per hour.

Although carbon black is formed by the pyrolysis of coal at temperatures between 900° and 1350° C, all the tars are not removed at the lower temperatures. Chemical analyses indicate that carbon black made at 900° C. still contains 20% volatile matter as compared to less than 1% volatiles in the black made at 1350° C. The electron micrographs of Figure 6 illustrate the presence of tar at the lower temperatures. At the lower temperature (Table II) the carbon content of the black produced is about 90%, while at 1350° C. it exceeds 96%.

Product gas analyses also show the effect of temperature. When the temperature was increased from 900° to 1350° C., the hydrogen content of the product gas increased from 48% to 80%, while the methane decreased from 25% to 4%. At the higher temperatures more methane was decomposed to hydrogen and carbon. Carbon black yields based on recovered product varied from 8.7% to 19% of the raw coal fed. Additional amounts of carbon black are visible in the char but are not recovered.

#### Effect of Varying Coal Feed Rates

Tests were made with varying feed rates of coal to determine the effect on the carbon black produced. Results of these tests are shown in Table III. Coal feed rates were about 1.5, 2, 2.5, and 3 lb./hr. and 12 cu. ft./hr. of nitrogen carrier gas was used. Consistent carbon black yields of about 15-16% were obtained at all coal feed rates. The properties of the carbon black were similar, the ash content ranging from 0.8 to 1.1% and the surface area about 15 m.<sup>2</sup>/g. The benzene extractable content of the black, however, increased with increased coal feed.

The yield of char varied from 58 to 61% of the coal feed. The volumes of product gas obtained are listed for each test along with a range of product gas analyses for all tests.

TABLE II. EFFECT OF TEMPERATURE ON CARBON BLACK YIELD AND QUALITY

Temp., ° C.	Carbon Black				Product Gas, % N <sub>2</sub> -Free			
	Yield, % of Coal Feed	Carbon %	Ash, %	Vola- tiles, %	H <sub>2</sub>	CO	CH <sub>4</sub>	C <sub>2</sub> +
(Coal Feed Rate 160-200 g./Hr., N <sub>2</sub> Flow 4 Cu.Ft./Hr.)								
900	8.7	89.6	0.2	20.6	48.1	17.2	24.5	6.7
1000	9.7	90.0	.7	15.6	58.3	13.8	23.3	1.5
1100	11.3	92.6	.1	6.5	67.5	14.5	15.2	0.6
1250	9.9	94.2	1.0	7.0	75.2	13.9	5.9	2.0
(Coal Feed Rate 676 g./Hr., N <sub>2</sub> Flow 10 Cu.Ft./Hr.)								
1350	19.0	96.6	0.4	0.7	80.1	14.1	3.5	0.8

TABLE III. TESTS USING DIFFERENT FEED RATES OF COAL (HVAB, 70%-200 MESH), 12 CU.FT./HR. NITROGEN, INITIAL TEMPERATURE 1250° C

Test No.	Coal Feed Rate, g./Hr.	Max. Temp. Reached, ° C.	Product Gas, Cu.Ft./Hr.	Yield		Char, gm./Hr.	% of Coal Feed	Carbon Black Properties		
				Carbon Black, g./Hr.	% of Coal Feed			Ash, %	Beuzene Extractables, %	Surface Area, m. <sup>2</sup> /g.
CBL-43	685	1360	11.25	102	14.9	418	61	1.0	1.6	14.0
CBL-34	925	1350	15.11	150	16.2	535	58	0.8	1.8	---
CBL-37	1210	1300	20.14	196	16.2	717	59	0.8	2.6	15.1
CBL-40	1352	1320	20.41	215	15.9	830	61	1.1	3.7	15.4

Range of Product Gas Analyses, %: H<sub>2</sub>, 72-84; CO, 12-21; CH<sub>4</sub>, 4.7-8.6; CO<sub>2</sub>, 0.5-1.3; HCN, 0.6-1.0; C<sub>2</sub>H<sub>4</sub>, 1-0.5; H<sub>2</sub>S, 0-0.8; O<sub>2</sub>, 0-0.5

### Effect of Varying Carrier Gas Flows

The residence time of the gas and coal in the reaction zone can be controlled by the flow of carrier gas. A series of tests was made in which the carrier gas flow was varied in 2-cubic foot increments between 8 and 20 cu. ft./hr. giving calculated gas residence times of 1.75 to 3.15 sec. The results of the tests are given in Table IV. At a constant coal feed of about 1.5 lb./hr. with increasing carrier gas flow, the yield of carbon black increased from 10 to 20%; the product gas increased slightly and the char yield decreased slightly. The ash content of the carbon black increased from 0.6 to 1.1%. Thus with shorter residence time, the yield of carbon black is increased as is its ash content. With high carrier gas flows, additional ash particles are physically carried by the gas stream from the char collector to the bag filter along with carbon black. The carrier gas flow should be controlled so as to give the maximum yield of carbon black without exceeding the maximum desirable ash limit of 1%.

### Evaluation of Carbon Blacks From Coal

Samples of coal-derived carbon blacks were evaluated with commercial blacks in rubber compounding tests by several industrial companies. Table V lists some of the physical-chemical properties of the blacks and rubber and cure properties of natural rubber formulated with these blacks. Carbon blacks listed are: two commercial thermal blacks P-33 (Fine, F.T.) and Thermax (Medium, M.T.); three blacks from hvab coal, one made at 1250° C., one at 1400° C., and the third at 1250° C., but made in an oxidizing atmosphere (20.6% O<sub>2</sub>); a carbon black made from cannel coal at 1250° C. and one made from Spencer Chemical Company de-ashed coal.

In general, the properties of the carbon blacks from coal are similar to those of the commercial thermal carbons. The coal blacks are higher in oil absorption, ash, and total sulfur which in a rubber compound, results in higher modulus, higher hardness, shorter elongation, and faster cure rate.

The free sulfur contained by all the coal-carbon blacks is a significant amount and is in all probability available for vulcanization and could contribute to the higher vulcanizate modulus.

The variance of values of the coal-black properties indicates that control of these properties can be maintained by proper selection of feed materials and operating variables. For example, when oxygen was used with hvab coal, the surface area of the carbon black increased from about 16 to 40 m.<sup>2</sup>/g. which is in the range of the next higher classification of black, the SRF or semi-reinforcing furnace grade. The oxygen atmosphere also changed other carbon black properties, increasing the benzene extractables and oil absorption values and in turn, imparting different qualities to the rubber formulated with it.

The properties of the rubber compounds made from coal black were similar to those made from commercial blacks using identical formulations (Table V). Generally, the coal carbon gave higher 300% modulus, higher hardness, and slightly lower tensile strength. Elongation with the coal product was both higher and lower--the hvab coal blacks gave lower elongations than the commercial product.

The cure properties of the rubbers compounded with coal-derived carbon black were equivalent to those compounded with commercial thermal blacks. In some cases the coal-black product cure rates were faster and some were slower, but they were generally in the same range.

TABLE IV. - TESTS WITH VARYING NITROGEN FLOWS; COAL (HVAB, 70%-200 MESH)  
FEED RATE 685 g./HR., INITIAL TEMPERATURE, 1250° C.

Test No.	N <sub>2</sub> Flow Cu.Ft./Hk.	Calculated Gas		Product Gas, Cu.Ft./Hr.	Max. Temp. Reached, ° C.	Yield %		Carbon Black Properties			
		Residence Time, Sec.				Carbon Black g./Hr.	Char, % of Coal Feed	Ash, %	Benzene Extract- ables, %	Surface Area, m. <sup>2</sup> /g.	
CBL-41	8	3.15		10.35	1360	71	10.4	62	0.6	2.3	14.0
CBL-42	10	2.77		11.00	1360	87	12.7	66	.8	2.0	15.1
CBL-43	12	2.47		11.25	1360	102	14.9	61	1.0	1.6	14.0
CBL-44	14	2.29		11.02	1340	107	15.6	61	.9	1.6	14.3
CBL-45	16	2.04		12.05	1340	104	16.8	61	1.0	1.4	14.7
CBL-46	18	1.87		12.72	1330	133	19.4	58	1.0	1.2	14.2
CBL-47	20	1.75		12.80	1325	138	20.1	58	1.1	1.4	15.3

Range of Product Gas Analyses, %: H<sub>2</sub>, 75-84; CO, 13-19; CH<sub>4</sub>, 3-5; CO<sub>2</sub>, 0-3.8; H<sub>2</sub>S, 0.2-0.8; O<sub>2</sub>, 0-0.3;  
C<sub>2</sub>H<sub>4</sub>, 0-0.5

TABLE V. - PROPERTIES OF COMMERCIAL AND COAL-DERIVED CARBON BLACKS  
AND THEIR NATURAL RUBBER COMPOUNDS

	Commercial		Carbon Black From Coal, Non-Oxidizing Atmosphere				Hvab Coal
	Thermal		Hvab Coal		Cannel Coal	Spencer De-ashed Coal	Oxidiz- ing Atm., 1250° C.
	Fine (P-33)	Medium (Thermax)	1250° C.	1400° C.			
<u>Carbon Black Properties</u>							
Benzene extracts, % ....	1.0	0.3	3.4	1.6	2.4	6.1	5.8
Transmission, % ..	1.0	2.0	1.0	-	2.0	2.0	1.0
Oil absorption gal, 100 lb. ....	5.0	4.0	6.5	-	6.8	7.7	10.2
Ash, % .....	0.9	0.16	0.40	0.5	0.66	0.17	1.44
Total sulfur, % ..	-	-	0.61	0.36	0.78	0.59	0.95
Nitrogen surface area, m. <sup>2</sup> /g. ....	12.0	7	10	15	11	14	12
Electron micro- scope surface area, m. <sup>2</sup> /g. ....	15.0	9	16	-	18	-	40
<u>Rubber Properties (Cured at 293° F.)</u>							
25' L300 .....	820	1080	1030	1010	900	1240	1390
25' Tensile .....	2080	2230	1830	1710	2120	2170	1700
25' Elongation ..	555	525	485	470	540	530	390
25' S.Hardness ..	59	55	63	63	64	67	77
<u>Rheometer Cure Properties at 320° F.</u>							
Minimum torque ..	1.7	1.0	2.2	0.7	1.5	2.8	5.3
Time to 7# rise, min. ....	3.5	3.9	3.5	4.8	3.0	3.0	3.0
Time to 90% torque, min. ....	10.7	11.9	9.8	11.5	8.4	9.0	8.6
Rate (in.-lb./ min.) .....	10.4	9.9	13.6	10.0	15.5	13.2	18.4

### Economic Outlook

An earlier cost study<sup>3/</sup> indicated that carbon black could be produced for about 3.1¢/lb. This estimate was based on a carbon black yield of 10% which was obtained in our earlier work. Since the yields have now been increased to 20%, a new cost study is under way but is not complete at this time. However, on a raw material basis only, one pound of coal costing 0.25¢ produces 0.2 pounds of carbon black worth about 1.25¢ (using a carbon black selling price of 6.25¢/lb.). On this basis, carbon black from coal looks quite attractive economically.

Although much interest has been shown in the process for which a U.S. Patent was granted,<sup>6/</sup> to our knowledge there is no carbon black being made commercially from coal today.

### CONCLUSIONS

Carbon black has been produced in bench scale by the pyrolysis of coal at 1250°-1350° C. Yields of carbon black from Pittsburgh seam coal (hvab) have been about 20% by weight based on the coal feed.

Carbon black properties can be controlled by selective control of operating variables. Residence time appears to be an important variable in the production and quality of carbon black from coal.

Carbon blacks from coal have been tested and compounded with rubber by several industrial companies. The black produced from coal has been evaluated as a substitute for commercial thermal black.

Preliminary cost studies indicate that commercially acceptable carbon black could economically be produced from coal.

### LITERATURE CITED

1. U.S. Department of the Interior, Mineral Industry Surveys, Carbon Black Quarterly Reports for 1968.
2. U.S. Bureau of Mines Minerals Yearbook, v. 2, 1965, pp. 279-291.
3. Johnson, G. E., W. A. Decker, A. J. Forney, and J. H. Field. Carbon Black Produced From Coal. Rubber World, v. 156, No. 3, June 1967, pp. 63-68.
4. A.S.T.M. Standards With Related Material. Part 19. Gaseous Fuels. Coal and Coke, 1966.
5. Fieldner, A. C. and W. A. Selvig. Methods of Analyzing Coal and Coke. BuMines Bull. 492, 1951.
6. U.S. Patent 3,424,556, G. E. Johnson. Production of Carbon Black From Coal, Jan. 28, 1969.

## ON THE AGROBIOLOGICAL ACTIVITY OF OXIDATIVELY AMMONIATED COAL\*

N. Berkowitz and S.K. Chakrabartty  
Research Council of Alberta, Edmonton;

and

F.D. Cook and J.I. Fujikawa  
Faculty of Agriculture, University of Alberta, Edmonton.

Since the late 1950's, much of the research effort devoted to the development of coal-based plant nutrients has shifted from humates to so-called 'nitrified' or 'nitrogen-enriched' coal (NEC). Aside from studies of the mechanism (1) and kinetics (2,3) of the oxidative ammoniation reaction by which this material is prepared, recent literature thus contains several reports of more or less extended growth trials with NEC in India (4), Canada (5) and Australia (6). And active interest in the outcome of these investigations, or in initiation of similar projects, has been expressed in the United States, the Soviet Union, New Zealand, and a number of Central European countries.

In large measure, this shift reflects growing awareness that ammonium humates or nitro-humates are unlikely to command much attention outside relatively small specialty or 'luxury' markets (5). But despite reports - including some from our own laboratories - that plant reaction to NEC frequently equals or betters gains accruing from the use of ammonium sulphate or nitrate, the nutrient value of NEC remains questionable. Indian findings (4) that NEC, typically less effective than nitrogenous mineral fertilizers during the opening years of an extended test program, subsequently equals or surpasses ammonium sulphate are not substantiated by Canadian (5) and Australian (6) experience. And observations that secondary treatment of NEC with  $\text{HNO}_3$  and aqueous  $\text{NH}_4\text{OH}$  yields products that do release substantial quantities of N have been found to be connected with the fact that such treatment also converts some associated mineral matter into assimilable nitrates (5).

---

\* Contribution 447 from the Research Council of Alberta, Edmonton, Alberta, Canada.

Since publication of their field trial results for the period 1958-64, Indian investigators (7) have come to concur in the view that NEC does not contain much 'available' N; and there is a concensus that their observations may have been directly influenced by increased moisture retentivity and improved structure of the impoverished soils in which the growth trials were conducted. (That coal or oxidized coals rich in humic acids can effect such improvements has been known for some time (8)). However, because gains resulting from application of  $\text{HNO}_3$ -oxidized NEC or mixtures of NEC with nitrogenous mineral fertilizers seemed on occasion rather greater than could prima facie be accounted for by the inorganic nitrogen (or urea-N) in this way introduced into a soil, belief in NEC's nutrient value has been revived by two alternative suggestions (5,6,9). One raises the possibility that NEC releases N at rates which, although too small to be measured by conventional laboratory tests, are yet great enough to affect plant life over the more extended period of a full growth cycle. And the second invokes possible synergistic behaviour of a mixture containing NEC and a conventional nitrogen source. The present study was undertaken with a view to testing the validity of these notions.

### Experimental

(1) Materials: Nitrogen-enriched coal was prepared by treating a subbituminous coal (70.5% C, 5.1% H, d.a.f.) with gaseous ammonia and air at 300°C. The reaction was carried out in a small electrically-heated fluid-bed reactor (3) and furnished three stock samples with, respectively, ~9%, ~11% and ~17% N.

Proceeding from these samples, a range of nutrient formulations which allowed simultaneous evaluation of all major compounding variables were prepared. Table 1 shows the form of this 'grid' as used in the growth trials. A similar 'grid', only differing in minutiae from that shown in Table 1, was employed for nitrogen-release rate measurements. In both sets, unreacted coal,  $\text{HNO}_3$ -oxidized coal, and mixtures of these with urea or ammonium nitrate were used as controls.

Total (analytical) nitrogen contents of test nutrients and control materials were determined by the standard Kjeldahl method and/or by a standardized gas chromatographic technique (which employed a Hewlett-Packard FM 185 C-H-N Analyzer). Nitrogen contents of plant matter harvested from the pots (cf. below) were measured by the Kjeldahl method.

Table 1. Materials 'Grid' used for Greenhouse Growth Tests with Grass

Coal	65/115	+ 5% $\text{NH}_4\text{NO}_3$	impregnated
		+ 5% urea	dry mixed
	<115	+ 10% urea	impregnated
			dry mixed
Coal, $\text{HNO}_3$ -oxidized	65/115	+ 10% urea	impregnated
NEC-I. (~17% N)	65/115	+ 5% urea	impregnated
			dry mixed
	<115	+ 5% $\text{NH}_4\text{NO}_3$	dry mixed
		+ 5% urea	impregnated
	+ 1% urea	dry mixed	
NEC-II (~9% N)	65/115	+ 5% urea	impregnated
			dry mixed
	<115	+ 5% $\text{NH}_4\text{NO}_3$	dry mixed
		+ 5% urea	impregnated
	+ 1% urea	impregnated	
NEC-II, $\text{HNO}_3$ -oxid.	28/48	+ 5% urea	impregnated
	<115	+ 1% urea	dry mixed
		+ 5% urea	impregnated

(ii) Nitrogen-release rates were studied by incubation of nutrient-amended soil and subsequent determination of  $\text{NO}_3^-$  by the standard phenol disulphonic acid method (10). The soil was a 1:1 v/v mixture of washed sand and black Chernozemic loam that had been thoroughly leached with distilled water, air-dried, and screened to <12 mesh. Test nutrients were hand-mixed into this substrate to provide 100 ppm (analytical) nitrogen, and the mixtures then placed in styrofoam cups over a vermiculite base

(cf. Figure 1). Incubation, in total darkness to prevent algal growth, was carried out in a controlled-environment chamber at 25°C and 95-98% r.h. for 19 days, and results cited below represent arithmetic averages of four replicates.

(iii) Growth Trials: Plant responses to the various test nutrients under greenhouse conditions were measured by growth of Reed Canary Seed in <12 mesh 1:1 v/v Chernozemic loam/washed sand, to which nutrients equivalent to 100 ppm (analytical) N had been added with the aid of a small hand-churn. Each plastic 5 in. greenhouse pot held 1000 gms. of soil and was seeded with ~1.0 gm grass seeds. Moisture conditions were in all instances maintained near field capacity, but in order to facilitate germination, moistened filter paper discs covered the seeds during the first few days of the trials.

After germination, the paper discs were removed, and growth allowed to continue to a height of 5-6 in. before being cut. The harvested material from each pot was then immediately placed into tared paper bags, oven-dried at 60°C, and weighed. Tests were terminated after the third cut, when it was evident that all supplies of 'available' nitrogen had been exhausted.

### Results and Discussion

Although the quantities of nutrient added to the soil mixture were in each case predicated on the supposition that all nitrogen forms were equally 'available' - and hence adjusted to provide 100 ppm analytical N - it is convenient to test the actual 'availability' of this added nitrogen by assuming that all N chemically fixed in coal and coal products is agrobiologically inert. Experimental results have therefore been graphed as functions of 'effective N', i.e. of nitrogen contained in the admixed urea or ammonium nitrate.

With respect to the results of N-release rate measurements, this procedure yielded a plot of the form shown in Figure 2, where release rates are expressed as percentages of the urea-rate. Table 2 identifies the various symbols which discriminate between the major nutrient types. Because of the relatively high nitrogen content of NEC itself, formulations of NEC and urea (or ammonium nitrate) cluster in the region of low 'effective N' (mostly at <25 ppm N); but like the other nutrient materials, and in common with them, they all lie close to a straight line which proceeds

from the urea-point (100/100) to intersect the ordinate within the range of values recorded with unamended soil. For the entire set, N-release is thus, within the error limits of the experimental method, directly proportional to the 'effective' nitrogen application.

An analogous result is obtained from the growth trial data, which were likewise treated as if all nitrogen in coal,  $\text{HNO}_3$ -oxidized coal and NEC were entirely inert.

Yields of (dried) plant matter obtained in each of the three harvests are shown in Figure 3 (whose symbols are identified in Table 2). The inset reproduces the 2nd harvest results for <30 ppm 'effective N' (which are virtually coincident with the corresponding 3rd harvest yields and have therefore been isolated for greater clarity of presentation). And the limits within which replicates of any one set varied are defined by the vertical lines through the data points.

Table 2. Representation of Test Nutrients

	Fig.2*	Figs.3-5
Untreated coal	—○—	—○—
$\text{HNO}_3$ -oxidized coal	—●—	—□—
NEC-I (~17% N)	—■—	—△—
NEC-II (~9% N)	—□—	—▽—
NEC-III (~11% N)	—■—	
NEC-II, $\text{HNO}_3$ -oxidized	—△—	—*—
Fuller's Earth	—●—	

\* Except for the few preparations marked \*, which contained ammonium nitrate, all nutrients carried 'effective N' in urea.

Nitrogen recoveries - i.e. the variation of each harvest's 'per pot nitrogen' with 'effective N' rates - are presented in Figure 4; and the (percent) nitrogen contents of the dried plant matter are shown in Figure 5. In both diagrams, the symbols are the same as those used in Figure 3 (cf. Table 2).

Inspection of the 1st harvest yields (cf. Fig. 3) shows that short-term growth which does not seriously deplete the available nitrogen supplies is an unreliable index of nutrient performance: when 'effective' N applications exceed 5-10 ppm, yields tend to be almost entirely insensitive to variations in available nitrogen\*. But taken in conjunction with subsequent harvest data, they point to a marked lack of utility of NEC.

Due, it appears, to minor amounts of hydrolyzable nitrogen which exists in NEC in reaction intermediates (1), most NEC samples caused slight initial improvements over the soil control (cf. 1st cut data, Fig. 3)\*\*. However, these nitrogen sources are evidently rather quickly exhausted. And by the time of the 2nd harvest, growth supported by NEC or mixtures of NEC with small amounts of urea or  $\text{NH}_4\text{NO}_3$  - which have by then also been substantially exhausted - is indistinguishable from growth in unamended soil or soil containing coal.

Nor does a further lapse of time - to the 3rd harvest, when all 'effective' N-supplies have been totally depleted - improve matters. Growth remains stunted at the soil control level.

There is perhaps, as comparison of the 1st and 2nd harvest data in Figs. 3, 4 and 5 suggests, another way of looking at plant growth. There appears to be a disposition for production of plant matter to take precedence over the demands of 'normal' plant chemistry; and so long as it is not actually acute, a soil-nitrogen deficiency will tend to be reflected in lowered plant-nitrogen rather than in reduced formation of plant matter. After a high 'effective' N application, 2nd harvest yields (and, consequently, 'per pot' nitrogen recoveries) will thus be greater than after a small application - but if the nitrogen supply is by that time beginning to be seriously depleted, the nitrogen content of the plant matter will be lower. Where plant composition rather than quantity is important - e.g., if

---

\* By implication, fertilizer testing above this (or some equivalent) minimum N-level is therefore liable to lead to quite erroneous inferences. It seems probable that failure to recognize this point has contributed to the conflicting reports on NEC performance.

\*\* An analogous initial gain is observed with  $\text{HNO}_3$ -oxidized coal in which, as already noted, varying amounts of 'available' N exists in mineral matter-based assimilable nitrates.

the protein content of the plant is, for various reasons, an overriding criterion - observations of growth per se may therefore be misleading. But as Figs. 4 and 5 clearly show, NEC makes as little contribution to composition as to growth: as soon as initial supplies of (hydrolyzable or admixed) 'effective' nitrogen are exhausted, plant responses to NEC-reinforced soil are in no way different from response to unamended soil.

Both facets of the growth trials thus lead to the conclusion that NEC - regardless of whether it is used alone or in combination with another nitrogen source - is an essentially inert and agrobiologically useless, material. No evidence was found to sustain the view that NEC functions as a slow N-release nutrient or that mixtures of NEC and urea or  $\text{NH}_4\text{NO}_3$  behave synergistically.

This conclusion is in no way modified by the length of the ammoniation reaction period (which governs the nitrogen level of NEC) or by the manner in which urea or ammonium nitrate are introduced into NEC-based formulations. Neither the N-release test nor the growth trials were able to differentiate between NEC with, respectively, ~9% and ~17% N; to distinguish between formulations containing urea or  $\text{NH}_4\text{NO}_3$  in particulate or impregnated forms; or to define effects of NEC particle size.

Significantly, NEC also failed to influence utilization of 'effective' N. Nitrogen balances established from the initial 'effective' N-application and the total N-recovery by plant matter over the entire growth period show an efficiency of ~50% regardless of the type or form of test nutrient\*.

There remains, of course, a possibility that the period of this study's growth tests was too short to detect a slow progressive chemical change leading to N-release from NEC. But a line of reasoning proceeding from this argument is difficult to sustain unless it is supposed that chemical change is induced by specific soil microorganisms. We would, in this connection, observe

(i) that even minimal amounts of nitrogen released from NEC would, had they in fact been released, have been

---

\* Because of the relatively small amounts of 'effective' nitrogen supplied to the soil, and because of the inevitable errors attending determination of analytical nitrogen, the actual range was fairly wide. But there were no indications whatever of systematic dependence of efficiency on nutrient type.

detected at the time of the 3rd harvest;

(ii) that possible slow abiotic oxidation of NEC in a well-aerated soil (and consequent formation of a nitrogen-rich humic acid capable of releasing a portion of its nitrogen content) is unlikely in view of the failure of  $\text{HNO}_3^-$  oxidation to produce such a change; and

(iii) that the chemical inertness of NEC (1) also rules out abiotic reduction to a nitrogen-releasing material.

#### Acknowledgments

We are indebted to Mr. J.F. Fryer for the numerous nitrogen analyses without which this investigation could not have been carried out.

#### References

1. Chakrabartty, S.K. and Berkowitz, N.; Fuel, 48, 151, 1969.
2. Mukherjee, P.N., Banerjee, S., Ramchandran, L.V., and Lahiri, A.; Indian J. Technol., 4, 119, 1966.
3. Brown, H.M., and Berkowitz, N.; Chem. Engng. Prog., Symp. Ser., 64 (No. 85), 89, 1968.
4. Lahiri, A., Mukherjee, P.N., and Banerjee, S; Planters' J. and Agriculturist (India), Aug. 1966, 385-6; 413-4.
5. Chakrabartty, S.K., Wood, J.C. and Berkowitz, N.; US. Bur. Mines IC 8376, 165, 1968.
6. Cudmore, J.F.; Austral. Coal Research Lab. Ltd., P.R. 68-4, 1968.
7. Lahiri, A.; personal communication to N.B.

8. De Silva, J.A., and Toth, S.J.; *Soil Sci.*, 97, 63, 1964.
9. Berkowitz, N., and Wood, J.C.; *Proceedings INDEX 67*  
(Gov't of Saskatchewan, Regina, Sask., 1968), p. 136.
10. Bremner, J.M.; 'Inorganic Forms of Nitrogen', *Methods of Soil Analysis II*, Amer. Soc. of Agronomy, No. 9.

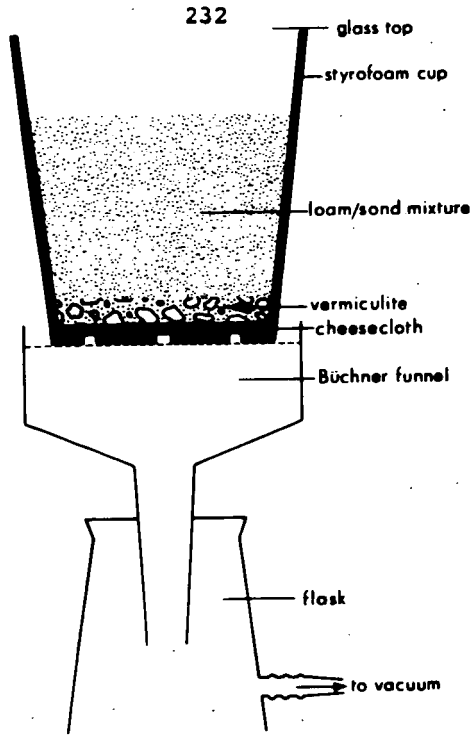


**Figure 1.** Container for Nitrogen Release Rate Measurements (as set up for preliminary leaching of soil mixture).

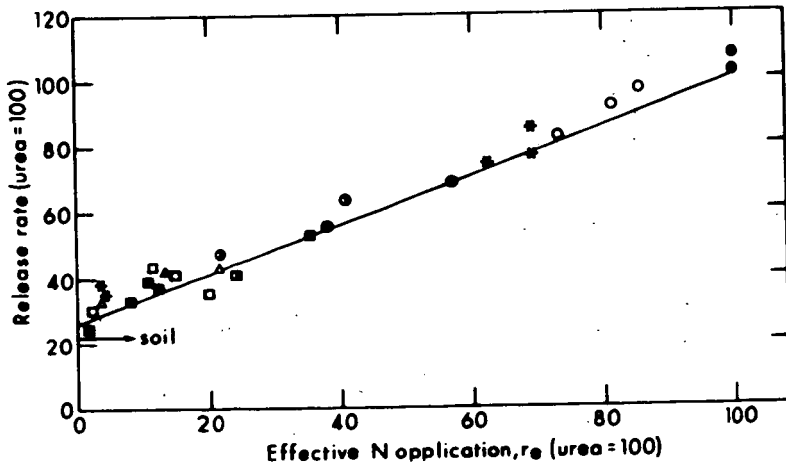


**Figure 2.** Nitrogen Release as Function of "Effective" Nitrogen Application. (For meaning of symbols, cf. Table 2).

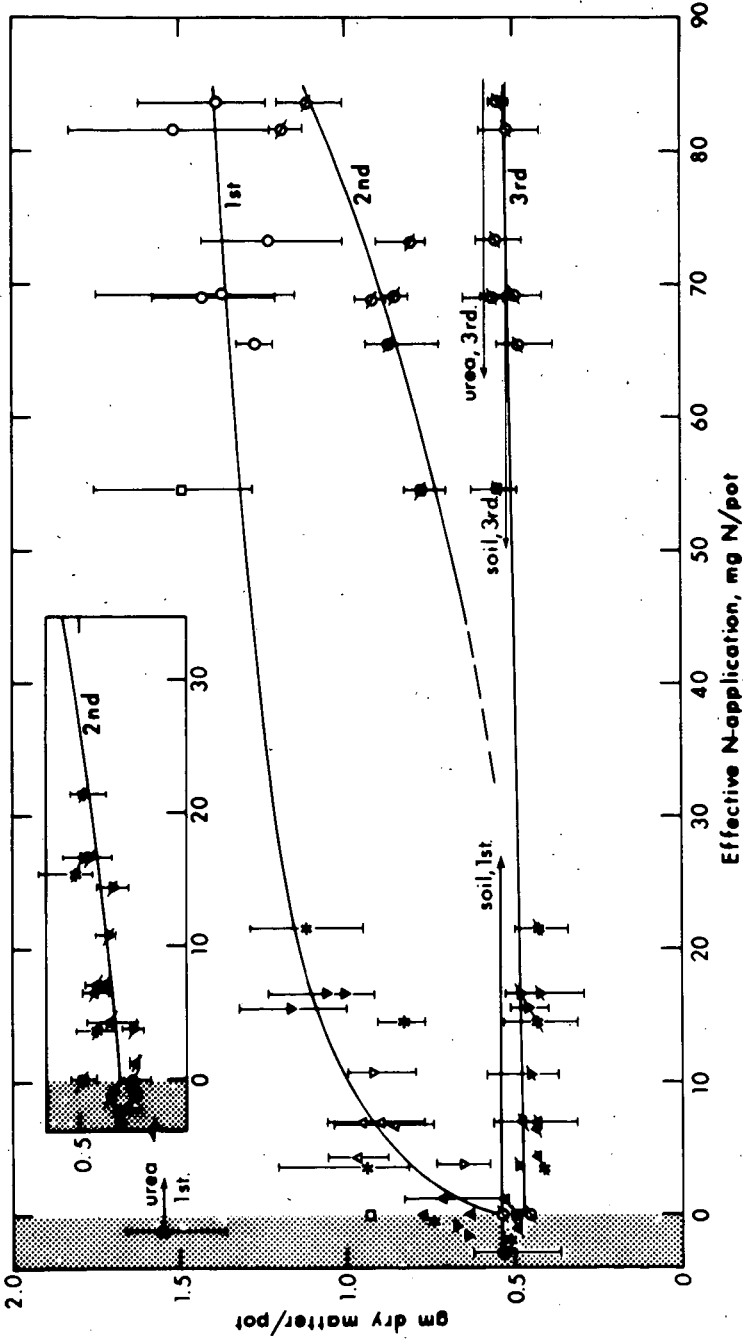
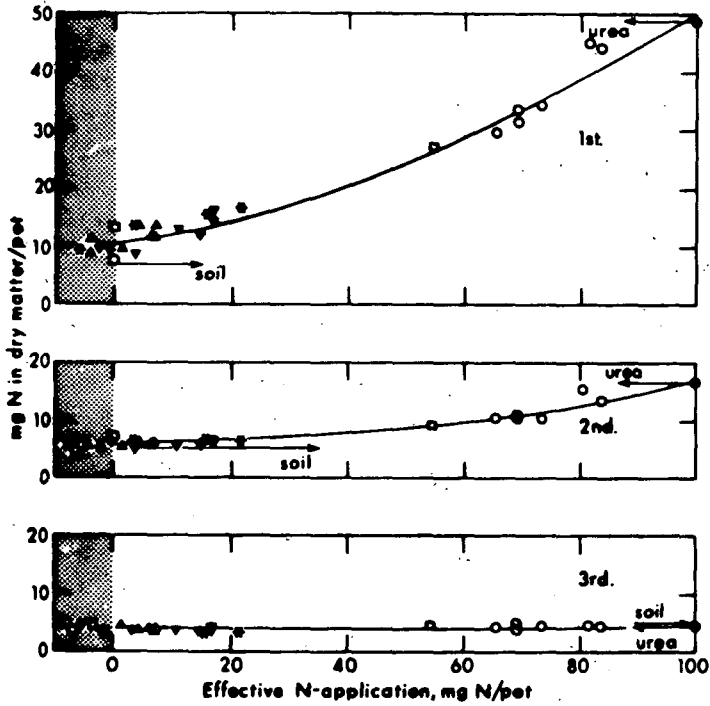
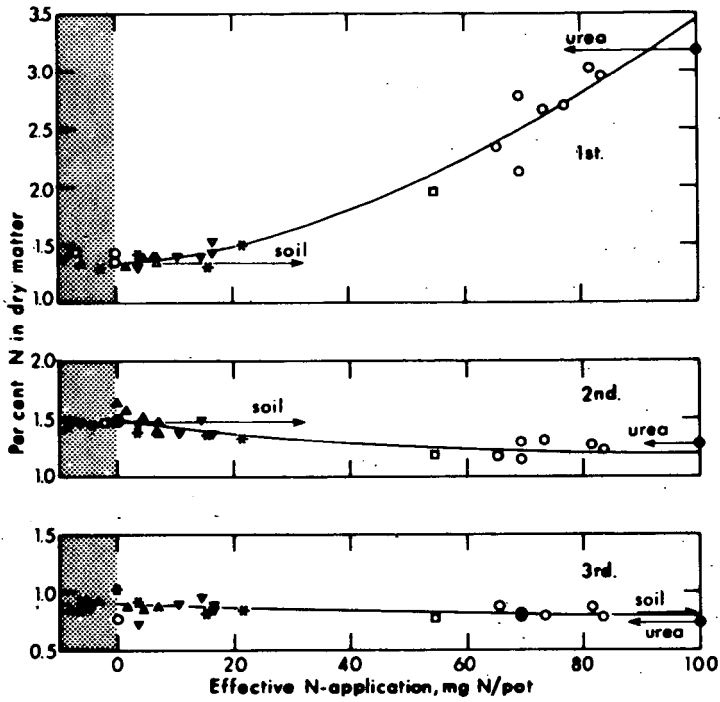


Figure 3. Growth Rate as Function of "Effective" Nitrogen Application (cf. Text and Table 2 for meaning of symbols).



**Figure 4.** Nitrogen Recovery as Function of "Effective" Nitrogen Application. (cf. Text and Table 2 for meaning of symbols).



**Figure 5.** Nitrogen Contents of (Dry) Plant Matter as Function of "Effective" Nitrogen Application. (cf. Text and Table 2 for meaning of symbols).

## NON-FUEL CHEMICALS FROM COAL

By Herbert J. West  
Skeist Laboratories, Inc.  
112 Naylor Avenue  
Livingston, New Jersey 07039

Introduction

Current research and development activities are demonstrating that liquid and gas fuels can be produced by hydrogenation of coal or coal-derived oil at costs which are in sight of being competitive with natural gas or fuels from petroleum. Most of this work is being done under contract to the Office of Coal Research, Department of the Interior, with the prime objective of assuring that we become self-sufficient in non-nuclear energy resources in the face of declining domestic petroleum and natural gas reserves.

Skeist Laboratories contracted to study the economic contributions to these operations from the recovery of non-fuel by-products. As our study progressed, it became increasingly evident that the production from coal of what we now call "petrochemicals" could eventually make just as great or even a greater contribution to our economy than the production of fuel. Major improvements in the design and construction of refinery and petrochemical equipment, together with production level requirements running into billions of pounds a year, have completely changed production economics in coal conversion from what they were at the time of earlier efforts in this technology.

Although new off-shore and foreign oil reserves frequently are being found, they are increasingly costly to discover. The ratio of domestic reserve to production demand is steadily decreasing; already, high-grade domestic crudes are priced over \$3.00 a barrel. The Alaska discoveries may postpone the petroleum shortage era; but despite predictions of low cost at the well, they are not likely to relieve the cost picture. Pipe lines to distribution sites are estimated to cost \$900 million, and maintenance and operating costs at -60°F. temperatures will contribute further to high transportation costs.

Let us assume, then, that within the foreseeable future, petroleum crudes become scarce enough or costly enough to threaten their usefulness as fuel. Also let us assume that nuclear energy will be cheap enough for electric automobiles to become an economic reality and for electricity to be the prime source of domestic heat. It has been estimated that before the end of the century, fast breeder reactors will be supplying power at as low as 0.2¢ per KWH. It is conceivable, therefore, that a petroleum shortage need not be critical in regard to energy requirements. Energy from coal conversion might complement nuclear energy, but the production of petrochemicals from coal could become of even greater significance. The demand for petrochemicals is expected to climb to 35 million tons in 1975, and possibly to 60-70 million tons by 1985.

### Processes for Coal Conversion

Several processes for coal conversion are under development. Those of major interest for potential chemicals recovery are designed to produce a synthetic crude for use as a refinery feed. One process\*, now being engineered for large-scale pilot-plant operation, first pyrolyzes coal in four steps under closely controlled conditions to convert about one-half the coal to gas and oil. The oil is hydrogenated to give a synthetic crude-oil refinery feed. The gas can be used to produce olefins and hydrogen as shown in Table 1. Crediting ethylene and propylene at current values could give hydrogen costs of less than 15¢/1000 cu.ft.

This low-cost hydrogen could be an extremely important factor in the overall economics of coal conversion, since hydrogen at costs by conventional steam reforming represent 30-40% of the cost of coal hydrogenation. The unconverted coal or "char" will be hydrodesulfurized and used as powdered fuel.

Another process operated on a large-scale pilot plant basis at Cresap, West Virginia, by Consolidation Coal solvates about 2/3 of the coal by heating with a kerosene-type solvent under pressure at about 700°F. After filtration, removal of solvent by distillation and hot-water washing of the extract, a high melting product is obtained which is hydrogenated to give the refinery feed. If desired, the coal extract can first be treated by typical tar-processing technology to recover tar acids and bases and other typical coal tar chemicals.

The third major process, which has many attractive features, is the H-coal process, developed by Hydrocarbon Research, Inc. Here pulverized coal is hydrogenated directly in an ebullating catalyst bed, by a process similar to fluidized bed technology. A synthetic crude is obtained directly.

Estimates of the cost of fuels obtainable by these processes are given in the reports to the Office of Coal Research by the contractors.

### Chemicals Recovery

The main purpose of this paper is to discuss the recovery of hydrocarbon chemicals from these synthetic crudes; but regardless of the ultimate objective of the operation, be it chemicals, liquid or gaseous fuels, the recovery of ammonia and sulfur is an essential feature to eliminate air and stream pollution. We do not propose to go into details of their recovery, but the volume is large and will make a significant contribution to the economics of the operation, as shown in Table 2.

\* COED (Char Oil Energy Development) FMC Corporation

TABLE 1

## HYDROGEN AND OLEFIN YIELDS FROM PYROLYSIS GASES

Coal consumed: 50,000 tons per diem

Gas volume: 400 MM cu.ft. per diem, CO<sub>2</sub>-H<sub>2</sub>S-free basis

Composition:	<u>Vol. %</u>
CO	22
H <sub>2</sub>	56
CH <sub>4</sub>	17
C <sub>2</sub> -C <sub>4</sub>	4-5

## ANNUAL VOLUME OF HYDROGEN AND OLEFINS:

	<u>MM lbs./year</u>	<u>Value MM \$</u>
Propylene	150	4.5
Ethylene	200	6.5
Hydrogen	135 billion cu.ft.	<u>27.0</u>
	Total	38.0

TABLE 2

## TYPICAL SULFUR, AMMONIA AND TAR ACID RECOVERIES PER ANNUM

Basis: A. Conversion via pyrolysis of 50,000 tons of coal per diemB. Conversion via solvation or direct hydrogenation  
of 15,000-17,000 tons coal per diem

Assumes coal with 3% sulfur content

	<u>A</u>		<u>B</u>	
	<u>M tons</u>	<u>Value MM \$</u>	<u>M tons</u>	<u>Value MM \$</u>
Sulfur	400	11	100	2.7
Ammonia	40-50	1.6-2.0	40-50	1.6-2.0
Tar acids*	40	<u>9.6</u>	40	<u>9.6</u>
Total value (rounded)		22		14

\* Estimates of recoverable material vary from 30,000 to 100,000 tons

All the volume figures throughout this presentation are based on a refinery, which when operating on all fuel, would produce 50,000 barrels a day of gasoline and fuel oil. This requires the pyrolysis of approximately 50,000 tons a day of as-received coal in the first of the foregoing processes, where only about one-fourth of the coal is converted to oil, or 15,000-17,000 tons of as-received coal a day in the other two processes.

Common also to all three processes is the availability of phenols and cresols, which can be extracted either before or after hydrogenation. The quantity of cresols potentially available would far more than saturate the market; but it would be desirable to extract as much as possible, as oxygenated hydrocarbons must be hydrogenated to extinction of oxygen before the reforming step, consuming valuable hydrogen. The volume of tar acids available is shown in Table 2.

In regard to our future petrochemical requirements, the high potential availability of aromatics is the most significant feature of coal hydrogenation. Table 3 shows a rough composition of a COED syncrude from Utah Coal compared with petroleum crudes. Unfortunately, no corresponding data are yet available on synthetic crudes from other types of coal, but it is believed that the distribution of product types does not vary significantly. The important feature is the high content of naphthenes and aromatic hydrocarbons, which indicates that after the several refining steps and severe reforming, the total aromatics content could approach 90%.

Table 4 shows a chromatographic analysis of another sample of Pittsburgh coal-derived naphtha. Several highly significant features are evident. The 10.2% of combined methylcyclopentane and cyclohexane suggests that it should be easier to recover cyclohexane from coal-derived naphtha than from petroleum naphthas, which contain much less. Methylcyclopentane isomerizes to cyclohexane by heat treatment. The potential availability from the 50,000 barrel operation would be about 5,000 barrels a day, or over 400 million lbs. a year.

The high content of decalins and tetralin theoretically could yield by reforming about 500 million lbs. a year of naphthalene at much lower costs than by dealkylating the alkyl naphthalenes in petroleum naphthas. We believe it should be possible to separate the naphtha of the composition shown in Table 4 into two fractions of 70% and 30%, reform the first fraction for monocyclic aromatics production and separate a decalin-rich cut from the second fraction for naphthalene production.

TABLE 3

## TYPICAL COED SYNCRUDE COMPOSITION VS. PETROLEUM CRUDES

	COED Syncrude	Naphthenic petroleum crude	Paraffinic petroleum crude
Paraffins	13.5	40-46	70-75
Naphthenes	57.8	47	19-23
Alkyl benzenes	7.9	7-13	7-12
Polycyclic and thio-aromatics	20.8		

\* \* \* \* \*

TABLE 4

## COMPOSITION OF COAL-DERIVED NAPHTHA AFTER ISOMAX HYDROCRACKING

	Vol. %	Reform Product
Paraffins	11.4	
Methyl cyclopentane + cyclohexane	10.2	Benzene
C7 Naphthenes	10.7	Toluene
C8 "	13.9	Xylene and ethylbenzene
C9 "	7.6	Trimethylbenzenes
C10+ "	6.0	Tetramethylbenzenes
Benzene	0	
Toluene	1.4	
Xylene	3.9	
Other alkyl benzenes	4.8	
Dicycloparaffins:		
Cis and trans-decalin	10.2	Napthalene
Tetralin (includes indanes)	3.5	
Other dicycloparaffins	14.8	
Hydrindane	1.2	
Napthalene	0.4	

100

Polymethylbenzenes. If all the naphthenes including the C<sub>6</sub>'s are reformed, about 50% of the naphtha would be converted to benzene and alkyl benzenes. The recoverable volumes of benzene, toluene and xylene are shown later. Of considerable significance to our plastics and coatings industries is the volume of tri- and tetramethylbenzenes obtainable from reforming of the C<sub>6</sub><sup>+</sup> naphthenes. Another analysis of coal-derived gasoline gives the percentages of significant components shown in Table 5, showing 16 times as high a content of durenes as in regular petroleum gasoline. Pseudocumene, although much lower, is present in significant quantities, and naphthenic pseudocumene precursors are presumably present also.

Polycyclic aromatics. Another series of analyses was made by the Atlantic Refining Co. on four fractions, including middle distillate and gas oil from the FMC Syncrude (Table 6). The important features are the high content of naphthalenes, tricyclic aromatics, acenaphthene, acenaphthylene and pyrene. Table 7 shows the potential availability of these compounds from 50,000 barrels of feed.

The tricyclic aromatics, although not individually identified, are probably of about the same distribution as those derived from coal tar, primarily anthracene, phenanthrene and fluoranthrene. Separation of these products, including acenaphthene and acenaphthylene, is long-established coal-tar processing technology; but new technologies in solvent extraction and fractional distillation could facilitate their recovery at very favorable costs. Also, it may be easier to isolate them in higher yield and purity from hydrogenated crudes than from coal tar since the content of many sulfur-, nitrogen- and oxygen-containing co-products, which complicate separation, has been reduced or eliminated by hydrogenation. The same possibility may apply to pyrene, which has been difficult to isolate from coal tar. Carbazole, in which, as explained later, there is revived interest, is found in the anthracene fraction in coal tar. About two-thirds of the nitrogen in the coal oil is removed as ammonia by hydrogenation to synthetic crude, but it could be extracted before hydrogenation.

#### End Uses for Polymethylbenzenes and Polycyclic Aromatics

There are numerous existing and potential uses for these materials. Some of the major end-uses are shown in Table 8. H. W. Earhart of Sun Oil Co. (see CW Report), Feb. 22, 1969, on polymethylbenzenes) lists a wide variety of real and potential uses for the tri- and tetramethyl benzenes in several fields, primarily plastics and coatings. Pseudocumene is already isolated by distillation from petroleum naphtha for oxidation to trimellitic anhydride, which is used mainly for conversion to tri-esters for plasticizers and to polyamide-imides for heat-resistant wire coatings. Durene, 1,2,4,5-tetramethylbenzene, is of high interest in the production of pyromellitic dianhydride, also used commercially to prepare heat-resistant imide polymers for wire.

TABLE 5.

SOME SIGNIFICANT COMPONENTS OF COAL-DERIVED GASOLINE  
AND REGULAR NON-PREMIUM GASOLINE (GAS CHROMATOGRAPH)

	% by Volume	
	<u>Coal derived</u>	<u>Typical regular petroleum gasoline</u>
Methylcyclopentane	2.2	1.5
Cyclohexane	3.5	0.4
Ethylbenzene	3.8	2.7
Pseudocumene	0.6	2.8
Durene	2.1	0.2
Isodurene	8.5	0.4

\*\*\*\*\*

TABLE 6.

SOME SIGNIFICANT COMPONENTS OF DISTILLATE CUTS FROM COED SYNCRUDE

	<u>Cut 1</u>	<u>Cut 2</u>	<u>Cut 3</u>	<u>Cut 4</u>
Boiling range	0.335	335-420	420-600	600-875
% distillate	3.8	8.3	25.9	48.9
Monocycloparaffins	71.4	55.1	19.7	4.3
Dicycloparaffins	9.2	8.7	11.0	3.6
Indanes and tetralin	0.9	16.4	23.7	8.3
Alkylbenzenes	7.4	9.9	9.2	4.8
Acenaphthene	-	-	1.2	6.9
Acenaphthylene	-	-	0.7	11.7
Tricydic aromatics			0.3	4.2
Pyrene			-	0.8
Chrysene			-	6.8

TABLE 7

VOLUMES OF POLYCYCLIC AROMATICS POTENTIALLY AVAILABLE  
FROM A 50,000 BARRELS/DAY REFINERY

	<u>MM lbs./day</u>	<u>MM lbs./year</u>
Naphthalene	1.6+	500+
Acenaphthene	.6	200
Acenaphthylene	.9	300
Pyrene	.08	26
Tricyclic aromatics*	.4	130

\* Probably at least 10% anthracene = 13 MM lbs/year; the other major component is phenanthrene.

\*\*\*\*\*

TABLE 8

END USES FOR POLYMETHYLBENZENES AND POLYCYCLIC AROMATICS

<u>Product</u>	<u>End Use</u>
Pseudocumene	Trimellitic anhydride for heat-resistant plastics and coatings.
1,2,4,5-tetramethylbenzene (durene)	Pyromellitic dianhydride for polyimide heat-resistant fibers and coatings.
1,2,3,5-tetramethylbenzene (isodurene)	Tetracarboxylic acid esters for non-volatile plasticizers.
Acenaphthene	Naphthalic anhydride for chemical specialties. Conversion via naphthalimide to perylene derivatives.
Acenaphthylene	Reactive ethylenic monomer for plastics.
Pyrene	Conversion to 1,4,5,8-naphthalene tetracarboxylic acid dianhydride for production of super-heat-resistant polyimides.
Anthracene	Production of anthraquinone.
Phenanthrene	Oxidation to diphenic acid for use in alkyd resins and polyesters.
Carbazole	N-vinyl carbazole for electrical grade polymers and photosensitive polymer systems.

enamel and fiber production. Its high content in the coal-derived naphtha reformat could eventually lead to a price comparable to that for paraxylene, i.e. less than 10¢/lb. vs. the current 50¢-60¢ range. The analyses indicate a potential availability of about 100 MM lbs. a year from the 50,000 bbl. refinery. Even larger quantities of the 1,2,3,5 isomer, isodurene, appear to be available. This could be oxidized to a tetracarboxylic acid for esterification to useful low-volatility plasticizers.

Pyrene is of paramount potential interest. Oxidation gives 1,4,5,8-naphthalene tetracarboxylic acid dianhydride, from which is made the exotic pyrrole polymer BBB or poly(benzimidazobenzophenanthroline) dione which, in fibers, retains strength up to 700°C. At \$400.00/lb., it is being produced and used to make drogue parachutes for spacecraft. Pyrene is difficult to isolate in high purity from coal tar, in which it is associated with benzodiphenylene oxides having the same boiling points and solubility. Since the content of materials of this type might be reduced or eliminated by hydrogenation, the isolation of pyrene from the heavy gas oil fraction from the synthetic crude might not be as difficult. The potential availability appears to be about 20 MM lbs./yr. Possibly its isolation at low cost could bring the price of its unique pyrrole polymer derivatives to a level suitable for industrial usage.

Acenaphthene and acenaphthylene, as shown in Table 7, are present in the synthetic crude to the extent of several hundreds of million pounds. Acenaphthene can be quantitatively oxidized in fixed or fluid-bed converters to naphthalene 1:8 dicarboxylic acid dianhydride which, by boiling with aqueous ammonia, gives a quantitative yield of naphthalimide. By alkali fusion, two molecules of naphthalimide condense to perylene tetracarboxylic acid diimide, used in small amounts to produce pigments. The imide rings can be hydrolyzed back to the dianhydride which, by reaction with diamines, could give polyimides with extremely high heat resistance. The situation could be like that for pyrene. Low-cost raw material could give product costs within a practical range. Naphthalic anhydride itself, potentially a low-cost product, has many interesting potential uses.

Acenaphthylene has been investigated on a limited scale as a reactive monomer capable of homo- and copolymerization, but the products to date have shown no outstanding performance. Presumably, it also can be oxidized to naphthalic anhydride, but we know of no evidence of this.

At a low enough price, anthracene would be the preferred raw material for anthraquinone, an important dyestuff intermediate. The quantity available per annum from the 50,000 bbl operation would be more than enough to meet all current requirements for anthraquinone. The production of this material is estimated at 10-12 million lbs./year, which, if

anthracene were the raw material, would require 12-15 MM lbs. of 90% anthracene. Modern distillation technology could possibly deliver a material containing only phenanthrene as a co-product. Anthracene can be separated from phenanthrene by recrystallization from furfural or pyridine bases. Phenanthrene to date has found but minor uses. It can, however, be oxidized to diphenic acid which, at a low enough price, could be used in fair volume in alkyd and chemical-resistant polyester resins and as an intermediate for many other interesting polymers.

Carbazole, as previously mentioned, may have been destroyed by hydrogenation but, if demanded, could be recovered from the crude before hydrogenation. The demand may increase substantially.

Poly-N-vinyl carbazole has found uses in electrical applications, and is now being used as a photosensitive polymer.

#### All-Chemical Refinery

Recovery of polycyclic aromatics has been emphasized mainly because, in most cases, they are not readily available from petroleum sources and production costs from coal tar have been relatively high. They represent but a small percentage of the total volume of hydrocarbons which can be produced from the synthetic crude. It is the production of olefins, dienes, benzene, toluene and xylene which we expect will make an invaluable contribution to our future economy. Synthetic crude is a much better feedstock than petroleum crudes for BTX production. The light naphtha cut is just as good a feedstock for olefin production, and the C<sub>2</sub>-C<sub>4</sub> hydrocarbons produced during hydrogenation can be processed to olefins.

Table 9 shows a concept of a production schedule for a chemical refinery. It is largely hypothetical since the input and output balances from coal to reformat feed are based on data submitted to OCR by Hydrocarbon Research, Inc., and the assumption is made that the composition of the reformat feed is comparable to that of the Isomaxate obtained from Pittsburgh seam coal-derived synthetic crude. The latter would reform to give the product distribution shown in Table 11, and is the only material for which we have a composition breakdown, as shown under naphtha feed in Table 11. However, we believe that the concept is an indication of what could be accomplished. In any case, such a production schedule would be highly flexible. The total volume and distribution of olefins and butadiene can be varied over wide ranges. Far more naphthalene could be produced if conditions warranted it, or any surplus of its precursor, decalin, could probably be isolated and converted to supersonic jet fuel. Decalin is currently priced at over 50¢/lb. Durene recovery could be increased severalfold if the demand increased. Cyclohexane could be added to the production schedule either by fractionation of the appropriate naphtha cut or by hydrogenating benzene. The latter method might prove to be better.

TABLE 9

CONCEPTUAL MAJOR PETROCHEMICAL PRODUCTION FROM  
50,000 BARRELS A DAY REFINERY

	<u>MM lbs./year</u>	<u>Price ¢/lb.</u>	<u>Value MM \$</u>
<u>Olefins and butadiene</u>			
Ethylene	585	3.25	19
Propylene	140	3	4.2
Butadiene	370	8.5	31.5
Butylene	60	5	<u>3</u>
			57.7
<u>Aromatics</u>			
	<u>MM gals. or lbs./year</u>		
Benzene	52.3 gals.	20	10.5
Toluene	65.7 "	16	10.5
Xylene	98.2 "	16.4	16.1
C <sub>9</sub> + aromatics	80	13.5	10.8
Pseudocumene	60 MM lbs.	6.5	3.9
Durene	10 " "	25	2.5
Naphthalene	256	3	<u>7.7</u>
			62.0
			<u>119.7</u>
	GRAND TOTAL		119.7

TABLE 10

## OTHER PRODUCTS FROM CONCEPTUAL SYNTHETIC CRUDE REFINERY

	<u>Volume</u>	<u>Price</u>	<u>Value MM \$</u>
<u>Chemicals</u>			
Hydrogen	22 billion cu.ft.	15¢/1000	3.0
Tar acids	82 MM lbs.	11.7¢/lb.	9.6
Sulfur	80,000 long tons	\$30/ton	2.4
Ammonia	50,000 short tons	\$40/ton	<u>2.0</u>
			17.0
<u>Fuel</u>			
Fuel oil	0.4 MM barrels	\$2.00	0.8
Surplus heavy naphtha	4 MM "	\$2.00	<u>8.0</u>
			8.8
<u>Polycyclic Aromatics</u>			
Anthracene	10 MM lbs.	20¢	2
Phenanthrene	"	10¢	1
Pyrene	"	30¢	3
Acenaphthene	"	20¢	<u>2</u>
			8
	Grand Total		<u>33.8</u>
	Products from Table 9		119.7
	Overall total		153.5

TABLE 11

## COMPOSITION OF REFORMATE FEED AND REFORMATE PRODUCT AFTER AROMATICS EXTRACTION

<u>Naphtha feed</u>	4287 MM lbs.	<u>Reformate product:</u>		
Composition:	<u>MM lbs.</u>		<u>MM lbs.</u>	<u>MM gals.</u>
Paraffins	414	Hydrogen	139	
Naphthenes:		Benzene	382	52.3
C <sub>6</sub>	417	Toluene	474	65.7
C <sub>7</sub>	442	C <sub>8</sub> aromatics	707	98.2
C <sub>8</sub>	573	C <sub>9</sub> aromatics	648	90.0
C <sub>9</sub>	311	Naphthalene	256	
C <sub>10</sub> <sup>+</sup>	164	Heavy naphtha	1228	
Toluene	61	Raffinate	262	
C <sub>8</sub> aromatics	167	C <sub>1</sub> hydrocarbon	33	
C <sub>9</sub> <sup>+</sup> "	234	C <sub>2</sub> "	36	
Dicycloparaffins	1236	C <sub>3</sub> "	56	
Other cyclics	<u>268</u>	C <sub>4</sub> "	<u>66</u>	
	4287		4287	

The total volume of hydrocarbons represents a recovery of about 900 lbs. from one ton of moisture and ash-free coal. BTX recovery is about 370 lbs. a ton vs. about 20 lbs. as originally obtained by conventional coal and coke technology. About 2000 million lbs. of C<sub>1</sub>-C<sub>4</sub> gases a year are produced in the initial coal hydrogenation and subsequent refining operations. After processing the C<sub>2</sub>-C<sub>4</sub> fractions plus the aromatics extraction raffinate to olefins and butadiene, it is believed that the C<sub>1</sub> fraction plus off-gases should be sufficient in quantity to provide most of the hydrogen requirements for the overall operation.

Other chemicals and fuels and their estimated value are shown in Table 10. The total value of all products from Tables 9 and 10 is \$153.5 million. The values are, we believe, conservative. Increased durenene or naphthalene production could add several million dollars to the total. The surplus heavy naphtha is credited at fuel value, whereas it could be a valuable source of other material such as decalin.

The overall material balance from coal to final products is shown in Table 12.

Table 13 shows the projected order of profitability of the refinery, using a rounded total product value of \$150 million. Basic hydrogenation and refining cost estimates are based on OCR contractor reports. The investments and operating costs for chemicals production are based largely on information provided by major petrochemical engineers. Depreciation is 15 years straight line. The return on investment after taxes is 8.5% and the pay-out time 6.6 years. This is for an operation processing about 55,000 barrels a day of synthetic crude oil and consuming via the H-coal or Consolidation Coal process about 4½ million tons of coal a year, moisture-free, ash-free basis. An operation twice this size, probably requiring an investment of about \$550 million would probably show a return of close to 10%.

In conclusion, it appears almost certain that the resurgence of coal as a chemical source could make several important contributions to our economy. It could aid in assuring self-sufficiency in energy resources, it could provide at low cost all the foreseeable requirements for what we now call petrochemicals for generations to come, and could also make available to industry new families of intermediates for fibers, plastics and chemical specialties.

Perhaps the most constructive production facility would be a two-purpose 100,000 bbls. a day refinery for both fuel and chemicals. Socio-economic factors would be important. Refineries could be located in distressed mining areas such as in Kentucky or West Virginia. Factors such as market demands, profitability data on individual items, freight charges, etc. could be integrated by computer to establish requisite optimum production schedules for overall maximum profitability. Finally, it should be noted that the extremely high polymethyl benzene content of coal naphtha reformat indicates

TABLE 12

OVERALL MATERIAL BALANCE FROM COAL TO ALL FINAL PRODUCTS* (per annum)						
		<u>MM lbs.</u>				
Input - Moisture, ash-free coal		8378				
Hydrogen		<u>695</u>				
		9073				
		<u>MM lbs.</u>		<u>MM lbs.</u>	<u>MM lbs.</u>	
Output:	Hydrogen	139	Benzene	382	Char-coke	1570
	Fuel gas	994	Toluene	474	H <sub>2</sub> O	981
	Ethylene	585	C <sub>8</sub> aromatics	707	H <sub>2</sub> S	220
	Propylene	138	C <sub>9</sub> + "	648	NH <sub>3</sub>	<u>99</u>
	Butadiene	370	Naphthalene	256		
	Butylene	<u>60</u>	Heavy naphtha	1228		2870
		2286	Fuel oil	<u>137</u>		
				3832		
	Total output:	2286				
				3832		
				2870		
	Unaccounted for			<u>85</u>		
				9074		

\* Based on HRI "H Coal" hydrogenation procedure

TABLE 13

## PROFITABILITY OF COAL CHEMICAL REFINERY\*

	<u>MM \$</u>
Basic investment for naphtha production, including off-site	217
Investment for chemicals production	86.5
Additional off-site investment	<u>16.5</u>
	320
Operating costs estimated at \$74 MM.	

	MM \$
Product value	150
15 year depreciation	21.4
Operating costs	74
Gross profit	54.6
After tax profit	27.3
Return on investment after taxes	8.5%
Cash flow	48.7
Pay-out time	6.6 years

\* Basic investment based on American Oil Report (Project 6120) to OCR. This report was an evaluation of the HRI "H Coal" project.

the possibility of producing premium 100+ octane fuel without recourse to lead. Many of these aromatics have research octane ratings exceeding 140.

Much work would, of course, be required to reduce many of these concepts to practice. Much more analytical data on process streams is needed. The fractionation of heavy naphtha would require considerable study to separate decalins and to the best of our knowledge, there are no available data on the reforming of decalin to naphthalene. The application of solvent extraction methods and fractionation techniques would have to be studied to recover the polycyclic aromatics. Analytical techniques must be refined.

The help and advice of many people was invaluable in obtaining the basic data for the Skeist report to OCR. We acknowledge, with thanks, the assistance of OCR contractor personnel at FMC Corporation, Hydrocarbon Research, Inc. and Consolidation Coal and of Mr. Harry Jacobs, Atlantic Richfield, Mr. Walter Linde, Lotepro Corporation and Mr. Everett Howard, UOP.

## SULFUR RECOVERY IN THE MANUFACTURE OF PIPELINE GAS FROM COAL

C. L. Tsaros, J. L. Arora, and W. Bodle

Institute of Gas Technology, Chicago, Illinois 60616

U. S. SULFUR NEEDS

U. S. sulfur consumption is growing at an increasingly rapid rate. Annual consumption increased from 5.5 million long tons in the middle 1950's to 7.8 million tons in 1965,<sup>15</sup> an annual increase of 3.6%. Consumption in 1967 was 9.3 million long tons, 8.3 million tons being provided by U. S. production, the rest from stocks and Canadian sour gas and refinery recovery.<sup>2, 13</sup> The annual average increase from 1965 to 1967 was 9%/yr.

Projections for 1970 and 1975, respectively, indicate U. S. consumption of 11 and 17 million long tons/yr.<sup>13, 15</sup> Market projections also allow for 2.7 and 5.0 million tons/yr for export in addition to the above. This is a big increase over the 1.3 million tons exported in 1967. If the exports are included, U. S. sulfur needs would increase 100% over 1967 figures by 1975.<sup>13</sup>

A large part of this increase may be met by desulfurization of fuels. It is estimated that about 12 million tons of sulfur is emitted yearly to the atmosphere in the U. S. by fuel combustion processes.<sup>6, 14</sup> This exceeds the current U. S. sulfur consumption. Not all of this is readily recoverable, however.

The public concern over air pollution, resulting in the need for desulfurization of fuels and/or flue gases; the availability of desulfurization processes; and the expanding need for sulfur will combine to make desulfurization a reality. Currently, about 70% of U. S. sulfur supplies are met by Frasch sulfur; over 80% of U. S. production is by this method. Future expansion will require other sources.

SULFUR IN U. S. COALS

In less than a generation we will have to meet part of the demand for liquid and gaseous fuels by conversion of coal and oil shale. This paper is limited to the recovery of sulfur during the conversion of coal to pipeline-quality gas by hydrogenation. In the manufacture of pipeline gas from coal most of the sulfur is also gasified. Regardless of whether the coal is burned conventionally or converted to gas, its sulfur content is of great importance.

The rank, sulfur content, and sulfur type of the coal reserves of the United States have been published by the U. S. Bureau of Mines.<sup>3</sup> Sulfur levels range from 0.2% or less to 7% by weight on a dry basis.<sup>10</sup> Of the total estimated U. S. coal reserves of all ranks, as of January 1, 1965, 65% is low-sulfur coal (1.0% or less). This 65% includes 91% of the lignites, over 99% of the subbituminous, and 97% of the anthracite coals. Fifteen percent of the coals are classified as medium-sulfur coals (1.1-3.0%), and 20% as high-sulfur coals (over 3.0%).

The latter two classes include 70% of the bituminous coals. Two-thirds of the high-sulfur coal is east of the Mississippi and comprises 43% of the total reserves in that section of the country.<sup>10</sup>

Sulfur occurs in coal in three forms: 1) combined with the organic coal substance, 2) combined with iron (pyritic), and 3) combined as sulfate.<sup>3</sup> Generally, organic sulfur predominates in low-sulfur coals. As total sulfur increases, both organic and pyritic forms increase. Sulfate sulfur in unweathered coals is usually less than 0.05%.

#### MANUFACTURE OF PIPELINE GAS

Conversion of coal to pipeline-quality gas by hydrogasification is shown in Figure 1, which is a simple block flow diagram giving basic steps in the process used. Ground, raw bituminous coal is pretreated by a mild air oxidation to prevent agglomeration during hydrogasification. Hydrogen is supplied by synthesis gas generated by the electrothermal gasification of hydrogasifier char. Hydrogasifier effluent is scrubbed to remove  $\text{CO}_2$  and  $\text{H}_2\text{S}$  and then sent to methanation to produce 950 Btu/CF heating value gas. In reviewing the recovery of sulfur for this process we have considered two cases: a high-sulfur coal containing 4.4% sulfur, and a low-sulfur coal containing 1.5% sulfur. These cases are based on pipeline gas plant designs for two different Pittsburgh seam coals. For the pipeline gas production capacity of 250 billion Btu/day, used throughout this study, sulfur inputs are 739 and 199 tons/day for high- and low-sulfur coals. Table 1 summarizes the distribution of sulfur in the gasification process.

Table 1. DISTRIBUTION OF SULFUR IN HYDROGASIFICATION PROCESS

	<u>Low-Sulfur Coal</u>		<u>High-Sulfur Coal</u>	
	<u>Tons Sulfur / Stream-Day</u>	<u>%</u>	<u>Tons Sulfur / Stream-Day</u>	<u>%</u>
Raw Coal	199	100	739	100
As $\text{SO}_2$ in Pretreatment Off-Gas	30	15.1	166	22.5
In Pretreatment Fines	5	2.5	15	2.0
In $\text{H}_2\text{S}$ From Hydrogasifier	158	79.4	487	65.9
Residue Char	6	3.0	71	9.6

During pretreatment about 15-25% of the sulfur is oxidized to  $\text{SO}_2$ . Most of the remaining sulfur is converted to  $\text{H}_2\text{S}$  during the hydrogasification of the pretreatment char. This includes virtually all organic and pyritic sulfur. Sulfur in the hydrogasifier char is essentially sulfide.

In this study we have considered sulfur recovery in two phases:

1) from  $\text{H}_2\text{S}$  only by the Claus Process, with  $\text{SO}_2$  vented or scrubbed out of the gas without elemental sulfur recovery, and 2) from both  $\text{H}_2\text{S}$  and  $\text{SO}_2$ . Figures 2 and 3 show the distribution of sulfur for the first phase only. In high-sulfur coal there is a large amount of pyritic sulfur. The char from hydrogasification contains 1.7% sulfur, largely as sulfide sulfur. We have assumed one-half of this sulfur is gasified and returns to the hydrogasifier as  $\text{H}_2\text{S}$  in synthesis gas.

This is a conservative assumption; pilot plant data indicate even more sulfur will be gasified. For the low-sulfur case, the hydrogasifier char contains only 0.1% sulfur and is assumed to pass through the electrogasifier unchanged.

### SULFUR RECOVERY FROM H<sub>2</sub>S

Hydrogen sulfide feed to the Claus plant is contained in acid gas stripped from the scrubbing solutions in the purification section. Because of the large amount of CO<sub>2</sub> present, the H<sub>2</sub>S concentration in this stream is low, 6 and 2% for the high- and low-sulfur coals. By modifying the scrubbing system to have two separate scrubbing liquid streams, it is possible to selectively recover 90% of the H<sub>2</sub>S, while absorbing only 25% of the CO<sub>2</sub> in a short, "quick contact" section of the absorber. By this method, the H<sub>2</sub>S concentrations in the sulfur recovery plant feed can be raised to 18.7 and 6%, respectively. Although the total amount of sulfur available is reduced, at higher H<sub>2</sub>S concentrations costs per ton of recovered sulfur are greatly lowered. Also, the percentage sulfur recovered from the Claus plant feed is raised so that in the low-sulfur case overall recovery is somewhat higher.

Table 2 summarizes the economics for recovery of sulfur from the H<sub>2</sub>S. Figure 4 gives a flow sheet representing the process scheme. Processing methods and costs for sulfur plants are based on published information and private communication with Pan American Petroleum Corp.<sup>4, 9, 11</sup>

Figure 4 shows the direct oxidation and split-flow processes used to produce sulfur from H<sub>2</sub>S depending on the concentration of H<sub>2</sub>S in the feed stream. Direct oxidation was used in all except the 18.73% H<sub>2</sub>S concentration stream case, where the split-flow process was used.

Generally, a two-reactor system is used for optimum sulfur recovery. The gases from first reactor are cooled for sulfur condensation, preheated, and sent to second reactor where additional sulfur is recovered.

After sulfur recovery from the second reactor, the gases go to an incinerator and are heated to 1200°F, where residual H<sub>2</sub>S is converted to SO<sub>2</sub>. If SO<sub>2</sub> from pretreatment off-gas is being recovered, the incinerator gases are cooled and sent to SO<sub>2</sub> extraction; otherwise, they are vented. Electrogasifier char is used as fuel for preheating the gases going to the reactor and for the incinerator.

#### Direct Oxidation Process

In this process air and the H<sub>2</sub>S stream are preheated and passed over the catalyst beds for conversion to sulfur.

#### Split-Flow Process

In split flow, one-third of the H<sub>2</sub>S, burned in a furnace boiler to produce SO<sub>2</sub>, is combined with bypassed H<sub>2</sub>S stream and is then passed over a catalyst bed to produce sulfur. The heat generated in burning H<sub>2</sub>S is used to produce steam as a by-product.

Table 2. SUMMARY OF COSTS FOR RECOVERY OF SULFUR FROM H<sub>2</sub>S IN HYDROGASIFIER EFFLUENT BY CLAUSS PROCESS

Feed to Claus Plant	Coal Type, % Sulfur			
	Low-Sulfur Coal, 1.5		High-Sulfur Coal, 4.4	
	Purification Off-Gas	Concentrated Purification Gas	Purification Off-Gas	Concentrated Purification Gas
H <sub>2</sub> S Concentration, mole %	2.03	6.95	6.0	18.7
Sulfur Recovery, %	70	86	85	91
Sulfur Recovery, tons/day	110	122	414	399
Sulfur Recovery, long tons/day	98.2	109	369.6	356
90% Stream Factor, long tons/year	32,260	35,810	121,410	116,950
INVESTMENT				
Claus Plant, \$	3,400,000	1,200,000	4,200,000	1,700,000
Incinerator With Stack, \$	300,000	300,000	300,000	300,000
Additional H <sub>2</sub> S Concentration Investment, \$	--	200,000	--	200,000
Total Fixed Investment, \$	3,700,000	1,700,000	4,500,000	2,200,000
OPERATING COSTS				
Char Fuel, \$4/ton, \$	332,000	378,000	381,000	349,000
Power, \$0.003/kWhr, \$	30,000	32,000	37,000	39,000
Sulfur Loading Cost, 25¢/long ton, \$	8,000	9,000	30,000	29,000
Labor, Maintenance, and Supplies, \$	32,000	36,000	73,000	70,000
Steam By-Product, 25¢/1000 lb, \$	--	--	--	-99,000
Subtotal, \$	402,000	455,000	521,000	388,000
Capital Charges, Includes 5% Depreciation, \$	385,000	130,000	499,000	203,000
Sulfur Recovery Charge, \$/yr	787,000	585,000	1,020,000	591,000
Sulfur Recovery Charge, \$/long ton	24.4	16.3	8.4	5.1

Table 2, Cont. SUMMARY OF COSTS FOR RECOVERY OF SULFUR FROM H<sub>2</sub>S HYDROGASIFIER  
EFFLUENT BY CLAUSS PROCESS

Feed Claus Plant	Coal Type, % Sulfur					
	Low-Sulfur Coal, 1.5			High-Sulfur Coal, 4.4		
	Purification Off-Gas	Concentrated Purification Gas	Purification Off-Gas	Concentrated Purification Gas	Purification Off-Gas	Concentrated Purification Gas
Sulfur Sale Price, \$/long ton	20	30	40	20	30	40
Annual By-Product Revenue, \$1000	-141.9	180.6	503.2	132.5	490.5	848.6
Decrease in Gas Price, ¢/10 <sup>6</sup> Btu	-0.17	0.21	0.59	0.16	0.58	1.0
20-yr Avg Price of Gas, ¢/10 <sup>6</sup> Btu	53.2	52.8	52.4	52.8	52.4	52.0
				49.9	48.5	48.5
				51.3	49.9	48.5
				3.09	4.53	2.06
				1.66	3.44	4.82
				2622.5	3836.7	1742.5
				2912.0	4081.4	2912.0

Three out of the four cases in Table 2 have lean acid-gas feed, 2 to 6%  $H_2S$ , and make use of the direct oxidation process. In the fourth case, 18.7%  $H_2S$ , the split-flow process is used. Raising the percentage of  $H_2S$  greatly reduces sulfur recovery plant investment for a given capacity, particularly in the range from 2 to 20%.

#### Economics of Sulfur Recovery From $H_2S$

Sulfur recovery ranges from 98 to 370 long tons/day for 1.5 and 4.4% sulfur in the coal. Recovery costs, with capital charges based on utility-type financing, vary from \$24 to \$51/ton as a break-even cost (Table 2). Capital charges are treated the same as for the pipeline-gas-from-coal plant except there is no return on investment or income tax. The cost is enough to cover operating and capital charges so the price of pipeline gas is the same as if there were no sulfur: 53¢/million Btu. Financing is 65% debt and 35% equity, depreciation is 5%/yr, and the interest rate is 5% on outstanding debt. Costs are summarized in Table 2.

The effect of the sulfur by-product on the price of pipeline gases is shown graphically in Figures 5 and 6. The base price of pipeline gas is 53¢/million Btu with no elemental sulfur recovery. Because of the higher unit cost of recovery and the small amount of sulfur obtained from low-sulfur coal, the effect of sulfur recovery on gas price is slight: 1¢ or less per million Btu. With high-sulfur coal the effect is much more significant, ranging from just under 2¢ to over 4.5¢/million Btu as sulfur market price increases from \$20 to \$40/ton. Raising the percentage  $H_2S$  in the feed has a significant effect on the cost per ton of sulfur, but only a small effect on the price of pipeline gas. A change of \$1 million in investment for a 250 billion Btu/day plant, representing 25-50% of the cost of the sulfur recovery section, will change the price of pipeline gas by about 0.25¢/million Btu.

#### SULFUR RECOVERY FROM $SO_2$ AND $H_2S$

Recovery of sulfur from  $H_2S$  still leaves substantial amounts of  $SO_2$  vented to the atmosphere from the coal pretreatment and sulfur plant incinerator off-gases. For high-sulfur coal the total is 239.3 to 254.3 tons/day of sulfur depending on whether the  $H_2S$  concentration in the feed to the sulfur recovery plant is raised by modifications in the pipeline gas purification section. This is one-third of the sulfur entering the plant with the coal. The effluent  $SO_2$  concentration is about 0.6%. For the low-sulfur coal, 66-78 tons/day of sulfur as  $SO_2$  is vented, with an average concentration of about 0.3%. These  $SO_2$  concentrations are similar to those in power plant flue gases; therefore, techniques applicable for  $SO_2$  removal from power plant flue gases should be applicable to flue gases from pipeline-gas-from-coal plants.

A large number of processes are in various stages of development at present. Review of these is beyond the scope of this study. The  $SO_2$  can be removed and discarded in chemical combination with limestone as in the Combustion Engineering Process,<sup>1</sup> extracted and liquefied as in the Wellman-Lord Process,<sup>1, 16, 17</sup> converted to sulfuric acid as in the Monsanto Cat-Ox Process,<sup>1, 6</sup> or converted to elemental sulfur as in the Alkalized Alumina Process.<sup>6</sup>

### SO<sub>2</sub> Removal

For removal of SO<sub>2</sub> from pretreatment and incinerator off-gases in our system without elemental sulfur recovery we have considered removal by the alkali-injection, wet-scrubbing process. Although definitive costs are not available, published data indicate a range of costs.<sup>1, 8, 18</sup> We have assumed an average price of \$10/ton of SO<sub>2</sub>. Since no additional sulfur is produced, the cost of removal must be added to the price of the pipeline gas without credit for by-products. For the low-sulfur coal the additional cost is about 0.5¢/million Btu; for high-sulfur coal, it is 1.7¢/million Btu. These added costs are indicated in Figures 5 and 6. The sensitivity is such that, for each \$1/ton change in SO<sub>2</sub> removal cost, the effect on pipeline gas price is 0.05¢ and 0.17¢/million Btu for low- and high-sulfur coals.

As a result of the additional costs for SO<sub>2</sub> removal, for low-sulfur coal the price of by-product sulfur will have to be about \$35/long ton to balance the costs of desulfurization (Figure 5). However, even with sulfur at \$20/ton, the penalty is only about 0.5¢/million Btu of pipeline gas. For a plant using high-sulfur coal, as long as by-product sulfur sells for \$20/ton or higher, pipeline gas price will not be penalized by costs of desulfurization (Figure 6).

Although current prices for sulfur are at the \$40/long ton level, future prices, with adequate or oversupply, could depress the price to \$30 or less. Since pipeline-gas-from-coal plants will operate in the future, we have considered \$40/long ton as a conservative maximum in a range of \$20-\$40/long ton.

In a pipeline-gas-from-coal plant, the production of large amounts of H<sub>2</sub>S during hydrogasification brings an advantage in sulfur recovery from SO<sub>2</sub> that is not present in a power plant. The SO<sub>2</sub> extracted from the pipeline gas plant "flue" gases can be sent to the sulfur recovery plant and reacted with H<sub>2</sub>S extracted from the hydrogasifier effluent according to the Claus reaction:



Less combustion of H<sub>2</sub>S is required to maintain the required H<sub>2</sub>S/SO<sub>2</sub> ratio of about 2. This may require more fuel, but it eliminates the need for separate reduction of SO<sub>2</sub> to recover the sulfur. A recent announcement briefly describes a process in which sulfur is produced by catalytic reaction of H<sub>2</sub>S and SO<sub>2</sub>. Some of the SO<sub>2</sub> reacts with methane to make more H<sub>2</sub>S. A pipeline gas plant already has the necessary H<sub>2</sub>S.<sup>12</sup>

Published information on the Wellman-Lord Process shows production of liquid SO<sub>2</sub>. In this process, SO<sub>2</sub> is removed by scrubbing the flue gas with a solution of potassium sulfite precipitated as potassium pyrosulfite. The crystals are recovered and dissolved in water, and SO<sub>2</sub> is stripped out with steam. Then the steam is condensed and the SO<sub>2</sub> is compressed and liquefied.

### SO<sub>2</sub> Recovery

For our application we would not need to liquefy the SO<sub>2</sub>. Based on published costs for the process<sup>16, 17</sup> and the pipeline gas capital charges described above, the cost of SO<sub>2</sub> extraction for our application might range from \$11 to \$15/ton of SO<sub>2</sub>. Contact with Wellman-Lord indicated that extraction of SO<sub>2</sub> in the pretreatment off-gas and in the sulfur recovery plant incinerator flue gas.

could be feasible and could be simpler than in a proposed power plant system making pure liquid  $\text{SO}_2$ . Although we do not have a specific design for our system, it appears that an  $\text{SO}_2$  extraction cost of \$10 to \$15/ton is a representative range for this process application.

We have made preliminary estimates of the cost of  $\text{SO}_2$  extraction based on published costs for the alkaliized alumina process.<sup>5,6</sup> This process requires the generation of a producer gas to regenerate the absorbent, producing  $\text{H}_2\text{S}$  which is then fed to the Claus plant to yield elemental sulfur. Published investment costs were adjusted to our capacities. Incremental  $\text{SO}_2$  removal costs ranged from \$25/ton for the high-sulfur coal to over \$50/ton for the low-sulfur coal. Since the high  $\text{H}_2\text{S}/\text{SO}_2$  ratio produced in the pipeline gas plant makes reduction of  $\text{SO}_2$  unnecessary, this process would be at the high end of the cost range for  $\text{SO}_2$  extraction in our application.

Figures 7 and 8 show the flows of sulfur through the pipeline gas and desulfurization systems for the 1.5 and 4.4% sulfur coals. Numbers are in tons/day. In these systems, sulfur is obtained from  $\text{SO}_2$  as well as  $\text{H}_2\text{S}$ . Flue gas from pretreatment and from the sulfur plant incinerator goes to  $\text{SO}_2$  extraction where 90% of the  $\text{SO}_2$  is recovered and sent to the Claus unit. With this system, the concentrated  $\text{H}_2\text{S}$  stream is obtained from pipeline gas purification. This reduces the cost of the  $\text{H}_2\text{S}$  recovery. Unrecovered  $\text{H}_2\text{S}$  is burned and recycled as  $\text{SO}_2$ . Sulfur recovery is increased from 110 to 160 long tons/day for low-sulfur coal, and from 370 to 532 long tons/day for high-sulfur coal. With high-sulfur coal the amount of  $\text{SO}_2$  extracted exceeds one-half the  $\text{H}_2\text{S}$ , so a small amount is liquefied.

#### Costs for Sulfur Recovery From $\text{H}_2\text{S}$ and $\text{SO}_2$

Table 3 summarizes costs of sulfur recovery for combined  $\text{SO}_2$  extraction and Claus plant operation; results are depicted graphically in Figures 9 and 10. Variables are the cost of  $\text{SO}_2$  extraction and the sale price for sulfur at the pipeline gas plant.

For low-sulfur coal (Figure 9) desulfurization improves the price of gas slightly, about 0.5¢/million Btu, if sulfur can be sold at \$30/ton. If sulfur from  $\text{SO}_2$  is not recovered but  $\text{SO}_2$  is scrubbed out and only the sulfur from  $\text{H}_2\text{S}$  is recovered (Figure 5), sulfur credits just about balance the costs for desulfurization.

With high-sulfur coal the effects are much greater because there is over 3 times as much sulfur recovered. Sulfur recovery substantially lowers the price of gas if the sulfur price is \$25/ton or better. At a sulfur price of \$30/ton or better and an  $\text{SO}_2$  extraction cost of \$15/ton, the price of gas is lowered by 3¢-5¢/million Btu. If  $\text{SO}_2$  is removed and only sulfur from  $\text{H}_2\text{S}$  recovered, then the price is about 51.5¢/million Btu. Even at \$20/ton and full desulfurization, recovery of sulfur from  $\text{H}_2\text{S}$  and  $\text{SO}_2$  has an advantage of 1¢ over the alternative. This is because, even though it costs \$15/ton  $\text{SO}_2$  (\$30/ton sulfur) to extract  $\text{SO}_2$  for sulfur recovery and \$10/ton (\$20/ton sulfur) to remove it as  $\text{CaSO}_4$ , the sulfur recovered more than pays for this differential cost of sulfur removal. The price of sulfur would have to drop to well below \$20/ton before it is less economical to recover it than to remove and discard it.

Table 3. SUMMARY OF COSTS FOR RECOVERY OF SULFUR FROM H<sub>2</sub>S IN HYDROGASIFIER EFFLUENT AND SO<sub>2</sub> IN PRETREATMENT AND INCINERATOR OFF-GASES BY SO<sub>2</sub> EXTRACTION AND CLAUSS PROCESS

	Coal Type, % Sulfur	
	Low-Sulfur Coal, 1.5	High-Sulfur Coal, 4.4
<u>Feed to Claus Plant</u>		
SO <sub>2</sub> to Extraction Unit, mole %	0.3	0.9
Equivalent SO <sub>2</sub> + H <sub>2</sub> S Feed, mole %	9.5	23.7
Sulfur Recovery, %	88	91
Sulfur Recovery, tons/day	181	596
Sulfur Recovery, long tons/day	161.6	532
90% Stream Factor, long tons/yr	53,090	174,760
<b>INVESTMENT</b>		
Claus Plant, \$	1,200,000	2,500,000
Incinerator, \$	300,000	300,000
Additional H <sub>2</sub> S Concentrator Investment, \$	200,000	200,000
Heat Exchange Incinerator Feed and Effluent, \$	1,700,000	1,700,000
Total Fixed Investment, \$	<u>3,400,000</u>	<u>4,700,000</u>
<b>OPERATING COSTS</b>		
Char Fuel, \$4/ton, \$	140,000	54,000
Power, \$0.003/kWhr, \$	9,000	7,000
Cooling Water, \$0.10/1000 gal, \$	5,000	5,000
Loading Cost, 25¢/long ton, \$	13,000	44,000
Labor, Maintenance, and Supplies, \$	43,000	73,000
Subtotal, \$	<u>210,000</u>	<u>183,000</u>
Capital Charges	353,000	528,000
Depreciation at 5%		
Revenue Required, \$	563,000	711,000

Table 3, Cont. SUMMARY OF COSTS FOR RECOVERY OF SULFUR FROM H<sub>2</sub>S IN HYDROGASIFIER  
EFFLUENT AND SO<sub>2</sub> IN PRETREATMENT AND INCINERATOR OFF-GASES BY SO<sub>2</sub>  
EXTRACTION AND CLAUSS PROCESS

	Coal Type, % Sulfur		
	Low-Sulfur Coal, 1.5	High-Sulfur Coal, 4.4	
<u>Feed to Claus Plant</u>			
H <sub>2</sub> S From Concentrated Purification Off-Gas, SO <sub>2</sub> From Extraction Plant	20	30	40
H <sub>2</sub> S From Concentrated Purification Off-Gas, SO <sub>2</sub> From Extraction Plant	20	30	40
<u>SO<sub>2</sub> EXTRACTION</u>			
Sulfur Sale Price, \$ /long ton	20	30	40
SO <sub>2</sub> Extraction, \$10/ton, \$	—	417,200	—
Annual Total Sulfur Recovery Cost, \$	—	980,200	—
Annual By-Product Revenue, \$	84,940	615,800	1,345,700
Decrease in Gas Price, ¢/10 <sup>6</sup> Btu	0.1	0.73	1.35
Price of Gas, ¢/10 <sup>6</sup> Btu	52.9	52.27	51.65
SO <sub>2</sub> Extraction at \$15/ton, \$	—	625,800	—
Annual Total Sulfur Recovery Cost, \$	—	1,188,800	—
Annual By-Product Revenue, \$	-127,400	403,400	934,300
Decrease in Gas Price, ¢/10 <sup>6</sup> Btu	-0.15	0.48	1.1
Price of Gas, ¢/10 <sup>6</sup> Btu	53.15	52.5	51.9
SO <sub>2</sub> Extraction at \$30/ton, \$	—	1,251,600	—
Annual Total Sulfur Recovery Cost, \$	—	1,814,600	—
Annual By-Product Revenue, \$	-753,800	-223,000	307,900
Decrease in Gas Price, ¢/10 <sup>6</sup> Btu	-0.89	-0.26	0.36
Price of Gas, ¢/10 <sup>6</sup> Btu	53.9	53.3	52.64
H <sub>2</sub> S From Concentrated Purification Off-Gas, SO <sub>2</sub> From Extraction Plant	20	30	40
H <sub>2</sub> S From Concentrated Purification Off-Gas, SO <sub>2</sub> From Extraction Plant	20	30	40
Annual Total Sulfur Recovery Cost, \$	—	2,871,200	—
Annual By-Product Revenue, \$	800,400	2,548,000	4,295,600
Decrease in Gas Price, ¢/10 <sup>6</sup> Btu	0.94	3.01	5.07
Price of Gas, ¢/10 <sup>6</sup> Btu	52.1	50.0	47.9
SO <sub>2</sub> Extraction at \$30/ton, \$	—	4,320,400	—
Annual Total Sulfur Recovery Cost, \$	—	5,031,400	—
Annual By-Product Revenue, \$	1,537,900	209,700	1,957,300
Decrease in Gas Price, ¢/10 <sup>6</sup> Btu	-1.81	0.25	2.31
Price of Gas, ¢/10 <sup>6</sup> Btu	54.8	52.75	50.7

The above applies, however, only to the situation where the  $\text{SO}_2$  is not released to the atmosphere. If  $\text{SO}_2$  can be vented, then there is not much economic advantage in recovering that sulfur which is converted to  $\text{SO}_2$  in the process. If air pollution standards require  $\text{SO}_2$  removal, then it appears more economical to recover it as sulfur than as sulfate.

In the manufacture of pipeline gas from coal by hydrogasification, high-sulfur coal is more of an asset than a liability. The production of  $\text{H}_2\text{S}$  facilitates sulfur recovery from both  $\text{SO}_2$  and  $\text{H}_2\text{S}$  and has the potential of reducing gas price by several ¢/million Btu. Hydrogen consumed in making  $\text{H}_2\text{S}$  is only 0.75¢/million Btu. Viewed as a source of sulfur, high-sulfur coal is a higher grade raw material for gasification, and the costs of desulfurization in a gas plant based on this coal will yield a greater return than with low-sulfur coal.

#### LITERATURE CITED

1. Bice, G. W. and Aschoff, A. F., "Status of  $\text{SO}_2$  Removal Systems." Paper presented at American Power Conference, Chicago, April 22-24, 1969.
2. "Current Business Statistics," Surv. Curr. Bus. 49,S-25 (1969) March.
3. De Carlo, J. A., Sheridan, E. T. and Murphy, Z. E., "Sulfur Content of United States Coals," U. S. Bureau of Mines L. C. 8312. Washington, D. C., 1966.
4. Grekel, H., Palm, J. W. and Kilmer, J. W., "Why Recover Sulfur From  $\text{H}_2\text{S}$ ?" Oil Gas J. 66, 88-101 (1968) October 28.
5. Katell, S., "An Economic Evaluation of the Alkalized Alumina System for the Removal of  $\text{SO}_2$  From Power Plant Flue Gases." Paper presented at American Association of Cost Engineers 13th National Meeting, Pittsburgh. June 30-July 2, 1968.
6. Katell, S., "Removing Sulfur Dioxide From Flue Gases," Chem. Eng. Progr. 62, 67-73 (1966) October.
7. Knabel, S. J. and Tsaros, C. L., Process Design and Cost Estimate for a 258 Billion Btu/Day Pipeline Gas Plant - Hydrogasification Using Synthesis Gas Generated by Electrothermal Gasification of Spent Char. Washington, D. C.: Office of Coal Research, 1967.
8. Kown, B. T., "Fresh Thought on  $\text{SO}_2$  Removal," Power Eng. 73, 41-44 (1969) May.
9. Palm, J. W., Pan American Petroleum Co., private communication of May 1969.
10. Parry, H. and De Carlo, J. A., "The Search for Low-Sulfur Coal." Paper presented at the IEEE-ASME Joint Power Generation Conference, Denver, September 18-21, 1966.
11. "Plant Recovers Sulfur From Lean Acid Gas" Chem. Eng. 70, 38-40 (1963) April 1.
12. "Pollution: Causes, Costs, Control," Chem. Eng. News 47, 33-64 (1969) June 9.

13. Rickles, R. N., "Desulfurization's Impact on Sulfur Markets," Chem. Eng. Progr. 64, 53-56 (1968) September.
14. Skeist Laboratories, Livingston, N. J., Chemical By-Products From Coal, Washington, D. C. : Office of Coal Research, 1968.
15. "Sulfur Hits a 47-Year High," Chem. Week 99, 35-36 (1966) December 17.
16. Terrana, J. D. and Miller, L. A., "New Process for Recovery of SO<sub>2</sub> From Stack Gases," Proc. Amer. Power Conf. 1968 30, 627-32.
17. Terrana, J. D. and Miller, L. A., "Wellman-Lord SO<sub>2</sub> Recovery Process," Proc. of the First Annual Air Pollution Conference, 53-59. Columbia: College of Engineering: Extension Division of the University of Missouri, 1968.
18. Tucker, L. M., "Sulfur Oxide Stack Emissions, Reactions, and Control." Paper presented at Meeting of American Petroleum Institute Division of Refining, Chicago, May 13, 1969.

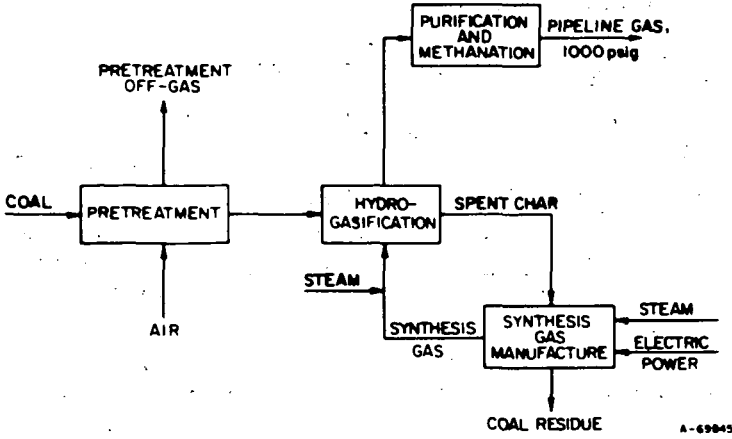


Figure 1. PIPELINE GAS BY HYDROGASIFICATION OF BITUMINOUS COAL

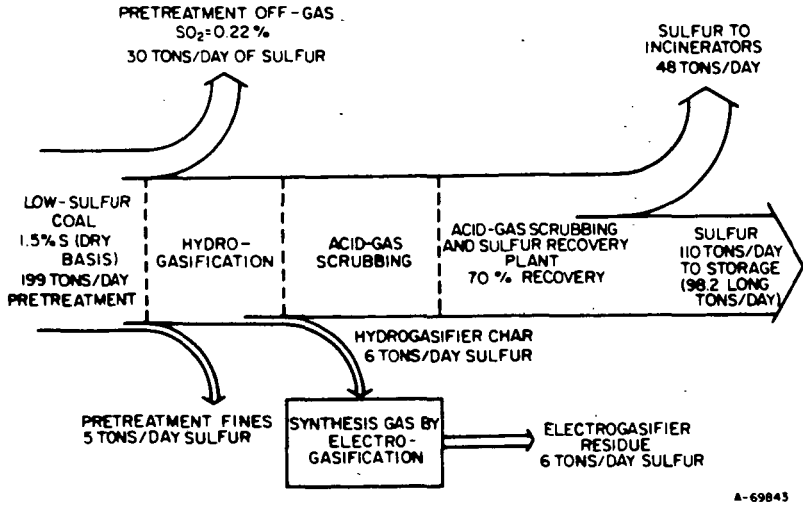
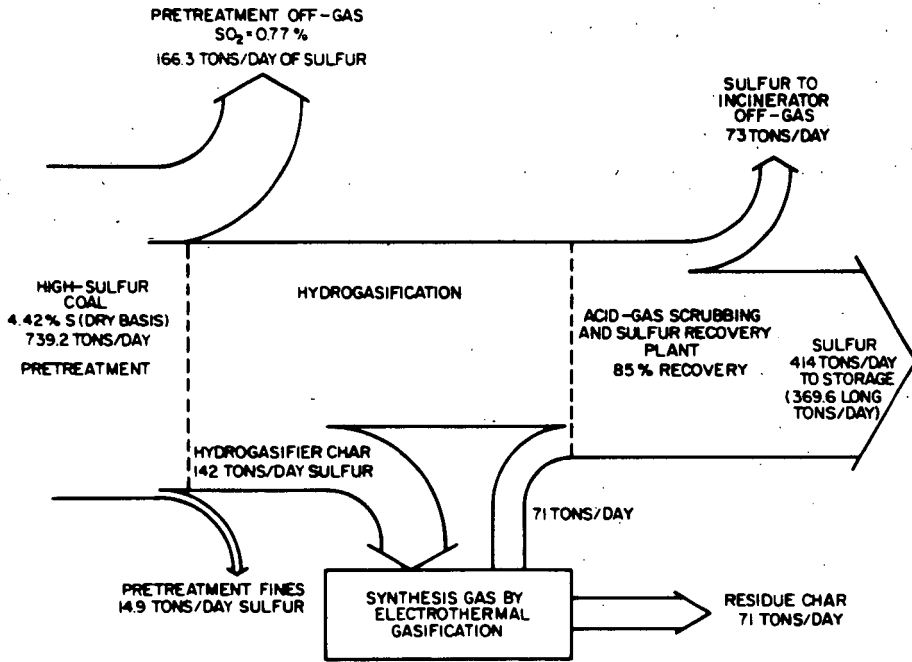


Figure 2. DISTRIBUTION OF SULFUR IN PIPELINE GAS PLANT FOR LOW-SULFUR COAL WITH NO SO<sub>2</sub> RECOVERY



A-69042

Figure 3. DISTRIBUTION OF SULFUR IN PIPELINE GAS PLANT FOR HIGH-SULFUR COAL WITH NO SO<sub>2</sub> RECOVERY

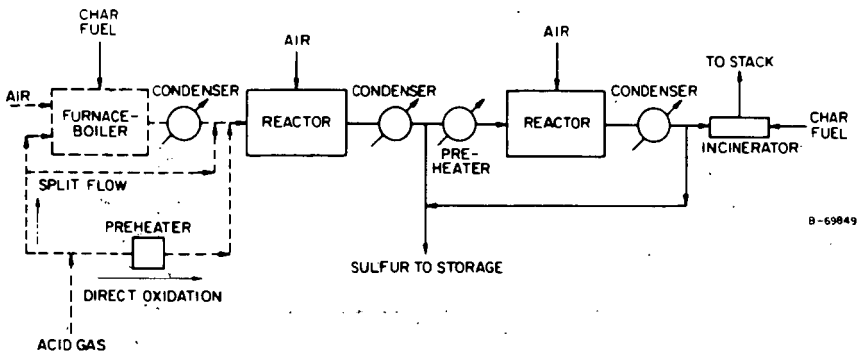


Figure 4. SULFUR RECOVERY SYSTEM

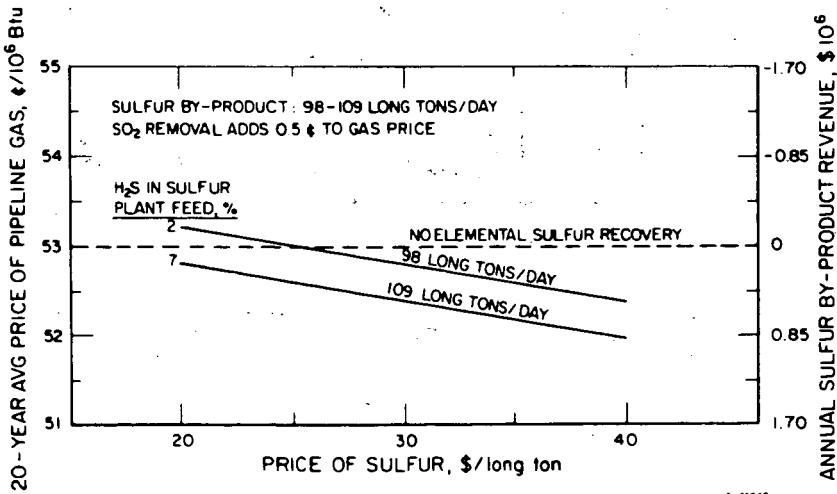


Figure 5. EFFECT OF SULFUR RECOVERY FROM H<sub>2</sub>S ON PRICE OF PIPELINE GAS FOR 1.5% SULFUR COAL

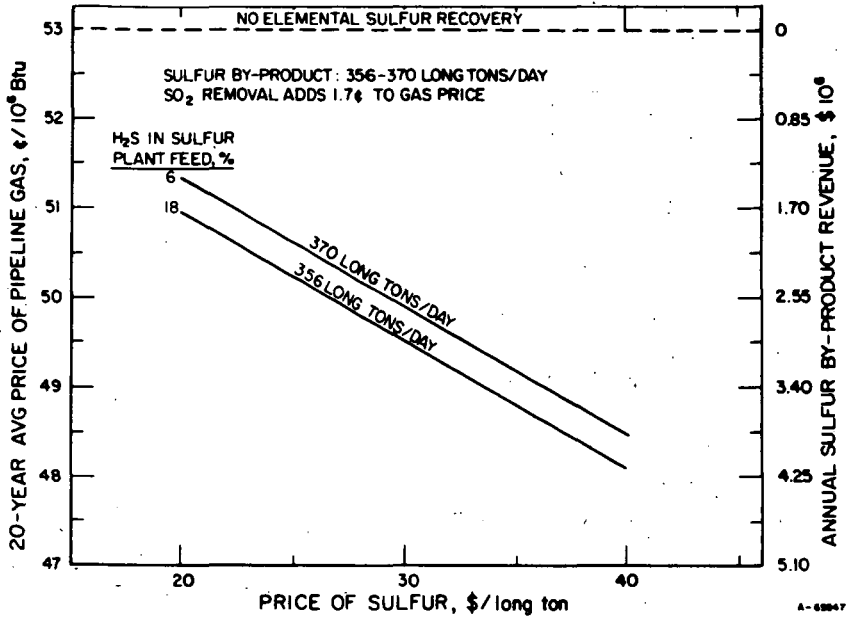


Figure 6. EFFECT OF SULFUR RECOVERY FROM H<sub>2</sub>S ON PRICE OF PIPELINE GAS FOR 4.4% SULFUR COAL

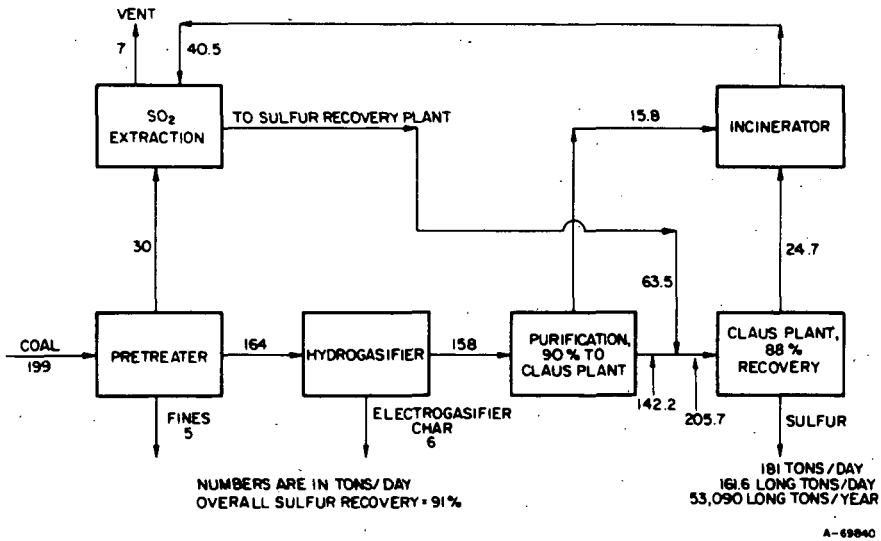


Figure 7. FLOW OF SULFUR IN PIPELINE GAS PLANT USING LOW-SULFUR COAL WITH SO<sub>2</sub> REMOVAL FROM PRETREATER AND INCINERATOR OFF-GAS

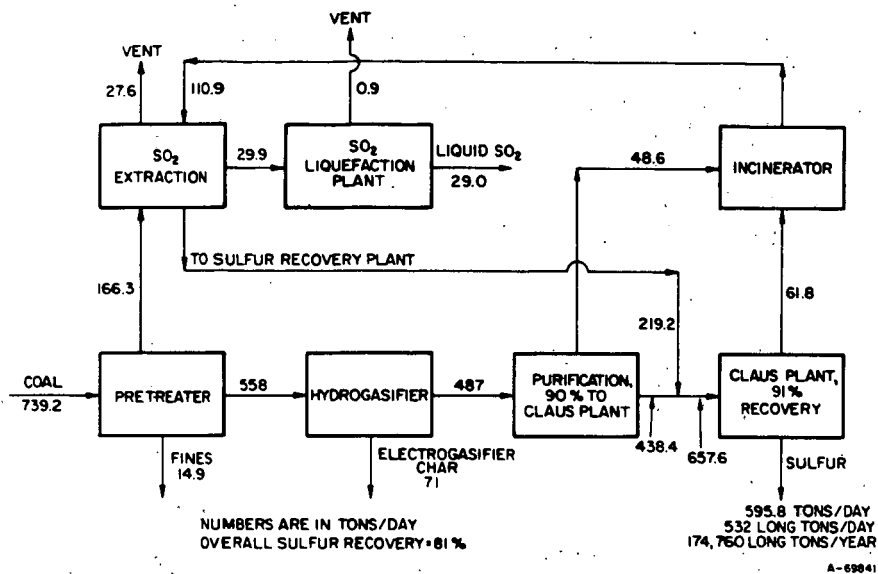


Figure 8. FLOW OF SULFUR IN PIPELINE GAS PLANT USING HIGH-SULFUR COAL WITH SO<sub>2</sub> RECOVERY FROM PRETREATER AND INCINERATOR OFF-GAS

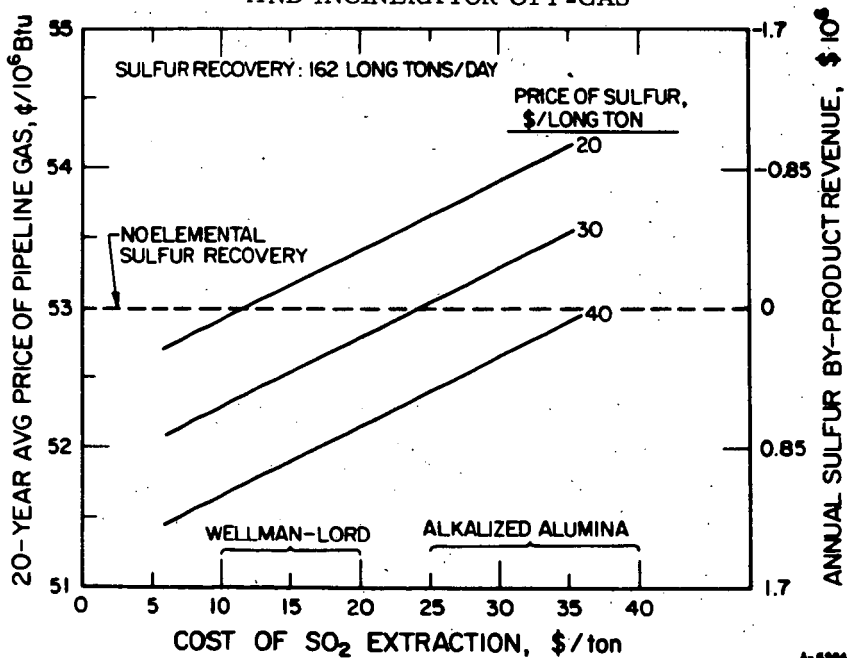


Figure 9. EFFECT OF COST OF SO<sub>2</sub> EXTRACTION AND SULFUR RECOVERY ON PRICE OF PIPELINE GAS USING 1.5% SULFUR COAL

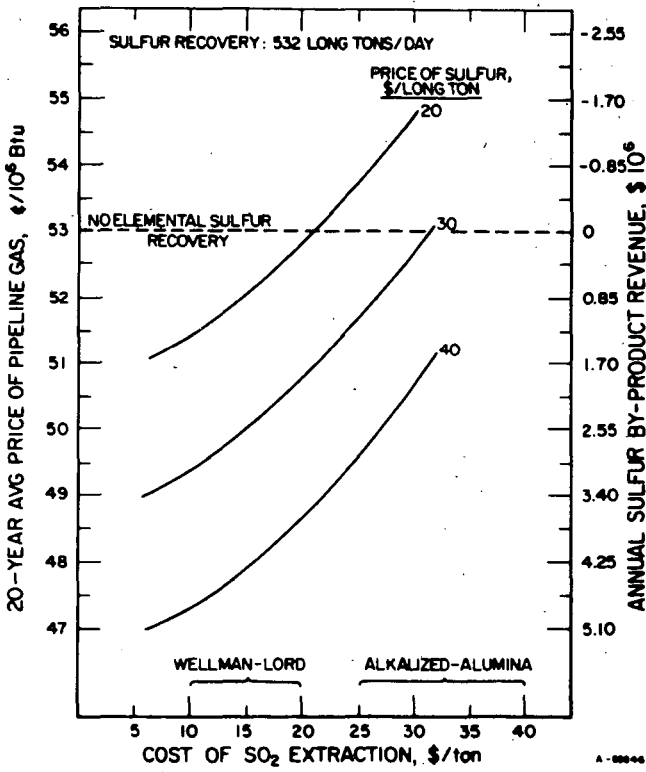


Figure 10. EFFECT OF COST OF SO<sub>2</sub> EXTRACTION AND SULFUR RECOVERY ON PRICE OF PIPELINE GAS USING 4.4% SULFUR COAL

## Hydrodesulfurization of Bituminous Coal Chars

C. A. Gray, M. E. Sacks, and R. T. Eddinger

FMC Corporation  
Chemical Research and Development Center  
P.O. Box 8  
Princeton, New Jersey

One of the products of many of the coal conversion processes now under development is a porous semi-coke or char. In the course of work under Project COED (Char Oil Energy Development), carried out by FMC Corporation under sponsorship of the Office of Coal Research of the U. S. Department of the Interior, a process has been developed for the desulfurization of such chars. The desulfurization of char proceeds in several chemical steps. These are:

1. Reaction of sulfur species with hydrogen to form  $H_2S$ .
2. Diffusion of the  $H_2S$  from the char into the bulk gas.
3. Absorption of the gaseous  $H_2S$  by an acceptor.
4. Regeneration of the acceptor with production of by-product sulfur.

This paper treats studies of the first two steps. A subsequent paper describes the acceptance of  $H_2S$  under process conditions and the regeneration of the  $H_2S$  acceptor.

Work by Consolidation Coal Company<sup>(1,5)</sup> established that high-temperature hydrogenation is effective in desulfurizing chars from Pittsburgh-seam coals. Equilibrium isotherms for the exchange of sulfur between gaseous hydrogen sulfide and sulfur in these chars were measured. These isotherms indicated that equilibrium concentrations of 0.5 percent hydrogen sulfide or less could be expected. However, kinetic data and data on the effect of process variables such as pressure, temperature and gas velocity were not available. Such data were needed to determine the technical and economic feasibility of incorporating char desulfurization into the COED concept. For these reasons, this experimental program was undertaken to:

1. Demonstrate the technical feasibility of desulfurizing COED chars by a high-temperature hydrogenation process.
2. Identify the important process variables associated with this process step.
3. Obtain kinetic data for this process.

#### Experimental Apparatus

The experimental system is shown in Figure 1. The reactor was a two-foot section of 3/4-inch, schedule 40, type 316, stainless steel pipe. A 22-inch long thermowell of 1/4-inch O.D. stainless steel tubing ran up the center of the reactor. A 14-mesh screen was welded to the thermowell about one foot from the bottom of the reactor to support the char bed.

The reactor was mounted vertically in a one-foot-long tubular electric furnace (Basic Products Corp., Model MK70). Power to the

furnace was controlled by an autotransformer. The temperature was monitored by a chromel-alumel thermocouple. Reactor pressure was measured with a gauge. Off gases were metered through a rotameter and a wet test meter in series, and vented to the atmosphere. Gas flow rate and reactor pressure were controlled with needle valves (1) and (4).

#### Run Procedure

A plug of ceramic wool was positioned on top of the support screen. Then a weighed sample char, from which the minus 200-mesh particles had been sieved, was charged on top of the wool plug. A second ceramic wool plug was placed on top of the bed to prevent any carryover of fines into the rest of the system.

The reactor was positioned in the furnace to locate the char bed in the center of the heated zone. The thermocouple was inserted into the thermowell to measure the temperature of the bed.

The furnace and reactor were brought up to reaction temperature with nitrogen being purged through the reactor. After the desired temperature had been reached, hydrogen was introduced into the system. This marked the start of the run. Gas flow rate and pressure were then adjusted to the desired levels. These adjustments took less than two minutes. For the two- and five-minute runs, the hydrogen rate was preset at room temperature, so that the desired conditions were attained at temperature. After the run, the reactor was dismantled, and the treated char weighed and analyzed for weight percent sulfur.

Char was originally analyzed using the standard Eschka method. Subsequently, analyses were made using an X-ray emission (XRS) method in order to expedite operations. Analyses of the off gas were attempted, but consistent results were not obtained.

Deviations between the two methods were random as to sign, and were within the combined precision of the two methods. The precision of the Eschka method is  $\pm 0.1$  percent sulfur; that of the XRS technique,  $\pm 0.05$  percent.

The experimental program was carried out using char from Crown (Illinois No. 6-seam) coal. The char had been processed in the COED process development unit at a maximum temperature of 1600°F(2). Tables I to III are compilations of the properties of this char before and after treatment with hydrogen at 1600°F. The sulfur content of the untreated char increased with decreasing char particle size, as did the ash content. This is presumably the result of a similar distribution of sulfur and ash in the crushed coal.

The distribution of sulfur between pyritic and organic forms is worthy of note. About seventy percent of the sulfur in this char was present as "organic" sulfur. This distribution is reasonably typical of coals of the Illinois No. 6-seam. The "pyritic" sulfur originally present in the coal has been converted, during pyrolysis, to ferrous sulfide, and/or pyrrhotite ( $\text{Fe}_7\text{S}_8$ ). The pyrite in the raw coal from which the char was derived was present as small particles from 3 to 25 microns in diameter. Microscopic examination showed that the bulk of the pyrite was present in fine veins of varying widths. The remainder was distributed, more or less at random, through the coal.

The desulfurization treatment had little effect on the properties of the char other than reducing the sulfur and moisture contents. Most differences in properties between treated and untreated chars are within the range of sampling error.

Because of the dependence of total sulfur content, and presumably also of inorganic/organic sulfur ratio on particle size, feed preparation and sampling were critical. Run feeds were prepared from large samples by multiple passes through a sample splitter. In general, only char from which the minus 200-mesh fraction had been removed was used. Within any group of feed samples from a parent batch, the standard error due to sampling was + 0.13 weight percent sulfur. From one master batch to another, far larger deviations were encountered.

## RESULTS

Initial work was directed along lines suggested by preceding investigations(1,5). The variables investigated were:

1. Temperature.
2. H<sub>2</sub>S concentration.
3. Char particle size.
4. Scale-up.

### Effect of Temperature

A graph of log percent sulfur removed from the char versus reciprocal temperature is shown in Figure 2. Runs were made at various temperatures at constant conditions of pressure, time and weight-space velocity (lb. H<sub>2</sub> per hr. per lb. char). These data clearly do not have the significance of a normal Arrhenius plot. They merely serve to point out that the rate of desulfurization is not particularly influenced by temperature at temperatures above 1600°F. At lower temperatures, the rate of desulfurization decreases.

### Effect of Hydrogen Sulfide

It has been reported(1) that H<sub>2</sub>S concentration is the most important variable in the desulfurization of char with hydrogen. Consequently, two hydrogen sulfide-hydrogen mixtures were prepared with H<sub>2</sub>S contents of 1.6 and 3.2 volume percent. The results from runs using these mixtures are shown in Table IV. Runs made with pure hydrogen are presented for comparison. It is evident that 1.4 percent H<sub>2</sub>S is sufficient to inhibit the reaction severely and that 3.2 percent H<sub>2</sub>S may be enough to reverse the reaction. Previous work showed that as little as 0.2 percent hydrogen sulfide can cause a 10 to 40 percent reduction in desulfurization rate.

### Effect of Particle Size

In the case of bulk diffusional mechanisms, reactant particle size is an important variable. To determine the effect of particle size, a sample of plus 28-mesh char (d > 0.0234 in.) was sieved from COED char. A part of this sample was then ground with a mortar and pestle to pass through 200 mesh (d < 0.0029 in.). Both samples were given identical desulfurization treatments.

The results from the runs with sized char are given in Table V. At all conditions, differences in residual sulfur between the plus 28- and the minus 200-mesh char are within experimental uncertainties. Thus, the desulfurization process appears to be independent of particle size. Runs made with the entire size distribution show less residual sulfur than equivalent runs with sized char. This may be due to the nature of the sulfur in the plus 28-mesh fraction used for the sized runs.

#### Effect of Scale-Up

Eighty percent desulfurizations was achieved in the 3/4-inch reactor system at 1600°F., 115 psia, weight-space velocity ( $S_w$ ) of 0.9, and 1-hour reaction times for 10-gm. char charges. A larger reactor of 2-inch schedule 80 stainless steel pipe was fabricated and replaced the 3/4-inch reactor in the desulfurization system shown in Figure 1.

The reactor was run with a charge of 100 grams of char at weight-space velocities of 0.29 to 0.65. Reaction times of 3 to 6 hours were required to achieve 70 to 80 percent desulfurization. Since the space velocity had been preserved in these runs, the long reaction times needed were surprising. Because this result suggested that the system was more complex than expected, an extensive experimental program was formulated.

The expanded program was formulated in terms of the variables of superficial velocity,  $U$ , volumetric space velocity,  $S_v$ , and pressure,  $P$ . The program was originally planned as a  $2^3$  factorial design with a midpoint. It turned out, however, that it was impossible to achieve two of the design conditions.

The experimental design is shown in Table VI. Runs were made for time periods of 2, 5, 15, 30, 45, and 90 minutes. A number of replicates were made.

The results of the expanded series of experiments are presented in Figure 3 as percent residual sulfur versus time. Some general conclusions that can be drawn from these figures are:

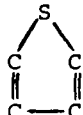
1. The most significant variable in terms of the shape and position of the curves is bed height (+ $U$ , - $S_v$  diagonal). Curves 1, 2, 4, 5 and 7 on Figure 3 ( $H = 0.158$  ft.) are similar but differ significantly from curves 3 and 6 ( $H = 0.632$  ft.).
2. Three regimes of desulfurization seem to exist:
  - a. An almost instantaneous or "flash" desulfurization to 40 to 60 percent residual sulfur in the shallow beds (Runs 1, 2, 4, 5 and 7) and 60 to 70 percent residual sulfur in the deep beds (Runs 3 and 6). This flash takes place in less than two minutes.
  - b. A slower but still appreciable desulfurization rate to 10 to 15 percent residual sulfur. In the shallow beds this took about 45 minutes, while in the deep beds sulfur was still being evolved after 90 minutes.
  - c. Negligible desulfurization after a residual sulfur content of 10 to 15 percent is reached.

The data do not lend themselves readily to simple quantitative treatment. Indeed, in a complex, heterogeneous material such as coal char, it would be naive to expect otherwise. As is noted above, there appear to be several distinctly different regions of the curves.

## DISCUSSION OF RESULTS

### General

Much of the prior work on the desulfurization of cokes and coal chars has led to the conclusion that the reaction of hydrogen with sulfur in the char to form  $H_2S$  is a reversible process at high temperatures. In coals and presumably in coal chars as well, there are a wide variety of sulfur-containing species. These include the following types of chemical structures:

Inorganic Sulfur	$FeS, FeS_2$
Thiophenic Sulfur	
Mercaptans	$H-S-C$
Thioethers	$C-S-C$
Disulfides	$C-S-S-C$

Presumably some sulfur species are also adsorbed on the char surface. Because a variety of forms of sulfur are involved, no simple equilibrium expression can be used.

At a given total pressure, the equilibrium between  $H_2S$  and sulfur in char can be expressed as an "inhibition isotherm". This is a plot of the  $H_2S$  to hydrogen ratio in the gas versus sulfur concentration in the char. A typical isotherm for sulfur in a char from Arkwright coal (Pittsburgh-seam) is shown in Figure 4A.

Figure 4B is an inhibition isotherm for the desulfurization of COED char from Crown coal. This isotherm has been synthesized from the two measurements on inhibition of the reaction by  $H_2S$  (Table IV), and from an estimate of the  $FeS$  content based on the pyritic sulfur content of the feed coal. Region I corresponds to about 60 percent of the total sulfur in the form of relatively easily removable organic sulfur with equilibrium gas-phase concentrations in excess of 0.3 percent hydrogen sulfide. Region II corresponds to about 30 percent of the total sulfur in the form of inorganic sulfides ( $FeS$ ) with an equilibrium concentration of 0.3 percent hydrogen sulfide. Region III corresponds to about 10 percent of the total sulfur, in the form of organic sulfur, sulfate sulfur, and stable inorganic sulfides ( $CaS$ ), with equilibrium concentrations less than 0.3 percent hydrogen sulfide. The isotherm is probably not linear in this region since little of this sulfur is removed by prolonged hydrogenation.

The inhibition isotherm in Region I was assumed to be a straight line because only two experimental points were available. The shape of Figure 4A shows that this is a reasonable approximation. The equilibrium concentrations of hydrogen sulfide over COED char in

this region are significantly lower than those reported for char from Pittsburgh-seam coal (Figure 4A).

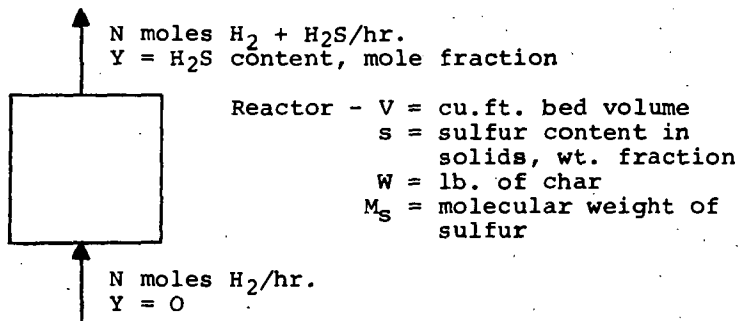
An equilibrium hydrogen-sulfide concentration of 0.3 percent was assumed in Region II. This figure was reported as the equilibrium concentration over FeS for Pittsburgh-seam char (Figure 4A) (1). The length of the FeS plateau (Region II) is fixed by the pyritic sulfur content of the char.

#### Equilibrium Desulfurization

Given the existence of a reversible desulfurization reaction, the simplest model of the desulfurization process in a well-mixed bed is one assuming that the off gases are always in equilibrium with the sulfur in the bed of solids (3). The rate of desulfurization can be computed from the weight-space velocity of hydrogen through the bed and from the inhibition isotherm.

For the system defined below, where the flow rate of gases leaving the bed is  $N$  moles/hr. containing  $Y$  mole fraction  $H_2S$ , the rate of sulfur removal is  $NY$ .

Figure 5



Neglecting the sulfur content of the gases in the reactor at any instant,

$$-N \cdot Y = \frac{d}{dt} \left( \frac{s \cdot W}{M_s} \right) \quad (1)$$

for any arbitrary equilibrium expression relating  $s$  and  $Y$ ,

$$Y = f(s)$$

this expression may be integrated

$$t = \frac{W}{N \cdot M_s} \int_s^{s_0} \frac{ds}{f(s)}, \quad \text{where } t = \text{time of desulfurization, hr.} \quad (2)$$

The weight space velocity,  $S_w$ ,  $\frac{N \cdot M_{H_2}}{W}$ , so that Equation (2) simplifies to

$$t = \frac{1}{16 S_w} \int_s^{s_0} \frac{ds}{f(s)} \quad (3)$$

The following equilibrium relationship describes the inhibition isotherm in Figure 4B.

$$0 < s \leq 0.0035, \quad Y = 0.865 s \quad (4)$$

$$0.0035 < s \leq 0.0130, \quad Y = 0.0030 \quad (5)$$

$$0.0130 < s, \quad Y = 1.153 - 0.0118 s \quad (6)$$

The equilibrium desulfurization curves calculated from Equations (4), (5), and (6) for six of the conditions studied are plotted in Figure 6. Weight-space velocity is the only parameter here, so that two curves suffice for all six sets of data. The solid lines in Figure 6 are the predictions of the equilibrium model. The dashed lines indicate the approximate course of the data. This comparison shows quite clearly that the equilibrium model is only valid for the removal of the first forty to fifty percent of the sulfur in shallow beds. This would correspond to the first step or flash removal of sulfur mentioned previously.

#### Non-Equilibrium Desulfurization

Quite clearly, the equilibrium desulfurization model begins to break down when fifty to sixty percent of the sulfur has been removed from the char. Interestingly, this corresponds to the point at which most of the organic sulfur has been removed, and only ferrous sulfide and the "irremovable" sulfur remain in the char.

The reaction of the ferrous sulfide could possibly be limited by a number of diffusional steps as well as by the kinetics of the reaction itself. It will be recalled, however, that char particle size had little or no effect on the desulfurization rate. From this it is concluded that boundary layer diffusion, and bulk diffusion within the char structure are not important limiting steps. The very weak temperature dependence similarly suggests that chemical effects are not limiting.

While diffusion through the char is not limiting, it is certainly possible that diffusion through the shell of iron, which would surround a pyrite particle being desulfurized, might be a significant step in limiting the rate of reaction.

The following discussion is presented with the objective of showing that this explanation is qualitatively in accord with the observed desulfurization data. Quantitative verification of the model would require detailed knowledge of the distribution, shape, and size of the ferrous sulfide within the char. Such information is not available. Indeed, the information available concerning the pyrite in the coal is very preliminary and quite crude.

for the purposes of the initial analysis, the ferrous sulfide particles are assumed to be approximately spherical. Considering the very low partial pressure of  $H_2S$  over  $FeS$  under process conditions, a pseudo steady-state treatment should be quite adequate. The physical situation is illustrated in Figure 7. The governing differential equation is:

$$N_s = - \frac{4\pi r^2 \epsilon \mathcal{D}}{\tau^2} \left( \frac{dC}{dr} \right) \quad (7)$$

Where  $N_s$  is the rate of sulfur removal from the particle and  $C$  is the concentration of  $H_2S$  in the gas,  $\epsilon$  is the porosity,  $\mathcal{D}$  the diffusivity of  $H_2S$ , and  $\tau$  is the tortuosity in the diffusion barrier. In the case in question,  $C = 0$  at  $R_0$ , the outer surface of the particle, and

$$N_s \approx 4\pi R^2 \frac{dR}{dt} \left( \frac{\rho_{FeS}}{M_{FeS}} \right) \quad (8)$$

where  $\rho_{FeS}$  and  $M_{FeS}$  are the density and molecular weight of ferrous sulfide.

The pseudo steady-state allows us to treat the inner boundary as stationary, in integrating Equation (7). The integrated form can then be integrated in the time domain. The result is:

$$\frac{6MC^2 \mathcal{D} \epsilon}{\rho R_0^2} t = 1 - \left( \frac{R}{R_0} \right)^2 \left[ 3 - 2 \left( \frac{R}{R_0} \right) \right] \quad (9)$$

This solution is shown in Figure 8.

The stoichiometric variable of interest is the fraction unreacted. This fraction  $\frac{V}{V_0}$  is shown as a function of time in Figure 8 on arithmetic coordinates.  $V_0$

Figure 9 is a synthetic desulfurization experiment in which the first 55 percent of the sulfur is removed by the equilibrium mechanism, and the last 10 percent is "irremovable". The data for experimental condition 5 were superimposed by trial and error on the same ordinate. From the comparison of these points with the curve, it is apparent that the above explanation is consistent with the observed curve shape, particularly when one realizes that there will be a distribution of particle sizes in the char. It remains, now to determine whether the group  $(6 \epsilon t / R_0^2 \tau^2)$  is of reasonable magnitude.

In the real case, the time required to achieve 20 percent of the initial sulfur was 18 minutes, or 1080 sec. The porosity,  $\epsilon$ , should be about 0.6, and the tortuosity  $\tau$  is probably about 2. Taking  $R^0$  as 0.001 cm, one calculates a  $\mathcal{D}$  of  $\sim 10^{-3} \frac{cm^2}{sec}$ . This figure is reasonable if the diffusion through the reacted shell is in the Knudsen or transition regime.

The agreement may, however, be purely fortuitous. Further verification of the rate limiting step proposed here must await a test of the theory on a different high sulfur char, preferably one which has been processed through a COED unit.

### Conclusions

The equilibrium nature of the removal of the first 50 to 60 percent of the sulfur seems reasonably well established. There are fairly wide deviations which are probably a combination of internal diffusional effects and experimental technique. The procedure was designed for runs of 15 minutes or longer. Random errors would be expected to be high for the 2-minute and 5-minute runs. The inhibition isotherm for this char is only poorly established, but it is evident that this explanation is in general agreement with the data. The fact that this explanation fails at about 50 percent sulfur removal is also well established.

In the region of 50 to 90 percent sulfur removal, it is evident that elevated hydrogen pressure increases the rate of sulfur removal. This, however, is consistent with most possible rate-controlling steps. Bed depth is the only other variable that has a strong effect. In fact, bed depth is by far the most significant variable. Had the experiments been conducted in fixed beds, this would not have been so surprising. The experiments were carried out under conditions where the beds were fluidized, however. It appears, therefore, that there must have been a significant degree of reabsorption of sulfur within the four-inch bed to account for the observed results. This also raises the question as to whether the one-inch bed was truly a differential bed. If not, the observed rates may be slower than those achievable in the presence of an acceptor intimately mixed with the char. The results of experiments in the presence of  $H_2S$  acceptors suggest that this is so.

From the experimental results, it is apparent that a significant fraction of the sulfur content of Illinois No. 6 char, produced by the COED process, can be removed in contact times which are industrially realizable. It is equally evident that the hydrogen atmosphere becomes saturated with the addition of very little hydrogen sulfide. Hence, either vast amounts of hydrogen must be circulated at high temperature, or a material must be mixed with the char which will absorb  $H_2S$  at  $1600^\circ F.$  and at very low partial pressures. This latter approach seems by far the more feasible.

Nomenclature

C	Concentration (moles/cm <sup>3</sup> )
C <sup>o</sup>	Equilibrium Concentration
$\mathcal{D}$	Diffusion Coefficient (cm <sup>2</sup> /sec)
f <sub>(s)</sub>	Inhibition isotherm (mole fraction)
M	Molecular weight - species indicated by subscript
N	Rate of flow (moles/sec)
N <sub>s</sub>	Rate of sulfur removal (moles/sec)
P	Pressure (psi)
r	radial distance (cm or microns)
R	Radial distance to reaction interface
R <sup>o</sup>	Radius of particle
s	sulfur content (wt. fraction)
S <sub>v</sub>	Volumetric space velocity (ft <sup>3</sup> /sec per ft <sup>3</sup> of bed)
S <sub>w</sub>	Weight space velocity (lb./hr. per lb. of char)
t	time (hr or sec)
U	Superficial velocity (ft per sec)
W	Bed weight (bm)
Y	Mole fraction H <sub>2</sub> S in the gas phase
ε	porosity
ρ	density
τ	tortuosity

References

- (1) Batchelor, J. D., E. Gorin, and C. W. Zielke, Ind. Eng. Chem., 52, 2, 161-168 (1960).
- (2) Jones, J. F., M. R. Schmid, M. E. Sacks, Y. Chen, C. A. Gray, and R. T. Eddinger, Char Oil Energy Development, Jan.-Oct. 1966.
- (3) Lenenspiel, O., Chemical Reaction Engineering, John Wiley & Sons, New York, 1962.
- (4) Schmid, M. R., J. F. Jones, and R. T. Eddinger, Chemical Engineering Progress, 64, 85, 26-30 (1968).
- (5) Zielke, C. W., G. P. Curran, E. Gorin, and G. E. Goring, Ind. Eng. Chem., 46, 1, 53-56 (1954).

TABLE I

ANALYSIS OF CROWN CHAR		
	BEFORE TREATMENT	AFTER TREATMENT
<b>PROXIMATE, wt. %</b>		
MOISTURE	4.4	2.5
VM	<u>3.6</u>	<u>5.9</u>
FC	75.4	76.0
ASH	16.6	15.6
<b>ULTIMATE, wt. %, dry</b>		
C	76.8	
H	1.4	
N	1.2	
S	<u>3.1</u>	<u>1.5</u>
O	0.1	
ASH	17.4	

TABLE II

ANALYSIS OF CROWN CHAR FEED		
SIEVE SIZE, TYLER MESH	WT. % ON SIEVE	WT. % S IN FRACTION
28	39	2.57
48	34	2.59
100	20	3.14
200	6	3.80
PAN	1	—

**SULFUR SPECIES**

ORGANIC	68 %
INORGANIC (PYRITIC)	29 %
SULFATE	3 %

TABLE III

**PHYSICAL PROPERTIES OF  
CROWN CHAR**

	BEFORE TREATMENT	AFTER TREATMENT
BULK DENSITY, lb/cu ft	20.7	20.7
PARTICLE DENSITY, gm/cc	1.08	1.01
PORE VOLUME, cc/gm	0.32	0.35
SURFACE AREA, M <sup>2</sup> /gm	123	114
MEAN MACRO- PORE DIAM., $\mu$	5	4.5

TABLE IV

**EFFECT OF H<sub>2</sub>S ON DESULFURIZATION  
AT 1600°F AND 115 PSIA**

INLET H <sub>2</sub> S, VOL %	REACTION TIME, HR.	PERCENT S REMAINING
0	1	12
0	2	22
1.6	2	72
3.2	1	118
3.2	2	105

TABLE V

EFFECT OF PARTICLE SIZE ON DESULFURIZATION AT 1600 °F, 15PSIA			
SIZE FRACT.	TIME, MIN.	SUPERFICIAL VELOCITY, ft./sec.	RESIDUAL SULFUR, % OF ORIG.
+ 28 - 200	5 5	0.53 0.51	68 66
+ 28 - 200	15 15	0.52 0.56	43 46
+ 28 - 200	10 10	0.22 0.19	65 72

TABLE VI

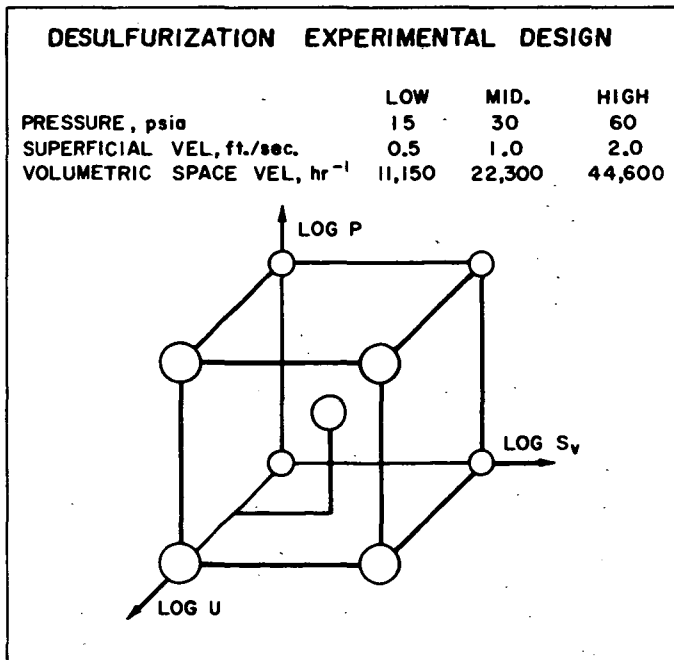


FIGURE 1

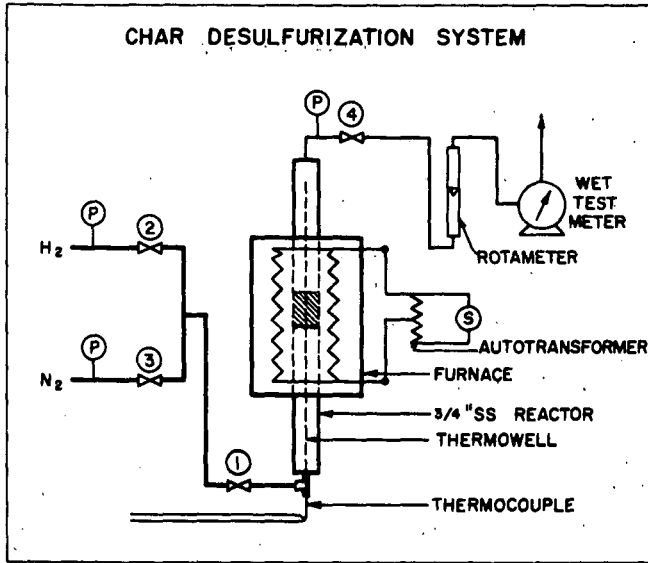
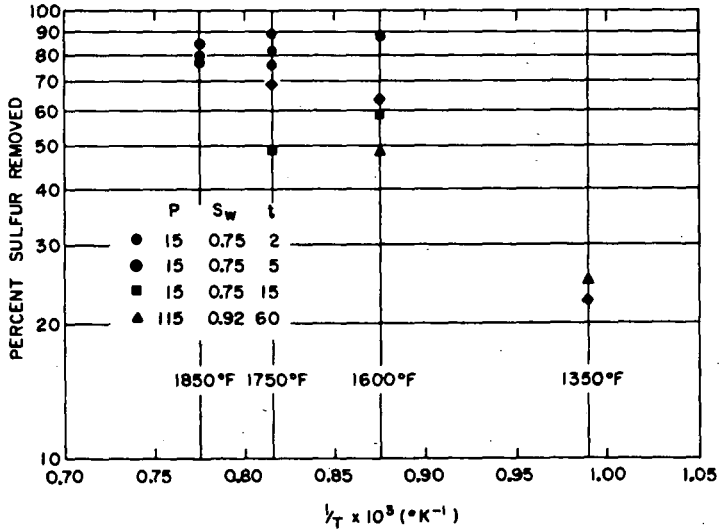


FIGURE 2

EFFECT OF TEMPERATURE ON  
DESULFURIZATION



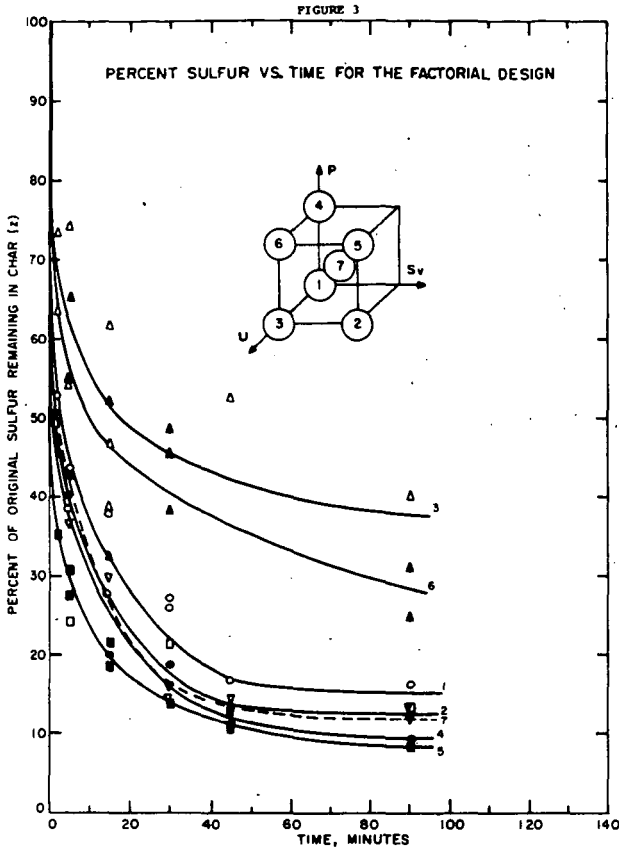


FIGURE 4  
INHIBITION ISOTHERMS FOR CHAR DESULFURIZATION

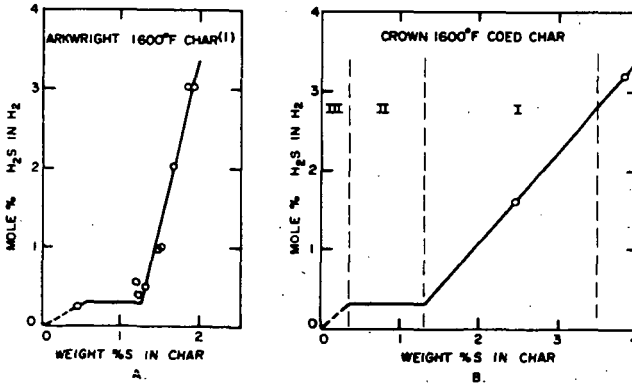


FIGURE 6

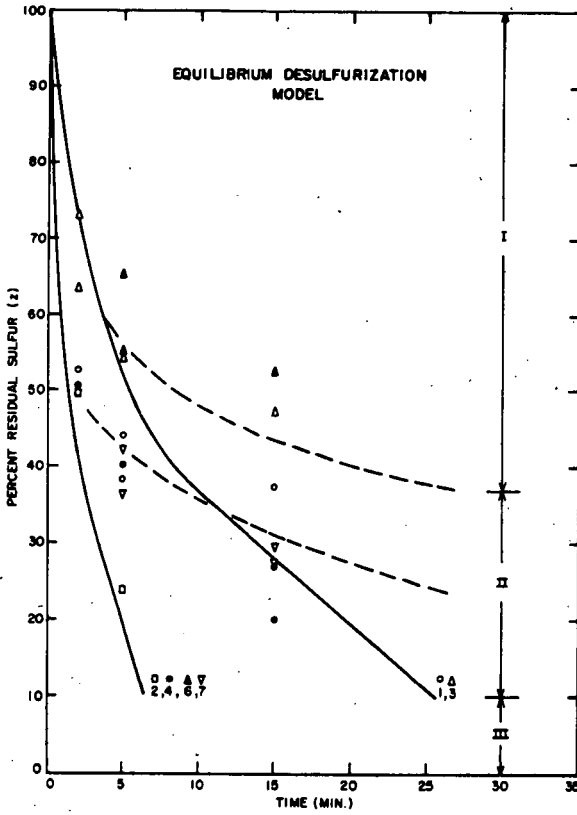
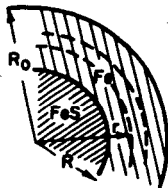


FIGURE 7

PSEUDO STEADY-STATE DIFFUSION



$$-\frac{4\pi r^2 \epsilon \rho}{\tau^2} \left( \frac{dC}{dr} \right) = N_s$$

At  $r = R,$

$$N_s = 4\pi R^2 \frac{dR}{d\theta} \left( \frac{\rho_{FeS}}{M_{FeS}} \right)$$

FIGURE 8

DIFFUSION THROUGH A REACTED SHELL

$$\left(\frac{6MC_0D_0}{\rho R_0^2 T^2}\right)t = 1 - \left(\frac{R}{R_0}\right)^2 \left[3 - 2\left(\frac{R}{R_0}\right)\right]$$

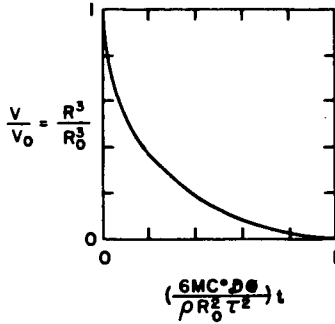
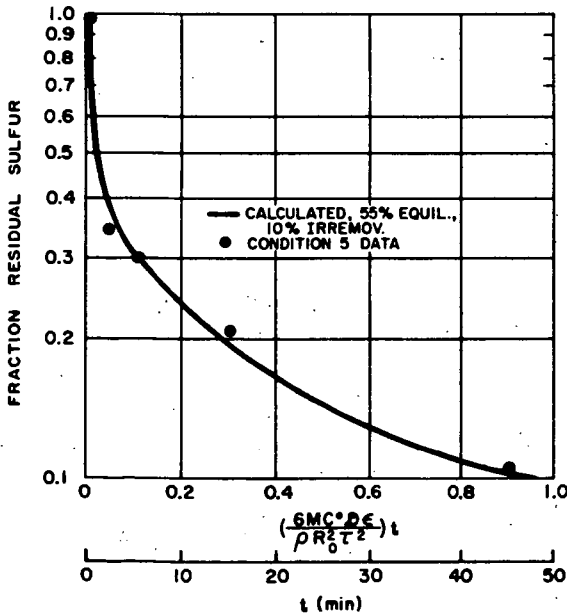


FIGURE 9

COMPARISON OF REAL AND HYPOTHETICAL  
DESULFURIZATION CURVES



## COED Char Desulfurization Process Studies

M. E. Sacks, C. A. Gray, R. T. Eddinger

FMC Corporation  
 Chemical Research and Development Center  
 P. O. Box 8  
 Princeton, New Jersey

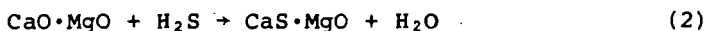
Project COED (Char-Oil-Energy-Development) sponsored by the Office of Coal Research, Department of the Interior, seeks to upgrade the value of coal by conversion to synthetic crude oil, gas, and fuel char. The original scope of Project COED was enlarged to include the production of low-sulfur fuel char to reduce air pollution. Preliminary experimental work (1) showed that the sulfur in COED char can be removed by treatment with hydrogen at 1600° and 1 atmosphere pressure. The rate of desulfurization was severely inhibited by low concentrations of hydrogen sulfide in the reactant gas. It was concluded that a hydrogen sulfide absorbent or acceptor, admixed with char, would be required to make a commercial process viable.

A block diagram of the proposed COED char desulfurization process is shown in Figure 1. Hydrogen and char from the COED pyrolysis plant plus acceptor would be fed to a desulfurization reactor. Here sulfur would be transferred from the char to the acceptor via a hydrogen sulfide intermediate. Desulfurized char and spent or sulfided acceptor would then be separated. Spent acceptor would be regenerated to yield active acceptor for recycle and by-product sulfur. This paper will summarize the results of the experimental program to specify the chemistry and mechanics of each of these steps. A preliminary process flowsheet, and the economics of the process derived from it, will also be presented.

Desulfurization

Desulfurization of COED char in the presence of hydrogen and an acceptor was investigated in a bench-scale rotary kiln. A sketch of this apparatus is shown in Figure 2. The 2-inch diameter kiln was mounted inside a resistance furnace and driven at 6 rpm by an electric motor, speed reducer, and pulley system.

USP calcium oxide and four different calcined dolomites were evaluated as hydrogen sulfide acceptors. Best results were obtained with a calcined dolomite. In 10 minutes, 85 percent sulfur removals were achieved with a hydrogen partial pressure of 15 psi. The sulfur content char from Illinois No. 6-seam coal was reduced from 3 to less than 0.6 weight percent. Only stoichiometric amounts of hydrogen and acceptor were required for the desulfurization reactions:



The rate of desulfurization was found to be independent of acceptor particle size in the range of sizes from minus 325-mesh to 6-mesh.

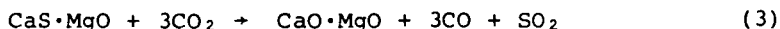
### Separation

After desulfurization, spent acceptor must be separated from desulfurized char. The difference in size consist and density between the acceptor and the char suggested that a fluidized bed could be used to separate them. The specific gravity of the acceptor is about 2, compared to about 1 for char. The proposed size consist for the acceptor is 6- x 10-mesh (Tyler) while COED char is all minus 16-mesh.

A 3-inch diameter glass column, equipped with a perforated grid plate and drain legs 1/2 inch and 6 inches above the grid plate, was used to determine the feasibility of separating char and acceptor in a fluidized bed. A sketch of this apparatus is shown in Figure 3. Results of these studies are shown in Figure 4. At a fluidizing velocity of about 2.5 ft./sec., acceptor sank to the bottom of the bed and char was fluidized above it. The acceptor stream, drawn off through the drain leg 1/2 inch above the grid plate, contained about 2 percent char. No acceptor was found in the char product drained from the drain leg 6 inches above the grid plate. Thus, it appears feasible to separate desulfurized char and spent acceptor in a fluidized bed.

### Regeneration

Several routes for the regeneration of spent dolomitic acceptor were investigated including carbonation with steam and carbon dioxide (2) and roasting in air or oxygen. The preferred regeneration scheme, however, was found to be the partial oxidation of spent acceptor with CO<sub>2</sub>.



A sketch of the apparatus used to explore acceptor regeneration is shown in Figure 5. A Globar-heated furnace was used to obtain temperatures above 2000°F. The reactor consisted of a sealed 3/4-inch I.D. alumina tube. A fixed bed of spent acceptor was formed between two ceramic wool plugs in the center of the bed. Inlet gases were metered through a rotameter. Off-gases were sampled and vented.

The regeneration of spent acceptor with carbon dioxide is catalyzed by iron (3). Acceptor particles were impregnated from solutions of ferric nitrate in methanol resulting in a seven-fold increase in regeneration rate as shown in Figure 6. This rate acceleration was accomplished by increasing the iron content of the dolomitic acceptor from 0.25 weight percent, the naturally occurring iron content, to 0.5 weight percent. Further increases in iron concentration did not increase rates. A microscopic examination of the impregnated acceptor particles showed that iron was concentrated in spots on the surface.

The effect of temperature on the rate of regeneration of iron-impregnated acceptor is shown in Figure 7. Below 2000°F., the rate is highly dependent on temperature with an apparent activation energy of about 103 kcal. Above 2000°F., the apparent activation energy is approximately an order of magnitude lower and appears to be a function of the space velocity. The behavior is indicative of a change in reaction mechanism at a temperature around 2000°F.

The rate of regeneration is zero order with respect to the CaS·MgO concentration of the acceptor. This is shown in Figure 9. Therefore, the rate-controlling step is not the rate of the reaction between solid CaS·MgO and gaseous carbon dioxide.

The rate of regeneration was also found to be independent of gas velocity and acceptor particle size. Therefore, diffusion of carbon dioxide from the gas to the surface of the acceptor particle is not the rate-controlling step.

The addition of carbon monoxide and inerts (nitrogen) to the carbon dioxide feed severely inhibited the regeneration rate. Runs were made at two conditions: 2200°F. and a space velocity of about 12, and 2000°F. and a space velocity of about 2. Results are summarized in Table I. At 2200°F., 10 percent carbon monoxide in the feed gas decreased the rate about 5 times, while 77.4 percent nitrogen decreased the rate about 3 times. At 2000°F., both 10 percent carbon dioxide and 77.4 percent nitrogen decreased the rate about 3.5 times. Thus, a regeneration process must be designed to keep both CO and inert concentrations in the carbon-dioxide reactant gas low.

The effect of space velocity on regeneration rate is shown in Figure 9. At space velocities below 3, the observed relationship between the space velocity and rate appears to be non-linear; at space velocities above 3, a linear relationship appears to hold. The fixed-bed reactor used in these experimental studies can be approximated by a plug-flow reactor at low space velocities and the differential reactor at high space velocities. This probably accounts for the change in shape of the curve (4). On the basis of these results it was concluded that the rate-controlling mechanism is either equilibrium or some surface phenomenon. The kinetic data were too scattered to distinguish between these types of mechanisms.

At a space velocity of 2, about 2 hours are required to achieve 60 percent regeneration.

The deactivation of dolomitic acceptor after repeated cycles of sulfurization and regeneration was studied by exposing the acceptor to alternate atmospheres of hydrogen sulfide and carbon dioxide. The deactivation was studied under two conditions: 1) sulfurization at 1600°F.--regeneration at 2100°F. and 2) sulfurization at 1600°F.--regeneration at 2200°F. The results are displayed as graphs of activity versus cycle number in Figure 10. Activity is defined as the moles of hydrogen sulfide absorbed per 100 atoms of calcium in the acceptor.

At a regeneration temperature of 2200°F., the dolomite was rapidly deactivated. After five cycles the activity was reduced to about 10. At a regeneration temperature of 2100°F., however, the dolomite maintained an average activity of 59 through 10 cycles. There was no clear trend toward loss of activity with increased cycling. It was concluded that dolomitic acceptor would remain about 60 percent active through at least 10 cycles if regeneration temperatures below 2100°F. were employed.

### Commercial Process

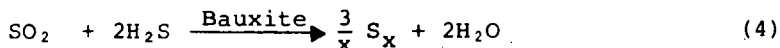
Based on these bench-scale results, a preliminary flowsheet for a commercial plant was made. The flowsheet is shown in Figure 11, and consists of four major sections: desulfurization in the presence of acceptor, separation of the desulfurized char from the spent acceptor, regeneration of the spent acceptor, and sulfur recovery.

In the desulfurization step, hot char at 1600°F. and hydrogen from the pyrolysis section of the COED plant, react with regenerated acceptor in a rotary kiln. The rotary kiln was chosen because of its ability to mix two dissimilar solids, char and dolomitic acceptor, and to operate with a relatively low gas flow and low pressure drop. Off-gases from the desulfurization reactor are returned to the gas purification section of the COED plant. The solid mixture of desulfurized char and spent acceptor is transported by gravity to the separator.

A fluidized bed was selected as the separation vessel. At a fluidizing velocity of about 2.5 ft./sec., the 6- x 10-mesh sulfided acceptor (specific gravity about 2) sinks to the bottom of the bed while the minus 16-mesh desulfurized char (specific gravity about 1) is fluidized above it. Essentially acceptor-free char is withdrawn from an overflow line at the top of the bed, cooled and sold as a low-sulfur boiler fuel. Sulfided acceptor, containing about 1 percent char, is withdrawn from the bottom of the bed and transported by a bucket elevator to the regeneration reactor. The separation vessel is fluidized by a recycle CO<sub>2</sub> stream. Off-gas from the separator, containing entrained char, is heated to 2600°F. in a wet wall furnace and serves as the fluidizing stream to the regeneration reactor.

The regeneration of spent acceptor is accomplished in a fluidized-bed reactor at 2000°F. Make-up dolomite is also added to the regenerator. Both regeneration and calcination occur in this reactor. Regenerated dolomite is recycled to the desulfurizer. Off-gas from the regenerator, containing CO<sub>2</sub>, CO and SO<sub>2</sub>, goes to the sulfur recovery section.

In the sulfur recovery section, SO<sub>2</sub>-containing off-gases from the regenerator are contacted with hydrogen-sulfide containing gases from the gas purification section of the COED plant. Elemental sulfur is recovered by the standard Claus process:



### Economics

Both capital and annual operating cost estimates for the COED char desulfurization process have been prepared. The estimates are based on adding a desulfurization section to a commercial COED plant processing 3.5 MM tons per year of Illinois No. 6-seam coal (1). 1.82 MM tons per year of 3-percent-sulfur char are processed yielding 1.75 MM tons of 0.6-percent-sulfur char and 91,300 long tons of sulfur.

Capital and annual operating costs are shown in Table II. Capital costs, including indirects, were estimated (5) at \$7.17 MM. Annual operating costs, including 13 percent capital charges, were estimated at \$2.6 MM. The annual return on investment, plant-level and before taxes, is highly dependent on the price of by-product sulfur. Assuming desulfurized char can be marketed at 100 percent of the value of coal on a Btu basis, the effect of sulfur price on return is shown in Figure 12. At the present price of sulfur (6), \$40 per long ton, the annual return on investment, plant-level and before taxes, is 23 percent. At a sulfur price of \$30 per long ton, however, the return is only about 10 percent. These estimates compare very favorably with both residual oil desulfurization (7) and stack gas clean-up schemes (8).

#### Acknowledgment

The authors thank the Office of Coal Research, Department of the Interior, and the FMC Corporation for permission to publish this paper.

#### Literature Cited

1. Jones, J. F., Schmid, M. R., Sacks, M. E., Chen, Y. C., Gray, C. A. and Eddinger, R. T., "Char Oil Energy Development, Final Report (January-October 1966)", Contract No. 14-01-0001-235, Office of Coal Research, Department of the Interior, 1966.
2. Squires, A. M., "A Reaction Which Permits the Cyclic Use of Calcined Dolomite to Desulfurize Fuels Undergoing Gasification", ACS National Meeting, Division of Fuel Chemistry, New York, 1966.
3. Riesenfeld, E. H. and Hesse, M., "Preparation of Sulfur and Sulfuric Acid from Sulfates of Alkaline Earths V.", J. Prakt. Chem., 100, 115-58 (1920).
4. Levenspiel, O., Chemical Reaction Engineering, John Wiley & Sons, New York, 1962.
5. Lang, H. J., "Simplified Approach to Preliminary Cost Estimation", Chem. Eng., June, 1948.
6. Oil, Paint and Drug Reporter, February 3, 1969.
7. Cortelyou, C. G., Mallott, R. C. and Meredith, H. H., "A New Look at Desulfurization", Chem. Eng. Prog., 64, 1, 53-59 (January 1968).
8. Eng. and Mining J., 169, 6, 91-100 (1968).

TABLE IEffect of Carbon Monoxide and Inerts on Regeneration Rate

<u>Run No.</u>	<u>Feed Gas Composition, %</u>	<u>Temperature, °F.</u>	<u>Space Velocity, lb. CO<sub>2</sub>/hr./lb. acceptor</u>	<u>Average Rate, lb. S/hr./lb. acceptor</u>
R-161	100 CO <sub>2</sub>	2200	11.8	0.19
R-162	90 CO <sub>2</sub> 10 CO	2200	12.3	0.036
R-166	22.6 CO <sub>2</sub> 77.4 N <sub>2</sub>	2200	8.8	0.062
R-182	100 CO <sub>2</sub>	2000	1.80	0.090
R-199	22.6 CO <sub>2</sub> 77.4 N <sub>2</sub>	2000	2.0	0.026
R-197	90 CO <sub>2</sub> 10 CO	2000	2.9	0.024

TABLE IIA

Cost Summary -  
COED Char Desulfurization Process

Fixed Capital Costs (\$1,000)

Desulfurizer	\$1,820
Separator and Cyclones	604
Bucket Elevator	26
Spent Acceptor Disposal	103
Acceptor Make-up System	163
Recycle Gas Heaters & Blower	1,221
Regenerator and Cyclones	498
Sulfur Recovery System	2,665
Sulfur Storage	27
Acceptor Surge Tank	<u>43</u>
TOTAL*	\$7,170

\*Includes all indirects and fee.

TABLE IIB

Operating Costs, \$/yr.

<u>Capital Related, \$</u>		
Taxes & Insurance	2	
Maintenance	6	
Depreciation (20-yr.)	5	
	<b>13</b>	\$932,000
<u>Labor-Related</u>		
3 men per shift @ \$60M/man-yr.		\$180,000
<u>Utilities</u>		
Electricity @ 6 mill/kwh		\$ 25,000
Cooling Water @ 2.5¢/M gal.		25,000
Boiler Feed Water @ 40¢/M gal.		50,000
		<b>\$100,000</b>
<u>Raw Materials</u>		
Hydrogen @ 25¢/M scf		\$409,000
Oxygen @ \$6.00/ton		503,000
Dolomite @ \$10.00/ton		400,000
Char @ \$3/ton		23,000
Iron @ \$500/ton		53,000
		<b>\$1,388,000</b>
<u>Total Plant-Level Cost, Exclusive of By-product Credit</u>		
		<b>\$2,600,000</b>

FIGURE 1

## COED CHAR DESULFURIZATION PROCESS

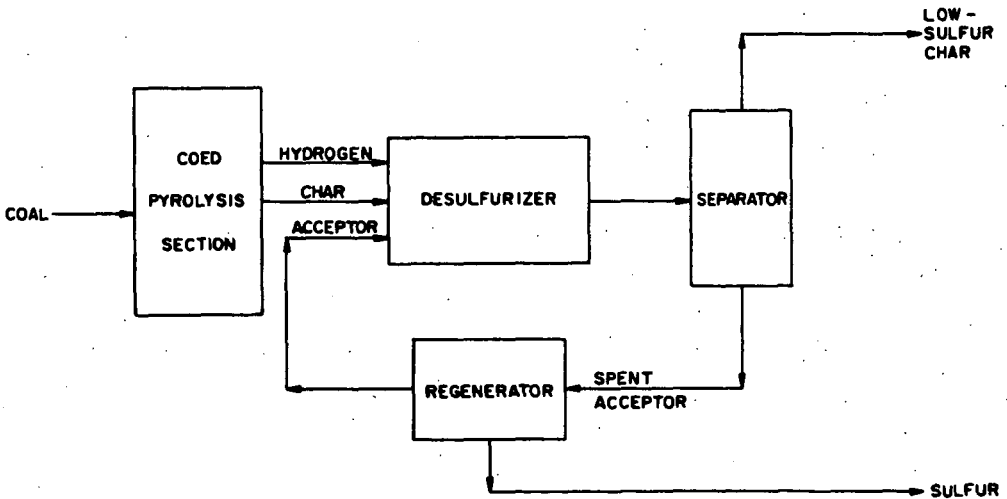
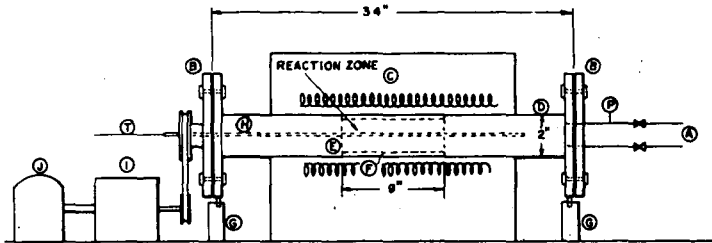


FIGURE 2

TWO-INCH ROTARY KILN FOR CHAR DESULFURIZATION



- |  |                           |
|--|---------------------------|
| Ⓐ GAS INLET AND OUTLET                                   | Ⓔ BEARINGS                |
| ⓑ 300 LB. SS FLANGES                                     | ⓓ 1/8" O.D. SS THERMOWELL |
| ⓒ RESISTANCE FURNACE                                     | ⓔ 64:1 SPEED REDUCER      |
| ⓓ REACTOR-2" - SCH 40-316 SS PIPE                        | ⓕ ELECTRIC MOTOR          |
| ⓔ BAFFLES TO KEEP CHAR-ACCEPTOR MIXTURE IN REACTION ZONE | ⓖ PRESSURE GAUGE          |
| ⓕ FLIGHTS  | ⓗ THERMOCOUPLE            |

FIGURE 3

FLUIDIZED BED SEPARATOR

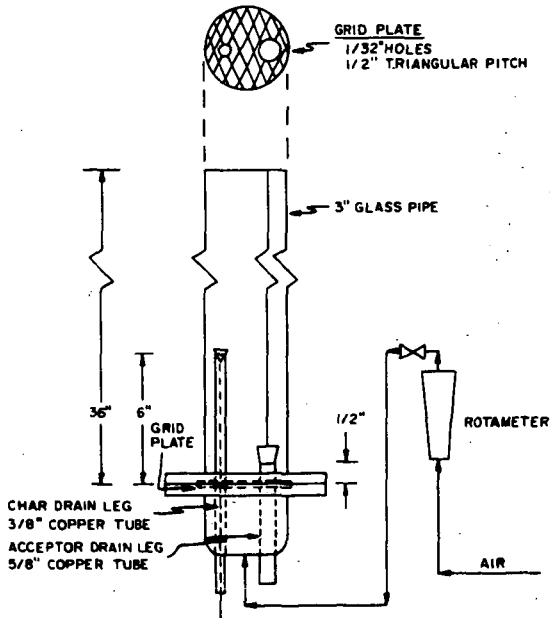


FIGURE 4  
SEPARATION OF CHAR AND ACCEPTOR  
IN A FLUIDIZED BED

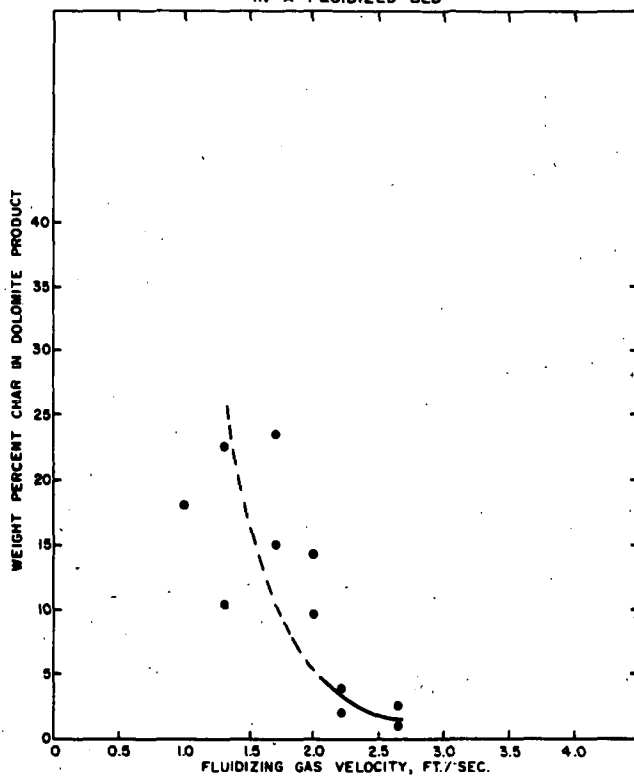


FIGURE 5  
APPARATUS USED TO STUDY ACCEPTOR REGENERATION

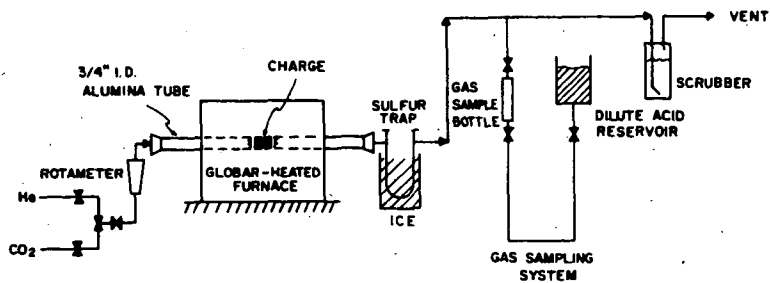


FIGURE 6  
EFFECT OF IRON CONCENTRATION ON  
ACCEPTOR REGENERATION

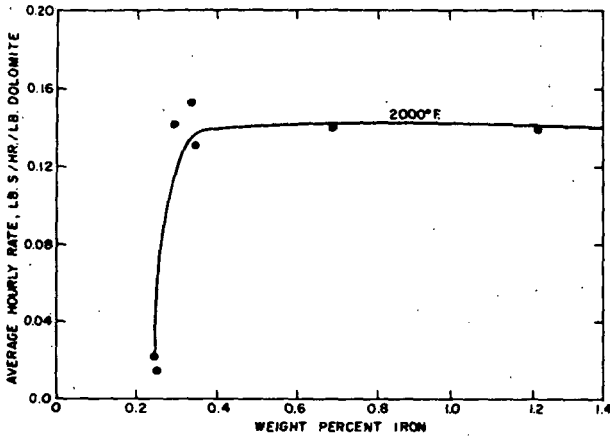


FIGURE 7  
EFFECT OF TEMPERATURE ON THE RATE OF REGENERATION

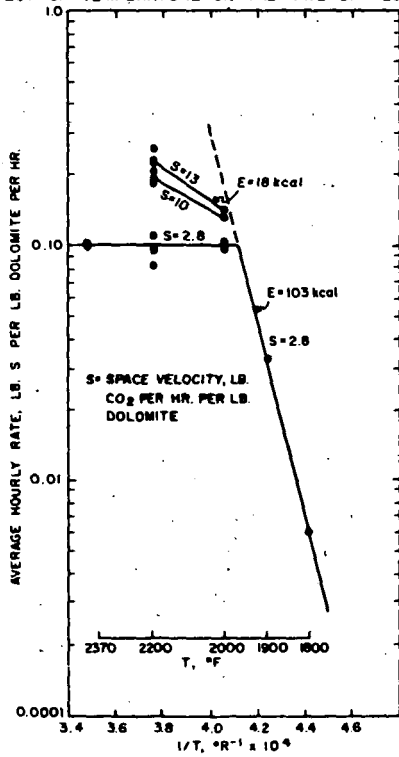


FIGURE 8

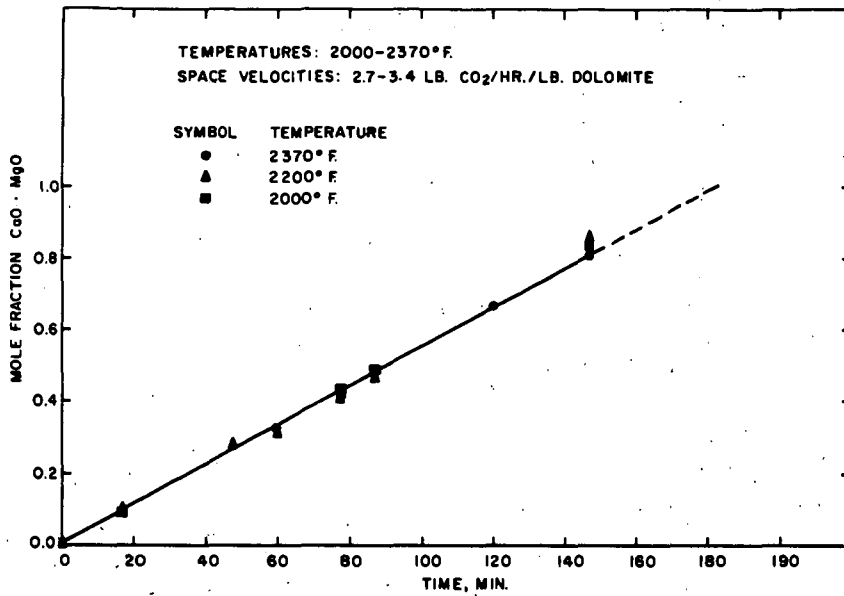
MOLE FRACTION  $\text{CaO} \cdot \text{MgO}$  VERSUS TIME

FIGURE 9

## EFFECT OF SPACE VELOCITY ON REGENERATION RATE

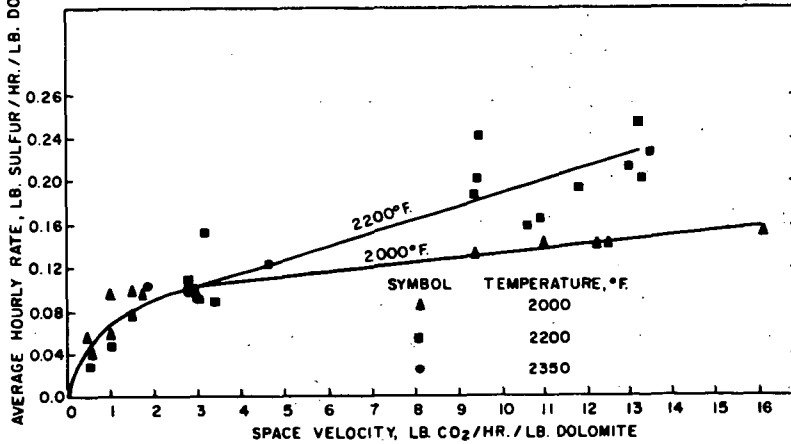


FIGURE 10  
DEACTIVATION OF ACCEPTOR UPON CYCLING

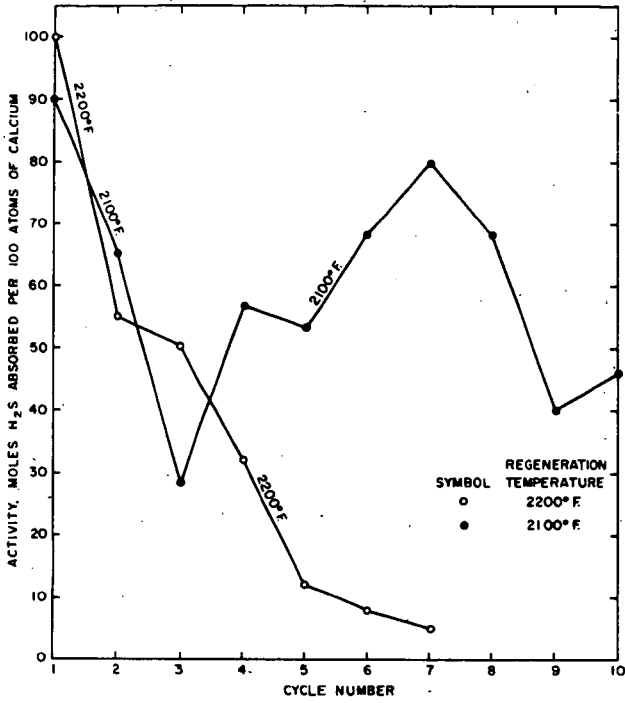


FIGURE 12  
EFFECT OF SULFUR CREDIT ON PROCESS ECONOMICS

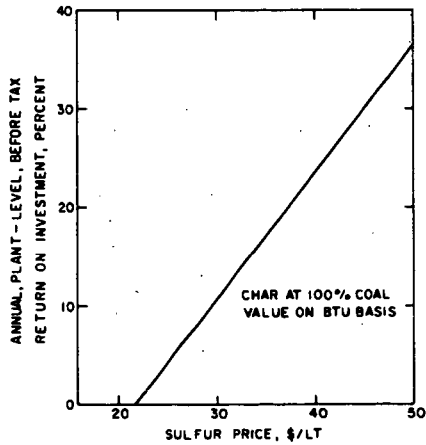
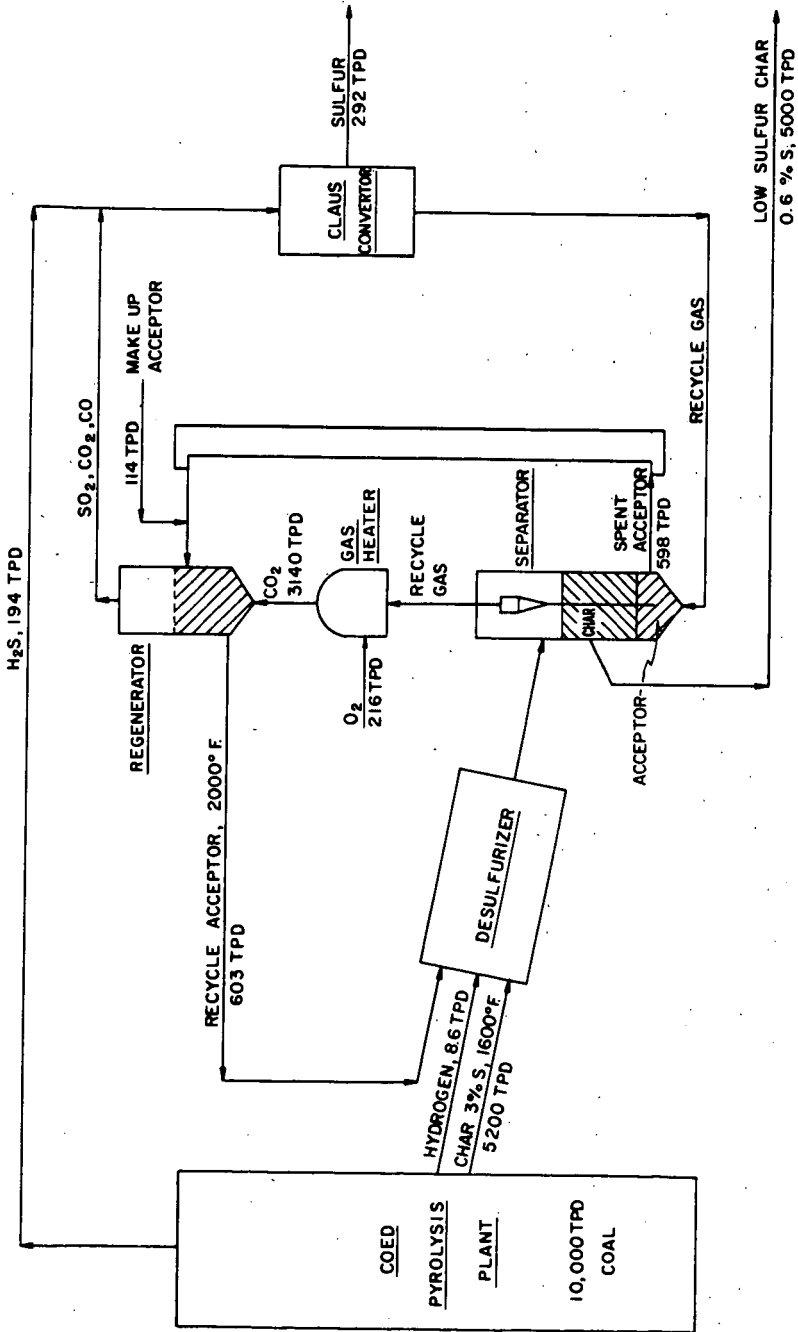


FIGURE 11  
COED CHAR DESULFURIZATION PROCESS



## THE CATALYTIC HYDROGENATION OF MULTI-RING AROMATIC COAL TAR CONSTITUENTS

Wendell H. Wiser, Surjit Singh,  
S. A. Qader, and George R. Hill

Department of Mineral Engineering  
University of Utah, Salt Lake City, Utah 84112

Bituminous coal is understood to consist primarily of fused ring structures joined together by various types of linkages to form an extensive network. These ring structures are quite highly aromatic, although considerable quantities of hydroaromatic configurations are also present. The size of these structures may vary from one to several rings, with an average-sized configuration containing three or four rings.

As one attempts to convert coal to useful liquid materials, it seems desirable to obtain high yields of benzene and its derivatives. These compounds have wide applicability as additives in gasoline to improve the octane rating, as raw materials for the manufacture of conventional explosives, as solvents and chemicals, etc. The higher members of the aromatic homologous series are solids at room temperature. (The melting point of naphthalene, a two-ring structure, is 80°C)

In the course of coal pyrolysis, a single-ring aromatic constituent existing in the lattice structure may possibly be liberated by rupture of the bond(s) joining it to the structure, followed by stabilization of the fragment thus produced. Similarly, higher members of the aromatic homologous fused series may be produced. These products may then be liberated as volatile products as determined by their respective vapor pressures.

While aromatic-type bonds are not expected to be thermally ruptured to any significant extent in this temperature range, the single carbon-carbon bonds within the hydroaromatic structures may be ruptured. This could lead to ring opening of saturated portions of the hydroaromatic structure, followed by cracking of the side chains thus produced, yielding gases and lower aromatics. It is probable that some of the benzene and its derivatives obtained in coal pyrolysis is produced in this manner.

These processes are greatly assisted by the presence of an agent which can produce atoms or small radicals to stabilize the thermally-produced fragments. Hence, dissolution in an appropriate solvent (e.g., tetralin) produces larger quantities of lower-boiling aromatic materials. Hydrogenation in the presence of an appropriate catalyst yields yet larger quantities of lower-boiling constituents.

The production of benzene and its derivatives may be increased by hydrogenation and hydrocracking of higher members of the aromatic series. For members of the series consisting of three rings or more, two possible approaches may exist. The first approach would consist of hydrogenation of a ring at the end of the cluster, followed by ring opening and cracking to produce a derivative of the next lower member of the aromatic series. This procedure could be repeated, yielding ultimately one molecule of benzene or a benzene derivative for each aromatic cluster thus utilized. The second approach may be the hydrogenation of a ring within the cluster other than an end ring, followed by cracking of this ring to yield two aromatic fragments. Completion of this procedure would yield at least two molecules of benzene or its derivatives for each cluster thus utilized.

The present paper describes initial investigation of these possibilities. In an effort to gain understanding of the basic principles involved, the study was initiated

using pure compounds. The first compound investigated was anthracene, a fused, linear, three-ringed compound. The catalytic hydrocracking studies were then extended to 9,10-dihydroanthracene.

### Experimental Procedure

The equipment consisted of an autoclave of one-liter capacity, equipped with a variable speed magnetic stirrer, a pressure gauge, and a thermocouple well. Auxiliary to the autoclave were a temperature recorder to follow the rate of heating, rheostats to assist in obtaining a smooth heating curve, and a temperature controller capable of maintaining constant temperature within  $\pm 3^\circ\text{C}$ .

The hydrogenation experiments were performed using 25 grams of anthracene of 98% purity, mixed with 2.5 grams of catalyst (nickel tungsten sulfide pellets of 1/8-inch diameter). The system was evacuated and then filled with hydrogen to a predetermined cold pressure such that the operating pressure at the temperature of the experiment would be 1500 p.s.i. Approximately 20 minutes were required to bring the system to operating temperature. Solid samples from the reaction products were dissolved in trichloroethylene and analyzed by means of a flame-ionization chromatograph, with an Apiezon-L separation column. Liquids and gases were analyzed by means of the gas chromatograph.

Studies concerning the continued reactions of the 9,10-dihydroanthracene at  $510^\circ\text{C}$  were performed using 25 grams of 9,10-dihydroanthracene of 95% purity, mixed with 2.5 grams of catalyst (Kaolin pellets of 1/8-inch diameter or fluid zeolite cracking catalyst). The techniques for hydrogenation and product analyses were similar to those described above.

### Results and Discussion

Typical curves from this study showing the rate of disappearance of anthracene during catalytic hydrogenation at various temperatures ranging from  $220^\circ$  to  $435^\circ\text{C}$  are shown in Figure 1. These data are presented as weight percent anthracene in the product as a function of time.

Figure 2 shows four chromatograms illustrating the progress of the reactions at  $390^\circ\text{C}$ . At 35 minutes, a considerable amount of hydrogenation to 9,10-dihydroanthracene had occurred, followed by some formation of 1,2,3,4-tetrahydroanthracene. At 60 minutes, hydrogenation of anthracene was nearly complete and a considerable amount of the 1,2,3,4,5,6,7,8-octahydro-derivative had been formed. Finally, at 240 minutes, the anthracene had disappeared, together with most of the 9,10-derivative, and ring opening and/or cracking of other anthracene derivatives to yield naphthalene derivatives was becoming significant.

Figure 3 shows four chromatograms which illustrate the progress of the hydrogenation reactions at comparable times as a function of temperature. At  $250^\circ\text{C}$  and 240 minutes, most of the anthracene had been hydrogenated, with appreciable quantities of 9,10-dihydroanthracene and 1,2,3,4-tetrahydroanthracene present in the system. Products representing higher stages of hydrogenation were not detected and no cracking was observed to occur. At  $300^\circ\text{C}$  and 200 minutes, more of the anthracene had been hydrogenated to the dihydro- and tetrahydro-derivatives, but there was still no evidence of higher stages of hydrogenation, or cracking to naphthalene derivatives. At  $390^\circ\text{C}$  and 240 minutes, essentially all of the anthracene had been hydrogenated, with rather small amounts of 9,10- and large amounts of 1,2,3,4-derivatives of anthracene present, but with an appreciable amount of 1,2,3,4,5,6,7,8-octahydroanthracene now present. Naphthalene derivatives, products of the hydrocracking of one or more of the anthracene derivatives, had appeared. At  $435^\circ\text{C}$  and 200 minutes, most of the 9,10-dihydroanthracene had been further hydrogenated, with a large quantity of the

octahydroanthracene present, but also with considerable amounts of naphthalene derivatives present. In addition, significant quantities of benzene derivatives were now observed. They were apparently formed by further hydrogenation and cracking of the naphthalene derivatives, or perhaps of the remnant of the 1,2,3,4,5,6,7,8-octahydroanthracene.

Figure 4 shows the rate of production of 9,10-dihydroanthracene during catalytic hydrogenation of anthracene. The data indicate that this is the first stable compound formed. At 220°C, yields of nearly 80% of this product, by weight, were obtained. As the temperature increased, the maximum quantity of this compound in the system decreased due to the continued hydrogenation in other positions on the molecule. At temperatures of 345°C and higher, the yield of 9,10-dihydroanthracene reached a maximum, then decreased at longer times due to continuing hydrogenation.

Figure 5 shows the rate of formation of 1,2,3,4-tetrahydroanthracene. It is observed that at temperatures of 250°C and lower, the yields of this product continued to approach a maximum value at long times and did not pass through a maximum. The data indicated only traces of products representing further stages of the hydrogenation process. At higher temperatures, the yields of 1,2,3,4-tetrahydroanthracene reached a maximum value for each temperature, then diminished due to continuing hydrogenation.

Figure 6 shows the rate of formation of 1,2,3,4,5,6,7,8-octahydroanthracene as a continuation of the process of catalytic hydrogenation of anthracene. Since only traces of this compound were formed at 250°C and lower, these temperatures are not represented. At 345° and 390°C, the quantities of this compound continued to increase with time, the data indicating only small quantities of further reaction products. At 435°C, a maximum quantity of 1,2,3,4,5,6,7,8-octahydroanthracene was observed, followed by a decrease as cracking of the molecule occurred, to yield naphthalene derivatives. Only small quantities of naphthalene derivatives were formed below 435°C.

Figure 7 shows the rate of formation of naphthalene and its derivatives. These compounds are apparently formed by opening a saturated ring on the end of the hydroaromatic molecule, perhaps followed by cracking of the side chain produced, to yield gas and a naphthalene derivative. At temperatures above 500°C, this reaction is appreciable, but cracking of these structures is very limited at lower temperatures.

As the hydrogenation reactions continued, a second saturated ring was apparently opened, perhaps followed by cracking of the side chains thus produced, yielding gas and benzene or its derivatives. Figure 8 shows the rate of formation of these compounds. These reactions occurred only at the higher temperatures at longer times.

The curves at 510°C in Figures 7 and 8 were obtained using 9,10-dihydroanthracene of 95% purity as the raw material, Kaolin catalyst, and hydrogen pressure of 300 p.s.i. The other curves at the lower temperatures in these two figures represent the continuing hydrogenation of anthracene described above.

An analysis of the data at a particular temperature (e.g., 435°C) reveals that maximum quantities of the various hydrogenation products appear in the following order: 9,10-dihydroanthracene (about 40 minutes), 1,2,3,4-tetrahydroanthracene (about 100 minutes), and 1,2,3,4,5,6,7,8-octahydroanthracene (about 140 minutes). The appearance of naphthalene derivatives is subsequent to or concurrent with the appearance of the octahydroanthracene, suggesting that the ring opening reactions to produce the naphthalene derivatives may occur primarily on the octahydro derivative of anthracene under the conditions of these investigations. This, however, has not been verified.

Kaolin, which has proven effective as a cracking catalyst, was tried using 9,10-dihydroanthracene as the raw material, a hydrogen pressure of 300 p.s.i., and a temperature of 510°C. The progress of the hydrocracking reactions is readily observed in Figure 9. At 60 minutes, a considerable quantity of 1,2,3,4-tetrahydroanthracene had formed, accompanied by some dehydrogenation to anthracene due to the equilibrium involving these three compounds. At this time, small quantities of naphthalene derivatives had appeared, but only a trace of benzene derivatives. At 120 minutes, the anthracene had essentially disappeared, accompanied by a further reduction in the quantity of 9,10-dihydroanthracene. There was an observable decrease in the quantity of 1,2,3,4-tetrahydroanthracene, accompanied by the production of a considerable quantity of 1,2,3,4,5,6,7,8-octahydroanthracene. The yields of naphthalene derivatives had become significant by this time (approximately 6.5 wt. percent) and small amounts of benzene derivatives had appeared. At 240 minutes, the anthracene derivatives had diminished greatly, accompanied by formation of rather large amounts of naphthalene derivatives (approximately 44 wt. percent) and a significant quantity of benzene derivatives (approximately 18 wt. percent).

The data for the hydrogenation of anthracene, as represented by the rate of disappearance of anthracene in Figure 1, may be analyzed by applying a first-order differential equation. If the average molecular weight of the products of reaction remains essentially constant (a good approximation until cracking becomes significant), weights may be used in the equation.

$$\frac{dx}{dt} = k'(a-x) \quad (1)$$

where "x" is the weight fraction of anthracene which has reacted at time "t", "a" is the initial weight fraction of the anthracene which may react at infinite time, and "k'" is the reaction velocity constant. Integrating equation 1 and evaluating the constant of integration with  $x = 0$  when  $t = 0$  yields:

$$\ln \frac{a}{a-x} = k't \quad (2)$$

A plot of equation 2 is shown in Figure 10, where the reasonably straight lines indicate that the hydrogenation of anthracene at 1500 p.s.i. hydrogenation pressure is first order in the temperature range of 220° to 435°C.

The rate of a chemical reaction is determined by the free energy of activation. The reaction velocity constant may be related to the free energy of activation by the following equation (1):

$$k' = \mathcal{H} \frac{kT}{h} e^{-\Delta F^\ddagger/RT} \quad (3)$$

or, since  $\Delta F = \Delta H - T\Delta S$ :

$$k' = \mathcal{H} \frac{kT}{h} e^{-\Delta H^\ddagger/RT} e^{\Delta S^\ddagger/R} \quad (4)$$

where  $\Delta F^\ddagger$ ,  $\Delta H^\ddagger$ , and  $\Delta S^\ddagger$  are the free energy, heat, and entropy of activation, respectively, "k" is the Boltzmann constant, "h" is the Planck constant, and  $\mathcal{H}$  is a transmission coefficient representing the fraction of activated complexes which leads to formation of products (usually considered equal to one).

Equation 4 may be written in the form:

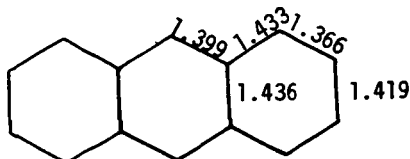
$$\ln \frac{h}{\mathcal{H}k} \frac{k'}{T} = \frac{-\Delta H^\ddagger}{R} \frac{1}{T} + \frac{\Delta S^\ddagger}{R} \quad (5)$$

Figure 11 represents a plot of equation 5 from which is obtained an activation enthalpy of 3.8 kcal/mole and an entropy of activation of -15.5 entropy units. The small activation enthalpy indicates that physical factors rather than chemical reactions control the overall rate of the process. The possibilities include diffusion of the anthracene to the catalyst surface, orientation and adsorption on the catalyst surface, desorption of the reaction products from the catalyst surface, and diffusion of these products away from the surface. This study does not provide information to identify the rate-controlling process.

In the formation of a covalent bond between two atoms, the resonance energy of the electrons involved increases in magnitude as the degree of overlapping of the atomic orbitals involved increases (2). (The word "overlapping" signifies the extent of coincidence of the regions in space in which the orbital wave functions have large values.) This resonance energy in large measure accounts for the energy of the covalent bond. Hence, other factors excluded, shorter bonds between two atoms would possess greater energy than longer bonds between the same two atoms.

If one considers the linear series, benzene (1 ring), naphthalene (2 fused rings), anthracene (3 fused rings), naphthacene (4 fused rings), etc., a very marked and progressive increase in reactivity is noted as the series is ascended (3). Thus, pentacene (5 linear fused rings) is highly reactive and heptacene (7 rings) is so reactive that it is impossible to obtain it in a pure state. This increase in reactivity is accompanied by an increase in tendency to yield addition rather than substitution products. Thus, anthracene is more likely to react by addition than by substitution under mild conditions.

Whereas a conjugated molecule (e.g., the polyenes) manifests alternate longer and shorter bonds, aromatic compounds do not. Hence, in benzene all bonds are equal to about 1.39 Å. Variations in bond distances occur in multiring compounds, but not alternately. Hence, the observed bond distances in the anthracene molecule are as follows (3):



The various positions on the multiring aromatic molecule manifest different degrees of reactivity. Hence, anthracene was observed in this study (as well as by other investigators) to add hydrogen in the 9 and 10 positions to form the dihydride, producing yields of this compound as high as 80% by weight under carefully controlled conditions. As the series is ascended, the stability of the dihydro-derivatives increases notably. Thus, dihydrobenzene is relatively unstable; 1,4-dihydronaphthalene is moderately stable; but 9,10-dihydroanthracene is a stable compound. With some of the higher members of the series, the tendency to form dihydro-derivatives is very marked, such that when heated, part of the compound is decomposed and part converted to the dihydride.

The addition of hydrogen in the 9 and 10 positions of the anthracene molecule (and in comparable positions away from an end ring on the higher aromatic homologues) would alter the aromatic nature of the bonds adjacent to these positions. One might expect a reduction in the resonance energy of the electrons associated with these bonds due to this alteration in aromatic nature, with a resulting weakening and lengthening of the bonds. It would then be theoretically possible to rupture these bonds in preference to other bonds within the fused structure. To date, such a rupture has not been observed to occur. Attempts to catalytically hydrocrack the 9,10-dihydroanthracene resulted in hydrogenation in the 1,2,3,4 positions with an

accompanying shift of hydrogen from the 9 and 10 positions. This shift is probably associated with the change in electron orbitals incident to the removal of the aromaticity of the ring involving the 1,2,3,4 positions.

Acknowledgment

This research was supported by the U. S. Office of Coal Research and the University of Utah under Contract #14-01-0001-271.

References

1. Glasstone, S., Laidler, K. J., Eyring, H., "Theory of Rate Processes," McGraw-Hill, New York, 1941.
2. Pauling, L., "The Nature of the Chemical Bond," Chap. III, Cornell University Press, Ithaca, New York, 1948.
3. Badger, G. M., "Aromatic Character and Aromaticity," Cambridge University Press, Cambridge, Great Britain, 1969.

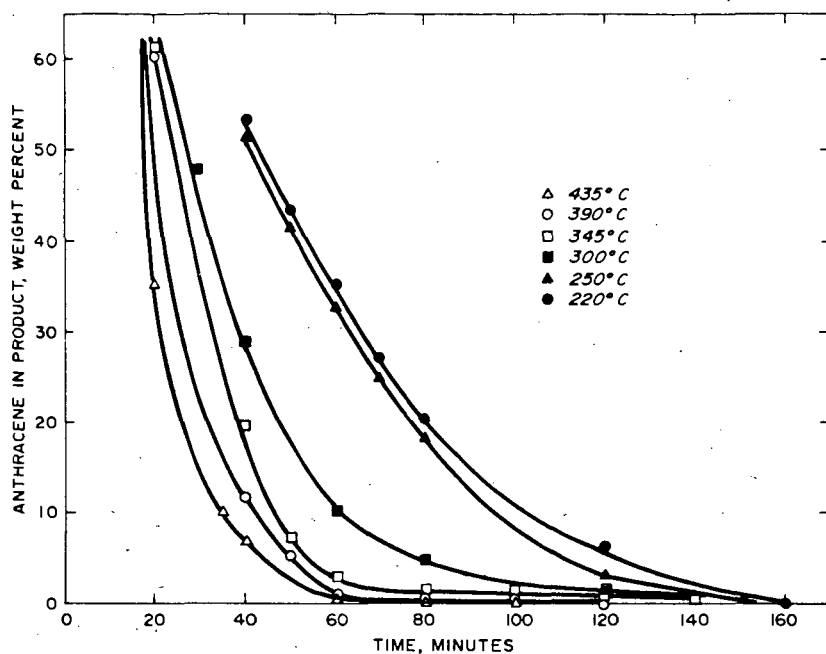


FIGURE 1 RATE OF DISAPPEARANCE OF ANTHRACENE DURING CATALYTIC HYDROGENATION.

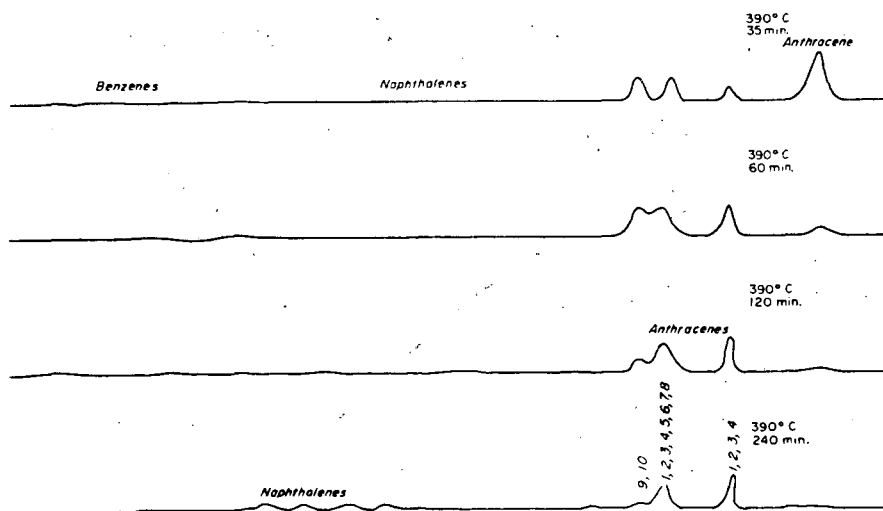


FIGURE 2 CHROMATOGRAMS SHOWING PRODUCT DISTRIBUTION ON HYDROGENATION OF ANTHRACENE AT 390°C, 1500 PSI, Ni-W-S CATALYST.

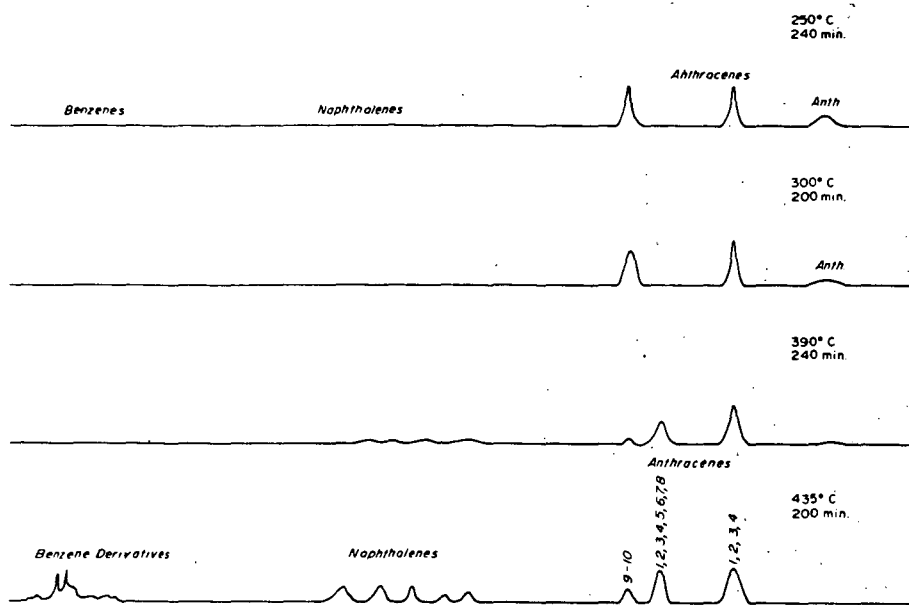


FIGURE 3 CHROMATOGRAMS SHOWING PRODUCT DISTRIBUTION ON HYDROGENATION OF ANTHRACENE AT 250°C TO 435°, 1500 PSI.

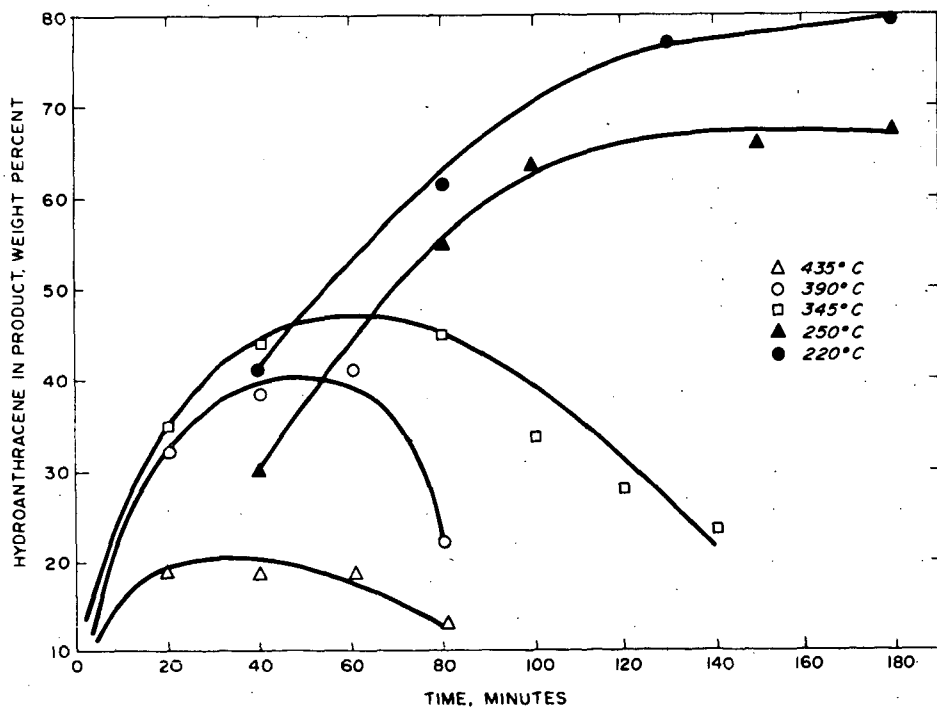


FIGURE 4 RATE OF FORMATION OF 9,10 - DIHYDROANTHRACENE DURING CATALYTIC HYDROGENATION OF ANTHRACENE.

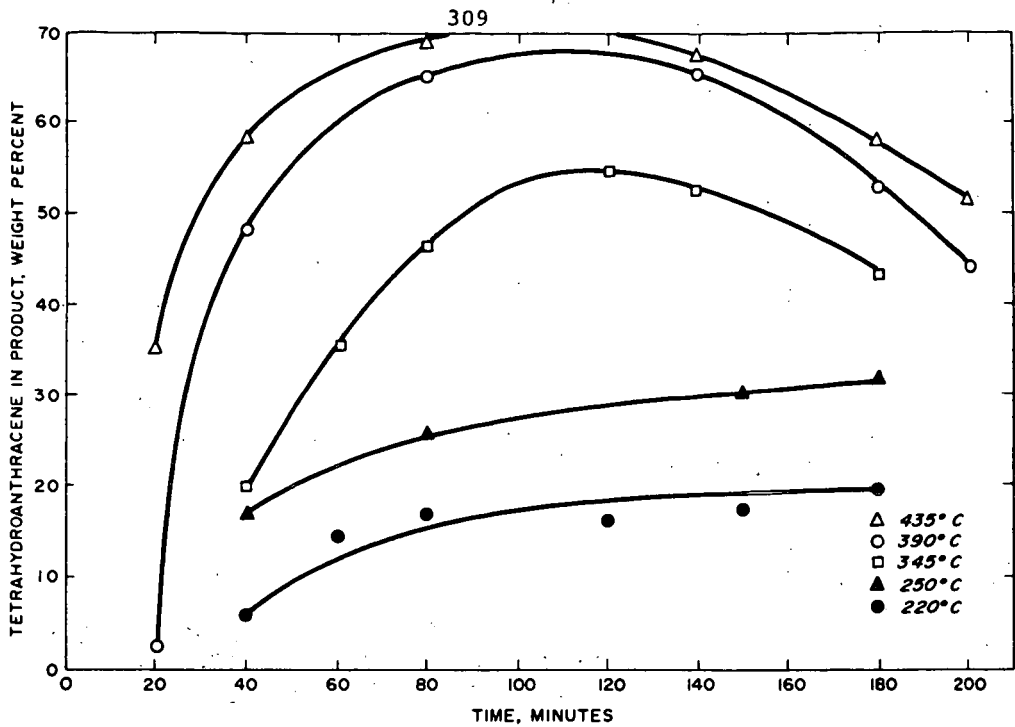


FIGURE 5 RATE OF FORMATION OF 1, 2, 3, 4 - TETRAHYDROANTHRACENE DURING HYDROGENATION OF ANTHRACENE.

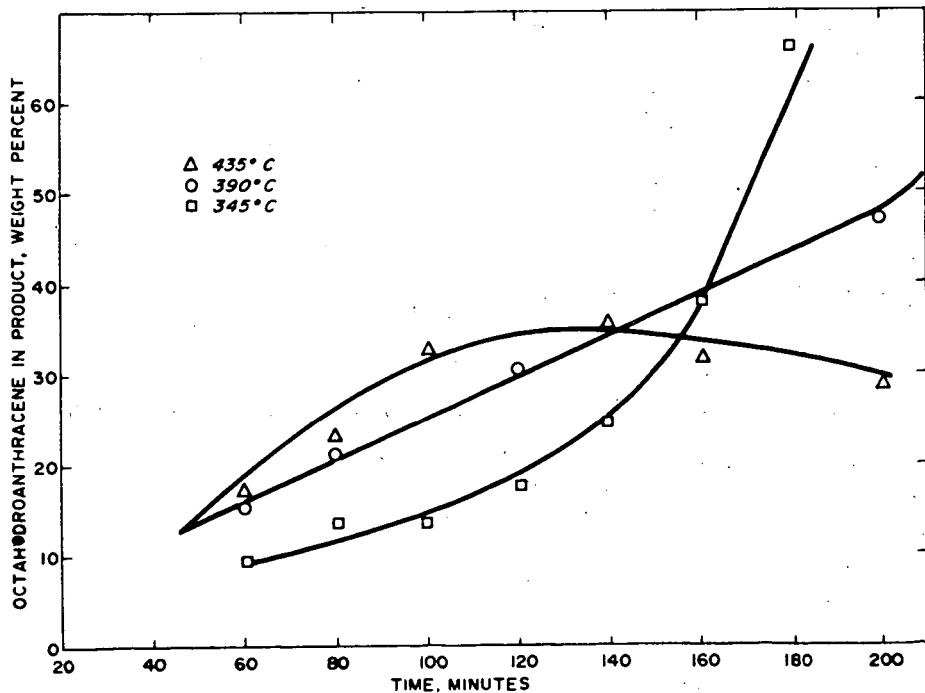


FIGURE 6 RATE OF FORMATION OF 1, 2, 3, 4, 5, 6, 7, 8, - OCTAHYDROANTHRACENE DURING HYDROGENATION OF ANTHRACENE.

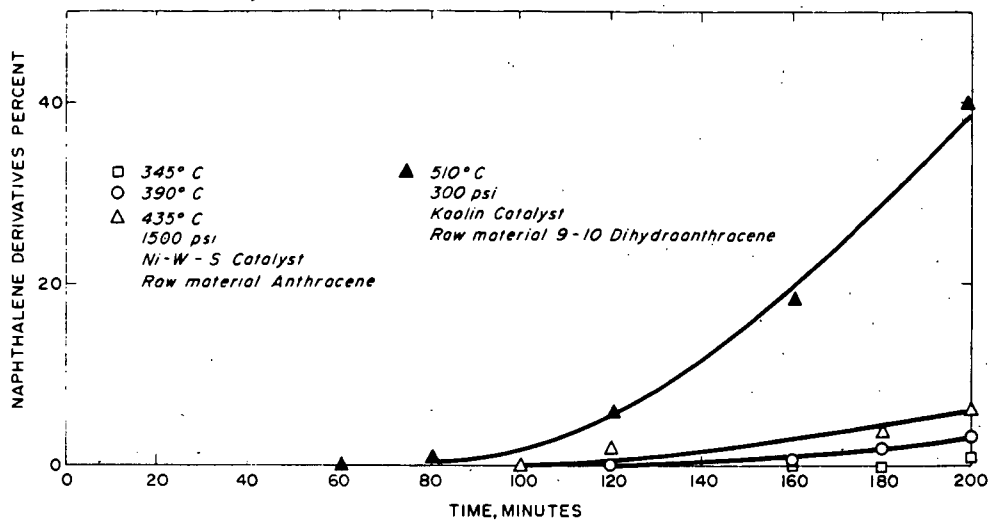


FIGURE 7 RATE OF FORMATION OF NAPHTHALENE DERIVATIVES DURING HYDROGENATION AND HYDROCRACKING.

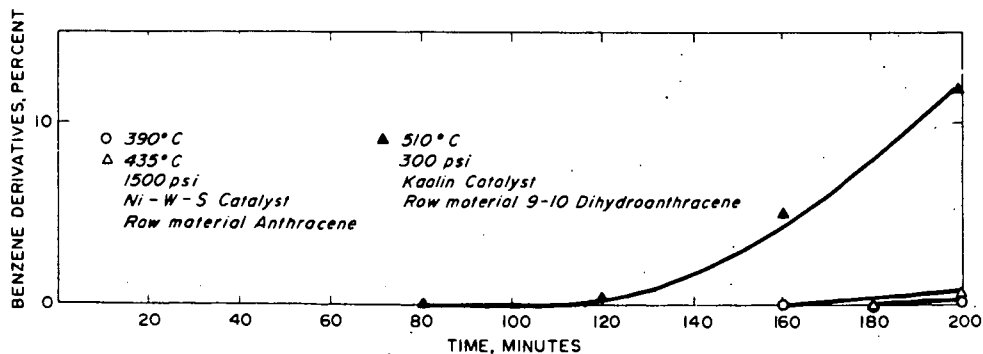


FIGURE 8 RATE OF FORMATION OF BENZENE DERIVATIVES DURING HYDROGENATION AND HYDROCRACKING.

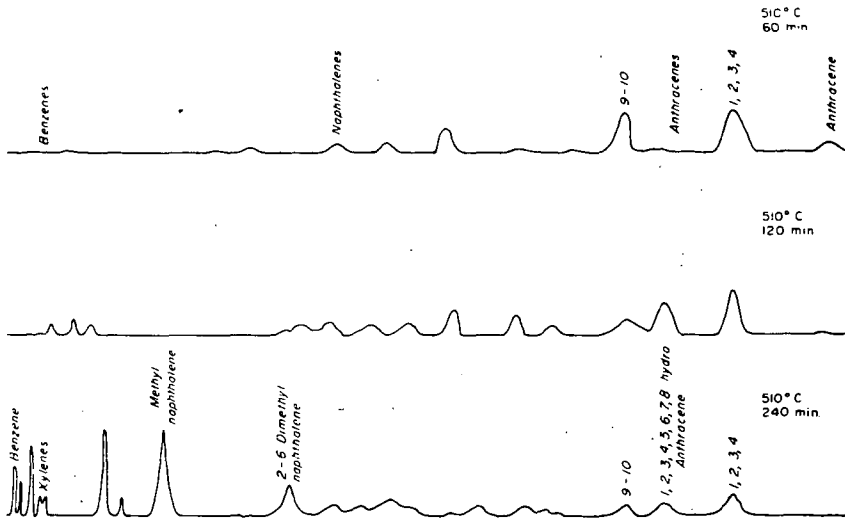


FIGURE 9 CHROMATOGRAMS SHOWING PRODUCT DISTRIBUTION ON CRACKING 9-10 DIHYDROANTHRACENE, 510° C, 300 PSI.

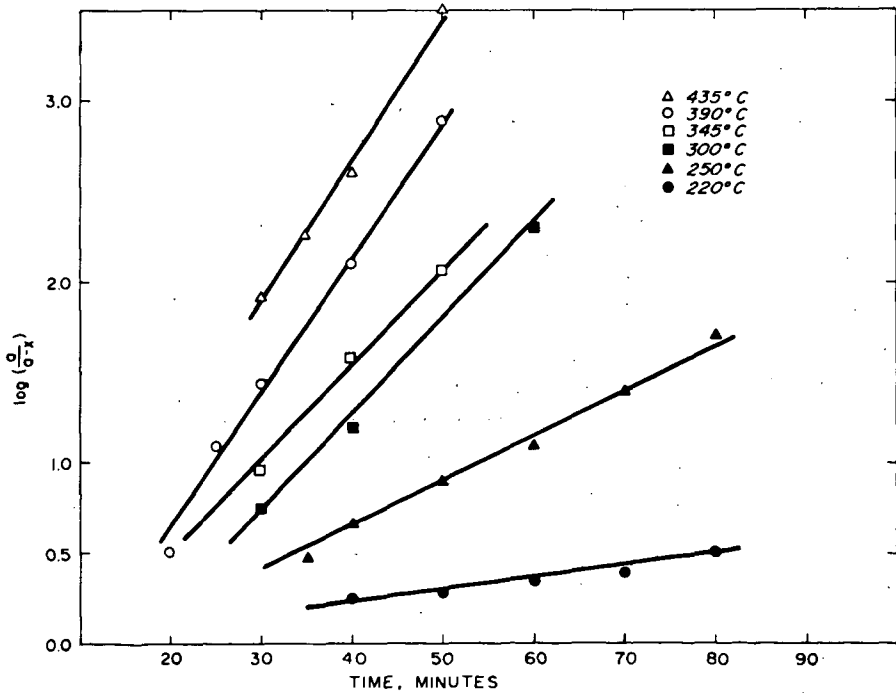


FIGURE 10 FIRST-ORDER PLOT FOR ANTHRACENE IN PRODUCT DURING HYDROGENATION OF ANTHRACENE.

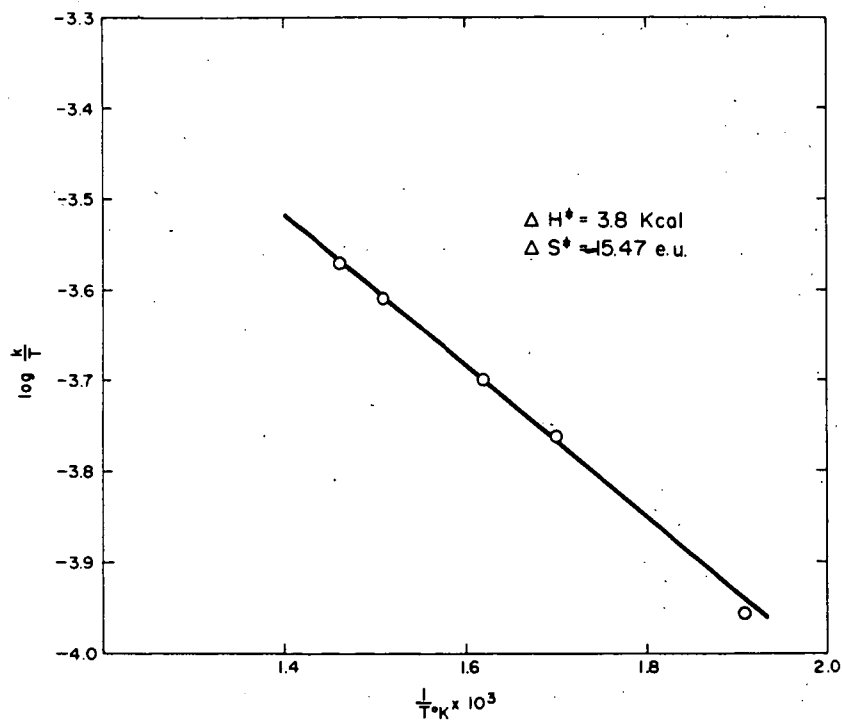


FIGURE 11 ABSOLUTE REACTION RATE PLOT OF HYDROGENATION OF ANTHRACENE.

## THE EFFECT OF A SIEMENS OZONIZER DISCHARGE ON THE REACTION OF ETHYLENE AND STEAM

T.C. Ruppel, P.F. Mossbauer, and D. Bienstock

U.S. Department of the Interior, Bureau of Mines,  
Pittsburgh Coal Research Center, Pittsburgh, Pa.Abstract

In the presence of a Siemens ozonizer discharge, ethylene and steam react exothermally to produce a large number of gaseous and liquid products. At 8.5:1 steam-ethylene molar ratio, 160 hourly space velocity, one atmosphere pressure, 240°C, 460 volt-amperes power drawn by the reactor, and 10,000 Hertz A.C. frequency, a single pass ethylene conversion of 70 percent was obtained. The gaseous products consist of hydrogen, carbon dioxide, carbon monoxide, ethane, methane, propane, propylene, and isomeric butanes, butenes, pentanes, pentenes, hexanes, and hexenes. The liquid fraction is more complex. Characterization of this liquid by analytical liquid chromatography, gas chromatography, and mass spectrometry indicated the presence of at least 75 components consisting mostly of paraffins, olefins, and oxygenates. The oxygenates are largely alcohols. The experimental data indicate that ethylene conversion increases with steam-ethylene molar ratio, input electrical power, and temperature, and decreases with increasing flow rate. There is no reaction at the stated conditions in the absence of an electric field.

Introduction

Novel techniques are being investigated by the Bureau of Mines to find new uses for coal or coal products. One technique under study uses an ozonizer discharge to induce chemical reactions with industrial potential. Initially, the gas phase reaction of carbon monoxide and steam to produce carbon dioxide and hydrogen in the absence of a catalyst was investigated (12). The effect of 60 Hz input power, pressure, space velocity, and temperature on carbon monoxide conversion was determined. In the present paper, we report on the reaction of ethylene and steam in the electric discharge.

From a chemical viewpoint, the ethylene-steam and carbon monoxide-steam reactions are entirely different. Whereas the carbon monoxide-steam reaction yields carbon dioxide, hydrogen, and a trace of methane (less than 1%), the products from the ethylene-steam reaction number at least 88. This can be inferred from Reaction 1 and Figure 1. There were 13 gaseous and 75 liquid products detected in the particular experiment described, all of which cannot be seen in the reproduced gas chromatogram.

Equipment and Procedure

The electrical discharge unit and operating procedure employed in this investigation have been described previously (12). Briefly, metered ethylene from a compressed gas cylinder is passed through a steam generator. The water in the steam generator is maintained at a precalibrated temperature so that the resulting ethylene-steam flow rate and molar ratio meet the requirements of the experiment. The mixture enters a Siemens-type reactor, undergoes reaction, and exits through a cold trap. The noncondensable gaseous product continues through a sample collection train of six gas collection bottles in series, and finally through a wet test meter for exit flow measurement. The cold trap is maintained at -21°C by means of an ice-salt mixture.

The Siemens-type ozonizer reactor, and the methods used for electrical, flow rate, and temperature measurements are described in Reference 12.

After the desired ethylene and steam flow rates were obtained and stabilized, the discharge was initiated.

The gaseous product was analyzed by means of gas chromatography and mass spectrometry. The liquid portion was characterized by analytical liquid chromatography, gas chromatography, and mass spectrometry.

### Results and Discussion

The primary characteristic of the ethylene-steam reaction in an ozonizer discharge is the complexity of the product mixture. A complete material balance for one set of conditions (Experiment No. 368) is given in Reaction 1. The organic liquid portion, immiscible with water, is characterized in Figure 1 and Table 1. Further characterization is in progress. Experimental results are given in Table 2.

<u>Experiment No. 368</u>		gas	-21°C cold trap	
		69.9 mole % ethylene		
		10.2 hydrogen		
		4.9 butanes		
		2.6 ethane		
		2.1 carbon monoxide		
		2.1 pentanes		
		1.8 hexanes		
50 mole % ethylene	<u>ozonizer discharge</u> →	1.6 butenes	+ 5.1 mole %	
50 water		1.2 propane	organics	
		1.1 hexenes	94.9 water (1)	
		0.9 pentenes		
		0.7 methane		
		0.7 propylene		
		0.1 carbon dioxide		
		<u>99.9</u>		
0.0202 lb/hr			0.00844 lb/hr	0.00970 lb/hr
0.000882 lb mole/hr			0.000277 lb mole/hr	0.000392 lb
0.30 SCFH		0.099 SCFH	mole/hr	

Table 1.- Characterization of Organic Liquid Product

Experiment No. 368	
Average molecular weight (ALC <sup>a</sup> )	----- 150
Maximum carbon number detected	
Gas chromatography	----- C <sub>13</sub>
Mass spectrometry	----- C <sub>14</sub>
Molecular types present	
Paraffinic (FIA and MS <sup>b</sup> ), approx.	----- 30% by vol.
Olefinic + Oxygenates (FIA and MS)	
Heavy ends, approx.	----- 20% by vol.
Light ends, approx.	----- 50% by vol.
Bulk density	----- 0.76 g/cc

a. Analytical liquid chromatography.

b. Fluorescent indicator analysis (ASTM D-1319-56T) and mass spectrometry.

Table 2.- Experimental Results

10,000 Hz A.C. frequency  
1 atmosphere pressure

Exp't. No.	Percent Ethylene Conversion <sup>a</sup>	Steam- Ethylene Molar Ratio	Space Velocity, hr <sup>-1</sup>	Tempera- ture, °C	Secondary Power, <sup>b</sup> volt- amperes	Secondary Voltage, r.m.s. volts
368	54.9	1.0	56	125	231	7000
377	66.1	8.5	160	240	380	6390
377A	68.0	8.5	160	240	420	6530
377B	70.0	8.5	160	240	460	6670
378	11.2	2.8	270	230	380	6620
378A	16.3	2.8	270	230	420	6920
378B	21.3	2.8	270	230	460	7220
379	10.2	1.0	100	245	380	6790
379A	14.0	1.0	100	245	420	7000
379B	17.7	1.0	100	245	460	7210
380	0	0.61	320	140	380	7060
380A	1.5	0.61	320	140	420	7380
380B	2.4	0.61	320	140	460	7700
381	11.2	7.0	140	140	380	7100
381A	36.7	7.0	140	140	420	7020
381B	53.5	7.0	140	140	460	6940
382	3.2	0.70	325	220	380	6690
382A	3.8	0.70	325	220	420	7160
382B	4.5	0.70	325	220	460	7620
383	2.0	3.0	270	140	380	7260
383A	7.5	3.0	270	140	420	7250
383B	13.1	3.0	270	140	460	7240
384	5.0	1.0	105	120	380	7290
384A	8.8	1.0	105	120	420	7500
384B	12.7	1.0	105	120	460	7720
385	0	8.5	160	240	0	0

a. Percent conversion =  $[(SCFH_{in} - SCFH_{out}) / (SCFH_{in})] (100)$ .

b. Volt-amperes drawn by the reactor.

As part of a larger program to delineate the effect of process variables on product characteristics, the effect of steam-ethylene feed molar ratio, space velocity, and temperature on ethylene conversion was determined.

The data were analyzed by means of a linear hypothesis statistical empirical model (9). With this model it is assumed that the conversion of ethylene is dependent on all variables studied to the first power only. The dependent variable could be chosen from any measured product characteristic: amount of organic product or single compound produced, ethylene or steam conversions, product density, average molecular weight, etc. We chose the percentage conversion of ethylene.

The following regression equation resulted from this model:

Percent  
Ethylene =  $17.35 - 2.31 (MR) - 0.0529 (SV) - 0.0191 (T) + 0.04079 (MR)(T)$ , (1)  
Converted

where: MR = steam-ethylene feed molar ratio  
 SV = space velocity,  $\text{hr}^{-1}$ , flow rate/reactor volume  
 T = temperature,  $^{\circ}\text{C}$ .

Equation 1 represents the experimental data of Table 2 at 420 volt-amperes secondary power. Secondary power does not appear as a variable in the regression equation because ethylene conversions obtained at 380, 420, and 460 volt-amperes secondary power were not obtained from experiments carried out in a randomized sequence. This could, and did in a test equation including secondary power, lead to spurious regression coefficients for terms containing secondary power. As seen in Table 2, molar ratio, space velocity, and temperature were randomized with respect to sequence. Randomization eliminates any apparent correlation of independent variables. However, Table 2 does indicate that ethylene conversion increases with power drawn by the reactor.

The effect of steam-ethylene molar ratio, space velocity, and temperature on ethylene conversion can be easily seen from Table 3, which was calculated from Equation 1.

Table 3.- Ethylene Conversions Calculated from Equation 1

10,000 Hz A.C. frequency 1 atmosphere pressure 420 volt-amperes drawn by reactor			
Percent Ethylene Conversion	Steam- Ethylene Molar Ratio	Space Velocity, $\text{hr}^{-1}$	Tempera- ture, $^{\circ}\text{C}$
12.0	1	100	100
14.1	1	100	200
1.5	1	300	100
3.5	1	300	200
15.5	3	100	100
25.8	3	100	200
5.5	3	300	100
15.2	3	300	200

An inspection of Table 3 shows that steam-ethylene molar ratio and temperature have a positive effect on conversion, whereas space velocity exerts a negative effect.

According to Table 2, maximum conversion of ethylene within the range of Equation 1 was found in Experiment No. 377A. The experimental value of 68.0 percent compares with a value of 67.7 obtained by calculation. Regions of interest suggested by the equation and Table 3 would be high steam-ethylene molar ratio, low space velocity, and high temperature.

It was found that no ethylene was converted to gaseous or liquid products in the absence of an electrical field in Experiment No. 385. These conditions matched those yielding the highest ethylene conversion, Experiment No. 377. Thus there is no thermal reaction at these conditions and it is the discharge which supplies the energy necessary for reaction. The authors' previous investigation (12), using the water-gas shift reaction ( $\text{H}_2\text{O} + \text{CO} = \text{H}_2 + \text{CO}_2$ ), has indicated that the discharge is necessary in that case also, and further that the quartz walls of the ozonizer are probably not involved. By analogy, it appears that the ethylene-steam reaction in an ozonizer discharge is also a homogeneous gas phase reaction.

We have obtained some preliminary experimental results at 60 Hertz A.C. frequency. With identical conditions, except frequency, the gaseous and liquid product characteristics appear to be identical. However the product yield is less. This variable will be studied further in future experiments.

The overall ethylene-steam reaction is exothermic. The heat of reaction is sufficient to keep the reaction temperature above the condensation point of steam. In practice, sectional heating and cooling were employed. The discharge by its nature has a tendency to localize, producing hot spots. These areas could become the sites for arc formation, with subsequent quartz reactor perforation and failure. A relatively even and stable discharge was obtained with the judicious intermittent use of small cooling fans and sectional heaters.

#### Comparison with Other Ethylene Reactions

There appears to have been no previous investigations of the ethylene-steam reaction in an electrical discharge. This includes any form of electrical discharge: arc, glow, microwave, ozonizer, or radiofrequency. However similar systems have been studied by others. The decomposition and polymerization of ethylene in nondisruptive discharges was studied by Andreev (1), Dem'yanov and Pryanisnikov (2), Eidus (3), Eidus and Nechaeva (4), Fujio (5), Jovitschitsch (7,8), Mignonac and De St. Aunay (10), Stratta and Vernazza (14,15,19), and Szukiewicz (16). The ethylene-air system has been investigated by Sugino, Inoue, Koseki, and Gomi (17), Vernazzi and Stratta (18), and the authors (13). Vernazzi and Stratta and the authors also investigated the ethylene-carbon dioxide system. Ethylene plus nitrogen was studied by Miyamoto (11). The ethylene-nitrogen-propane system in a glow discharge was investigated by Hinde and Lichtin (6) for the purpose of elucidating the mechanism of olefin reactions with active nitrogen. Most of the above citations were concerned with ozonizer discharges at or around atmospheric pressure; however the A.C. frequencies employed varied greatly.

The above investigations can be qualitatively summarized by the following reactions:

#### References 1,2,3,4,5,7,8,10,14,15,16 and 19

Ethylene	$\xrightarrow{\text{nondisruptive discharges near atmospheric pressure}}$	acetylene butadiene butene-1 ethane hexene-1 hydrogen methane liquid + solid products	(2)
----------	---	--	-----

#### Reference 17

1.68 ethylene 5.00 air	$\xrightarrow{\text{ozonizer atmospheric pressure}}$	acetaldehyde carbon dioxide diformyl peroxide ethyl alcohol ethylene oxide formaldehyde hydrogen methane methyl alcohol propargyl alcohol water	(3)
---------------------------	--	---	-----

#### Reference 18

1 ethylene 5 air	$\xrightarrow{\text{ozonizer near atmospheric pressure}}$	carbon dioxide water	(4)
---------------------	---	-------------------------	-----

Reference 13

1 ethylene	ozonizer	carbon monoxide
1 air	<u>10,000 Hz A.C. freq.</u> →	formaldehyde
	atmospheric pressure	hydrogen
		methyl alcohol
		paraformaldehyde
		water
		other liquid products
		(5)

Reference 11

2 ethylene	"silent discharge" →	acetylene
1 nitrogen	near atmospheric pressure	hydrogen cyanide
		liquid + solid products
		(6)

Reference 18

ethylene	ozonizer	carbon monoxide
carbon dioxide	<u>1:4 to 4:1 ratios</u> →	hydrogen
		methane
		liquid sat'd. hydrocarbons
		(7)

Reference 13

1 ethylene	ozonizer	butanes
1 carbon dioxide	<u>10,000 Hz A.C. freq.</u> →	butenes
	atmospheric pressure	carbon monoxide
		ethane
		hexanes
		hydrogen
		pentanes
		pentenes
		liquid products
		(8)

In practically all cases the above reactions did not proceed to completion. The residence time was too short for the complete reaction of feed material.

Factorially designed experiments are in progress to simultaneously determine the effect of A.C. frequency, molar ratio, power drawn by reactor, pressure, space velocity, and temperature on the various dependent variables previously mentioned. Following these experiments it should be possible within the limitations of the chemistry involved, to produce product with specified characteristics.

Conclusions

The ethylene-steam reaction holds potential engineering applications. It is novel, exhibits good reactivity from a technical viewpoint, can be carried out under mild conditions, and produces a myriad of alcohols, olefins, and paraffins. As a mixture analogous to crude petroleum, Fischer-Tropsch synthesis product, or the product from destructive distillation of coal, the ethylene-steam reaction product may prove to be a rich source of synthetic organic chemicals.

Within the limits of this investigation, the following conclusions can be drawn:

(1) Ethylene conversion is higher at higher steam-ethylene molar ratios, power inputs, and temperatures, and at lower space velocities.

(2) No ethylene or steam was converted to products in the absence of an electric field.

Literature Cited

1. Andreev, D.N., Bull. acad. sci. U.R.S.S., Classe sci. math. nat., Ser. chim., 1039 (1938); Chem. Abs. 33, 6575 (1939).
2. Dem'yanov, N.Y., and Pryanishnikov, N.D., J. Russ. Phys. Chem. Soc. 58, 472 (1926); Chem. Abs. 21, 3344 (1927).
3. Eidus, Y.T., Bull. acad. sci. U.R.S.S., Classe sci. math. nat., Ser. chim., 737 (1938); Chem. Abs. 33, 3269 (1939).
4. Eidus, Y.T., and Nechaeva, N.N., ibid., No. 1, 153 (1940); Chem. Abs. 35, 3540 (1941).
5. Fujio, C., Bull. Chem. Soc. Japan 5, 249 (1930); Chem. Abs. 24, 5644 (1930).
6. Hinde, P.T., and Lichtin, N.N., Advan. Chem. Series 80, 250 (1969).
7. Jovitschitsch, M.Z., Monatsh. 29, 1 (1908); Chem. Abs. 2, 1418 (1908).
8. Ibid., 29, 5 (1908); Chem. Abs. 2, 1418 (1908).
9. Mendenhall, W., "Introduction to Linear Systems and the Design and Analysis of Experiments," Wadsworth Pub. Co., Belmont, Calif., 1968.
10. Mignonac, G., and De St. Aunay, R.V., Compt. rend. 189, 106 (1929); Chem. Abs. 23, 4668 (1929).
11. Miyamoto, S., J. Chem. Soc. Japan 43, 21 (1922); Chem. Abs. 16, 2248 (1922).
12. Ruppel, T.C., Mossbauer, P.F., and Bienstock, D., Advan. Chem. Series 80, 214 (1969).
13. Ibid., unpublished results.
14. Stratta, R., and Vernazza, E., Industria chimica 6, 133 (1931); Chem. Abs. 25, 4186 (1931).
15. Ibid., 8, 698 (1933); Chem. Abs. 27, 5254 (1933).
16. Szukiewicz, W., Roczniki Chem. 13, 245 (1933); Chem. Abs. 27, 4487 (1933).
17. Sugino, K., Inoue, E., Shirai, K., Koseki, T., and Gomi, T., Nippon Kagaku Zasshi 86, 1200 (1965).
18. Vernazza, E., and Stratta, R., Industria chimica 5, 137 (1930); Chem. Abs. 24, 5644 (1930).
19. Ibid., 6, 761 (1931); Chem. Abs. 26, 1198 (1931).

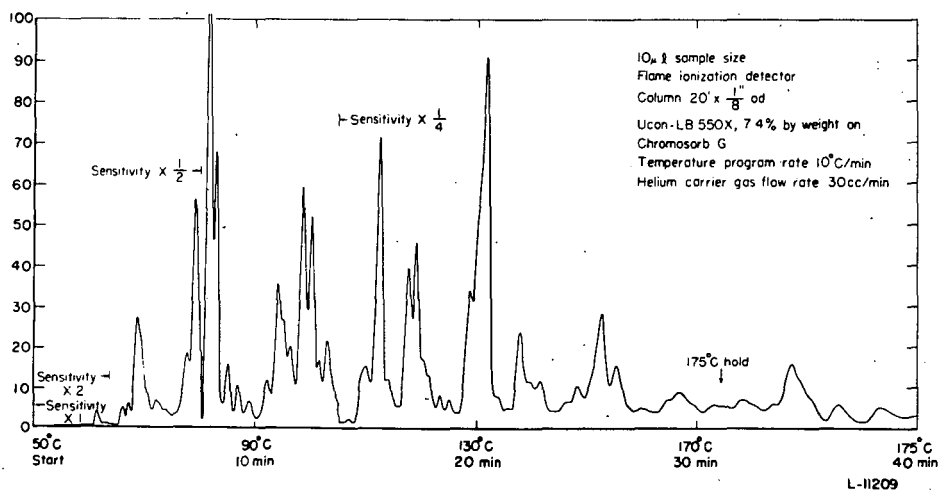


Figure 1.- Typical Gas Chromatogram of the Organic Liquid Products from the Ethylene-Steam Reaction in an Ozonizer Discharge.

THE CONVERSION OF COAL TO ACETYLENE  
IN ARC HEATED HYDROGEN

R.E. Gannon, V.J. Krukonis, T. Schoenberg

AVCO Corporation/ATD  
Lowell Industrial Park  
Lowell, Massachusetts 01851I. INTRODUCTION

In recent years intense research has been directed toward the development of coal treating processes designed to produce hydrocarbons for the chemical industry. The major portion of this effort has been aimed at producing pipeline gas and coal-derived liquid fuels, such as gasoline, by processes involving high pressure, catalytic hydrogenation carried out in fluid bed (1), slurry (2,3) and transport reactors (4).

While the processes for producing gaseous and liquid fuels by conventional techniques were being developed, exploratory experiments to investigate the rapid pyrolysis of coal to gaseous products were in progress. In these studies energy sources such as d.c. arcs (5,6), lasers (7), flash lamps (8), plasma jets (9-12) and arc image furnaces (13,14) have been used to heat coal at temperatures above 1500°C. The results of these studies show that the rapid pyrolysis of coal produces a gaseous mixture of which acetylene is the principal hydrocarbon constituent. These results are consistent with the free energy data of Wagman, et al (15) and Howard, et al (16) (Figure 1) which show that at ordinary temperature the paraffinic and olefinic hydrocarbons are more stable than acetylene, but with increasing temperature the free energies of these hydrocarbons become progressively more positive until at temperatures above 1200°C they are less stable than acetylene. In gaseous mixtures above 1200°C, therefore, acetylene should be the predominant species. Upon cooling the mixture, however, much of the acetylene is lost as it becomes more unstable toward its elements as well as toward other hydrocarbons. The fact that acetylene is identified in the cooled gas mixture, however, indicates that the rate of the formation is greater than the rate of the decomposition reactions. From these considerations it is obvious that to produce appreciable quantities of acetylene it is necessary to heat the reactor mixture to temperature above 1200°C to obtain a mixture rich in acetylene and then to quench this mixture rapidly in order to preserve as much of the acetylene as possible. Features of a plasma jet reactor which allow the reaction mixture to be heated to approximately 2000°C and rapidly cooled to ambient conditions in a matter of milliseconds obviously exhibits potential as a reactor for the conversion of coal or other hydrocarbons to acetylene.

II. EXPERIMENTALA. APPARATUS

The work described in this paper is concerned with the formation of acetylene through the exposure of coal to hydrogen which has been heated by passing it through an electric discharge. The basis for this technique was demonstrated by previous workers (9, 10, 11) who showed that acetylene could be produced by heating coal in an argon plasma jet. It was further shown that the acetylene formation could be enhanced by including small amounts of hydrogen in the argon stream. Each group of workers, however, was limited to hydrogen concentrations below 30% by the severe erosion of the electrodes of the plasma generator when operated at higher hydrogen fractions.

At AVCO it was found that a plasma generator equipped with a tungsten-tipped cathode and a water-cooled copper anode could be operated using pure hydrogen gas without measurable erosion of the electrodes. This unit was therefore adapted to a reactor chamber which would allow the introduction of coal directly into the plasma jet followed by immediate cooling to room temperature in a water-cooled chamber and water-cooled exit pipes. A schematic drawing of the reactor is shown in Figure 2. The plasma generator is a 30 kw unit which when operated with hydrogen is 75% efficient, i.e., 75% of the electric energy is converted to gas enthalpy. This was determined by measuring the energy absorbed by cooling water circulated around the electrodes. Similarly it was determined that when operated with argon it was only 50 to 55% efficient.

To obtain an estimate of the reaction temperature and temperature profiles, provision for measuring the temperature at twenty four stations within the reactor were made. Tungsten-5% rhenium, tungsten-26% rhenium thermocouples from the nozzle, viz.,  $3/4$ ",  $1\frac{1}{4}$ " and  $1\frac{3}{4}$ ". These thermocouples and housings provided the capability for measuring temperatures up to 5000°F. The millivolt output of the thermocouples was fed to a multiposition recorder so that the time-temperature history at each of the three vertical positions could be obtained simultaneously. The radial temperature distribution was obtained by eight measurements made at  $\frac{1}{4}$ " intervals from the centerline of the reactor at each of the three vertical distances. Figure 3 shows the measured temperature profile in the reactor at distances of up to  $1\frac{3}{4}$ " from the nozzle. The left side of each curve shown was drawn by symmetry to the measured right side.

For the operating conditions shown on the figure, the temperature of the hydrogen leaving the nozzle was calculated to be 5200°F. The measurements show that this temperature declined to 4100°F at  $3/4$ " from the nozzle and then to 2400°F at  $1\frac{1}{4}$ " and to 1900°F at  $1\frac{3}{4}$ ". The radial temperature distribution shows a steep gradient at the  $3/4$ " distance but only a slight gradient at  $1\frac{3}{4}$ " as the jet expands as it progresses away from the nozzle.

Temperature measurements with coal feeding were attempted but could not be extended for more than several seconds because the coal reacted rapidly with the beryllia sheath and then with the tungsten-rhenium thermocouples. When the coal was introduced, the centerline temperatures of the two furthest thermocouples,  $1\frac{1}{4}$ " and  $1\frac{3}{4}$ " from the nozzle, dropped about 500°F before the thermocouples failed. The thermocouples closest to the nozzle, however, did not record a temperature decline indicating that the coal was not reaching the hottest part of the jet.

The coal is fed to the reactor from a 6000 gram hopper by means of a screw feed system. The speed of the screw feeder and consequently the coal feed rate is controlled by a variable speed motor. Hydrogen, typically 2.4 SCFM, is introduced to the coal feed line after the screw feed to act as a carrier gas. The coal-hydrogen mixture is conducted into a circular manifold from which it is injected into the plasma through a series of small holes around the inside diameter, as illustrated in Figure 4. Controlled coal feed rates of between 125 g/min and 550 g/min are possible with this arrangement.

The effluent gases from the coal-hydrogen reaction are sampled by means of a probe in one of the exit lines. Gas chromatography is then used to analyze the collected gases using a Porapak N column and a flame ionization detector to analyze for the hydrocarbons and a silica gel column and a thermal conductivity detector to analyze for H<sub>2</sub>, CO, CO<sub>2</sub> and air.

## B. RESULTS

In studying the feasibility of producing acetylene by subjecting coal

to arc heated hydrogen it is evident that three critical parameters must be measured: 1) the yield of acetylene per pound of coal used 2) the energy required to produce a pound of acetylene 3) the concentration of acetylene in the exit gases. Because each of these parameters should be dependent on the process variables, it is important to designate the operating conditions at which the critical parameters are optimum, i.e., a high yield and concentration and a low specific energy requirement (SER). Considering the process, two variables, the rate of coal feed and the enthalpy of the hydrogen from the arc appear to be of primary importance. For this reason, the three parameters, yield, concentration and SER were studied first as a function of enthalpy at a constant coal feed rate and then as a function of coal feed rate at a constant gas enthalpy.

In the initial runs it was determined that the conversion process was more efficient when the reactor was operated at pressures between 0.2 and 0.5 atmospheres. The subsequent runs were therefore performed under reduced pressure. Pittsburgh Seam Coal, of a -100 + 200 consist was used in all runs in this study.

The results showing the effect of gas enthalpy and coal feed rate on yield, concentration and SER are shown in Figures 5 and 6. For this data, yield is defined as pounds of acetylene produced per pound of coal (including ash and moisture content) introduced, concentration is the moles of acetylene per mole of exit gas and SER is the kilowatt hours of electricity to the system (including losses to the electrodes and walls) required to produce one pound of acetylene.

### III. DISCUSSION

The general effect of gas enthalpy on the critical parameters of the process are predictable and consistent with the results shown in Figure 5. That is, it would be expected that the acetylene yield and concentration should increase with increasing enthalpy and that the SER should go through a minimum where enough energy is available to convert the coal to acetylene with a minimum of energy being lost in the exit gases.

In considering the effect of coal feed rate, illustrated in Figure 6, it is predictable that the yield should decrease with increasing coal feed rate. It should also be expected that as the coal feed was increased the average enthalpy of the coal-gas mixture would decrease. Using this reasoning it would be predicted that once the ideal coal feed rate for the fixed gas enthalpy of the test was reached, the concentration should reach a maximum and then decrease as the average enthalpy of the mixture decreased with increasing coal feed. Similarly it could be predicted that the SER value should go through a minimum as an increasing percentage of the energy is used as sensible heat for the additional coal. These predictions are not substantiated by the data given in Figure 6 as the concentration appears to attain a maximum at a coal feed rate of 130 g/min, and to remain nearly constant to feed rates of over 250 g/min. The SER values behave in a similar manner, achieving a low value of about 7 kwh/lb. at 130 g. of coal/min. and remaining constant to the maximum coal feeds tested.

The departure from the predicted behavior as the coal feed was increased can be explained on the basis of the competing reactions of forming acetylene at high temperatures on one hand and then allowing it to decompose before it is effectively quenched. To substantiate the premise that appreciable amounts of acetylene decompose before it is quenched a series of experiments to study the rate of acetylene decomposition was performed. In these experiments a gas mixture of 6% acetylene and 94% hydrogen was introduced through the ports where the coal is normally injected. The amount of decomposition of the acetylene was then determined as a function of gas enthalpy. The results, given in

Figure 7, showed that at high gas enthalpy (4.0 kw/SCFM) as much as 36% of the original acetylene decomposed and at 1.8 kw/SCFM, the enthalpy level for the data given in Figure 6, 16% of the acetylene decomposed. Extrapolation of this data indicates that as the enthalpy is decreased below 1.8 kw/SCFM by the addition of coal, the rate of acetylene decomposition will also decrease. The plateaus in the concentration and SER values shown in Figure 6 can then be interpreted as indicative of a balance in the competing reactions where although less acetylene is formed because of the decrease in average enthalpy (caused by the additional coal) less acetylene is decomposed for the same reason. At some higher coal feed rate, the enthalpy of the mixture will fall below the level required to form 8% acetylene and a corresponding decrease in the final acetylene concentration will be observed.

Since the early work with the argon plasma coal reactions (9-11) Newman and his co-workers (12) at the National Coal Board in England have also adapted a hydrogen plasma jet to produce acetylene from coal. The lowest SER value reported in this work corresponds to about 8.5 kw/hr and was achieved with a gas enthalpy of about 3.0 kw/SCFM at a coal feed rate of 160 g/min. This SER value is appreciably higher than the lowest values given in Figure 5 and comparison of the data suggests that the experiments at the National Coal Board were performed at excessive gas enthalpies. In addition it was shown that the radial coal injector, illustrated in Figure 4, distributed the coal more uniformly and consequently more efficiently than a straight tube injector apparently similar to the one used by Newman et al. Russian workers (17) also developed a hydrogen plasma jet and used it to form acetylene from methane. Their SER values, however, were two to three times higher than those reported in this paper.

Evaluation of the process as a commercial method of producing acetylene can be based on a recent study by the Stone and Webster Engineering Co. (18). This study was designed to evaluate an arc-coal process of producing acetylene in which the coal is injected into the inter-electrode region. The same critical parameters are important in each process and the same mine-mouth operation considered by Stone and Webster can be utilized in the evaluation of the arc heated hydrogen process.

The current price of acetylene depends on the size of the contract, the location and the process. For large contracts acetylene costs about 8¢/lb when produced by the carbide or partial oxidation process. (19) If we select 7¢/lb as a target cost for producing acetylene by the arc heated hydrogen process we can use the Stone and Webster data for designating the combination of operating parameters required to make the process viable. Using a conservative price for electricity of 5.25 mils and considering a 300 million pound per year plant it can be shown that a process in which the yield is 18%, the concentration 12% and the SER value 4.5 kw/lb, or a case in which the yield was 30%, the concentration 12% and the SER value 5.75 kw/lb, would meet the target cost. These values are admittedly based on conservative data; that is, no credits other than fuel credits were taken for by-products and it was indicated that electricity costs of about 4.0 mils could be negotiated for an acetylene plant with a load of about 100 mw. If reasonable credits are taken for the chemical value of the by-products and 4.0 mil power is used, a cost reduction of about 1.5 cents per pound could be realized or a process in which the SER value was about 6.5 kw/lb would be considered viable.

The most promising direction for additional improvements in the process would appear to be toward utilizing the highest temperature portions of the plasma jet to better advantage. As was indicated in the plasma temperature measurements, the coal was not reaching the central portion of the jet and consequently the highest energy gases were not being utilized in the conversion reaction. Better

coal penetration may be achieved by feeding a portion of the coal through a hollow cathode or by feeding the coal counter-current to the plasma jet.

Another method in which the reaction of coal with arc heated hydrogen could be utilized to advantage is in combination with the previously cited (6) process in which the coal is injected directly into the arc. In such a process a large portion of the coal is volatilized in the inter-electrode region and the effluent gas mixture consists of acetylene and other hydrocarbon species as well as arc heated hydrogen. Injecting coal into this plasma jet, as shown in Figure 6, should serve to react with the arc heated hydrogen to form additional acetylene, as previously shown, and to quench the high temperature hydrocarbon species to preserve a high percentage of the acetylene. The combination of the two processes would be analogous to the Huels process (20) in which liquid hydrocarbons are injected directly into the arc as well as downstream of the arc. Initial tests in which the combined processes were tried with coal injection showed a 10 to 15% increase in the acetylene concentration with a corresponding decrease in SER values. A decrease in acetylene yield was also noted. This can be traced to the additional coal, added downstream, which apparently isn't converted to acetylene as efficiently as the primary coal charge injected directly into the plasma.

#### ACKNOWLEDGEMENT

Support of the program was provided by the Office of Coal Research on Contract Number 14-01-0001-493. The technical assistance of A. Bothe, T. Henze, R. McDonough, and R. Ruediger in planning and performing the described experiments is gratefully acknowledged.

#### REFERENCES

1. Kavlick, V.J., and Lee, B.S., Amer. Chem. Soc., Div. Fuel Chem., Preprints 10, (4), 131-9 (1966).
2. Curran, G.P., Struck, R.T., and Gorin, E., Amer. Chem. Soc., Div. Fuel Chem., Preprints 10, (2), C-130--C-148 (1966).
3. Lefrancois, P.A., Barclay, K.M., and Skaperdas, G.T., Amer. Chem. Soc., Div. Fuel Chem., Preprints 10, (4), 198-205 (1966).
4. Eddinger, R.T., Friedman, L.D., and Rau, E., Fuel 45, (3), 245-52 (1966).
5. Krukonis, V.J., and Schoenberg, T., Paper 5-132, 7th International Conference on Coal Science, Prague (1968).
6. Krukonis, V.J., Gannon, R.E., and Schoenberg, T., Paper to be presented at the 19th Canadian Chemical Engineering Conference Edmonton, Alberta, October, 1969.
7. Sharkey, A.G. Jr., Schultz, J.L., and Friedel, R.A., Coal Sciences, Adv. in Chem. Series 55, 643-644 (1966).
8. Rau, E., and Seglin, L., Fuel 43, (2), 147-57 (1964).
9. Bond, R.L., Ladner, W.R., and McConnel, G.I.T., Coal Sciences, Adv. in Chem. Series 55, 650-665 (1966).
10. Kawa, W., Graves, R.D., and Hiteshue, R.W., U.S. Bureau of Mines, Rept. Invest. 6829 (1966).

11. Kawana, Y., Makino, M., and Tatsuo Kimura, *Kogyo Kagaku Zasshi*, 69, (6), 1144-50 (1966).
12. Newman, J.O.H., et al, 7th International Conference on Coal Science, Prague (1968).
13. Littlewood, K., McGrath, I.A., Paper C9, 5th International Conference on Coal Science, Cheltenham (1963).
14. Rau, E., Eddinger, R.T., *Fuel* 43 (3), 246 (1964).
15. Wagman, et. al, *J. Res. Nat. Bur. Stand.*, 1945, 35, p. 467.
16. Howard, Wood and Kaltenbacher, *Chem. Eng. Prog.* , 1961, 57 , (11) p. 50.
17. Kozlov, G.I. et. al, *Int'n. Chem. Eng.*, 8, No. 2, April, 1968, p. 289.
18. Office of Coal Research, R.& D. Report No. 34 "AVCO Arc-Coal Process" OCR Contract No. 14-01-0001-493, April 1968.
19. O'Hara, J.B., *Chem. Eng. Prog.*, 63, April 1967, p. 61.
20. Gladisch, H., *Hydrocarbon Proc. & Pet. Ref.*, 41 (6), 159 (1962).

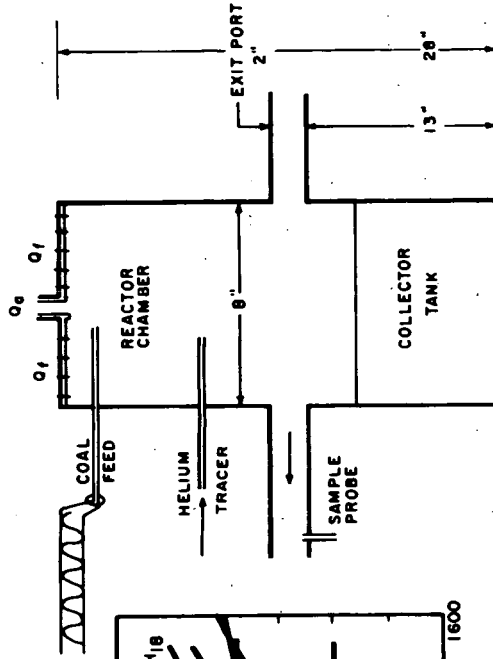


Figure 2 ARC HEATED HYDROGEN REACTOR

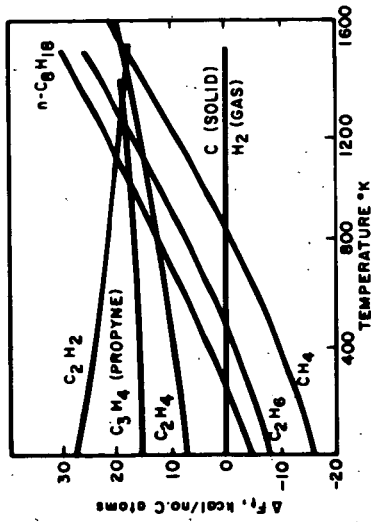


Figure 1 FREE ENERGIES OF FORMATION OF SELECTED HYDROCARBONS

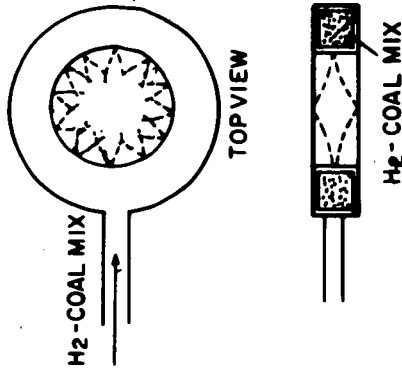


Figure 4 COAL FEED MANIFOLD

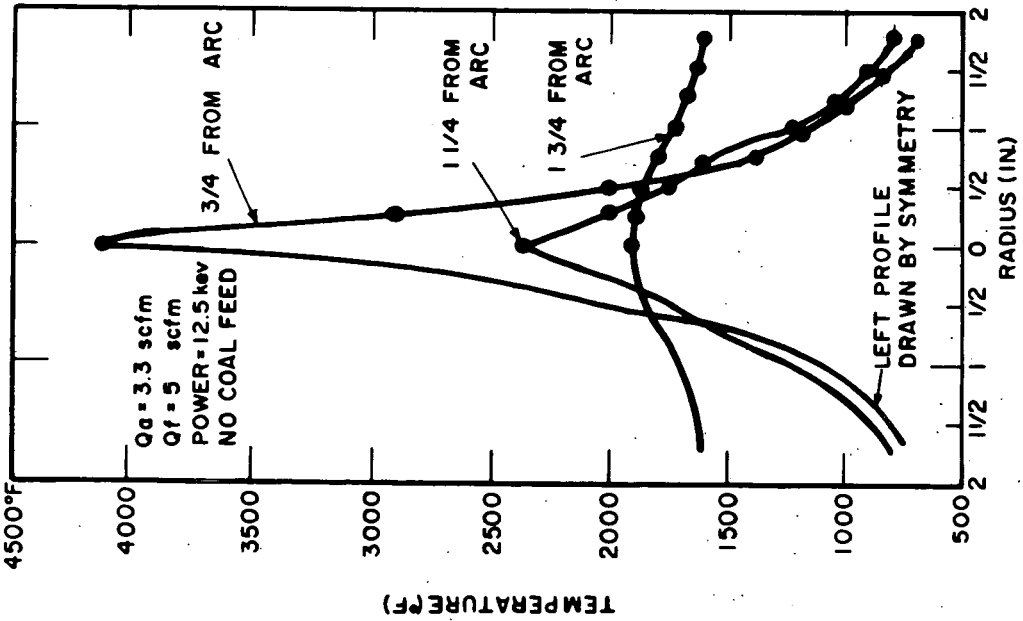


Figure 3 TEMPERATURE DISTRIBUTION IN REACTOR

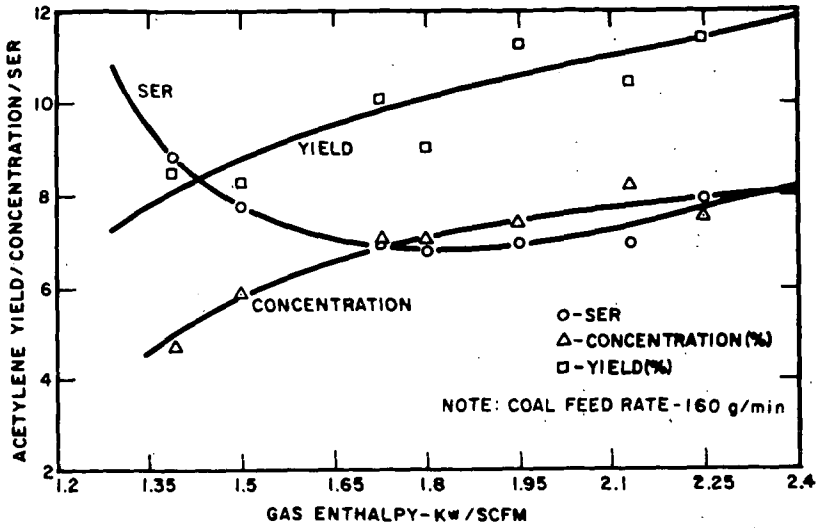


Figure 5 ACETYLENE YIELD, CONCENTRATION AND SER AS A FUNCTION OF GAS ENTHALPY

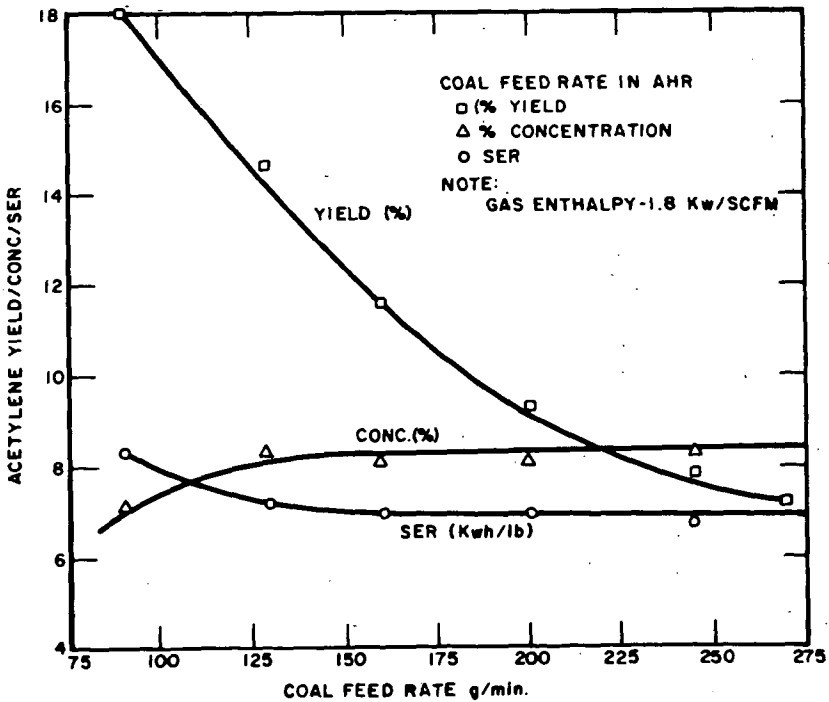


Figure 6 ACETYLENE YIELD, CONCENTRATION AND SER AS A FUNCTION OF COAL FEED RATE

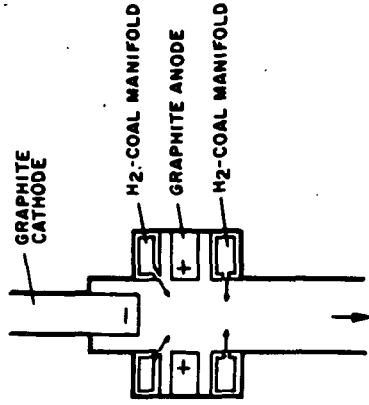


Figure 8 ARC REACTOR WITH DUAL COAL FEED

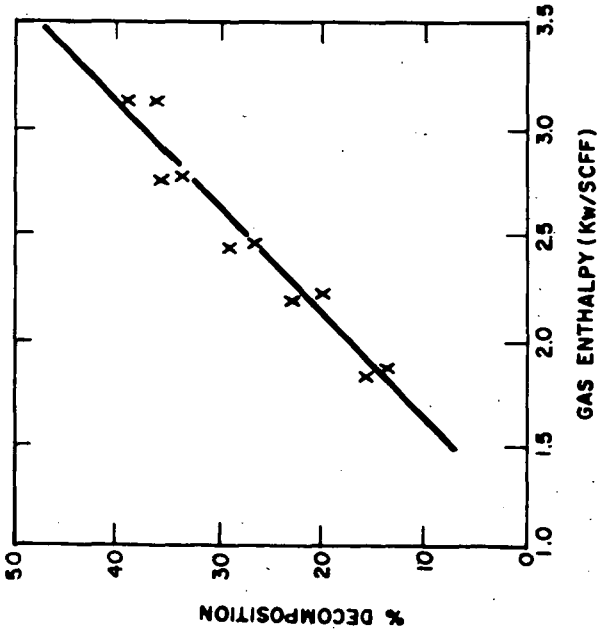


Figure 7 ACETYLENE DECOMPOSITION AS A FUNCTION OF GAS ENTHALPY

Kinetics of Formation of Hydrogen Cyanide  
from Methane and Ammonia in a Microwave Plasma

Thorikild Juul-Dam and Norman F. Brockmeier

The Department of Chemical Engineering  
The University of Texas, Austin, Texas, 78712

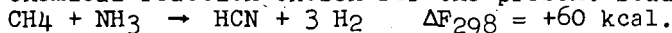
**Abstract** The reaction of  $\text{CH}_4$  with  $\text{NH}_3$  to produce HCN was studied at 10 and 25 torr pressure in a microwave plasma. Varying the reactant flow rate from 60 to 1050 cc./min. NTP and the microwave power from 70 to 500 watts produced conversions to HCN from 9 to 78 percent. Application of the theory of diffusion controlled discharge operation resulted in constant  $E/p$  and average electron energy at a given pressure. Combining this conclusion with the observation of invariant specific power and electron density justified replacing reaction time with specific energy in the rate equations. Mathematical models based on first order kinetics were consistent with measured reaction rates for the disappearance of  $\text{CH}_4$  ( $k_1 = 0.036$  liter/W-hr) and the formation of HCN ( $k_2 = 0.035$  liter/W-hr).

**Introduction** One useful way to classify discharges for chemical synthesis is on the basis of the temperature ratio of the electrons to the bulk gas,  $T_e/T_g$  (Spedding, 1969). In thermal discharges, such as a high current D.C. arc or a plasma jet,  $T_e/T_g$  approaches unity, and the bulk gas temperature is usually of the order of 10,000°K. In non-thermal discharges, such as high frequency and microwave discharges at pressures below 0.5 atm.,  $T_e/T_g$  may range from about 10 to nearly 100. The bulk gas temperature may be as low as 300°C (Brockmeier, 1966). Thus the non-thermal discharge provides a means for generating a significant number of high energy electrons without heating the bulk gas to a great extent. The purpose of the present study is to investigate the production of HCN under these conditions.

The microwave discharge has some definite advantages because it provides a highly reactive environment at relatively low temperature. Products that are thermally unstable can be synthesized. Reactions that have a favorable free energy change, but which normally require a catalyst or high temperature to achieve a reasonable rate, should proceed in a microwave discharge. The absence of metal electrodes aids in preventing contamination and possible undesirable catalytic effects.

Investigators have been studying the effects of microwave radiation on gases since the first generators became available about 25 years ago, but in all of these studies, except that of McCarthy (1954), there has been very little effort to measure the effects of power, flow rate, temperature, and pressure on the reaction rate in the microwave plasma. Recently, Cooper, et al. (1968), have reported a more comprehensive study of the discharge parameters that affect the chemical yield. The oxidation of HCl to chlorine was correlated as a function of the quantity (power)<sup>1/2</sup>/pressure, which was proportional to the proper variable,  $E/p$ .

The chemical reaction chosen for the present study was the following:



This reaction is not thermodynamically favorable until the temperature is raised above 900°C. The HCN is unstable below 2000°C (Sherwood and Maak, 1962). The recovery of a significant amount of HCN at the cooler temperatures (300-800°C) prevailing in a microwave reactor depends first on generating suitable activated precursors and second on these precursors combining along a reaction pathway that leads to HCN concentrations "frozen" at values greater than the equilibrium values.

This chemical reaction is particularly suitable for study in a microwave reactor. Under most conditions in the operating plasma, large concentrations of hydrogen will be present, therefore the operation can be analyzed within the framework of the diffusion-controlled theory.

Theoretical A microwave field affects only the charged particles in the reaction tube, and essentially only the electrons, because they are so much lighter than the ions present. The Boltzmann transport equation, which is an equation of continuity, represents the changes in the number and density of electrons and is the starting point for most theories of microwave discharges in a gas. These theories have been formulated by several investigators for both the initial breakdown and the steady state discharge (Rose and Brown, 1955; Brown, 1959 and 1966; Kontaratos and Demetriades, 1965). The solution to the Boltzmann equation for a steady state discharge has been discussed by Brown (1959, 1966), and an exact solution can be obtained for two limiting cases, low and high electron density.

The conditions in an operating discharge differ somewhat from the conditions at the initial breakdown. The operating discharge has a significant concentration of positive ions, somewhat greater than the electron density because the heavier ions diffuse to the walls more slowly. The electron density,  $n$ , is significantly greater than the breakdown value because of the exponential growth law for free electrons. The interaction between these charged species generates a space charge field that enhances the diffusivity of the positive ions and decreases the diffusivity of the electrons. The effect of the space charge field,  $E_s$ , is taken into account in solving the Boltzmann transport equation by superposing  $E_s$  on the microwave field:

$$E = E_s + E_p e^{j\omega t} \quad (1)$$

At microwave frequencies the effective field for energy transfer,  $E_e$ , is substituted for the peak field in equation (1)

$$E_e^2 = E_p^2 \cdot \nu m^2 / (\nu m^2 + \omega^2) \quad (2)$$

where  $\nu m$  is the collision frequency for momentum transfer and  $\omega$  is the radian frequency of the field ( $\omega = 1.54 \times 10^{10} \text{ sec}^{-1}$  at 2450 MHz). The effectiveness of energy transfer changes markedly as the relative values of  $\nu m$  and  $\omega$  vary with pressure. If equations (1) and (2) are used to calculate the field,  $E$ , the equation of motion for an electron may be solved to get the specific power, or power input per unit volume of gas (Cooper, et al., 1968).

$$\bar{P} = ne^2 E^2 / (2m\nu m) \quad (3)$$

It has been shown (Brown, 1959; MacDonald, 1966) that three proper variables are sufficient to describe breakdown conditions in electric discharges:  $E\Lambda$ ,  $p\lambda$ , and either  $E/p$  or  $p\Lambda$ . The electron density,  $n$ , must be added to this list to describe the operating discharge.

The diffusion controlled breakdown theory has been solved using the assumption of constant collision frequency ( $\nu m \neq f [u]$ ) to obtain the breakdown field over a pressure range from 0.1 to 100 torr. Figure 1 shows the results of MacDonald and Brown (1949) comparing the theory with experimental results for hydrogen at 2800 MHz. Also on the same plot are the curves for steady operating conditions, where  $n_0$  is the electron density at the centerline of the tube. Similar curves have been reported by others using air (Rose and Brown, 1957) and helium (Reder and Brown, 1954). Figure 1 indicates that  $E/p \approx 10$  for pressures above 10 torr. Another important observation is that if  $n_0 > 10^9 \text{ cm}^{-3}$ ,  $E$  is practically constant as  $n_0$  is increased. It can be shown (Cooper, et al., 1968) that the average electron energy,

$u$ , is determined by  $E/p$ , so the value of  $u$  is also steady at the above conditions. Since the rate of formation of excited species is determined by  $E/p$ , the distribution of these reactive species will also be practically constant at a given pressure if  $n_0 > 10^9 \text{ cm}^{-3}$ . The electron density in the present system is estimated as at least  $10^{10} \text{ cm}^{-3}$ .

For certain reactor and waveguide geometries, and especially that used in this work, one effect of increasing the incident power is to extend the electric field farther outside the waveguide into the flowing gas. The region in which the electric field is strong enough to sustain a discharge is the same as the extent of the visible glow. At constant pressure the length or volume of the visible discharge may be directly proportional to the power absorbed in the microwave reactor, especially at low to moderate power levels. In the linear region, the reciprocal of the slope is the specific power, or power absorbed per unit volume, which is a constant.

Equation (3) shows the relationship between the specific power and electron density. It has been shown above that, at constant pressure in the high electron density limit, the values of  $E$  and  $v_m$  will be steady. Therefore, the electron density will be constant if the specific power remains constant over this range of conditions. This implies that over a moderate range of power levels, the result of increasing the power is simply to lengthen the microwave reactor, without causing any significant change in the average electron energy, the electron density, or the kinds of reactions occurring. The longer reaction zone has the same environment as at lower powers, and the contact time is increased proportionately with the power.

Experimental The apparatus used for this study is shown schematically in Figure 2. The microwave power was supplied by an Eimac PPS-2.5A Power Pack at a fixed frequency of 2450 MHz using a continuous wave magnetron with an output adjustable between 200 and 2500 watts. A crescent-shaped variable attenuator was installed in the waveguide to permit operation below 200 watts. An impedance meter consisting of a movable probe in a slotted waveguide was used to measure the voltage standing wave ratio (VSWR). The power incident on the reactor was detected with a loop-type directional coupler and read on a microwave power meter. The power actually absorbed in the discharge region was calculated from the incident power reading and the VSWR. A tapered waveguide section with a slot for the reactor coupled the power into the plasma (Fehsenfeld, et al., 1965).

The microwave reactor was a 13 mm. OD quartz tube. A Liebig condenser was mounted around it to permit cooling the tube with a high-velocity air stream. A fitting in the exhaust end of the tube was used to install a chromel-alumel thermocouple in a thin-walled quartz shield for those runs in which temperatures were measured.

Research grade methane and ammonia were used as feed gases without further purification. Each feed rate was measured at atmospheric pressure with a Matheson No. 600 series rotameter. An evacuated glass bulb was used to obtain a sample for gas chromatography using a hydrogen flame detector. In addition, a condensed sample was obtained by operating the three toggle valves to direct the product stream through a glass trap cooled with liquid nitrogen. The condensed products were dissolved in water and titrated for cyanide and ammonia.

Results Experimental results were obtained over the following ranges of operating conditions: gas pressures from 10 to 25 torr, absorbed powers from 70 to 500 watts, and gas feed rates from 60 to 1050 cc./min. measured at NTP, that is, 21°C and atmospheric pressure. For most of the runs, the feed ratio of methane to ammonia was 1:2. The use of this feed ratio rendered methane the limiting component for the formation of HCN in all of the experiments. The major products from the reactor were HCN, hydrogen, and nitrogen. In addition, there was a minor amount of

acetylene, and very small quantities of ethane, ethylene, and other hydrocarbons.

In many studies of reaction kinetics in electric discharges, the specific energy,  $U/V$ , has been used rather than reaction time,  $t$ , to correlate the results (Vasil'ev, et al., 1937; Borisova and Eremin, 1967). This has also been done here, for reasons explained in the theory section and because calculation of specific energy from the measured power and feed rates was more accurate than calculation of space time.

The results of chemical analyses are shown in the following figures. The disappearance of methane followed an apparent first-order kinetic expression at 10 torr, Figure 3. The rate constant for methane decomposition was  $3.6 \times 10^{-2}$  liters/W-hr. At 25 torr, the measured rate constant equalled that at 10 torr.

Figure 4 depicts the production of HCN as a function of specific energy at 10 torr. At low  $U/V$  ( $< 18$  W-hr/l) this figure exhibits a linear relationship with an initial slope practically the same as the slope of the line in Figure 3 for methane decomposition. At higher  $U/V$  the line curves, approaching asymptotically a value of approximately 80 percent conversion of methane to HCN for a  $U/V$  greater than 80 W-hr/l. Experiments at 10 and 25 torr pressure yielded essentially the same results, just as in the case of the methane decomposition.

At higher specific energies ( $> 40$  W-hr/l), very small amounts of an as yet unidentified dark brown solid were produced.

In a separate series of experiments, the axial temperature profiles were measured just below and part-way into the exhaust end of the operating discharge. At 10 torr, the absolute temperature increased about 10 percent as the power was increased nearly fourfold. The conclusion is that large variations in power cause only minor changes in the temperature profiles in the discharge. For each profile, the temperature near the center of the glowing plasma was  $1000^\circ\text{C}$ . The higher the gas rate, the higher the temperature is at the edge of the glow: as the flow rate was increased from 60 to 180 to 900 cc./min., the respective temperatures were 250, 350, and about  $500^\circ\text{C}$ .

The energy requirement per gram of HCN was calculated at different values of specific energy. The minimum energy requirement was 70 W-hr/gm. of HCN at a specific energy of 4.6 W-hr/l, corresponding to a 17 percent conversion to HCN.

Discussion The correlation of results by means of a straight line in Figure 3 indicates that the decomposition of methane in a microwave plasma can be described by a first-order reaction rate expression at 10 torr:

$$\ln(1 - X_A) = -k_1 (U/V) \quad (4)$$

Because of the first order expression, no volumetric expansion factor is required.

The decomposition of methane in the presence of ammonia in a microwave plasma leads to the formation of HCN by a series of at least two elementary reactions. In a series mechanism, the formation rate for the product is controlled by the rate of the slowest reaction in the series. The HCN will also be decomposed by exposure to the discharge. The series of reactions forming HCN will be summarized by  $A \rightarrow R$  and the decomposition of HCN will be abbreviated to a single reaction  $R \rightarrow S$ , so that



The form of equation (5) implies that only first-order reactions are considered in this mechanism. The corresponding integrated rate expression becomes

$$\frac{N_R}{N_{A_0}} = \frac{k_2}{k_2 - k_3} \left[ 1 - \exp \left[ - (k_2 - k_3) U/V \right] \right] \exp (-k_3 U/V) \quad (6)$$

where  $U/V$  has replaced time, and  $N_A$  is the molar feed rate of methane.

Equation (6) is the mathematical model that was used to generate the curve shown in Figure 4. This model gives a nearly straight-line correlation at low  $U/V$ , which begins to curve significantly at about 30 W-hr/l as the HCN begins to react to a large extent. However, the HCN is quite stable, since 80 percent conversion to HCN can be achieved, indicating that  $k_3$  is small. If  $k_3 \ll k_2$ , equation (6) may be simplified to  $N_R/N_{A_0} = [1 - \exp(-k_2 U/V)] \exp(-k_3 U/V)$  (7)

The values of  $k_2$  and  $k_3$  at 10 torr were calculated by determining the best fit to the experimental data in Figure 4. The same procedure was used for data at 25 torr. The results are shown in Table I.

Table I  
Rate Constants Calculated from Equation (6)

Pressure, torr	$k_2$ , l./W-hr	$k_3$ , l./W-hr
10	$3.5 \times 10^{-2}$	$3.65 \times 10^{-3}$
25	$3.5 \times 10^{-2}$	$3.65 \times 10^{-3}$

Since  $k_3$  is an order of magnitude smaller than  $k_2$ , equation (7) is an accurate approximation to the kinetic model. Note that for low values of  $U/V$ , the exponential containing  $k_3$  is practically unity wherefore equation (7) reduces to equation (4), which describes the methane decomposition. In the limit of zero conversion, at zero  $U/V$ , the rate of formation of HCN is identical to the methane decomposition rate. The value for  $k_1$  calculated from Figure 3 agrees with the initial slope of Figure 4 ( $k_2$ ) to within 5 percent. Therefore, the decomposition of methane appears to be the rate-controlling step in the formation of HCN, with the result that  $k_2$  equals  $k_1$ . This model is consistent with the experimental results up to about  $U/V = 60$  W-hr/l at both 10 and 25 torr.

At specific energies greater than 60 W-hr/l, no model has been found to describe the results. The products from the HCN decomposition (S) probably tend to reform some HCN.

#### Nomenclature

A = methane

$E$  = electric field strength, volts/cm.

$E_e$  = effective field strength, volts/cm.

$E_p$  = amplitude of electric field, volts/cm.

$E_s$  = space charge electric field, volts/cm.

$e$  = electronic charge, coulomb.

$k_1$  = rate constant for decomposition of methane, l/w-hr.

$k_2$  = rate constant for formation of hydrogen cyanide, l/w-hr.

$k_3$  = rate constant for the decomposition of hydrogen cyanide, l/w-hr.

$m$  = electron mass, gram.

$N$  = moles of chemical compound, moles

$n$  = electron density,  $cc^{-1}$

$n_0$  = centerline electron density,  $cc^{-1}$

$\bar{P}$  = specific power, watts/cc.

$p$  = pressure, torr.

$R$  = hydrogen cyanide

$S$  = decomposition products of hydrogen cyanide

$T_e$  = electron temperature, °K

$T_g$  = gas temperature, °K

$t$  = reaction time, min.

$U$  = absorbed power, Watts

$u$  = average electron energy, electron volts

$V$  = feed rate, cc/min at 21°C and 760 mm Hg.

VSWR = voltage standing wave ratio

$X_A$  = fractional conversion of methane

$\Lambda$  = characteristic diffusion length, cm.

$\lambda$  = free space wavelength, cm.

$v_{\text{m}}$  = collision frequency for momentum transfer,  $\text{sec}^{-1}$ .

$\omega$  = radian frequency of field,  $\text{sec}^{-1}$ .

Literature Cited

- Borisova, E.N., Eremin, E.N., Russ. J. Phys. Chem., 41, 69 (1967).  
 Brockmeier, N.F., PhD. thesis in chemical engineering, Massachusetts Institute of Technology, Cambridge, Mass., 1966.  
 Brown, S.C., "Basic Data of Plasma Physics," M.I.T. Press, Cambridge, Mass., 1959.  
 Brown, S.C., "Introduction to Electrical Discharges in Gases," Wiley, New York, 1966.  
 Cooper, William W., Mickley, Harold S., Baddour, Raymond F., I & EC Fundamentals, 7, 400 (1968).  
 Fehsenfeld, F.C., Evenson, K.M., Broida, H.P., Rev. Sci. Inst., 36, 294 (1965).  
 Kontaratos, N., Demetriades, S.T., Phys. Rev., 137(6A), 1685 (1965).  
 McCarthy, R.L., J. Chem. Phys., 22, 1360 (1954).  
 MacDonald, A.D., "Microwave Breakdown in Gases," Wiley, New York, 1966.  
 Reder, F.H., Brown, S.C., Phys. Rev., 95, 885 (1954).  
 Rose, D.J., Brown, S.C., Phys. Rev., 98, 310 (1955).  
 Rose, D.J., Brown, S.C., J. Appl. Phys., 28, 561 (1957).  
 Sherwood, T.K., Maak, R.O., I & EC Fundamentals, 1, 111 (1962).  
 Spedding, P.L., The Chemical Engineer, CE 17 (January/February, 1969).  
 Vasil'ev, S.S., Kobozev, N.I., Eremin, E.N., Zhur. Fiz. Khim., 7, 619 (1936); Khim. Tverd. Topliva, 8, 70 (1937).  
 MacDonald, A.D., Brown, S.C., Phys. Rev., 76, 1634 (1949).

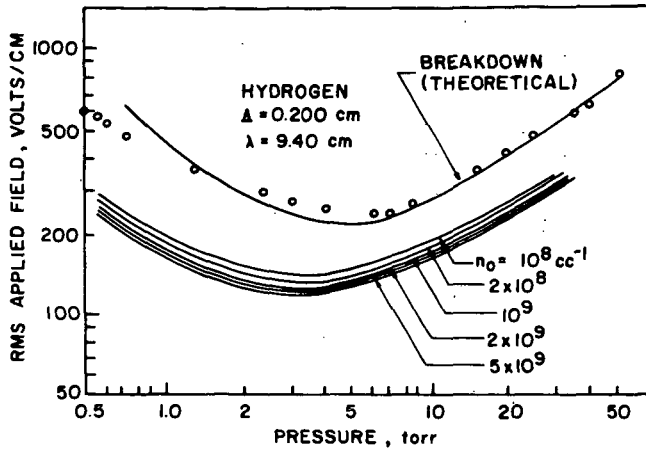


FIGURE 1. EXPERIMENTAL CURVES FOR STEADY-STATE MICROWAVE DISCHARGES.

○ : EXPERIMENTAL DATA

FROM : MACDONALD AND BROWN, 1949

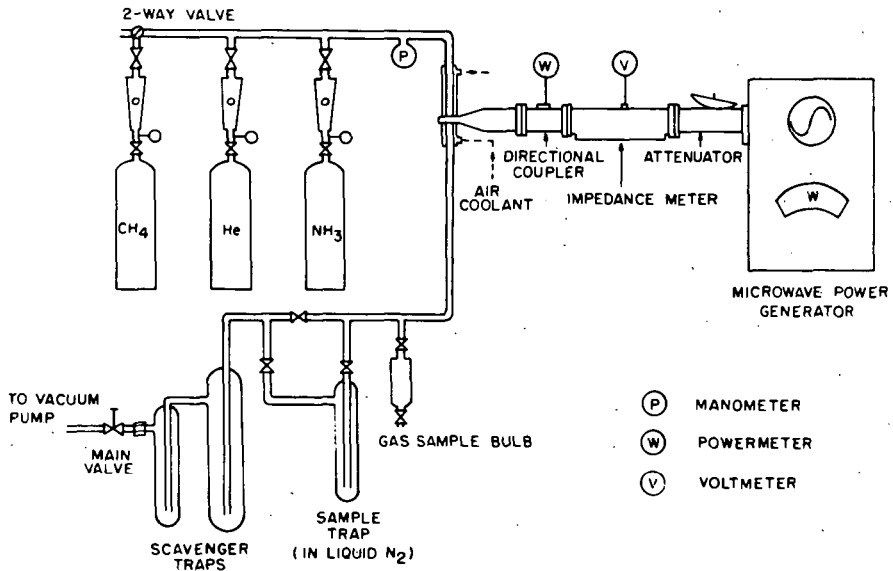


FIGURE 2. SCHEMATIC DIAGRAM OF APPARATUS.

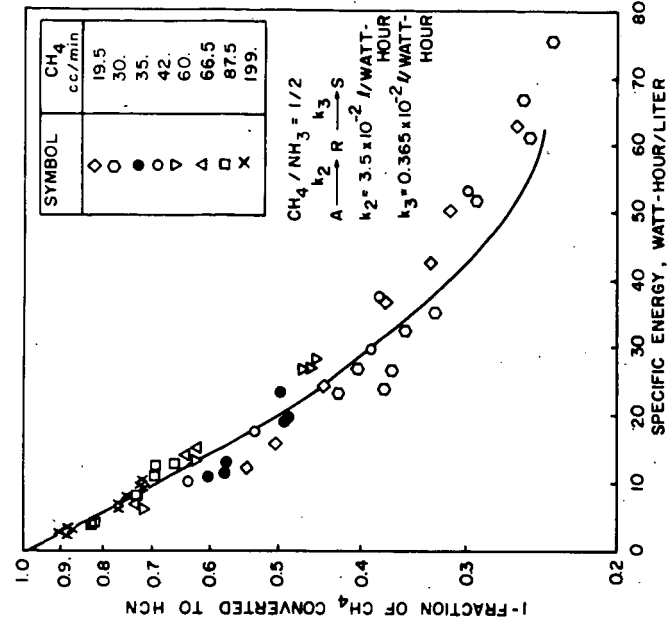


FIGURE 4. EFFECT OF SPECIFIC MICROWAVE ENERGY ON THE FORMATION OF HCN AT 10 torr PRESSURE.

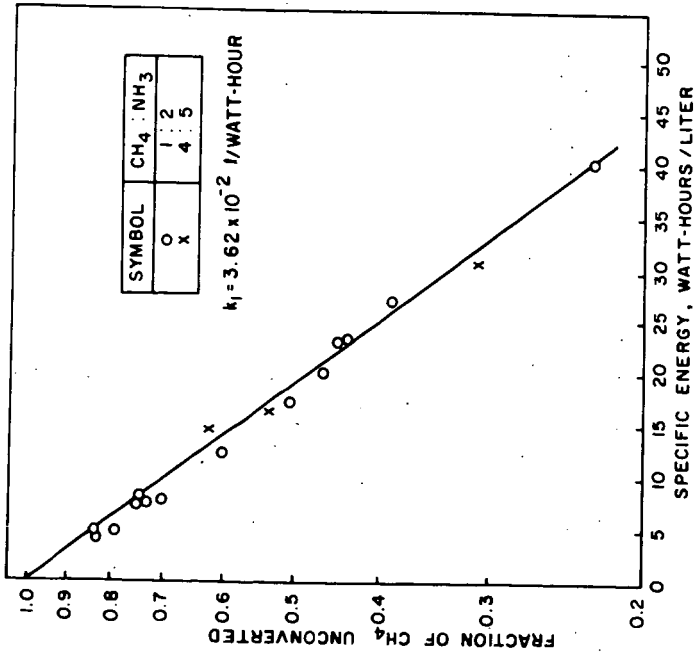


FIGURE 3. EFFECT OF SPECIFIC MICROWAVE ENERGY ON THE DECOMPOSITION OF CH<sub>4</sub> AT 10 torr PRESSURE.